



THE UNIVERSITY *of* EDINBURGH

This thesis has been submitted in fulfilment of the requirements for a postgraduate degree (e.g. PhD, MPhil, DClinPsychol) at the University of Edinburgh. Please note the following terms and conditions of use:

- This work is protected by copyright and other intellectual property rights, which are retained by the thesis author, unless otherwise stated.
- A copy can be downloaded for personal non-commercial research or study, without prior permission or charge.
- This thesis cannot be reproduced or quoted extensively from without first obtaining permission in writing from the author.
- The content must not be changed in any way or sold commercially in any format or medium without the formal permission of the author.
- When referring to this work, full bibliographic details including the author, title, awarding institution and date of the thesis must be given.

NEURAL MECHANISMS OF DANCE
COMMUNICATION IN HONEYBEES

ANNA HADJITOFI



Doctor of Philosophy
School of Informatics
University of Edinburgh

2024

Anna Hadjitofi:

Neural mechanisms of dance communication in honeybees

Doctor of Philosophy, 2024

SUPERVISORS:

Professor Barbara Webb

Professor Tim Landgraf

EXAMINERS:

Professor Andrew Barron

Professor Henry Thompson

Declaration of Originality

I, Anna Hadjitofi, declare that this thesis was composed by myself, that the work contained herein is my own except where explicitly stated otherwise in the text, and that this work has not been submitted for any other degree or professional qualification. The work of others has been appropriately referenced. A full list of references is given in the bibliography.

December 22, 2024

Abstract

This thesis brings a new approach to the study of honeybee dance communication: evaluating computational models against observed behaviour to understand how dance communication could be implemented by the insect brain. After a foraging trip, a bee has internal knowledge of the flight vector to the food which it communicates by producing a stereotyped motor pattern known as the waggle dance. This creates mechanical cues that surrounding nestmates can assimilate to obtain their own flight vector. Independently of communication, the acquisition and utilisation of vectors for navigation is believed to occur in the central complex in the insect brain. Our key hypothesis is that this circuit is sufficient, with minor adaptations, to explain both the production and assimilation of dance information.

First, we propose how an anatomically grounded model of path integration for foraging, based on the central complex, could be adapted to produce the dance in the hive. We assume the existence of vector memory, where a snapshot of the bee's path integrator state at the food source can later be utilised by the steering circuitry to guide a return journey. We also impose a parameter to limit the angular velocity of the bee when wagging based on properties of natural dances. By simulating neural activity for foraging routes, we demonstrate that natural features emerge from the subsequent dancing behaviour produced by the circuit, including waggle and return phases. The simulated dances also exhibit patterns of angular scatter that align with those observed in real bees for different feeder distances. Our results suggest that performance of the dance could arise from a pre-existing neural circuit that underlies large-scale navigation and supports the idea that the dance is a miniature re-enactment of the foraging flight.

We then explore how this circuit could be used by the receivers of information: nestmates following the dance. We present a new dataset of nestmates as they follow a dance and uncover a previously unreported feature of their antennal positioning that correlates to their relative angle to the dancer. Knowing its own orientation to gravity on the vertical comb, this could allow followers to deduce the dancer's orientation, which indicates the direction of the food relative to the sun. Integrating the estimates of this direction during the waggle phase could then enable the follower to obtain a vector to the food. Based on recent evidence of antennal inputs and spatial encoding in the central complex of the fruit fly, we propose how the circuit could be adapted to use the antennal information to perform these computations and recover the signalled dance vector. Using the real positional data of the followers as input, the simulated circuit predicts that their recovered vectors would be appropriately centred on the signalled direction. It also predicts the distribution to be up to $\pm 90^\circ$ wide from this direction.

To follow up this result, we devise an experiment to compare these predictions with the real flight vectors expressed by bees. Inspired by the forced-detour paradigm in ants, we track the correction angle of bees navigating to a feeder after an imposed detour, as a measure of the estimated food location. Similar to the circuit's predictions, we observe a characteristic spread of vectors centred on the feeder. Our work thus indicates that the central complex could underlie the encoding, decoding and expression of spatial information in dance communication.

Lay Summary

The honeybee waggle dance is a remarkable form of communication, whereby a bee that has found food performs a *dance* inside the hive to signal its location. The direction of the dancer's movement relative to gravity on the vertical honeycomb tells other bees where to find the food relative to the sun, and its duration correlates with the distance to the food. Although scientists have known about the waggle dance for a long time, the details of the underlying mechanisms in the brain remain poorly understood. For example, how nestmates can observe and translate the dancer's movements into a flight path they can use to find the food is unknown.

This thesis uses a computational approach to investigate how neural circuits in the bee brain could produce and interpret the waggle dance. We focus on the involvement of a region of the insect brain called the central complex, which is known to be a centre for navigational processing. Our work implements computer simulations of this neural circuit and compares their behaviour to real-world observations. First, we demonstrate how properties of the central complex that underlie large-scale navigation could be adapted to perform the dance as a miniature re-enactment of the original foraging trip. Following this, using high-speed high-resolution cameras, we film bees observing dances and uncover how the movements of the dancer could be sensed by other bees through the positioning of their antennae to deduce the signalled direction of the food. We then propose how the central complex could process this antennal positioning, along with the bee's knowledge of its own orientation relative to gravity, to obtain a flight path to the food. Finally, we conduct a novel experiment to measure how accurately bees' have estimated the signalled location after observing a dance. Using real data from tracked bees as input to the proposed model, we obtain predictions for the flight paths of bees recruited to a food source. Both the model's predictions and experimental results show a similar pattern: recruited bees would be scattered in a wide, fan-shaped vicinity of the food source.

We show how neurobiological properties of the same circuit can accommodate key aspects of the honeybee dance communication, including a forager performing the dance and a nestmate translating the dance into their own flight path. Although the waggle dance is a unique form of location-sharing that is not known to exist in any other insect, our results suggest that it could arise from the repurposing of existing navigational mechanisms and neural circuitry that is common across the insect world.

Acknowledgements

It has been a privilege to have had the opportunity to spend several years studying a topic of great interest to me. This would not have been possible without my family, and in particular, my parents, for their unwavering support in my endeavours without exception. This thesis is also a product of your legacy and I dedicate it to you.

I would like to also express my sincere gratitude to my principal supervisor, Barbara Webb, for her guidance and mentorship throughout my PhD. I will never forget your dedication and support whilst putting together our *Current Biology* paper, and thank you for your patience as I returned to my behavioural data for what must have felt like the hundredth time to analyse something new.

I also feel very fortunate to have been part of the Insect Robotics Group. I would like to thank its members, past and present, for creating such a welcoming and friendly environment. Thank you for the many insightful discussions and sharing of knowledge about the world of insect navigation. Sorry for always *pollinating* the conversations with stuff about bees.

I am also grateful to my second supervisor, Tim Landgraf, for his feedback at my annual review meetings and for kindly hosting me in his lab group to conduct the detour experiment in Berlin. The detour experiment would also not have been possible without Marie Messerich. Thank you for tirelessly setting up the tunnels and training the bees with me every day, and in the thirty degree heat. You also almost certainly took more of your fair share of the bee stings for the both of us. Along with the other members of Tim's lab, thank you for making it easy to be away from home.

My thanks also go to Mark Barnett and Matthew Richardson for their invaluable bee expertise and support in providing and handling the honeybee colonies over my first two summer seasons. The opportunity to collect behavioural data as well as become confident in handling bees played a large role in shaping the trajectory of my PhD. I would also like to extend my thanks more generally to the Edinburgh and Midlothian Beekeepers' Association (EMBA); it was always interesting and insightful to have the perspective of avid beekeepers.

I would also like to thank the organisations that funded my project: the European Research Council, The Eva Crane Trust as well as The Janet Foreman Fund.

Finally, I would like to thank my partner, Nuri, for his endless patience and moral support, from the decision to pursue a PhD in Edinburgh to the final proof reading of this thesis. You know more than anyone else about the work that has gone into this thesis and I hope you know that this journey would have been immeasurably harder without you. Thank you for always being there for me.

Dedication

For my parents, Karen and Andrew.

“Perhaps the greatest question about the bee’s communication system left unanswered by the work of von Frisch is how the bees following a dancer detect the information in the waggle dance.”

— Thomas Seeley, in the *Foreword* to *The Dance Language and Orientation of Bees* by Karl von Frisch, 1993.

Contents

1	Introduction	I
1.1	The language of the hive	3
1.2	Advances in understanding the insect brain	4
1.3	Scope	5
1.4	Contributions	6
1.5	Outputs	6
2	Background	9
2.1	Strategies of insect navigation	9
2.1.1	Path integration: beyond homing	12
2.2	Honeybee communication	14
2.2.1	The honeybee colony	14
2.2.2	Modelling a foraging trip as a dance	16
2.2.3	Characterising following behaviour	23
2.3	The insect central complex	30
2.3.1	Vectors in the insect brain	30
3	Path integration in dancing	35
3.1	The origins of dance behaviour	36
3.2	Directional dance error: constraints and control	37
3.3	A path integration control system	41
3.4	Comparison with natural dances	45
3.4.1	Alternating turns	45
3.4.2	Angular divergence	47
3.4.3	Round dances	49
3.5	Discussion	51
3.6	Methods	53
3.6.1	Honeybee dance datasets	53
3.6.2	Path integration model	55
3.6.3	Data analysis and statistics	57
4	Assimilating the flight vector information	59
4.1	Perspectives on following behaviour	60

4.2	An observational study of follower bees	62
4.2.1	Dynamic variation of relative body axes	62
4.2.2	A relationship between antennal positioning and angle to dancer	64
4.3	A proposed circuit to recover the dance vector	66
4.3.1	Vector assimilation by the central complex	66
4.3.2	Real antennae data as input	69
4.4	Discussion	74
4.5	Methods	76
4.5.1	Honeybee data	76
4.5.2	Rate-based assimilation circuit	77
4.5.3	Data analysis and statistics	80
5	Testing dance recruitment	83
5.1	A detour experiment in bees	84
5.1.1	Approaches to studying foraging accuracy	84
5.1.2	Training phase	86
5.1.3	Testing phase	86
5.2	Accuracy of location estimation and sharing	89
5.2.1	Flight trajectories post detour	90
5.2.2	Precision of dances	94
5.2.3	Predictions of the assimilation circuit	96
5.3	Discussion	99
5.4	Methods	100
5.4.1	Experimental protocol	100
5.4.2	Video analysis	104
5.4.3	Data analysis and statistics	106
5.4.4	Acknowledgements	108
6	Conclusion	109
6.1	Overview	109
6.2	Rethinking the dance	110
6.3	Future directions	113
	Bibliography	117
A	Supplementary Material	145

List of Figures

1.1	Infrared photograph of a honeybee performing the waggle dance	2
2.1	Three different though not mutually exclusive modes of navigation in insects	10
2.2	Representing vectors as sinusoids	13
2.3	An overview of honeybee anatomy	15
2.4	Typical stages in the life of the worker honeybee and order of duties	16
2.5	Conceptual illustration of polarised skylight and the signalling of direction .	18
2.6	Translational optic flow experienced by a bee moving through its environment	19
2.7	Domain of categories used to study following behaviour	24
2.8	Frontal view of a three-dimensional reconstruction of the honeybee brain .	31
2.9	Example of the vector memory extension to a path integration circuit	34
3.1	Comparison of recruitment systems within the Apidae family	37
3.2	Angular divergence across consecutive waggle phases	39
3.3	Measuring the change in course during the waggle phase	40
3.4	A network for path integration based on the insect central complex	42
3.5	From foraging to dances using vector memory	44
3.6	Natural and simulated paths of three features of dance communication	46
3.7	Alternating turns during natural and simulated dances	47
3.8	Angular scatter during natural and simulated dances for distant and nearby food sources	48
3.9	Traces of natural and simulated dance paths for nearby food sources	51
3.10	Example waggle phase trajectories from Landgraf et al.	54
4.1	Requirements of following from behind the dancer versus from any position	61
4.2	Positioning of follower bees and their antennae when following waggle phases	63
4.3	Point of view from camera positioned perpendicular to honeycomb	64
4.4	Calculating antennal positioning using the full length or halfway point	65
4.5	Proposed mechanism to assimilate the foodward vector (overview)	67
4.6	A central complex circuit to recover the allocentric dance angle	68
4.7	Deviation of follower bees' foodward vectors obtained from the assimilation circuit	70
4.8	Vector averaging over consecutive waggle phases improves angular accuracy .	72
4.9	A non linear function improves the mapping of antennal angle to dancer angle	73

4.10	Labelling and visualisation pipeline of follower bees	77
4.11	Connectivity of the assimilation circuit	80
5.1	Top-down views of experimental area in Berlin	87
5.2	Equipment for the detour experiment	88
5.3	Relative configuration of training and detour tunnels tested	89
5.4	Distributions of flight angles post detour relative to the tunnel exit	91
5.5	Returning foragers tested on multiple detour release sites	92
5.6	Mean distributions of flight angles post detour relative to the tunnel exit	93
5.7	Foodward angles signalled in the waggle phases of dancers ordered by their post detour accuracy	94
5.8	The angles of waggle phases performed by six dancers relative to gravity within a 2.5 hour period	95
5.9	The angles of waggle phases followed by new recruits and their post detour flight angles	97
5.10	The assimilated vectors of six new recruits and their post detour flight angle	98
5.11	Ant detour data from Collett et al.	99
5.12	Sky conditions throughout the detour experiment	101
5.13	Post detour flight angles in relation to sky conditions and feeder angle	102
5.14	Automated tracking of bees' flight paths	105
A.1	Angular divergence across consecutive waggle phases (additional view)	146
A.2	The hypothetical gain in performance when using antennal modulation for a uniform distribution of nestmates around the dancer	147
A.3	Additional results of the assimilation circuit	148
A.4	Surrounding area of site for the detour behavioural experiment in Berlin	149
A.5	The angles of waggle phases performed by six dancers relative to the feeder within a 2.5 hour period	151
A.6	The assimilated vectors of six new recruits with their mean vectors weighted by their length	152

List of Tables

2.1	Stimuli available for detecting and localising dancers in the hive	28
2.2	Stimuli available outside of the hive for locating the final resource	29
2.3	Corresponding names in <i>Drosophila melanogaster</i> and other insects	32
3.1	Circular statistics for dances for nearby resources	50
5.1	Randomisation test results for the angles of the vectors followed and assimilated by recruits	108
A.1	Circular statistics for post detour flight angles	150

1

Introduction

At the height of summer, a honeybee colony can be up to 50,000 strong and exists as a complex biological system that depends heavily on communication. Many messages propagate through the hive every minute: from widespread chemical signals like the alarm pheromone to more distinct signals, such as the ‘tooting’ of the queen. Amidst the apparent chaos, there are, in fact, pockets of organisation. This thesis puts one important type of bee communication in focus: the waggle dance. The waggle dance is a form of referential communication whereby foragers perform a *dance* that indicates the location of valuable resources to nestmates inside the hive via a mixture of body motion, mechanical and chemical cues¹⁰⁰. In particular, the rapid waggling of her abdomen along the vertical comb communicates the approximate location of the resource relative to the hive. For this communication to succeed, nestmates following the dance are required to detect the dancer’s orientation relative to gravity and duration of waggling and translate this into their own flight vector with a direction relative to the sun⁹⁸ and distance from the hive^{87;301}, which they can follow to the resource (Fig. 1.1).

By virtue of being a dynamic and social interaction within the hive, the honeybee dance is difficult to study in an isolated laboratory setting. To date, researchers are yet to directly record neural activity from actively dancing bees. Many characterisations of the dance have instead stemmed from observations of behaviour, often afforded by the use of glass observation hives. Until the late 20th century, honeybee dance research primarily relied on real-time observation and dances were decoded with stopwatches and protractors positioned over the glass. During this time, models of the behaviour had a tendency of being more qualitative in description than concrete, and may have prioritised more obvious parts of the behaviour. For example, although literature fondly refers to the dance exhibiting a classic figure-eight pattern on the comb, observing a busy hive on a sunny day will likely reveal distortions to the dance path and a far more diverse repertoire of movements than expected³¹⁹. Moreover, until the early 2000s, two further categories of dance (round and sickle) were believed to exist separately to

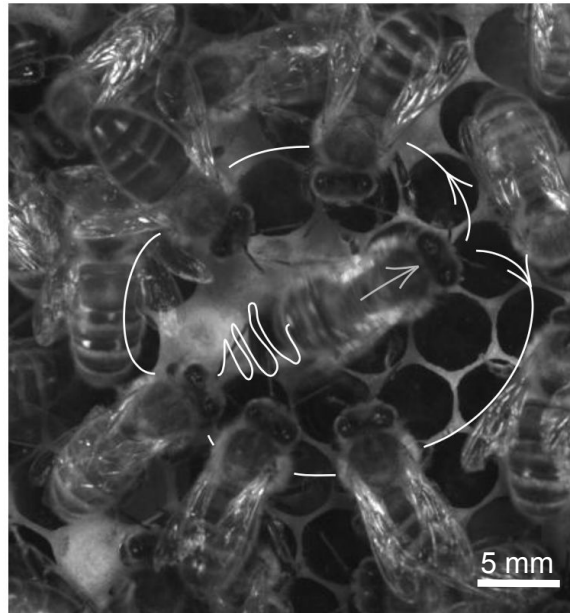


Figure 1.1. Infrared photograph of a honeybee performing the waggle dance (centre) within a hive. The dance has been described by von Frisch¹⁰⁰ as repeating circuits of a waggle phase, in which the bee rapidly waves their abdomen from side to side, followed by a return phase, where the dancer returns to the starting point (white lines). Consecutive return phases can alternate clockwise and counter-clockwise, giving the dance a figure-eight shape. The dance conveys a flight vector, where the angle and duration of wagging correlates with the direction and distance to the resource, respectively. Nestmates remain in close contact to obtain the dance vector. Photo by Anna Hadjitofi, Sept. 2022.

the waggle dance, but there was minimal clear criteria defining them and researchers would estimate their distinctions by eye. Utilising a number of honeybee dance datasets (old and new), this thesis offers a fresh analysis of key dance elements with a view towards reconciling empirical observations with potential models that explain the behaviour.

Computational neuroethology aims to understand the behaviour of animals through computational modelling and simulations of their nervous systems⁴⁴. The models can take properties of the animal into account, such as its neural circuitry, sensors, actuators, and behaviour. They can therefore be used to test specific hypotheses for the neural processing underlying the behaviour and highlight the assumptions required to make the model work as proposed. We follow a combined approach that utilises behavioural data along with computational models to formulate aspects of dance communication and test hypotheses about its underlying neural substrate. Neural models can be built at varying levels of detail: low-level models focus on the biophysical properties of neurons, while high-level models offer an abstract, algorithmic perspective which is more suited for explaining behavioural data. We use simple neural models, where the output of a modelled neuron is the weighted sum of its input, optionally transformed by a non-linear function, and preserve the connectivity between layers of neurons to align with established anatomy. These models are then evaluated against behavioural data to assess their ability to reproduce and explain observed behavioural patterns.

Research has established that several insects, including honeybees, can represent their location in the form of a vector by continually integrating their speed and direction travelled from a point of origin, a process called path integration³⁴⁸. While the state of this vector at the foraging site is believed to form the basis of information conveyed in the dance (i.e. the vector's length and angle)^{12;99;257}, the mechanisms underpinning the execution of the dance itself and the assimilation of this vector by recipient nestmates has received far less attention. This thesis draws inspiration from the perspective that dance communication operates on a common representation that is accumulated, expressed and exchanged amongst the bees: a flight vector to the resource. This raises the intriguing possibility that a common neural mechanism could underlie both the communication and navigational aspects of the behaviour. The overarching goal of the contributions made in Chapters 3 to 5 is to explore the neural mechanisms underlying the communication, with a focus on a candidate neural circuit based on path integration and its ability to explain observed behavioural data. While each chapter focuses on a different aspect of the communication – performing the dance, recovering the signalled dance vector and navigating to the resource – we maintain an emphasis on principles of this shared neural circuit being a common underlying mechanism.

1.1 The language of the hive

Insects are estimated to have originated on Earth 480 million years ago¹²⁰ and form a dominant phylum with roughly one million species identified and an expected 5.5 million overall³⁰⁶. Despite their small size, insects display a wonderfully complex set of behaviours and have developed a wide range of adaptations to different environments. Their neural systems – often containing fewer than a million neurons²⁰⁴ – efficiently govern complex visual systems³⁰⁸; robust navigation strategies¹³²; and diverse styles of locomotion, including crawling, flying, and swimming. Fossil evidence on honeybees (genus *Apis*) is sparse but Price and Grüter²⁵⁰ conservatively estimate that dance behaviour originated at least 20 million years ago. The evolution of the dance has progressed alongside the *Apis* phylogeny, from simple sun-referenced dances on horizontal combs in species that are basal to the genus, to gravity-referenced dances on vertical combs in the darkness of enclosed nests in derived species, such as *A. mellifera*. The dance is especially beneficial when food sources differ in quality and are hard to find¹⁸ but its importance extends to swarm behaviour too. Scout bees not only identify suitable nesting sites but must recruit fellow scouts to assess their findings. This leads to a dynamic voting process where dances for less suitable sites gradually diminish, resulting in the promotion of the optimal site and the colony's subsequent relocation to it^{182;286}. How does the compact honeybee brain orchestrate this long-established and fascinating form of communication?

As a model for understanding animal communication systems, the waggle dance has generated a long and rich line of research. In 1973, Karl von Frisch¹⁰⁰ was awarded a Nobel Prize for his pioneering work in this area. To date, it remains one of the most sophisticated, known forms of invertebrate communication. However, more than seventy years after its discovery much of the underlying biology is still not yet understood. Whilst incremental research has paved the way for identifying the likely sensory inputs to the system, an understanding of how these

inputs are integrated to govern the overall behaviour remains elusive. For example, the dance exhibits powerful transformations of celestial cues to terrestrial coordinates: the direction to a resource is obtained relative to the sun during flight but is somehow translated to be relative to gravity when dancing on the vertical comb and compensates for the sun's diurnal path across the sky. Although there have been manual attempts to simulate the dance via engineering pre-programmed dance parameters into a robot (e.g. RoboBee^{171;172}), there is yet to be an implementation of a mechanism that can generate the dance based on its underlying biological principles. We address this gap in Chapter 3 by providing the first insights into such a mechanism. Similarly, despite several hypotheses, how nestmates following a dance utilise the noisy pattern of stimuli they perceive and map this to subsequent search behaviour is equally, if not more, ambiguous. Follower bees extend their antennae towards the dancer and experience repeated contact during the waggle phase, which has led researchers to hypothesise that the antennae must be important for the exchange of information^{108;262}. However, researchers had yet to provide an observationally supported account of how the dancer's movements could be sensed and processed by the follower bee to assimilate its own internal flight vector to the resource. In Chapter 4, we provide such an account and explore how stimuli received from the antennae enables followers to decode the dance and assimilate their own vector. Following this, in Chapter 5, we test our proposed model with a field experiment.

1.2 Advances in understanding the insect brain

While the honeybee dance has historically been explored through experimentation on bees alone, in this thesis, we also make use of new data emerging from other insects as an opportunity to expand our understanding of the neural underpinnings of the dance. Insects are ideal organisms for studying the neural basis of behaviour due to their small, accessible brains. Traditionally, neuroanatomical data has been collected through meticulous manual tracing of individual neurons²⁶⁸. However, recent breakthroughs in automatic tracing methods have made it possible to obtain a map of connections between neurons – a 'connectome' – of the central region²⁶⁹ and even the whole²⁷⁰ of the fruit fly brain. This surge in neuroanatomical data coupled with modern neurophysiological tools has allowed us to study the underlying neuronal circuitry of some insects in unprecedented detail. Notably, in fruit flies, calcium imaging permits researchers to examine how specific neuron populations respond to stimuli^{287;289} and optogenetic manipulation provides a way to causally link neuron activity to behaviour⁶³. In recent decades, these approaches have yielded significant insight into the central complex, a brain region that houses the circuitry responsible for the insect's compass-like navigation¹³⁹. While there are some differences in its gross morphology¹³⁷ and connectivity²⁴⁷, the central complex has been found in all insects examined to date and its core functions remain remarkably conserved. Neurobiological discoveries in one insect species may therefore be applicable to others.

The models presented in this thesis are built upon the principles introduced by new findings about the circuits within the central complex of other species. Of particular interest to the waggle dance are discoveries demonstrating that insects represent their current distance and

direction travelled (a vector) through sinusoidal activity patterns in neurons in the central complex. These were based on observations in the fruit fly *Drosophila melanogaster*^{189;190}, as well as in the sweat bee *Megalopta genalis*³⁰⁵. Biological^{189;356} and computational models³⁰⁵ of navigation have also revealed an elegant steering circuit that underlies an insect's orientation to a goal, where offset anatomical connections produce a comparison of the current heading to the goal direction. These findings have positioned the central complex as a likely neural substrate for path integration¹³⁹ and offer anatomically-grounded models of such navigational abilities. Recent studies have also characterised a pathway connecting mechanosensory input from the antennae to compass neurons in the central complex, elucidating how fruit flies can use the position of their antennae to detect the wind direction^{311;363} and how this information influences their internal compass^{56;238}. We propose how these findings might be relevant for dancing in Chapter 3 as well as obtaining the signalled dance vector in Chapter 4.

1.3 Scope

This thesis focuses on how the components of the signalled vector – distance and direction to the resource – are communicated in the dance, assimilated by follower bees and then used when attempting to navigate to the resource. In the context of performing the dance, this is based on the path of the dancer on the comb and how aspects of the wagging correlate with the distance and directional information. The waggle dance is multifaceted and in addition to the characteristic wagging, it encompasses a multitude of secondary behaviours, such as evasive manoeuvres and interruptions for trophallactic food exchange. Related scents^{254;324} and heat^{302;303} are also emitted by the dancer, as well as wind currents produced by their simultaneous wing beating whilst wagging²¹⁴. In Chapter 2, we discuss why some of these cues are more likely to be used to localise a dancer within the hive, rather than in the exchange of the dance vector. The functional significance and concept behind exchanging vector information in the dance has not always existed without controversy. In fact, it took von Frisch many years to convince colleagues that vector information was indeed decoded and used by nestmates to find the resource, over counter arguments that they could simply be following odours to the resources²²². This thesis does not imply that olfactory information is not useful in locating the resource, but rather that recruited nestmates can use the signalled vector to approximate the target location more closely than if no additional cues were available.

Follower bees also experience a myriad of stimuli during the dance and it is difficult to identify what parameters they can perceive and/or utilise. For example, several measures of duration in the dance correlate with feeder distance (e.g. duration of waggle phase or return phase only, or both), and there are undoubtedly numerous potentially perceptible features of antennal contact with the dancer too. Motivated by the recent advances in understanding the pathways of antennal positioning to the central complex in other insects, we take a targeted approach and study the angle of nestmates' antennae whilst following the dance as a key feature for assimilating the dance vector. Our results demonstrate that nestmates can use this feature alone to obtain an initial estimate of the location and we leave the integration of other possible sensory signals, which could further refine this estimate, as future work.

1.4 Contributions

1. A biologically plausible model of path integration in insects produces natural features of the dance. This suggests that performance of the dance itself could arise from a pre-existing neural circuit that underlies large-scale navigation and supports the speculation that the dance is a miniature re-enactment of the foraging flight. (Chapter 3)
2. Nestmates following the dance exhibit a novel relationship between their antennal positioning and their angle relative to the dancer. This feature could enable them to determine their angle to the dancer, and thus, the angle to food. (Chapter 4)
3. Using the position of follower bees' antennae as input, a neural circuit first proposed to underlie path integration can be adapted to decoding the dance. Using this 'assimilation circuit', follower bees can obtain their own flight vector that they can follow to the food. This allows us to infer the estimated food location after observing a single follower bee, which has never been possible before. (Chapter 4)
4. A new experiment in bees, inspired by the enforced-detour paradigm in ants, provides a test of dance recruitment and an evaluation of the presently proposed assimilation circuit. The findings suggest that both dancers and new recruits fly an appropriately centred but widely distributed direction when returning to a known food source or navigating to a new one for the first time. (Chapter 5)

1.5 Outputs

Publication

Parts of the research leading to this thesis resulted in the following peer-reviewed publication. Some passages have been quoted verbatim from the respective source.

Hadjitofi, A. and Webb, B. 2024. 'Dynamic antennal positioning allows honeybee followers to decode the dance', *Current Biology* 34(8), 1772-1779. <https://doi.org/10.1016/j.cub.2024.02.045>. (Chapter 4)

Engagement

Hadjitofi and Webb¹²² was published in a high-impact journal and garnered interest from several media outlets. This led to opportunities for public engagement and included live interviews on BBC Radio Scotland and That's TV (Channel 8), a guest appearance on the DataSkeptics podcast, and an invited article for the Scottish Beekeepers Association magazine. The research was also covered by online journalism websites, including The Transmitter, Metereod, and The Edinburgh Reporter.

Conference presentations

- ‘A hypothesised network for signalling vector information in the honeybee waggle dance,’ At the *International Congress of Neuroethology*, Lisbon, Portugal, Jul. 2022. (Chapter 3)
- ‘What is the role of the central complex in communicating vector information in the honeybee waggle dance?’ At the *Conference on Structure and Function of the Insect Central Complex*, Janelia Research Campus, VA, USA, Oct. 2022. (Chapters 3 and 4)
- ‘A mechanistic approach to assimilating vector information in the honeybee waggle dance,’ At the *International Conference on Invertebrate Vision*, Bäckaskog Slott, Sweden, Aug. 2023. (Chapter 4)
- ‘A model and a test of honeybee dance recruitment,’ At the *International Congress of Neuroethology*, Berlin, Germany, Jul. 2024. (Chapters 4 and 5)

Datasets

Hadjitofi, A. and Webb, B. 2024, ‘Honeybee antennal positioning data when following dances’, *figshare*. <https://doi.org/10.6084/m9.figshare.24715977>. (Chapter 4)

Code

- ‘Dance2Vec’: Simulation of honeybee antennae and assimilation circuit accompanying Chapter 4. <https://github.com/annahadji/dance2vec>.
- ‘BeeFlightTracer’: A tool for tracking flying bees in static cameras and reproducing results in Chapter 5. <https://github.com/annahadji/bee-flight-tracer>.
- ‘BeeBasler’: Configuration and orchestration of recording honeybees using Basler’s pypylon library. <https://github.com/annahadji/beebasler>.
- ‘BeePi’: Configuration and orchestration of recording honeybees using the Raspberry Pi camera module. <https://github.com/annahadji/beepi>.
- ‘VideoPyer’: A video player and annotation tool built using Python and Tkinter. <https://github.com/annahadji/videopyer>.

2

Background

2.1 Strategies of insect navigation

In this section, we provide a behavioural overview of the strategies that insects can use to represent a resource's location and navigate to and from it (Fig. 2.1). We discuss how the different approaches reveal path integration as a promising candidate that yields the most appropriate representation of a location for dance communication: a flight vector leading to the resource. We also elaborate on the proposal that path integration might support other modules of behaviour required within the dance too.

Visual route following

In route following, insects use a series of *snapshots* – extracted features of their visual field at a location – to retrace their outbound path when returning home from a distant goal. It has been well-documented that ants^{7,50,51,145} and bees³⁶⁴ can learn a visually guided route as a series of views that can be seen when facing along that route. To perform the route, the insect moves forward in the direction of the panorama in sight that matches a view from the series. If an insect is not too far from known areas where familiar features are abundant, this strategy allows it to stay on course. It can also be more resilient to local changes in the environment, such as a broken branch, than similar disruptions to an odour trail would be. Visually guided routes have the disadvantage that they require learning to take place at the level of the individual and it is unlikely that such a representation could be communicated with conspecifics.

Vector-based navigation

A vector is a linear path with a specific length and angle, starting from a reference, such as the nest, and ending at a destination. Many biologists, starting with Piéron²⁴⁶, have displaced

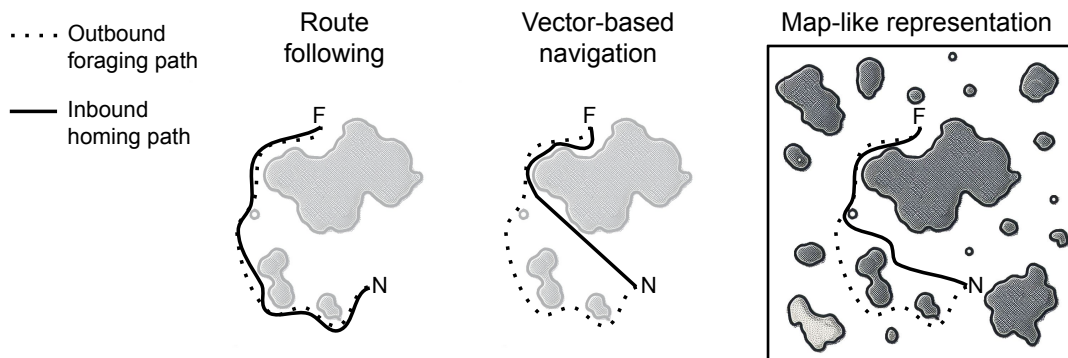


Figure 2.1. Three different though not mutually exclusive modes of navigation in insects, exemplified through their homing paths (solid black line) after discovering a feeder on a foraging trip (dotted black line). N and F represent the nest and feeder, respectively.

insects from their starting position and released them at a new one. The insect’s direction and distance of travel are often unchanged as though it were unaware of the displacement. This suggested that they could be navigating by following internal vectors. As an animal travels from a reference point, it continuously integrates its changes in direction with the distance covered through a process called ‘path integration’, which has since been firmly established in insects and other animals^{216;348}. This cumulative summing of the animal’s outward path generates an internal global ‘homeward vector’ that specifies a straight trajectory from the animal’s current position to the reference point. The homeward vector is continuously updated, even on the inbound journey, enabling the animal to steer around obstacles and continue until home. This strategy thus allows the animal to return home by the shortest possible route, and navigate between two points without having to learn the details of the route that connects them. It also explains novel shortcut routes between known feeders when insects are out foraging: addition of the current state of the homeward vector with the memory of a vector state from another food site would produce a vector directly from the current arbitrary location to the food^{55;112}. Insects encode their heading direction with respect to several celestial cues, including the sun³⁴⁴, intensity gradient⁷⁹, and the Milky Way galaxy⁵⁷, which act as stable external cues to limit accumulating angular errors during the integration. Using vectors does not exclude the use of visual snapshots, but path integration alone is useful when navigating in novel, dissimilar areas and has a relatively low error when used over shorter foraging distances.

Map-like spatial representation

Tolman³²⁶ formally proposed the concept of a cognitive map to be a system whereby relational information is used to build a representation of space, where the true geometric positions of points in space are preserved. In operational terms, using such maps should enable animals to compute and steer novel courses between familiar sites within their habitual foraging or home areas. Inspired by experimental analyses of orientation behaviours in mammals^{236;326}, Gould¹¹⁵ was one of the first to suggest that honeybees could navigate using such maps. Since then, there has been a plethora of displacement experiments that claim to provide evidence of such behaviour in bees^{42;201;206;207;340;359}. When captured and released in familiar foraging environments, bees continued along their original goal vector from the release site, seemingly

unaware that this would not lead to the intended location. However, after an initial period of this mis-orientation, it was claimed that the bees flew novel short-cuts that were biased towards the location^{206;207;340}. Several studies on both bees^{72;156;203} and ants³⁴⁵ have challenged this narrative, leading to a debate within the field^{45;43;55;346}. Opponents of the cognitive map hypothesis argue that the results of displacement experiments can be explained by simpler mechanisms. For example, not only is it difficult to ascertain that a novel short-cut is truly novel but it is also possible that familiar landmarks or *views* are being recognised from a new angle. Nonetheless, the concept has been a powerful stimulator of behavioural experimentation that continues to recent years³⁴⁰. Interestingly, *stop* signals directed from nestmates towards live dancers when they had perceived danger at the advertised site¹⁴¹ suggests an apparent ability to associate location identity to a vector, which is relevant to the claim that nestmates can project the vector perceived from a dancer into their own map³⁴⁰.

Other sensory modalities

Olfaction. Olfaction also facilitates honeybees to search for food sources and return to them. Exposure to learned odours provided inside the hive can trigger the recall of navigational memories associated with the specific learned food site²⁵⁴. Moreover, honeybees are known to mark their nest, as well as food sources, with Nasonov pheromone which might attract other bees to these goals when nearby^{88;95}. They may also mark food sources with repellents that inform conspecifics of sources that temporarily provide no food¹¹¹. Similar mechanisms also exist in ants, where odour trails can guide workers to and from resources³⁰⁴.

Magnetoreception. The earth is a huge magnet, with magnetic field lines emerging from the south magnetic pole, curving around the globe, and re-entering at the north magnetic pole. The angles between local magnetic vectors and the horizontal are known as ‘inclination’. These angles, along with the field intensity, form gradients that run from the two poles to the equator on each hemisphere²⁹⁴. Many animals³⁵⁷ can use the magnetic field lines as a directional cue to migrate long distances. Experiments from the 1990s indicate that bees possess magnetoreception^{52;159;176;177;186;272;327}. Recent experiments confirm that bees can be trained to elicit a proboscis extension in response to a magnetic stimulus¹⁷⁸, and that disturbances to the field reduce their visitation to affected flowers²¹⁸ and their ability to home⁸⁹; however, suppressing or rotating the field when dancing does not affect the success of recruiting nestmates to the feeder¹⁷⁰.

Electroreception. Honeybees, like other insects, accumulate electric charge in flight, and when their body parts are moved or rubbed together. While bees are mostly positively charged, flowers are often negatively charged²⁷. The charge of a flower can also be altered based on its pollination status³⁴³ and its visitation by bees^{47;219}. Research suggests that bumblebees³¹⁰ can detect the electric field of flowers and use it to improve speed and accuracy of learning rewarding resources⁴⁷. In honeybees¹¹⁸, electric stimuli mimicking those given off by a dancer can trigger antennal movements in conspecifics, however, the details underlying what information nestmates can extract from this signal towards locating the resource is unknown.

2.1.1 Path integration: beyond homing

The accumulation of a homeward vector via path integration offers an informative representation of a site's location: a straight-line path that can be inverted to express both distance and direction to the site from the hive. Whilst the homeward vector is discharged along the inbound route¹⁶³, foraging insects can store the state of its path integrator at a feeder and use it to later return to the location from their nest^{49;94;217}. This is referred to as a 'foodward vector', or a 'vector memory' in a more general sense. The storage of this vector has been demonstrated by several experiments in desert ants. Ants that are forced to deviate from their direct path to food turn towards the food once free to choose their direction of travel⁴⁹, as they do when performing home vectors too²⁷¹. They can also perform foodward vectors after being relocated from the feeder back to the nest, showing that, once acquired, a foodward vector can be expressed independently of the home vector¹⁶³.

Correlation of the distance and directional components of a site's foodward vector with the duration and orientation of the waggle phase, respectively, has led to a common postulation that bees utilise the information resulting from path integration when signalling a location via dancing^{12;99;193;257}. For example, bees communicate a direction pointing in a straight line to a resource even if their actual flight involved detours around obstacles, such as a building or a mountain ridge¹⁰⁰. Moreover, radar tracking of follower bees recruited to a new resource reveal that they fly a directed path that bears resemblance to the vector encoded in the waggle dance they observed²⁵⁷. Further evidence supporting the correlation of this vector with parameters of the dance is detailed in Section 2.2.

In addition to providing the basis for the vector information that is conveyed in the dance, the performance of the dance itself may arise from a path integration control system. Whilst path integration is often thought of as a homing mechanism operating on the scale of large distances²²¹, whether bees can also use it on a much smaller spatial scale to track their movement on the surface of the comb has been discussed less frequently. In Chapter 3, we examine the paths of dances that arise when using a network for path integration to control consecutive foodward and homing behaviours on a small-scale within the hive. In support of this hypothesis, there is recent behavioural evidence of path integration being involved in tight food-centred searches which occur over the scale of a few centimetres in the fruit fly^{21;34;153} and in walking bumblebees²⁴³. Although the local searches by these insects appear random, they are in fact centred on a fictive food location, suggesting that the animal is keeping track of its estimate of the location even in the absence of visual, olfactory, and pheromone cues. This centring may be similar to the return phase in bee dances, where the dancer returns to the approximate start position of the dance between waggle phases¹⁷⁴. While general similarities between bee dances and fruit fly searches for sugar were first noted by Dethier⁶⁴ in 1957, a computational model demonstrating the involvement of path integration in performing the dance has yet to be tested.

The accumulation of a foodward flight vector when foraging and its subsequent use for return trips to the feeder might also share fundamental similarities with the process of follower bees

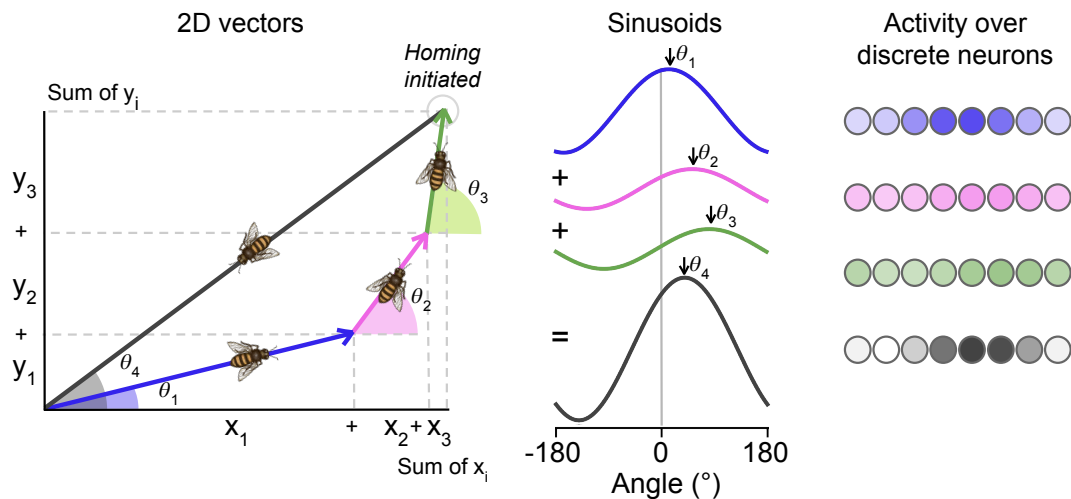


Figure 2.2. Path integration and the representation of vectors as sinusoids. **Left,** Each coloured two-dimensional vector represents a segment of the outbound journey and θ_i represents the corresponding directions of travel. Variables x_i and y_i are the Cartesian components of the segments which compute the homeward vector when summed. **Middle,** Any two-dimensional vector can be represented as a sinusoid whose amplitude represents the magnitude of the vector and whose phase represented the angle of the vector³²⁹. **Right,** These can also be discretised into spatial activity patterns over populations of discrete neurons. Adding these sinusoids point wise is equivalent to performing vector addition.

assimilating the dance vector and following it to the resource. In Chapter 4, we suggest that a follower bee assimilates the dance vector by integrating her estimates of the waggle phase angle over the course of the dance's waggle phase. This is akin to integrating the estimates of her travelling flight vector during path integration over the course of the foraging trip (Fig. 2.2). This conceptual unification proposes an intriguing possibility: the underlying neural circuitry facilitating these behaviours could be shared or overlapping. In support of this, there appears to be no dance-specific sensory projections in the brains of worker honeybees (that partake in dancing) when compared with male and queen honeybees (that do not dance), as well as even other species that lack dance communication³⁵. In recent years, research has uncovered that insects employ neural representations that are directly relevant to processing of vectors^{189;190}. This includes representing a flight vector as sinusoidal activity across a neural population, where the phase encodes the angle of the vector and the amplitude represents its length³²⁹, i.e. polar coordinates of a location in two-dimensional space. Examples of the schematic representations of vectors used in this thesis are shown in Fig. 2.2 and the specific circuitry and neurons involved in vector processing in the insect brain are later detailed in Section 2.3. By leveraging the growing knowledge of how bees perform the behaviours required for general navigation, this thesis explores the overarching theme that path integration and its underlying neural mechanisms play a role in both the encoding and decoding of dance communication in honeybees.

2.2 Honeybee communication

In this section, we provide background on the honeybee and a behavioural overview of how bees model the foodward flight vector from path integration into a dance. We also discuss the existing hypotheses for how followers decode the dance into their own foodward flight vector.

2.2.1 The honeybee colony

Taxonomy

Honeybees are classified under the genus *Apis*, which encompasses around seven to eleven extant species^{6;81;188} known for their honey production and social behaviour. Although they differ in the form of their nests (i.e. cavity versus open nests, and vertical versus horizontal combs), all use nest-based communication to share information about the location of resources^{19;74;183}. Whilst we discuss relevant findings for several species of honeybee, this work primarily focuses on the Western honeybee, *A. mellifera*, one of the most extensively studied bee species. Unless stated otherwise, the term ‘honeybee’ refers to *A. mellifera* in this thesis.

Anatomy

Honeybees belong to hymenoptera, one of the largest orders within the class of insects. Their basic anatomy exhibits three main parts: the head, thorax and abdomen²⁹⁵ (Fig. 2.3a). The head integrates two compound eyes and three ocelli, two antennae, the mouth and proboscis. The head is connected to the thorax by the vertex. The thorax contains the flight muscles and connects to two pairs of wings and six legs. The abdomen contains the stomach, intestines and sting defence apparatus (Fig. 2.3b). The Nasonov scent gland is located in a fold between the last two abdominal segments and can be exposed by flexing the tip of the abdomen¹⁹⁹.

Their antennae are divided into three main sections: the scape, pedicel and flagellum (Fig. 2.3c). The scape is attached to the head and rises from the antennal socket. Attached to the end of the scape is the pedicel, a much shorter segment that forms an elbow-like joint that allows rotation in many directions. The position of each antenna is controlled by two muscle systems: the scape is moved by four muscles within the head, and two muscles within the scape control the distal segments (pedicel and flagellum)¹⁶². The honeybee spends the majority of her life within the dark hive. In this light-deprived environment, the antennae are crucial sensory organs. They are highly mobile and lined with thousands of touch fibres and odour cavities²⁵³, making them essential for a bee’s sense of touch, smell and taste. Research has also uncovered roles of the antennae in orientation sensing too. Mechanosensory feedback from the stretch and deflection of the antennae is transduced from the Johnston’s organ¹⁴⁴ (JO) in the pedicel and is a key sensory input for insect flight^{197;265;363}. It has also been shown that *Drosophila melanogaster* can use the displacement of their antennae to encode wind direction³¹¹ as well as orient with respect to it¹⁹⁵. Moreover, although honeybees have no sense organs for the perception of sound pressure waves, if the air displacement of a sound pressure wave is large enough, bees can detect this with their JOs in the antennae^{69;155;157;331}.

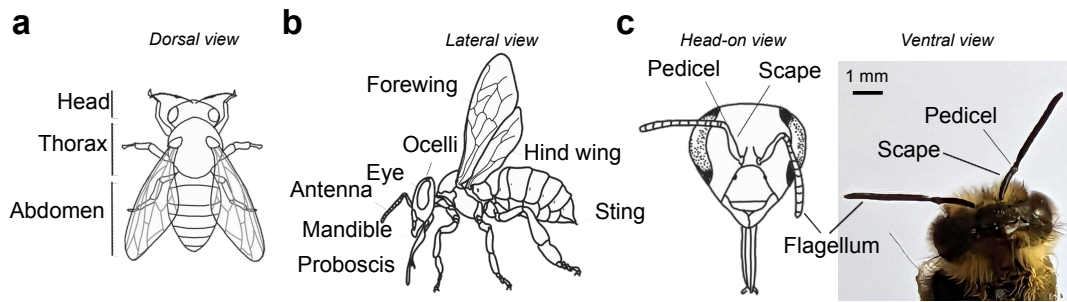


Figure 2.3. An overview of honeybee worker anatomy. Anatomy based on Snodgrass²⁹⁵. Drawings and photo by Anna Hadjitofi, Sept. 2023. **a**, Dorsal view of honeybee. **b**, Lateral view. **c**, Head-on (left) and ventral (right) view with labels for the three main segments of the antenna. The antennae are flexible and can adopt many positions. On the left, the antennae are in a more relaxed bent position, whereas in the photograph on the right they are stretched out away from the head.

When a nestmate approaches a dancing bee, they stretch out their antennae which are then touched repeatedly by the dancer as it waggles by^{108;262}. Although this physical interaction led researchers to believe that the antennae were crucial for interpreting the dance, for a long time we have not known *how* they could be involved. In Chapter 4, we study the positioning of nestmates' antennae whilst following dances within the hive and measure the angle of the antennae as the angle defined by the (1) base to tip of the flagellum relative to the bee's head direction and (2) base to pedicel, as viewed from a camera perpendicular to the comb.

Social behaviour

Honeybees live in colonies reaching tens of thousands of individuals and form eusocial societies where one fertile female, the queen, lays eggs and is inseminated by fertile males, the drones. The worker bees are sterile females that represent the vast majority of the hive and display age polytheism, meaning that they perform various tasks throughout different stages of their lives^{180;281} (Fig. 2.4). Within the colony, the workers construct combs of hexagonal cells from wax, where the queen lays eggs and workers store pollen and nectar. Dances typically take place on an area of comb near the entrance to the hive, referred to as the 'dance floor', which is often concentrated with nectar processing activities.

As with many central place foragers, bees begin foraging only after they have performed 'orientation flights', which are first performed immediately around the hive before leading to different sectors of the surrounding environment^{38;61}. These enable the bee to memorise the location of the hive in relation to its visual panorama and geographic landmarks⁶². Workers typically become dancers and dance followers after five to six weeks, when they fully transition to foragers and fly out to localise food sources. However, young nurse bees can become foragers prematurely if the colony's demographics require it²⁴². The colonies that we have studied as part of this thesis have been situated in two or three frame observation hives and contained around 5000 individuals of mixed ages. We present data from any bee that show signs of dancing or dance-following behaviour – defined respectively in Sections 2.2.2 and 2.2.3.

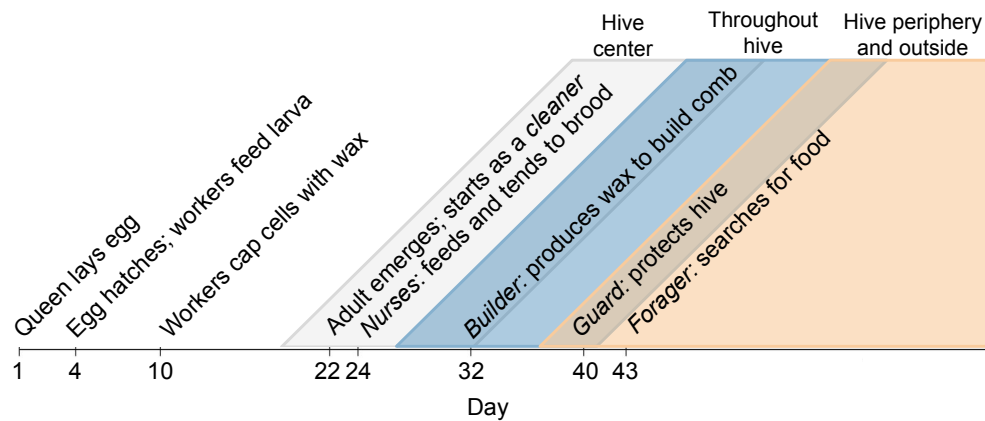


Figure 2.4. Typical stages in the life of the worker honeybee (in days) and order of tasks performed in the hive. Data generalised from Seeley²⁸¹.

2.2.2 Modelling a foraging trip as a dance

How does a dancer move?

Upon returning from a successful foraging trip (e.g. finding nectar, pollen, resin, water or a new nest site), a honeybee will enter the hive and perform the dance in the dark on the vertical comb. The dance is a repeating series of circuits composed of waggle and return phases. During the waggle phase, she throws her abdomen from side to side in a pendulum-like motion at a frequency of about 15-25 Hz, and emits airborne pulses of vibrations at 30 pulses per second, with each pulse lasting around 20 ms^{208;213}. The dancer holds tight to the comb whilst gradually moving forward, without ceasing to waggle. The waggle phase is followed by a return phase, in which the dancer circles back to the approximate starting point of the previous waggle phase. These returns typically alternate clockwise and counter-clockwise for consecutive dance circuits, giving the dance its characteristic figure-eight shape. The duration of the waggle phase and its orientation relative to gravity are believed to respectively encode a measure of distance and the angle to the resource relative to the sun^{98;100}; effectively conveying a flight vector to the resource. As discussed in Section 2.1.1, these signalled components are likely derived from the foodward vector obtained from path integration.

Given the flat plane of the comb, many, if not all, studies analyse the movement of dancers and nestmates from their two-dimensional Cartesian coordinates on the comb. Von Frisch mostly analysed dances in real time, using a stopwatch to measure duration and a protractor to measure orientation. However, a dance circuit can last for only a few seconds and many details cannot be captured by an unaided human eye. Precise views of the dance were made possible with high-speed video recordings which could be watched back frame by frame. For example, Tautz et al.³²¹ discovered that during waggling, the bee takes small, uncoordinated steps when their bodies can no longer extend and each leg clings to the rim of a cell on the comb for as long as possible. It is now common to use manual or automated methods to track dancing and following behaviour from video recordings obtained from a camera positioned perpendicular to the comb, an approach that we also follow in this thesis.

Direction: celestial cues to geocentric coordinates

How do foraging bees determine the direction of a resource?

One of the primary directional cues used by central place foraging insects is the sky (or ‘celestial compass’). Insects combine their detection of the sun’s position and a correction for its movement during the day to establish a consistent geocentric (Earth-based) estimate of their heading with respect to absolute North. This compensation for the sun’s daily movement enables them to signal a constant foraging direction in Earth-based coordinates to nestmates, as well as return to the resource at different times of day. For example, a returning forager can orient itself such that the sun, represented by the point of maximal brightness in the sky⁹⁸, is in the same relative position in its visual field as it was in the previous outbound flight to the known location. Light propagates as a wave in which the electric and magnetic fields are oriented orthogonally to the direction of propagation¹⁹⁸. In unpolarised light oscillation directions are uniformly distributed, but in linearly polarised light the fields oscillate in specific, orthogonal axes (Fig. 2.5a). As sunlight passes through the atmosphere, it creates a distinct pattern of polarisation across the sky, with the degree and orientation of polarisation differing relative to the sun’s position (Fig. 2.5b). This pattern is invisible to us but is visible to many other animals, including bees²⁶³. It provides a wide-field celestial cue which is more reliable than a single light source such that bees can use this pattern to derive compass information from a patch of blue sky when the sun is obstructed. With the source of celestial cues originating so far away, they have the benefit that their orientation only changes when animals perform rotational motion but not translational (Fig. 2.5c).

Integrating ground velocity information

How do foraging bees determine the foodward vector to the resource?

To accumulate an accurate foodward vector through path integration, a bee needs to integrate its ‘ground velocity’ during the outbound journey to the food (i.e. the speed and direction travelled relative to the ground). This can be challenging in flying insects, as they can be travelling in a direction that is not consistent with their heading direction, termed ‘holonomic motion’, for example, due to displacement by wind. In the 1990s, experiments manipulating the visual features encountered by bees revealed the role of translational optic flow in estimating ground velocity^{85;86;300;301}. When an animal moves in a particular direction, the images on the retina slip backwards from a single point of expansion, away from the direction of movement. Translational optic flow refers to the rate at which the images moves across the retina when navigating (Fig. 2.6). One compelling experiment involved raising a feeder via a tethered balloon^{85;86}. Despite flying further and expending more energy, dancers signalled shorter distances to nestmates as the balloon ascended, due to reduced optic flow from the ground. Further studies using tunnels to constrain the flight paths of foragers supported this principle: bees trained to forage from resources in tunnels with patterned walls, that increase the perceived optic flow, searched for the food at greater distances when tested in a narrower reward-free tunnel and at shorter distances when tested in a wider tunnel³⁰¹. When deprived of image motion, bees searched uniformly, unable to gauge distance. Positioning equidistant resources

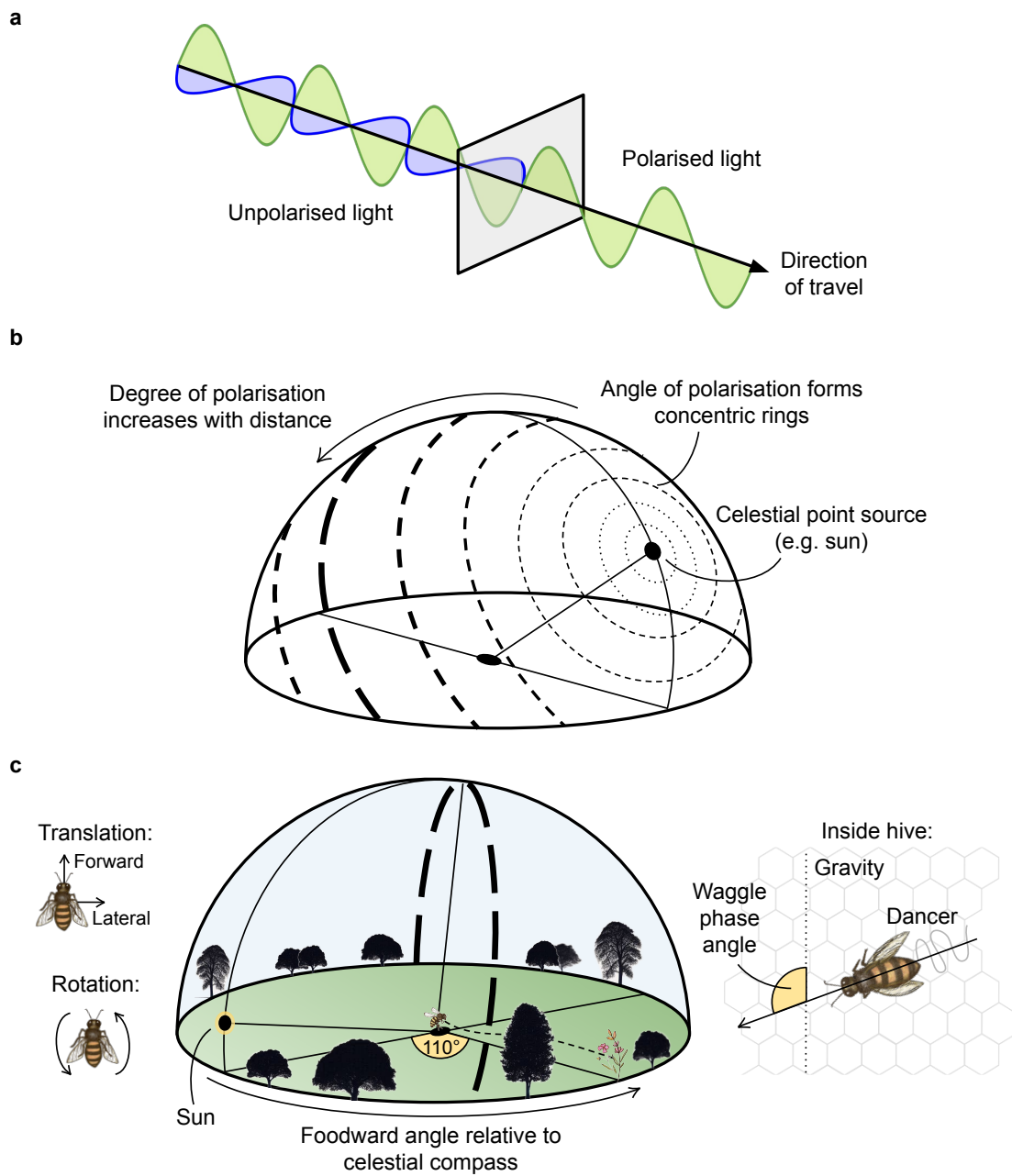


Figure 2.5. Conceptual illustration of polarised skylight and the signalling of direction in the dance. **a**, Unpolarised light oscillates in all axes on a plane perpendicular to the direction of travel (only two shown for clarity), whereas polarised light oscillates in one axis. **b**, An illustration of the polarisation pattern over the natural sky. Unpolarised sunlight is polarised by atmospheric scattering, with the direction (or ‘E-vector’, dashed lines) and degree (line thickness) of polarisation differing relative to the sun’s position. Light is most strongly polarised in an equatorial ring corresponding to viewing directions perpendicular to the sun’s direction. **c**, Using this celestial compass and a correction for time compensation, a foraging honeybee can establish the direction to the resource and signal this to nestmates via the orientation of their waggle phase relative to gravity on the comb. Left depicts rotational (clockwise and counter-clockwise) and translational (forward and backward) movement. Only the ring of maximal polarisation is shown for brevity.

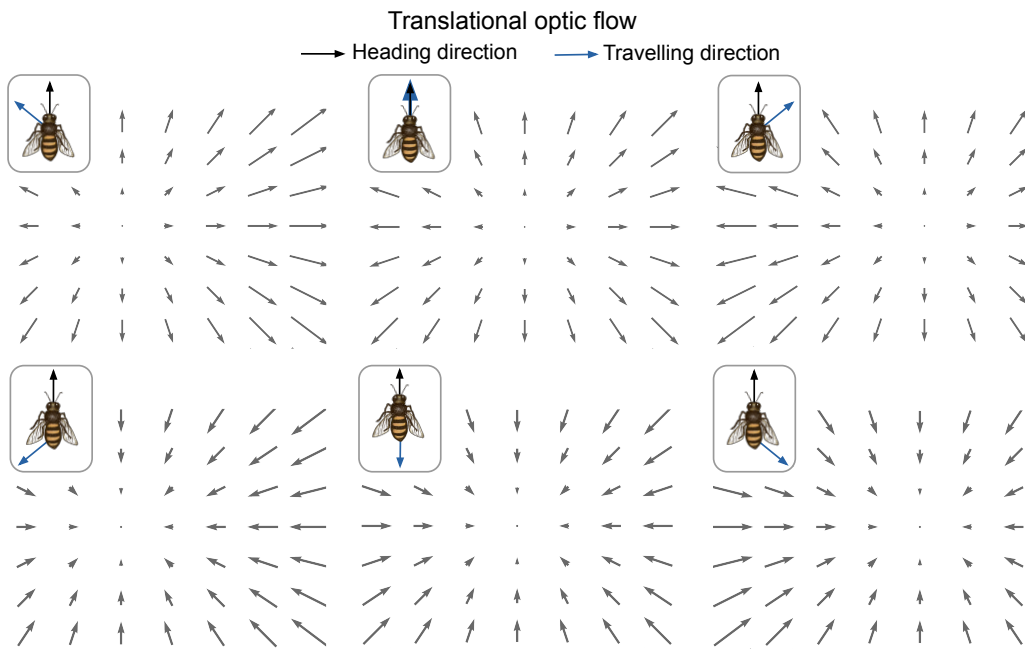


Figure 2.6. Translational optic flow (grey arrows) experienced by a bee moving through its environment. The heading direction (black) may not align with the travelling direction (blue), due to displacement by wind or side-slipping when walking, for example.

in diverse environments (e.g. amidst water or a forest) also confirmed that the optical flow cues play a dominant role in distance measurement, rather than flight time alone^{13;323}.

This optic flow provides information in an egocentric (body-centred) frame of reference, meaning that the bee perceives this movement relative to its own body. However, when combined with the compass described above, bees can transform this velocity information from an egocentric to a geocentric frame of reference, also known as an allocentric frame of reference¹⁹⁰. This enables them to accumulate their true travelled vector relative to the world. In Section 2.3, we detail a recently uncovered neural circuit in the insect central complex that performs this transformation. Using optic flow to estimate ground velocity has the advantage that the same flow will be generated whether a bee's movement is produced actively by wing beats or through transport by the wind. Moreover, although it is unlikely that foragers and recruits would fly an identical route to a resource, bees use optic flow to maintain constant ground speeds and heights^{9;248;301}, which may minimise variance in their perceived optic flow.

In the early 2000s, patterned tunnels manipulating the perception of optic flow became a standard tool to create *virtual* flight paths for bees and study how they encode spatial information^{8;9;14;58;87;160;193;202;248;249;290;293;298}. Although various configurations that differ in shape, dimensions and patterning have been tested, the tunnels have a transparent roof or mesh so that the bees can still estimate their direction using celestial cues (the sky). Manipulating bees into perceiving that they have flown a much farther distance (i.e. several hundred metres) than they have (i.e. six metres) can make behavioural experiments more practical. In Chapter 5, we design and conduct a detour experiment that utilises patterned tunnels to study the accuracy of location estimation and sharing by foragers as well as newly recruited bees.

Signalling the foodward vector

How do dancers signal the direction to the resource?

The signalling of direction is perhaps one of the most well-defined parameters of the dance. Open-nesting honeybee species in Asia, such as *A. florea*, have exposed nests where the comb is typically built around a tree branch. *A. florea* perform their dances with a view of the sky on the horizontal section of the nest, where the direction of the waggle phase correlates directly to the resource relative to the current position of the sun¹⁸³. In contrast, the Western species *A. mellifera* dance on vertical combs within a dark nest cavity^{98;100}. Inside the nest on a vertical surface, gravity serves as reference: the angle between the sun and resource as seen from the nest is reproduced on the vertical comb and serves as a signal of direction to the resource (Fig. 2.5c). Researchers estimate the direction of a waggle phase by either measuring the dancer's mean body orientation across the waggle phase or the angle of the path that the dancer describes in the waggle phase. The latter is often taken as the angle of the straight line connecting the bee's position in first and last frames of visible wagging. In lower frame rate video recordings (e.g. 30 frames per second (fps)), the wagging is accompanied by blurring of the dancer's wings or abdomen. Von Frisch¹⁰⁰ reported that *A. mellifera* could change reference cues and alternate between performing gravity- and sun-oriented waggle phases if a mirror was used to reflect the sun from the bottom of the otherwise dark hive. However, dances with a visual reference appear to be more precise than those with a gravity reference³¹⁶, resulting in the difference between the angles of consecutive waggle phases being around 20° smaller on average.

While the Earth rotates at a steady rate relative to the sun, the perceived movement of the sun through the sky also varies depending on the observer's geographical latitude and the time of year⁷⁶. The angle of the sun from North is referred to as the sun's azimuth. Bees compensate for these temporal variations and signal the direction to the resource relative to the sun's current position^{75;184;255}, even when the original foraging trip took place in overcast conditions⁷¹ and even if the forager dances over several hours while remaining inside the nest with no view of the sun, as in *marathon* waggle dances described by Lindauer¹⁸¹. Underlying this ability appears to be the combination of an internal biological clock and an influence by the external diurnal events. Over 60 years ago, Renner²⁵⁵ famously transported bees that were trained to forage at particular times in Paris to New York on an evening red-eye flight. Interestingly, bees displayed jet lag-like behaviour, foraging at the original Paris-time when under constant lighting conditions but slowly updated to local time when exposed to natural surroundings in a field over three days.

How do dancers signal the distance to the resource?

By gradually moving feeders further from the nest, von Frisch¹⁰⁰ claimed that dancers perform round dances for nearby resources (less than 50 m) and the waggle pattern for resources further afield. He characterised round dancing as the forager making “swift, tripping steps” to run in a circle before suddenly reversing the direction of travel and circling around again, before repeating (p. 29). He also noted that how far bees would run around the circle before reversing, as well as the total number of reversals, could vary greatly. Round dancing was the first piece

of evidence that von Frisch considered a symbolic signal of distance – *near* versus *far*. Few studies since have further characterised the structure of the path in round dances and they are often loosely identified based on von Frisch’s description. However, in 1988, Kirchner et al.¹⁵⁸ reported that round dances appeared to contain extremely brief waggle phases. Since these observations, the duration of the waggle phase has generally been established as the most informative encoding of distance to the resource, with longer durations signalling further distances (see also von Frisch¹⁰⁰, pp. 98-106).

There are actually many duration-related correlations in the dance and over time, it has been considered that follower bees might measure the duration of the entire dance circuit, waggle phase only (either from the wagging or sound pulses), the length of the waggle on the comb, the divergence of dance directions³⁴⁹ or count either the number of waggles or sound pulses. In fact, some of these measures of have been used almost interchangeably in the past. Why there is more than one correlation with distance in the dance is an interesting and unanswered question. Von Frisch’s standard measure for how distances were encoded was ‘tempo’, which he recorded as the number of dance circuits per 15 seconds, and this was often used by earlier studies as a proxy of the distance signal. Recent evidence has indicated that the circuit duration obscures differences in dialects between honeybee species that the waggle or return phase alone otherwise reveal¹⁶⁷ and that return phases are noticeably shorter for feeders with a higher concentration of sugar³⁶⁹. This means that comparisons between earlier and recent work within the field may not always be reliable.

Identifying how honeybees map their distance flown to a duration of some dance parameter has also been challenging. Firstly, there seems to be no universal calibration for how flight distance translates into dance duration, with different species³⁰⁷, subspecies¹⁶⁷, and even individual bees²⁷⁹ possessing variations in their feeder distance-duration calibration. Even within *A. mellifera*, studies report conflicting linear^{167;276;278;279;351} or non-linear^{97;337} relationships between feeder distance and duration. Differences in published curves across studies are rarely, if ever, obtained for the same spatial route. Given that bees gauge distance flown via optic flow, it is possible that some of the differences are the result of flying through dissimilar environments. Furthermore, inconsistent training distances across studies (ranging from 0.4 km to 11 km) and the use of different dance components (duration of the waggle, return or circuit) as metrics may have added to the uncertainty. A review by Kohl and Rutschmann¹⁶⁵ revealed a suspicious association between the maximum training distance used: a non linear component was only detected when using training distances further than 1 km. Thus, studies relying on linear calibration functions established over shorter training distances would have routinely underestimated foraging distances that were being signalled by longer waggle durations. We use the distance-duration calibration slope estimated by Kohl and Rutschmann¹⁶⁵ when mapping a feeder distance to waggle duration in the simulation experiments in Chapter 3.

Do dancers signal the outbound or inbound journey?

The distance to a resource could in principle be represented by the outbound or inbound flight paths, or even both. Many have reported that the distance is primarily gauged on the way to a food source^{13;87;100;133;193;293;299}. Von Frisch¹⁰⁰’s classical experiment where bees were led

around a mountain ridge to a resource, showed that whilst bees signalled the airline shortcut direction from the hive, they still signalled the outbound flown distance even though they had flew over the ridge on their way back to the hive. However, there is evidence that bees monitor the distance travelled on the inbound route too^{33;78;24;300}. For example, Edrich⁷⁸ claimed that dancers that have never experienced the outbound flight path, as a result of being displaced to an unfamiliar location 5 km away, are still capable of performing highly accurate dances. However, bees could take up to 50 minutes to return home and his depiction of a dance performed immediately after the bee arrives home (see Fig. 3 in Edrich⁷⁸) displays various oddities that seem to improve after the bee had been allowed to visit the resource again. Brines³³ also reported that waggle dances can be evoked when a forager only experiences a return trip. He displaced foragers whilst feeding near the nest to a new final feeder location. He noted the importance of a forager being at the final location before finishing feeding, after which she then performed orientation flights, or else she would not return. But what, if any, is the advantage of learning the distance on the journey to a resource, rather than on the route back? After all, a naïve forager often flies a tortuous path before finding a food source. This is an unanswered question but signalling the outbound distance would at least set a safer upper bound on the distance a recruit should expect to fly to find the resource.

Bees might also store multiple versions of the distance information: a personal one and a communal one⁵⁹. This was discovered by depriving the bee of celestial cues along segments of an outbound foraging trip. The personal version (the subsequent trip of the bee) ignored the distance travelled without the celestial compass, whereas the communal version (shared by dancing) included these segments. Thus, there could be independent systems controlling the information available for personal navigation versus dancing, or that given a context, it is possible to extract the relevant data from a unified representation.

Misdirection and angular divergence in the dance

Depending on resource quality, the number of dance circuits performed can vary between 1 and 100 in a single bout of dancing²⁸⁴ and previous work has reported that successful recruits had followed on average 8¹⁴⁶, 17¹²¹, 15^{315;361} or 20-23 waggle phases²⁰⁷. Although it is not always emphasised in literature, many dance paths exhibit a degree of distortion or noise which can lead to a variation in the angle of food signalled: the waggle dance is by no means a perfectly precise behaviour. There is also the caveat that it is impossible for experimenters to truly state the actual direction being signalled in dances via external observation; such parameters can only be estimated. Nonetheless, estimates of the direction appear to show that consecutive waggle phases in dances exhibit a degree of directional scatter that decreases with increasing feeder distance^{16;102;103;330}; a phenomenon termed ‘angular divergence’. This has been claimed to result in a bimodal distribution of leftward and rightward deviations about the intended direction (up to $\pm 40^\circ$) with some overlap³¹⁶. Moreover, when *A. mellifera* dance horizontally on their vertical comb, where gravity is not aligned with the waggle phase orientation, they exhibit greater angular variation than dances performed close to vertical^{54;274}. From dances signalling natural resources across several days, Okada et al.²³⁵ identified that the angle of waggle phases varied from phase to phase most commonly within the range of $\pm 15^\circ$ from

the mean. Thus, there are potentially many values of angles to the resource that are signalled within a dance. In Chapter 5, we further examine the angular scatter in dances in relation to their performance in an experiment measuring their accuracy at returning to a feeder.

It is regarded within the community that follower bees reduce the effect of this noise by averaging several waggle phases to estimate the intended direction^{53;97}. Evidence suggests that only four consecutive waggle phases are needed to sufficiently estimate the variation across the entire dance and offer a good representation of the mean obtained if decoding all waggle phases in the dance⁵³. Moreover, Tanner and Visscher³¹⁵ show that the distribution of recruits arriving in traps that are set out in a $\pm 45^\circ$ array either side of the feeder is best fit by the prediction of a waggle phase-averaging model, rather than last- or single- waggle phase models.

2.2.3 Characterising following behaviour

How do interested nestmates respond and react to a dance?

For a human observer, nestmates following the dance appear as a single bee or group of bees that extend their antennae in order to make contact with the dancer as she passes by, especially during the waggle phase¹⁰⁸. Although cavity nesting species dance in complete darkness, comparative studies suggest that open nesting species similarly rely on tactile antennal contact to communicate, despite having visual input¹⁰⁶. Nestmates can also be seen moving along with the dancer (including on the return phase and for several dance circuits) and are most typically found side-on or behind the dancer but can be positioned in front too^{30;152}. After following the dancer for one or more dance circuits, she may then leave the hive to search for the resource.

Historically, diverse criteria have been used to identify follower bees for inclusion in subsequent analyses. Many of these require the active movement of the nestmate alongside the dancer throughout circuits and exclude those who engage with the dancer via their antennae but do not actively follow the dancer around the comb^{30;70;99;106;108;320}. However, dances do not necessarily solicit immediate action from recruits and there is ultimately no way of proving that such nestmates are not decoding the dance information. Reviewed by Biesmeijer and de Vries²², there are three main contexts in which a nestmate may be following a dance:

- A novice forager can find her first food source either by following a waggle dance and obtaining her own flight vector to the resource (being a recruit), or by searching independently without following dances (being a scout)^{180;280}.
- An experienced forager whose foraging has been interrupted, for example by nightfall or a rainstorm, can resume her foraging either by following dances (being a reactivated forager) or by examining the source on her own (being an inspector)^{23;107}.
- An experienced forager that is already engaged in foraging may need to find a new food source when her old one fades, and can do so either by following a dance (being a recruit) or searching independently (being a scout).

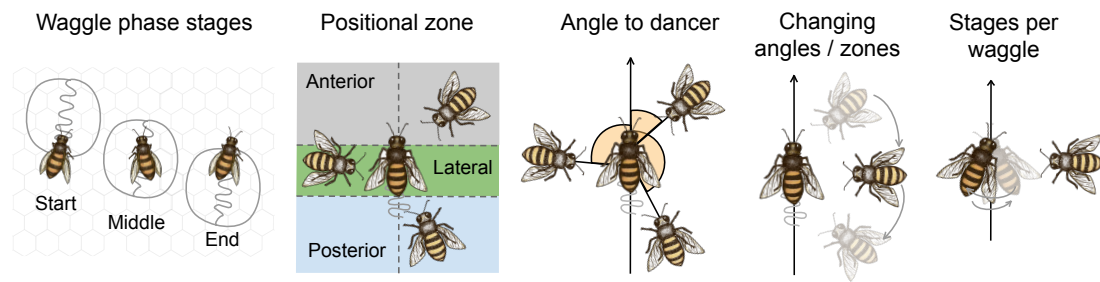


Figure 2.7. Domain of categories within which features of following behaviour are studied. The dance vector is signalled over the course of a waggle phase. During this, followers may have little choice over which positional zone they occupy and may experience a number of relative angles, which may change over time. The dancer oscillations may affect the follower’s ability to maintain contact.

It is also possible that there are bees occupying the vicinity for other reasons, such as waiting to unload nectar from the dancer²⁸³. Whether there are differences in the characteristics of following behaviour in these contexts is not yet known; we only see that some bees actively pursue the dancer around the comb and some do not³⁰, but almost all show conspicuous interest with their antennae. In Chapter 4, we take an inclusive view that following behaviour can be identified based on whether or not a nestmate is extending out her antennae towards the dancer. Such nestmates may occupy any position facing towards the dancer, exhibiting varying or consistent angles during following, as well as show interest for a portion of the waggle phase, an entire circuit, or multiple circuits. In support of this definition, nestmates that display these behaviours have been found to act as successful recruits. For example, Kietzman and Visscher¹⁵² observed that nestmates can be successfully recruited to the feeder irrespective of the position they followed from and even if they only followed one waggle phase. The natural next question is, how do these followers decode the dance?

Stimuli available for follower bees

How do followers bees decode the dance?

Follower bees are required to detect the dancer’s orientation relative to gravity and duration of the waggle phase and translate this into a flight vector with a direction relative to the sun⁹⁸ and distance from the hive^{87;301}. Over the years, it has emerged that there are seemingly many stimuli that follower bees are exposed to during the performance of the dance. Here, we propose separating these stimuli into three categories: (1) stimuli that assist in detecting, localising and broadly orienting towards a dance in the comb (Table 2.1), (2) stimuli that have been proposed in the past to aid nestmates in assimilating the signalled dance vector (discussed below) and (3) stimuli that are available outside of the hive and may help to find the resource alongside the assimilated vector (Table 2.2). Since our work focuses on how nestmates assimilate the vector information, we detail the stimuli in group (2) in the context of past and present hypotheses discussed below. Fig. 2.7 shows the categories within which researchers have typically studied these stimuli and other features of following behaviour to understand their role in information processing.

The airflow hypothesis

The oscillation of the dancer's wings^{297;367;368} and abdomen whilst wagging create oscillatory airflows as well as a narrow jet airflow²¹⁴ around the dancer. Generated at the tip of the wings and moving backwards, the jet is fan shaped and broader in the dorsoventral direction than in the lateral directions. In contrast to the oscillatory airflows, where the masses of air are flowing to and from, the air flows in only one direction in the jet, i.e. away from the dancer. It has been hypothesised that this jet could be used to inform follower bees of the signalled foodward direction. This line of inquiry, led by Axel Michelsen over approximately 15 years, has not been revisited recently but a historical overview of this research is provided by Michelsen^{209;210}. Based on measurements with small hot-wire anemometers, Michelsen²⁰⁸ proposed that antennae positioned behind the dancer and within the angle of wagging (e.g. $\pm 30^\circ$) would be capable of detecting a well-defined maximum airflow whenever the dancer's abdomen pointed in their direction. Comparing the timing of the signals reaching the two slightly spaced antennae could inform the follower which side of the axis of the waggle phase it was on. While it remains unclear whether bees possess the neural circuitry to process temporal information of a jet of air hitting either antennae, their ability to compare odour concentration gradients between their two antennae has been well-documented^{26;194;313}. If so, they postulated that followers might use the temporal pattern of the airflow they perceive to try to reach a position behind the dancer. The resulting parallel alignment was theorised to be the simplest way for a follower to approximate the waggle phase angle (and thus, foodward angle), as it would be equal to the her own orientation relative to gravity.

The groups' insights were mostly obtained from measuring the air currents emitted from a mechanical model bee that could *dance* and had metal wings which were vibrated by an electromagnetic driver^{211;212}. They later discovered that the generation of these jets by real dancing bees could be much more variable and dancers could seemingly switch them on and off by adjusting their wings. The velocity of these jets could also sometimes be equal to the background level of airflows in the hive. Thus, while the jet airflow could inform a follower that she is positioned behind the dancer, it is likely that followers must have access to other cues too. Furthermore, Kietzman and Visscher¹⁵² observed that successfully recruited nestmates occupied various positions around the dancer, even those without direct exposure to the jet (e.g. from the side and front).

The tactile hypothesis

Given the apparent motivation of follower bees to extend their antennae towards the dancer and receive contact, touch has also been a point of focus during the search for reliable channels of communication. The tactile hypothesis refers to the idea that follower bees can infer the waggle phase angle through passive antennal contact with the dancer's body^{30;108;262}. This requires that a follower must know her own orientation relative to both gravity and the dancer to determine the foodward angle in her own frame of reference. This hypothesis removes any constraints on where the followers can obtain the information from and is supported by observations that followers keep their antennae outstretched and stable during the waggle

phase; as this may minimise altering the perceived signal according to their own movements. However, it has previously been unclear how she transduces her angle to the dancer from the contact or deflections of her antennae. This is because the questions of whether and to what extent the wagging movements of a dancer are tactilely transmitted to the followers have rarely been studied.

There are only two pieces of existing work within this domain. The earliest is by Rohrseitz and Tautz²⁶², who measured the angle of followers' body orientations and whether their antennae were in contact with the dancer at the midpoint of each swing of the dancer's abdomen (e.g. see far right of Fig. 2.7). They proposed that followers could be guided to the favourable position at the rear end of the dancer by a decreasing value of a feature they termed 'coincidence': the duration of simultaneous contact with the dancer and both of their antennae. Gil and Marco¹⁰⁸ additionally measured the deflections of the antennae by the angle between the follower's antennae scapes at the end of each wagging movement. The magnitude of the followers' antennal deflections increased when they faced the dancers from the side, and the variability of such deflections diminished when they faced the dancers from behind; however, there was no consistent relationship within a single feature of the deflections that made it possible to decode *any* angle to the dancer. Both studies selected specific time points at which to measure features of antennal contact, however, our hypothesis proposes that follower bees *continually* integrate their estimates of the dancer's orientation during the waggle phase (Section 2.1.1). In Chapter 4, we revisit the tactile hypothesis and examine the followers' antennal positioning at a higher resolution across multiple points of the dancer's abdominal swings (and not just the midpoints or change points).

Stopwatch-like activity in bees

In their study, Gil and Marco¹⁰⁸ also found that the higher the number of wagging movements, the higher the number of antennal deflections and contacts that the followers experienced. They suggested that this could offer a potential mechanism for decoding the distance of the resource. However, von Frisch¹⁰⁰ estimated that the error from using the number of waggles as a correlation of feeder distance was 29% greater than using the duration of the waggle phase (pp. 101–102). The value of a signal is also dependent on the precision with which it can be received. Although it has been claimed that bees may be able to count the number of landmarks (up to five) passed on the way to a resource⁴⁵, whether bees could count and grasp sharp differences in much greater numbers of wagging movements is not confirmed.

Since then, research has also studied how nestmates might use the airborne vibratory signals available from a dance to infer the distance. Recall from Section 2.2.2 that the wagging dancer emits airborne pulsed vibrations at around 30 pulses per second, with each pulse being around 20 ms^{208;213}. A series of experiments led by Hiroyuki Ai^{23;35} found that simulating these waggle vibrations on the honeybee's antenna at the Johnston's organ affected a local interneuron in the brain (DL-Int-1). This interneuron normally fires spontaneously, but the train of vibration pulse stimuli caused it to stop and become hyperpolarised (less excitable). Upon the offset of the pulse train, the interneuron showed increased activity (post-inhibitory

rebound). Another interneuron, DL-Int-2, a presumed postsynaptic neuron of DL-Int-1, showed increased continuous spiking activity under the pulse stimuli. The authors suggest this inhibitory network resembles the functions of a stopwatch, potentially playing a role in decoding the duration of the waggle phase pulsing. In Chapter 4, we suggest that this activity could be used by followers to gate their accumulation of the dance vector in memory. This hypothesis proposes that the accumulation can be constrained to particular contexts – namely, from the onset of stimuli present in the waggle phase (pulses of vibrations) to its offset, when the vector is then stored. Ai et al.³ also characterised a third neuron (bilateral DL dSEG-LP) whose activity appeared to be phase locked to the vibration pulses even if the temporal pattern of stimuli was changed. If honeybees use the number of pulses to encode distance (as opposed to the total duration of pulsing), then this neuron may be a potential candidate for processing this information.

Contexts in honeybee recruitment studies

In several of the studies examining the experience of follower bees in the hive, it is unknown whether or not these followers would actually be recruited to the feeder or indeed, the extent to which they would be able to find it. Studies of honeybee recruitment thus fall into three main categories: those that study the following behaviour within the hive^{29;30;106;108;161;262}, those that study the subsequent foraging success after being recruited^{87;99;119;143;170;211;257;285;322;340}, or finally, those that correlate the followers' in-hive experience with their subsequent success^{84;121;146;152;315;318}. This latter approach makes it possible to compare predictions of a follower's recovered dance vector against the actual flight vector that she expressed (or flew), but is often limited by the effort and challenges associated with tracking individual bees throughout their foraging flights. Across the studies within this category, the experiences of followers that have been measured include the amount of time spent following the dancer, the number of waggle phases followed, their position and angle relative to the dancer as well as the time spent in antennation (the time spent touching each other with their antennae). While the number of waggle phases followed by a nestmate has consistently been proven to be a reliable predictor of a nestmate being more likely to find the food, to this day, there is limited evidence that the other factors exert the same influence. Although an earlier study by Judd¹⁴⁶ in 1994 asserted that followers had to experience a position behind the dancer to be successful at finding the feeder, more recent work has since relaxed this constraint^{152;318}. Thus, the mechanism that follower bees use to decode the dance appears to be flexible with respect to the stimuli that researchers have measured so far.

It is also worth noting that different approaches have been used to determine the success of recruits at different levels of detail. These methods range from simple binary measures, indicating whether or not the recruits arrive at the original feeder, to more detailed aspects of their success, such as the distribution of recruits caught in feeder traps that are arranged around the original location of the food. Finally, a few research groups have been able to utilise tracking systems, such as harmonic radar, to monitor the entire search flight of recruits^{207;257;340}. In Chapters 4 and 5 we discuss the results of some of these studies in the context of understanding how accurate recruits are at estimating the location of the signalled food.

Table 2.1. Stimuli available for detecting and localising dancers in the hive.

	Description	Notes
Temperature	Bees exhibit a higher temperature of their thorax when dancing ^{302;303} .	Foraging honeybees are highly endothermic and need to warm up the thoracic muscles for flight ²⁶⁶ . Whether this warming of the dancer effects the rate of recruitment is unknown but it is possible that thermal activity is a distinguishing feature of a dancer and helps prepare follower bees for flight.
Olfactory & chemical cues	A mixture of hydrocarbons is released by dancers and leads to an increase in foraging and significantly more bees exiting the hive ^{109;324} .	Thom et al. ³²⁴ suggest that the pheromone acts as an attractant, luring unemployed foragers to the dance floor. A more recent study by Balbuena et al. ¹⁰ suggests that incoming foragers might already release these signals on entering the hive. Thus, they might at least serve as a motivational cue that stimulates foraging activity.
Electric fields	Electric fields emitted by dancing bees induce passive antennal movements in stationary bees ¹¹⁸ .	The electric fields emanating from the surface charge of bees are very likely to be relevant stimuli for identifying a dancer. It is also an intriguing possibility that such fields may correlate with the duration of the waggle phase (and thus, distance to resource) or that a follower might somehow extract their angle to the dancer using them, however, these hypotheses are yet to be tested.
Vibrations transmitted via the comb	<p>Dancers produce two types of vibration during the waggle phase:</p> <ul style="list-style-type: none"> • A low frequency (15-25 Hz) vibration from side-to-side abdominal movements²¹⁴. • A high frequency (250-300 Hz) vibration from vibrating her wings for short pulses of 20 ms²⁹⁷. <p>Whilst dancing, they firmly grip the rims of the cell walls of the comb which aids the propagation of these vibrations to the comb itself^{232;320}.</p>	Sensed by the subgenual organ on the legs, these vibrations on the comb appear to attract followers to dances ²⁶⁷ . However, dancers often perform within close proximity which could cause frequent interference. Thus, although correlating with the waggle phase duration, many believe it is unlikely that these signals are strong enough to be reliably decoded as a precise distance (or directional) cue to the resource ²⁰⁸ . Michelsen et al. ²¹² also suggests that information transfer is possible from a mechanical dancer that imitates both vibrations but does not touch the comb.

Table 2.2. Stimuli available outside of the hive for locating the final resource, that can be used in addition to following the dance vector.

	Description	Notes
Floral scents	Recruits are attracted to the scents and odours from the food carried in by foragers ⁹⁶ .	When a successful forager returns with nectar, she brings back the food scent in the crop itself or clinging on her body. Recruits are able to use these floral scents as guiding cues for search flights, especially when scented feeders are upwind ^{96:355} .
Nasonov pheromone	Honeybees can expose glands to mark food sources with Nasonov pheromone ^{88:95;350} .	Scent marking can also explain why unaccompanied new recruits, prefer the same entrance used by trained bees, even if it is harder to access ⁹² . In the 1940s, von Frisch dismissed the idea that bees solely rely on the pheromone to find the resource with an experiment that covered the Nasonov glands with shellac (glue) to prevent them from releasing odours while foraging and reported that the recruits' abilities to locate the foods were undiminished (described in Gould ¹¹⁴). Similarly, although Griffin et al. ¹¹⁹ found that the pheromone was important for helping recruits to find a signalled resource 5 m from the hive, this bias reduced for feeders that were 10 to 20 m away and disappeared for feeders at 30 m.
'Buzzing' flights and the presence of bees	The presence of bees at a feeder can attract recruits searching for the feeder ³²² .	Tautz and Sandeman ³²² reported the importance of 'buzzing' flights by foragers around a feeder that were necessary for encouraging recruits to land on the feeder. These flights reportedly looped around and across the feeder, maintaining a distance of about one metre and lasting up to 15 seconds with a characteristic loud buzzing.
Electrostatic fields	The difference between the electrostatic charge of bees and floral sources.	See Section 2.1.
The presence of experimenters	It is plausible that in open field experiments, bees that are accustomed to human interaction during training may utilise humans as visual cues or indicators of food being nearby.	The arrival of bees, both trained and recruited, to a feeder is often recorded by experimenters waiting at the feeding site. I have personally observed that in doing so, bees could gradually associate my presence with a sugar reward. For example, even upon entering the field containing their hive, some bees would actively approach and fly around me in a non aggressive manner, even before the introduction of feeders. A few individuals appeared to learn that even landing on me would likely lead to them being then placed directly on a feeder.

2.3 The insect central complex

The central complex has been found in every insect examined to date and is widely believed to be the navigational centre of the insect brain^{137;245;333}. It is therefore relevant to the accumulation of a flight vector when foraging as well as oriented behaviours within the hive, such as dancing. It is a highly organised region of the brain that unites inputs from the left and right in four primary neuropils that span the midline: the protocerebral bridge (PB), the ellipsoid body (EB), the fan-shaped body (FB), and the paired noduli (NO) (Fig. 2.8). Columnar neurons recurrently connect the individual neuropils to each other, while tangential neurons provide a large number of inputs from, and a smaller number of outputs to, the rest of the brain^{93;131;339}. It is worth noting that there are differences in nomenclature between neuropil and neuron names in fruit flies and other insects, with the EB and FB often respectively referred to as the lower division of the central body (CBL) and upper division of the central body (CBU) in other insects (see Table 2.3 for the full list relevant to this work). The computations carried out by this complex, yet ordered entanglement of neurons are a burgeoning area of research. In this section, we focus on the functional role which is of immediate interest to the honeybee dance: the representation of flight vectors in the brain.

2.3.1 Vectors in the insect brain

Ground velocity

As discussed in Section 2.2.2, behavioural experiments have established that honeybees can use the perceived translational optic flow to estimate their ground velocity. In 2017, Stone et al.³⁰⁵ were the first to characterise optic flow-sensitive neurons in the sweat bee, referred to as TN cells. TN cells selectively provide input to the NO of the central complex. There are four TN cells, split into two types, with each type existing in both the left and right hemispheres. TN₂ neurons respond to horizontal motion $\pm 45^\circ$ from the front of the insect and TN₁ respond to $\pm 45^\circ$ from the back. Each cell fires proportionally to the component of velocity in its preferred direction, thereby collectively tracking the ground velocity in four cardinal directions around the insect. Similar neurons have also been identified in the fruit fly (LNO cells)^{189;190} and additionally respond when flies move laterally or side-slip when walking (shown in the Extended Data Fig. 4j-q of Lyu et al.¹⁹⁰).

Heading direction

Calcium imaging of columnar neurons connecting the EB and PB (EPG neurons) in the fruit fly has revealed that head direction is represented by a distinct peak or *bump* of activity across the EPGs, that uses both external and self-motion cues to rotate through the population in a manner consistent with the insect's rotation within its environment^{110;289}. This has been confirmed for restrained flies walking on an air-supported ball²⁸⁹ as well as tethered flies flying in a virtual reality arena¹⁵⁴. Similar to proposed models of head direction cell functioning in mammals¹⁶⁴, the EB acts as a ring attractor, with its dynamics characterised by local excitation

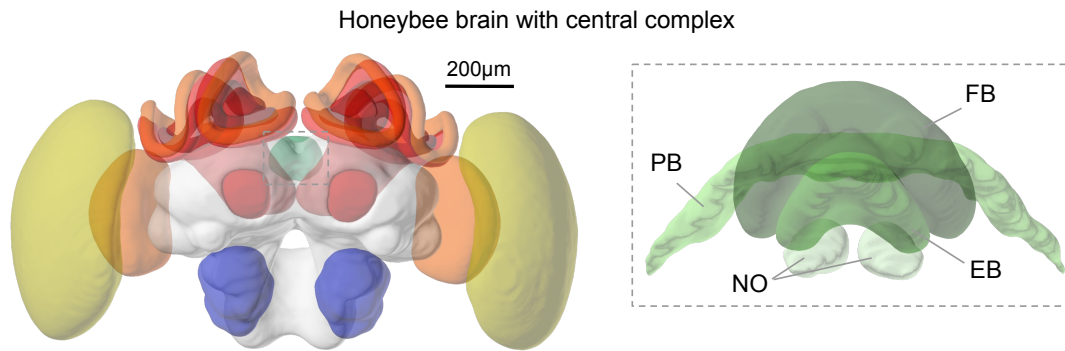


Figure 2.8. Frontal view of a three-dimensional reconstruction of the honeybee *A. mellifera* brain. Different neuropils shown as coloured volumes, with the central complex neuropils in green (obtained from the insect brain database¹²⁸, www.insectbraindb.org; data from Brandt et al.³²).

that reinforces activity at the bump location, and long-range inhibition that suppresses activity in neurons with different direction tuning³³². Information about external cues is thought to reach the EPGs via populations of directionally tuned neurons known as ring neurons, which exist as different groups that respond separately to visual cues²⁸⁸, polarised light¹²⁶, and airflow²³⁸. Thus, the network can use multiple sensory modalities to form an accurate representation of the head direction. The tracking of head direction is most accurate in the presence of external cues; although the EB directional bump can exist and persist in the absence of external cues too^{117;333}. These updates are believed to be idiothetic but it is not yet known whether they are driven by proprioception or motor efference⁹¹. In vertical cavity-nesting species, honeybees orient their dances with respect to gravity in the hive. In this work, we hypothesise that gravity exists as another external cue that can similarly evoke and update a directional bump in the EB. Some insects sense gravity via their antennae^{148;197}, whilst in bees it appears likely that they use the hairs on their neck and between their thorax and abdomen^{35;187}. Manipulations of the mechanosensory neck hairs, including gluing the head rigidly to the thorax, disrupt geotactic behaviour and leads to disoriented dancing¹⁸⁷. The pathway of gravity-induced mechanosensory input to the central complex and a resulting neurophysiological response is yet to be tested experimentally.

Travel direction

The EPG neurons send axonal outputs to the glomeruli that form the PB, which inherits copies of the bump³⁶⁰. Another population of neurons, known as $\Delta 7$ neurons, are interposed between EPGs and many cells that are downstream of the PB. These are believed to help shape the EPG heading signal into a sinusoid within the downstream populations¹³⁹. Crucially, this sinusoidal representation – where the phase correlates with the heading angle – enables the circuit to implement vector computations. An exciting recent discovery in the fruit fly has in fact supported this concept^{189;190}, where the translational optic flow signals from the NO are multiplied with the heading signals from the compass system. The flow signals modulate the relative amplitudes of four sinusoids that exist in four PFN cell populations (for the left and right, and both forward and backward movement), which convey the bump from the EB to the

Table 2.3. Corresponding names in *Drosophila melanogaster* and other insects.

	<i>Drosophila</i>	Other insects
Central complex neuropils	PB	PB
	FB	CBU
	EB	CBL
	NO	NO
Tangential neurons	LNO	TN
	ER	TL
	Δ_7	TBI
Columnar neurons	EPG	CL _I
	PFN	CPU ₄
	PFL	CPU _I
FB interneurons	h Δ	Pontines

PB and are otherwise yoked to the insect's head direction¹⁹⁰. Downstream, the connectivity pattern of these neurons onto h Δ B neurons in the FB supports a vector sum computation that pools together the insect's estimate of its egocentric (body-centred) translational direction with its estimate of allocentric (world-centred) heading direction, to accurately predict its allocentric travel direction. This offers an elegant solution to the problem of how insects can still track their direction of travel when it differs to the direction they are facing. It has been proposed that the integration of this vector, or its components³⁰⁵, over time should enable insects to form a working memory of their path travelled through the environment. A recent study⁵⁶ has also identified a population of PFNs that encode wind direction that is sensed via displacement of antennae in the fruit fly, and display peak sensitivity at $\pm 45^\circ$ similar to the optic flow input above. In a following study¹⁹⁵, the authors proposed that similar modulation of the head direction bump could allow for an allocentric estimate of wind direction. In Chapter 4, we propose that a nestmate following a dance can use the position of their antennae to similarly (and with the same circuitry) convert its egocentric orientation to the dancer to an allocentric estimate of the dancer's direction which signals the food.

Steering

Over 60 years ago, Mittelstaedt²¹⁵ suggested that animals control their path through the environment by measuring the discrepancy between their current heading angle and a desired goal angle. Since then, Webb and colleagues have proposed neural network implementations of this idea in insects^{113;124;217;305}. Constrained by anatomy in the sweat bee, *Megalopta genalis*, Stone et al.³⁰⁵ proposed a model for path integration and steering, where a layer of CPU_I neurons effectively compares inputs from a layer of TBI neurons – carrying the current head direction bump – and a layer of CPU₄ neurons (homologs of PFNs) – carrying a desired goal direction from memory – to generate a steering command encoded across its population. CPU_I cells converge in a premotor control region, called the lateral accessory

lobe^{80;129;130;179}, and work in the moth has shown that this region is involved in generating steering commands²²⁴. The proposed CPU₄ layer is composed of two accumulators, one for movement on each of the left and right sides, where each memory cell of either accumulator encodes the total travel along one of eight cardinal compass directions encoded by the TB_i cells. Each accumulator is updated depending on the excitatory activity of the TN optic flow-based cells encoding movement on one side of the body, modulated by the inhibitory activity of the TB_i heading layer. The CPU₄ cells thereby accumulate the speed travelled in the direction opposite to the current heading and charge a home vector as the insect moves away from a reference point. A shift in connectivity between TB_i-CPU₄-CPU_i cells helps establish the strength of a rightward or leftward turning signal: the excitatory CPU₄ layer output is modulated by the inhibitory TB_i layer output 45° to the left, or right, respectively. The insect turns if the signals from one side are greater than those from the other. The CPU₄ accumulators continue to be updated while following the home vector back to the nest. Once there is no imbalance in the accumulators, it indicates that the nest has been reached and an emergent search pattern ensues. Similar neuroanatomical motifs have been observed in the desert locust¹³¹ and monarch butterfly¹²⁹. Recent functional studies have also confirmed this steering circuit in the fruit fly³⁵⁶, where PFL3 neurons (potential homologs of CPU_is) are anatomically positioned to receive right-left shifted copies of the current head direction and generate a steering command by comparing these to inputs from the FB^{139;252;356}.

Vector memory and return trips

How foodward (or goal) vectors are encoded in memory is unknown, but it is reasonable to suggest that they are stored separately in the same format as the information encoded by the integrator. A computational model mimicking this encoding successfully replicates many features of these vectors and navigational strategies utilising them²¹⁷. Moël et al.²¹⁷ extended the path integration network by Stone et al.³⁰⁵ to introduce memory synapses that store the CPU₄ accumulator states at salient locations. When wanting to revisit the location, the vector memory is reactivated and used to inhibit the current state of the CPU₄ integrator cells, resulting in a steering signal in the direction of the location (a foodward route) (Fig. 2.9). If starting at the nest, with the integrator containing a zero home vector, this negative inhibitory influence means that the bee will act as though its current location is exactly opposite to where the feeder is located. Consequently, the steering circuit, aiming for *home*, will guide the bee from its actual location (the nest) toward the food. Since the path integration continues to run in parallel and reflects the bee's actual displacement, lifting this inhibition of the CPU₄ cells at any time results in the bee returning to a homeward route. In Chapter 3, we explore how this model could be used for performing the waggle dance.

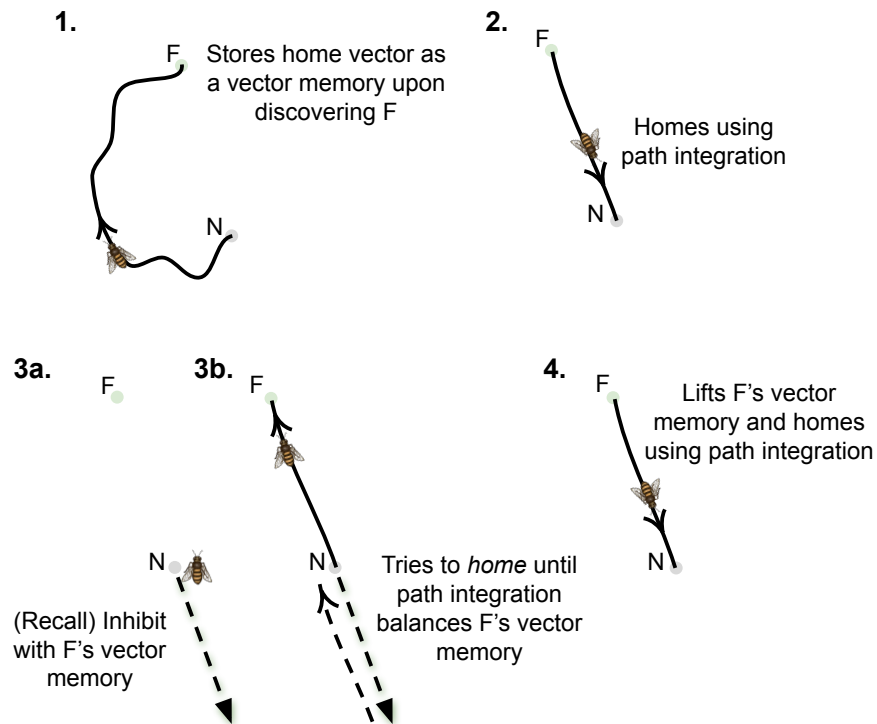


Figure 2.9. Example of the vector memory extension to a path integration circuit. 1, During a random foraging route, a bee discovers a feeder (F, green) and stores the current state of its home vector as a vector memory. 2, It then uses its home vector to return to the nest (N, grey). 3a, Whilst at the nest, the bee recalls the feeder's vector memory. This inhibits the current state of its path integrator to reflect a *virtual* (imaginary) position which is opposite to the feeder's actual position. 3b, As the bee now tries to *home* from this virtual position, it will result in steering signals towards the feeder's real position. 4, Lifting the feeder's vector memory recall at any time allows it to return to the nest.

3

Path integration in dancing

Despite extensive research on many aspects of the honeybee waggle dance, the control mechanisms governing its execution within the hive remain poorly understood. Esch⁸³ once highlighted that waggle dances were seemingly similar to re-enactments of the foraging trip on a small scale, i.e. a dancer orients in a direction correlating with the direction towards the food and travels or *waggles* along it for a duration correlating with its distance. However, despite his observation and the established role of path integration in controlling path direction when foraging and returning to a feeder (see Section 2.1), its involvement in performing the dance has remained largely unexplored. Path integration is often referred to as a homing mechanism that operates on the scale of large distances, enabling insects to efficiently travel home after tortuous foraging routes many kilometres in length²²¹. However, there is growing evidence that it also exists on a small scale. When foraging ants arrive back near the nest but cannot immediately find it, they initiate a local centred search on the scale of a few metres³⁵⁸. Fruit flies also use path integration to perform tight food-centred searches that cover only a few centimetres^{215;153;325}, which is comparable to the spatial scale that a honeybee's dance circuit can be performed over¹⁷⁴.

In this chapter, we explore the idea that path integration could be involved in performing the waggle dance and highlight that this concept is supported by the general structure of the dance as well as its evolutionary origins. We use a computational approach to propose how a path integration control system can be used to perform the dance, in addition to its established use in long range behaviours, such as homing and returning to a feeder. We show that a network modelled on the insect central complex³⁰⁵ can account for several features of the dance, including classic waggle and return phases, as well as measures of angular divergence. To the network, we add the oscillations of the abdomen and assume a hypothetical vector memory proposed by Moël et al.²¹⁷. We also add physical restrictions to the angular velocity of the dancer's path when waggling informed by our new analysis of natural dances.

3.1 The origins of dance behaviour

Honeybees exist within the Apidae family, which also encompasses bumblebees, stingless bees and orchid bees⁴⁰. A comparison of these social bee species offers an interesting perspective on how dance behaviour might have arisen. Kajobe and Echazarreta¹⁴⁷ reported that stingless bees, *Meliponula ferruginea* and *M. nebulata*, partake in piloting flights. This is arguably the most basic form of location sharing, where experienced foragers exit the hive in distinct foraging bouts and directly lead recruits to the food source, without relying on communication within the nest. Whilst foragers also returned in bouts carrying the same resource, the number of individuals in a return bout could be less than in an exiting bout, suggesting that recruits may not follow the whole distance. Similarly, when returning to the feeder, *M. panamica* foragers perform an initial section of zig-zagging that persists up to 50 m from the nest and points towards the resource. These flights are followed by recruits until they are able to complete the journey on their own⁸². Both examples suggest that these forms of location sharing behaviour exist as piloting-like flights of foragers following their own path integration vector to return to the feeder. The synchronisation of foraging trips has also been reported in honeybees when the food source is unscented³²². Some species of stingless bee deposit odour droplets every few metres extending from the resource all the way to the nest^{138;150;151;185} or a shorter portion of it (30 m)²²⁹. In each of these contexts, recruited nestmates can conveniently acquire the foodward vector directly via their own path integration system when guided along the route. However, scent trails risk inadvertently leading competition to the same food source and obstacles, such as dense foliage, risk an inexperienced recruit losing track of the leader guiding the trip²²⁷.

Research has shown that many bee species also exhibit excitatory movements or pulsed vibrations *within* the hive that attract and incite nestmates to search for food^{68;82;226;228;230}. For example, bumblebees do not participate in guiding but rather display ‘food alerting’ behaviour, where they perform extended excitatory runs around the nest upon successfully finding food⁶⁸. Moreover, a variety of vibrations are produced by different species of stingless bees⁸², with even the length of pulsed vibrations depending on the feeder distance in some species^{82;231}. Esch⁸² proposed that behaviours guiding nestmates to food sources, such as the zig-zag flights, could be precursors to the waggle dance, with the addition of distance information conveyed through sound pulses (Fig. 3.1). This supports the hypothesis that the waggle dance gradually evolved as a refinement of simpler communicative foraging systems, all utilising the same orientation system based on vector navigation, rather than emerging as a distinct and separate adaptation. This is further reflected within the *Apis* phylogeny itself. Dances of open-nesting honeybee species which are basal to the genus point directly towards the resource and most closely resemble a small-scale foraging flight to *guide* nestmates to the resource. The intermediate stages that led to communicating on such a small-scale, and even relative to gravity in cavity nesting species, are still poorly understood²⁵⁰, but the existence of similarities in communicative behaviour across species supports the idea that an evolutionary conserved pathway - namely, one capable of path integration - underlies such behaviours.

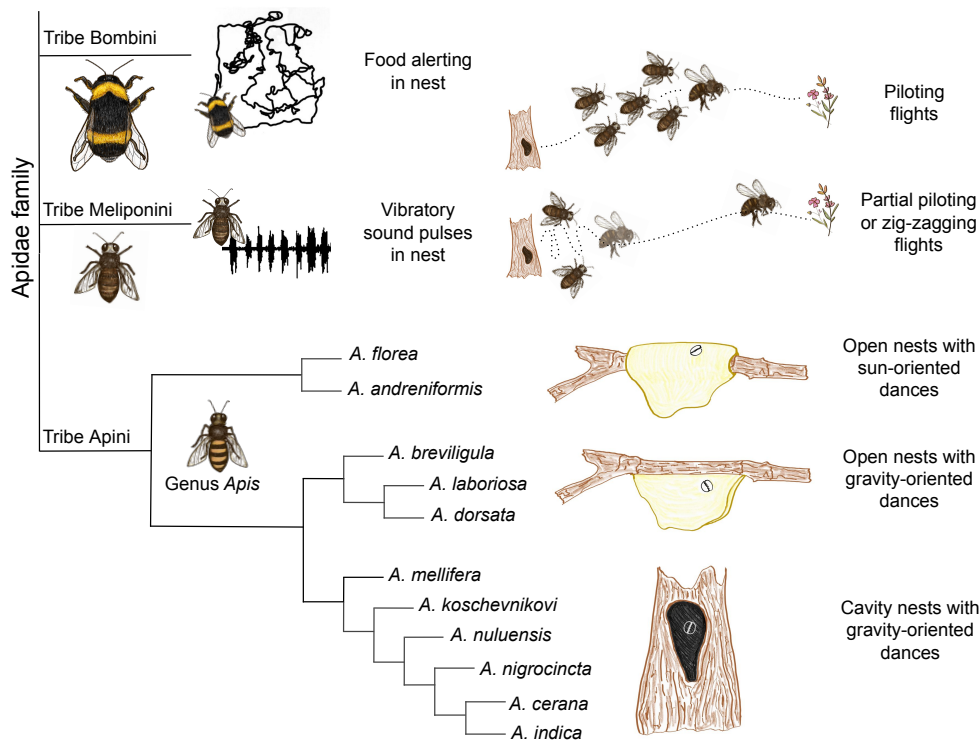


Figure 3.1. Overview of recruitment systems within the Apidae family. Tribes Bombini (bumblebees), Meliponini (stingless bees) and Apini (honeybees) shown. Phylogeny adapted from Barron and Plath¹²; Lo et al.¹⁸⁸. Bumblebee food alerting trace in nest adapted from Fig. 2.1.1 in Dornhaus⁶⁷. Vibration sound pulse waveforms in stingless bees adapted from Fig. 9 in Nieh and Roubik²³¹. All other drawings by Anna Hadjitofi.

3.2 Directional dance error: constraints and control

We were interested in examining whether natural dance paths display features that are further indicative of a path integration control system. Towards this, we obtained and analysed datasets for two honeybee species, *A. florea* and *A. mellifera*, collected by Timothy Schaefer's¹⁹² group and Tim Landgraf's¹⁷⁴ group, respectively. This allowed us to compare dances with difference reference points (i.e. the sun or gravity) and substrates (i.e. on top of other bees or on the comb). As discussed in Section 2.2, waggle phases are often performed with a degree of angular scatter. Towne and Gould³³⁰ tested the resulting scatter at several feeder distances and observed a four-fold decrease when signalling a food source at 700 m compared to 100 m. This decreasing scatter with increasing feeder distance prompted many questions as to whether bees were strategically tuning the scatter to distribute recruits over a constant patch size^{125;330}; or whether bees were physically incapable of dancing with great precision for nearby sources. In the 2000s, researchers hypothesised that if bees were strategic, then they must dance more accurately when signalling a new nest site, where the goal is typically much smaller. After 15 years of experimentation^{16;17;278;314;317;328;349}, a final cross-species review by Beekman et al.¹⁹ concluded that bees are simply physically constrained when performing short waggle durations, irrespective of signalling a nesting or feeding site. In this section, we analyse the directional properties of waggle dances to investigate these apparent constraints.

Angular scatter and motivational state

We first tested whether the angular scatter measured in dances could arise from accumulating errors over consecutive waggle phases. Does the dancer begin her dance aligned with the feeder direction but gradually loses her way over time? Interestingly, there is no trend towards increasing angular scatter over consecutive waggle phases in either species (Fig. 3.2a,c), suggesting that any scatter is not due to accumulating errors from performing more waggle phases. The angular divergence was calculated as the mean absolute angular difference between consecutive waggle phases (the signed angular differences are shown in Fig. A.1). Fig. 3.2d visualises the cumulative fraction of dances with various differences between the angle of the first waggle phase and the mean divergence across the rest of the dance. It is interesting that not even the majority of first waggle phases are performed with the greatest precision, as one might expect that the bees correctly align themselves with the foodward angle before any dancing or wagging behaviour occurs. This may indicate that bees dance within a motivational context in which the reward itself activates the dance movements and leaves little time to correct their orientation to the foodward angle prior to wagging. An early commentary by Dethier⁶⁴ supports the idea of *sudden* excitatory behaviour of insects in response to a sugar reward. He observed the gyrations of hungry fruit flies in response to a sugar drop, whose intensity and duration of increased turning behaviour positively correlated with the sugar concentration. This was interpreted as an excitatory search for the food. Shakeel and Brockmann²⁹¹ observed that honeybees also initiate a similar search and that when prevented from walking, the probability of initiating the excited searching (or dancing) decreased with time after sugar ingestion. Furthermore, De Marco et al.⁶⁰ reported that a higher sugar concentration can lead to an even bigger increase in the directional scatter of waggle phases at the beginning of the dance. It is thus plausible that the first waggle phase lacks precision due to a heightened motivational state triggered by the resource itself, rather than an error in the original vector. We explore a possible explanation as to why the remaining waggle phases might also be imprecise in the up-coming sections.

Timothy Schaerf's group¹⁹² also recorded whether a dancer was carrying pollen in the 'pollen baskets' located on their hind legs. The angular scatter within a dance appears to be irrespective of this (Fig. 3.2b, $P = 0.26$), suggesting that the additional weight or presence of pollen on the legs does not influence the precision of the dance differently to nectar.

Adjusting the waggle phase trajectory

The idea that the dance is initiated before the dancer can precisely orient to the feeder is also consistent with the activation of a vector memory to return to the feeder, i.e. it is the activation of the memory that drives the orientation towards the food in the first place (see Section 2.3). A path integration control system would also predict that once activated, the bee should continually attempt to adjust the angle of the general waggle path to the foodward angle, instead of wagging forward with a fixed *off* angle. Research has not yet quantified the potential curvature of waggle phase trajectories and commonly measures the direction of a waggle phase using the straight line connecting the thorax at the start and end of the wagging^{19;54}. To follow this up, we investigated whether the angle of the dancer at the start

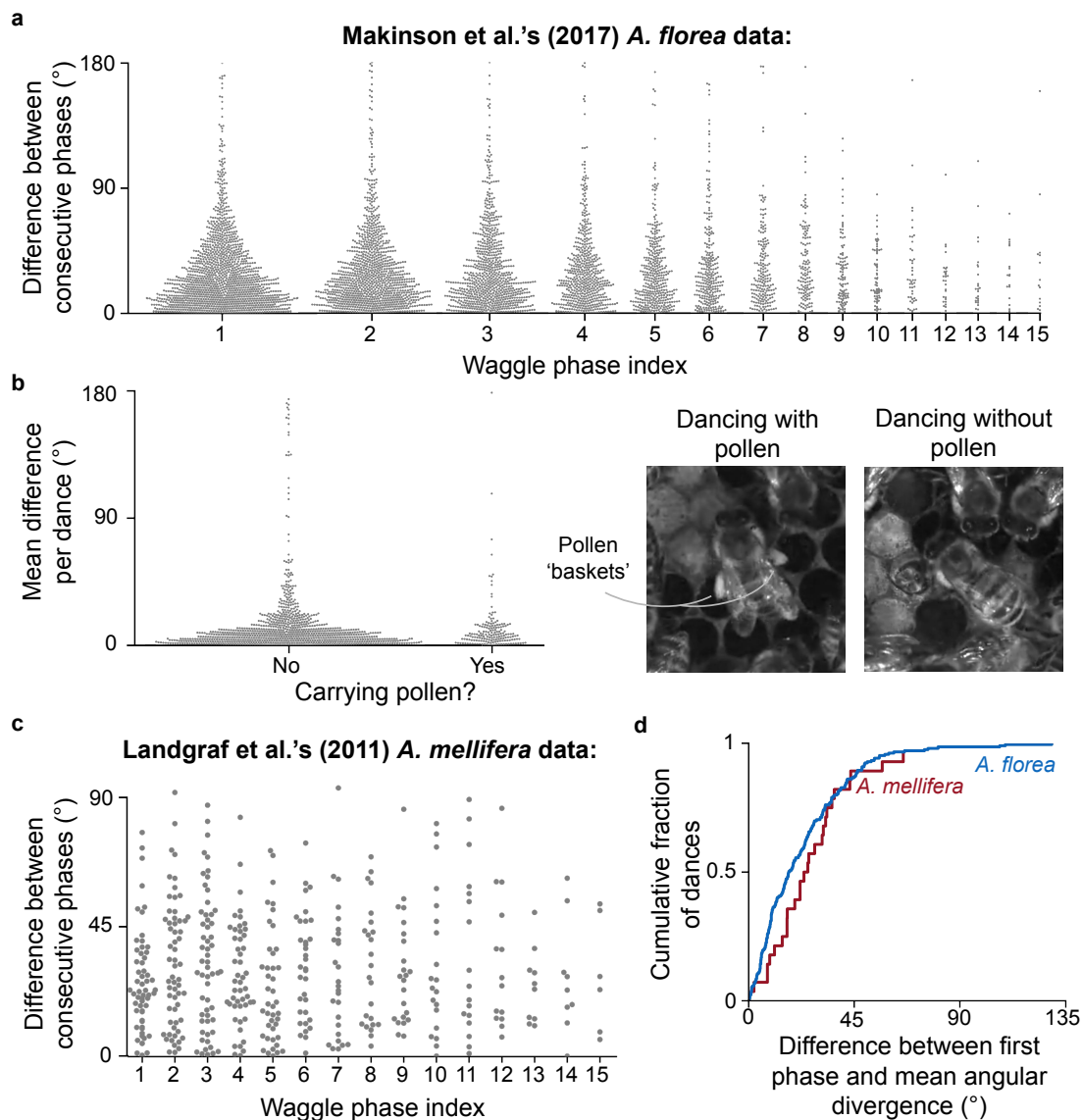


Figure 3.2. Angular divergence across consecutive waggle phases. Absolute difference in the angles between consecutive waggle phases in **a-b**, *A. florea*, computed from dances ($n = 1333$) collected by Makinson et al.¹⁹² and in **c**, *A. mellifera*, computed from dances ($n = 63$) collected by Landgraf et al.¹⁷⁴. Makinson et al.¹⁹² calculated the angle of a waggle phase as the angle of the line connecting the bee's thorax at the beginning and end of a waggle phase relative to gravity (manually annotated). Signalled resources were unknown but **b**, whether the bee was carrying pollen was recorded ($H = 1.25$, $P = 0.26$). Photos taken by Anna Hadjitofi Jun. 2023. Landgraf et al.¹⁷⁴ used an automated method¹⁷³ to track the dances of foragers trained to a feeder 230 m away. **d**, Cumulative distributions of the absolute difference between the first waggle phase relative to the absolute mean differences in the angles between consecutive phases in dances containing at least six circuits. Both data sources were analysed and used with permission. See also Figs. 3.10 and A.1.

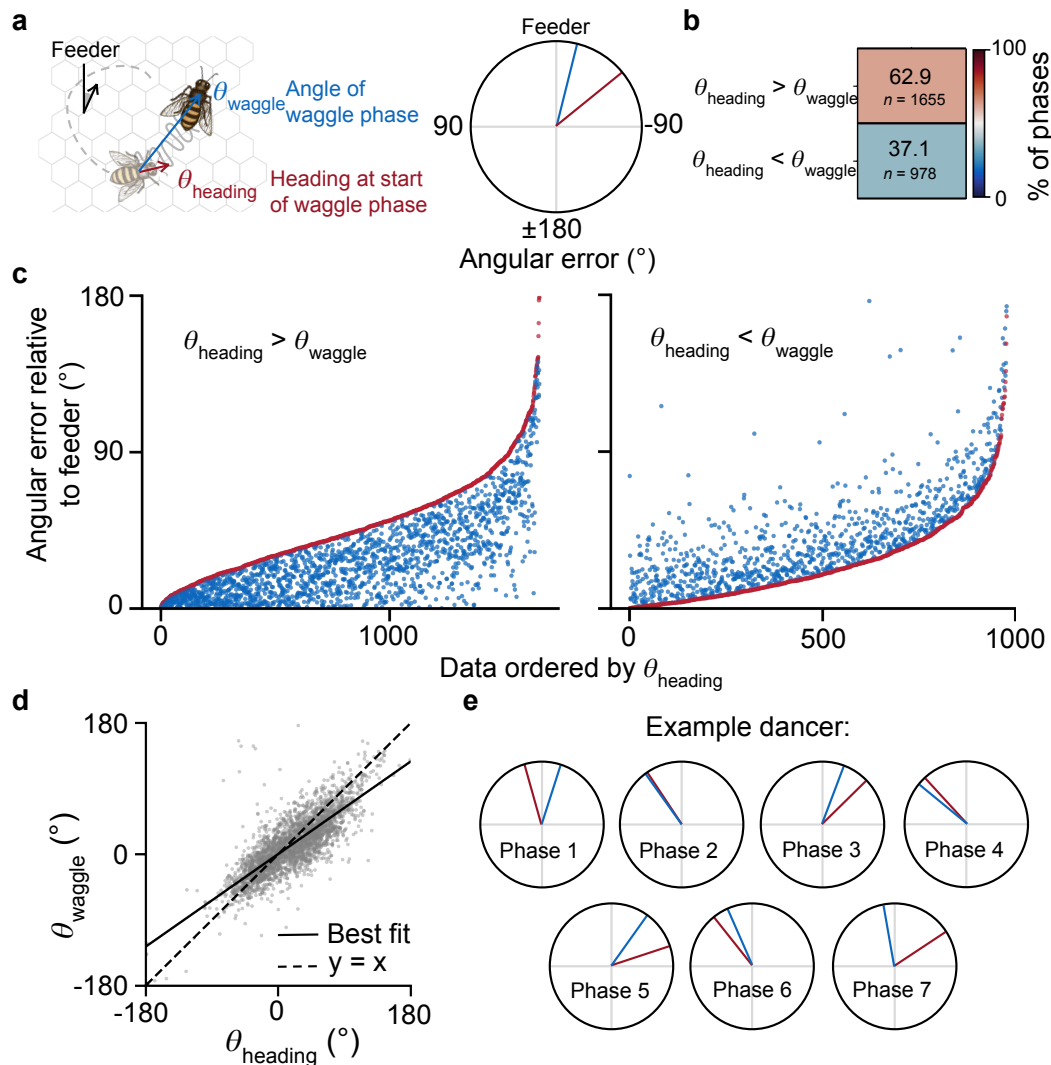


Figure 3.3. Measuring the change in course during the waggle phase. **a**, The heading angles of dancers ($n = 67$) at the start of their waggle phase (red, θ_{heading}) was compared against the angle of their entire waggle phase (blue, θ_{waggle}) relative to the feeder. **b**, Percentage and raw counts of waggle phases where θ_{heading} was further from the feeder angle than θ_{waggle} (red) and vice versa (blue). **c**, Absolute angular error of waggle phases where θ_{heading} (red) was further than θ_{waggle} (blue) from the foodward angle (left) and vice versa (right). **d**, Angular error of θ_{heading} against θ_{waggle} for all waggle phase. The solid line depicts the line of best fit (slope = 0.7, $r = 0.79$, $P < 0.0001$) and the dashed line depicts the relationship expected if there was no change between the angle at the start and the angle across the entire phase. **e**, Measured angles for an example dancer over seven waggle phases performed.

of the waggle phase differs from the overall angle obtained across the entire phase (Fig. 3.3a). Can dancers adjust the course of their trajectory during a waggle phase? We trained bees (*A. mellifera*) to forage from a feeder and recorded their dances within the hive. From the recordings of 67 dancers (2633 waggle phases), we measured the headings of dancers relative to the feeder in the first frame of wagging and obtained the angle of the waggle phase using the conventional method: the line connecting this point to the thorax in the last frame of visible wagging. Almost two-thirds of all waggle phases were performed with the dancer's initial heading deviating further from the foodward angle than the overall angle of the waggle phase (Fig. 3.3b). Fig. 3.3c shows the absolute angular error between the start angle (red) and waggle angle (blue) for each phase, separated into phases where the angle of the dancer at the start was further from the feeder than the angle of the entire waggle phase (left) and vice versa (right). Fig. 3.3d shows the line of best fit through the full range of (signed) errors compared to the diagonal line, which would be observed if there was no adjustment to the angle throughout the waggle phase. Consistent with the prediction of a path integration circuit, this comparison suggests that there is an inclination towards bees adjusting their angle to better align with the foodward angle if their initial angle deviates from it. The slope of the line of best fit (0.7) suggests that there is a 30% improvement in this alignment. The fact that this is not a perfect alignment (i.e. a horizontal line) suggests that bees are physically constrained when attempting to update their path direction when wagging. The mean change in the angle of the path estimated from the dataset is $53.04^\circ/s$ (s.d. = $48.89^\circ/s$). Although this is a novel observation, it is plausible that wagging would restrict path adjustments, considering the rapid oscillations of their abdomen and their grip on the comb with their legs³²¹.

3.3 A path integration control system

To bridge the gap between the observed dance behaviour and its underlying neural mechanisms, we now introduce how a computational model of path integration could explain how bees perform the dance. The central complex (see Section 2.3) is a highly conserved region of the midbrain involved in the processing of polarised light¹³⁰, orientation control for walking and flying²⁸⁹, as well as various forms of arousal³³⁴. Neurophysiological studies have offered insights into the neural circuits supporting these functionalities^{91;139}. Based on neuroanatomical evidence of the sweat bee's central complex, Stone et al.³⁰⁵ proposed a computational model of a subset of the circuitry illustrating that it can support the intrinsic computations needed for path integration when foraging. The model exploits the fact that a vector can be represented as a sinusoidal pattern of activity across a neural population, where the phase and amplitude encodes the direction and distance to a point of origin respectively. Sinusoids can then be combined to produce a directional control signal. As the insect forages, CPU₄ neurons *charge up* by integrating ground velocity input from optic flow (TN cells) and polarised light information from the head direction circuit (TBI cells). This accumulates a flight vector, distributed across the CPU₄ population, which represents the direction and distance to the nest. On the homeward path, structured connections draw a comparison between the current head direction and the CPU₄ memory direction to steer home (Fig. 3.4a).

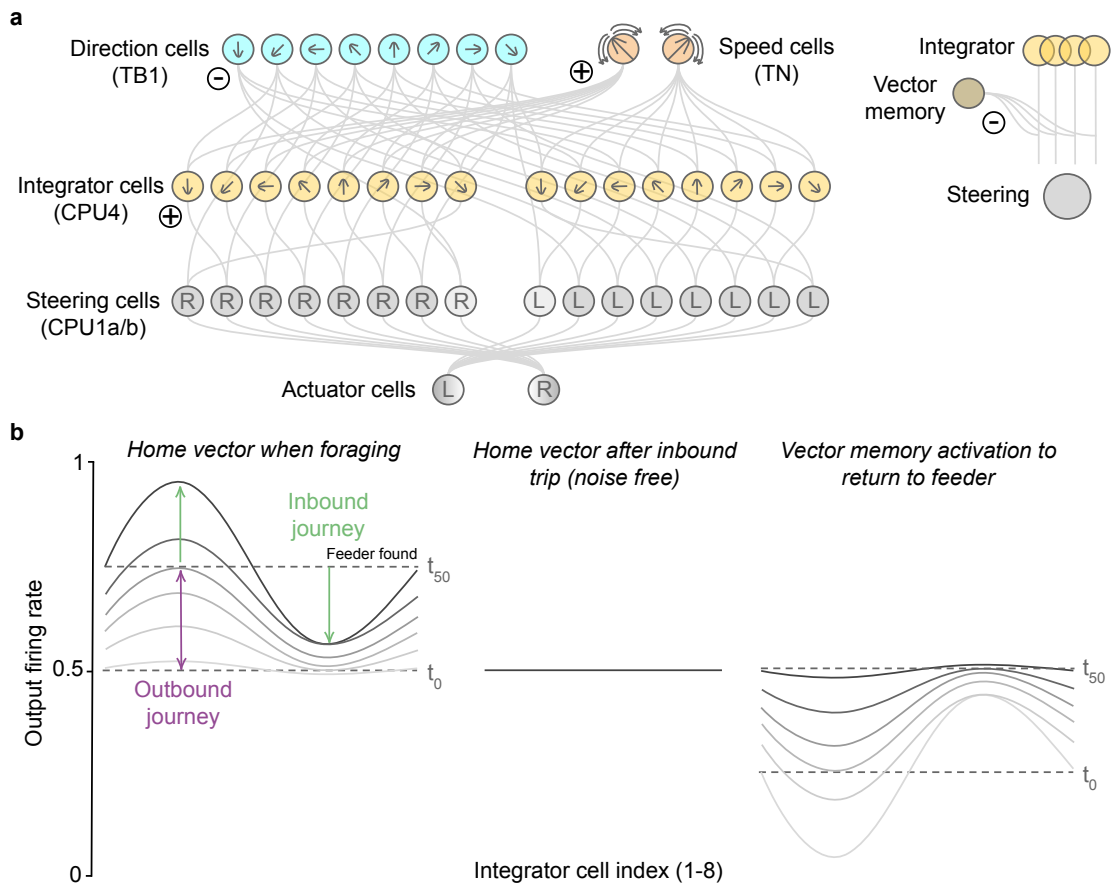


Figure 3.4. A network for path integration based on the insect central complex. **a**, Neural connectivity of the principal cell types enabling the accumulation of a home vector, modelled by Stone et al.³⁰⁵ and extended to include vector memory recall by Moël et al.²¹⁷. Connections between TBIs omitted for brevity. **b**, Examples of the sinusoidal activity representing the desired steering direction over time when (left) foraging, (middle) arriving back at the nest and (right) when vector memory recall is used to return to the feeder. Distance can be represented using the inbound journey (green) or outbound journey (purple). The angle (or phase) of the home vector is determined using the fast fourier transform²³³. Only cell indices 1 - 8 are shown for brevity.

The model has been extended to include the concept of vector memory²¹⁷, where the state of the path integrator (CPU4s) can be saved at salient locations, such as a feeder, and later used to inhibit the current state of the integrator cells to steer a return journey to the feeder (Fig. 3.4b). Further details of the model and neuron types are given in Section 2.3. We propose that this circuit could also underlie the performance of the dance itself: honeybees can use an existing vector memory on a small scale to emulate travelling to the feeder via the waggle phase on the comb. Since the path integration continues to run in parallel to the activation of a vector memory, during the waggle phase, the dancer also charges a home vector that retains an estimate of the starting point of the dance. Upon deactivating the vector memory, this small-scale home vector could then be utilised by the steering circuit to perform the return phase of the dance circuit. This model thus presents a plausible neural mechanism that is capable of producing the general structure of repeating waggle and return phases in the dance.

Model details

Fig. 3.5 illustrates the path trajectories generated by this circuit (Fig. 3.4) when simulated under various conditions: foraging, returning to the feeder, and the proposed dancing behaviour. A bee initiates a homeward route after discovering a feeder on a foraging trip (left). She can later activate her vector memory of the feeder to return to it (middle) or signal its location via dancing on the comb (right). These paths are reconstructed by decoding the neural activity of CPU₄ integrator cells into the bee's estimated distance (amplitude) and direction (phase) relative to her starting point, providing snapshots at 10 ms intervals.

Expression of the foodward vector. We use the most recent calibration for *A. mellifera* defined by Kohl and Rutschmann¹⁶⁵ for mapping the distance of the decoded foodward vector to a waggle duration which the dance model uses to gate the expression of the vector memory. There is also evidence that the presence of odour can gate whether or not fruit flies orient with respect to the wind direction¹⁹⁵. These findings were observed in FB local neurons called hΔC in the central complex, making it plausible that a particular cue could control a brief period of activating a vector memory. Another option is that the foodward vector continually discharges as the vector memory is activated, until there is no imbalance left in the two CPU₄ accumulators. This indicates that the feeder has been reached, after which the vector memory deactivates and thereby initiates the return phase. This option assumes that the network can operate at a different spatial scale within the hive, such that the foodward vector is discharged at an accelerated rate than if the bee was following it to fly to the actual resource. Behaviourally, it is difficult to disambiguate which option is more likely. Whilst it is generally unknown how bees establish their calibrations for mapping the feeder distance to a waggle duration, or an accelerated rate of discharging, recent work suggests that bees deprived of following any dances before they first dance develop a long-lasting inability to accurately convey distance in their own dances⁶⁵, suggesting a potential social learning component.

Return phases. The return phase is triggered when the vector memory is deactivated at the end of a waggle phase. The connectivity of the steering circuit dictates that the dancer turns to the side which immediately minimises the discrepancy between her current heading angle and the starting point of the dance. The dancer's final heading angle at the end of a waggle is sampled from a von Mises mixture distribution, allowing for natural variation around the central waggle direction with a bias towards $\pm 20^\circ$ offsets. We set a threshold that reactivates the vector memory for the next waggle phase when the dancer returns to a location within 5 mm of the starting point of the dance.

Distance and direction inside the hive. For open-nesting species of honeybees which dance on horizontal combs, the model could operate in the same directional frame of reference as it does for performing regular return trips to the feeder: with respect to the sun and polarisation pattern in the sky. Vertical cavity nesting species dance with respect to gravity, and it is unknown how bees are able to translate the foodward angle between celestial cues and gravity, or how gravity information is represented in the central complex. In this work, we assume that gravity could exist as another cue that can similarly evoke and update a directional bump in the EB (via TB₁ cells in Fig. 3.4). Regarding maintaining a measure of distance travelled inside

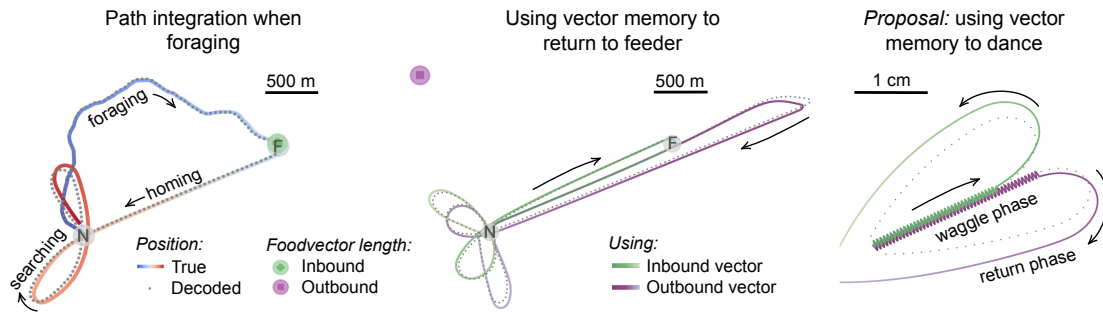


Figure 3.5. From foraging to dances using vector memory. **Left**, The feeder’s vector memory obtained when foraging can be reactivated in order to **Middle**, return to the feeder or **Right**, emulate the waggle phase, and lifting its inhibition initiates homing or the return phase. The paths show the decoded self-position from simulated neuronal activity of the path integration memory layer (see Fig. 3.4). The length of the foodward vector can either be represented using the inbound route (green, the straight line connecting home and feeder) or outbound route (purple, the total time travelled before discovering the feeder).

the hive, Lyu et al.¹⁹⁰ showed that LNO_I cells in the fruit fly, homologs of TN cells, display similarly strong tuning to egocentric translation direction in the context of side-slipping when walking in darkness as they do when experiencing optic flow stimuli simulating flight. It is thus plausible that these cells could exhibit a similar nature of activity to record displacement in the context of the dance, as they do in flight. We assume that TN cells display maximal activity when flying at 6 m/s outside of the hive, and dancing at 1.4 cm/s within the hive. Given our findings in Section 3.2, we also add a restriction to the steering circuit that limits the maximum angular velocity of heading angle adjustments during wagging (ranging between $\pm 10^\circ/s$ and $\pm 80^\circ/s$). For example, $\pm 30^\circ/s$ means that a dancer that starts wagging at 45° relative to gravity will be, at most, oriented towards 15° or 75° after one second of wagging.

Outbound and inbound foraging routes. As discussed in Section 2.2, bees can use the information from either the outbound or inbound foraging route in their dances. The memory update for the CPU₄ integrator cells used by Stone et al.³⁰⁵ makes it possible to extract representations of either measure,

$$CPU4^t = CPU4^{t-1} + h(TN^t - TB1^t - k) \quad (3.1)$$

where t is the current timestep, TN is the ground velocity response, $TB1$ is the compass-sensitive response, h determines the rate of memory accumulation ($h = 0.005$ when flying and $h = 0.025$ when in the hive) and k is the uniform rate of memory loss ($k = 0.05$). CPU₄ memory cells are initialised with a charge of 0.5 and have an activity that range between 0 and 1. Whilst the amplitude of the home vector represents the inbound distance (the straight-line distance to the nest), the overall mean displacement of the sinusoid from its baseline starting activity provides a measure of the outbound distance (total time travelled). These properties are visualised in Fig. 3.4b (left). The memory cells also begin to saturate as their sinusoidal activities approach 1, which is consistent with the gradual plateauing of the feeder distance to waggle duration calibration curves observed for long foraging distances¹⁶⁵.

3.4 Comparison with natural dances

In this section, we compare the dance paths that emerge from this path integration model against three features of natural dances: alternating turns, angular divergence as well as round dancing for short feeder distances. Fig. 3.6 shows three examples of natural dance paths from Landgraf et al.¹⁷⁴ demonstrating these features, alongside the equivalent that emerge from simulations of the model. The metrics for each feature of the model are calculated over for the same number of dances or waggle phases as in the corresponding natural dance dataset used for comparison.

3.4.1 Alternating turns

Von Frisch¹⁰⁰ described a typical waggle dance as repeating circuits of waggle and return phases, where the dancer alternates which side they turn to at the end of consecutive waggle phases. These alternations are a notable feature as they would be responsible for creating the figure-eight shape of the dance that is often referred to. From the perspective of a path integration control system, a dancer could be biased to turn to a particular side at the end of the waggle phase if she finished off-centre with respect to its starting point, due to the wagging, for example. She would then be attracted to turn to the side that immediately minimises the discrepancy between her current heading angle and the starting point of the dance, reinforced by the offset anatomical connection in the steering circuitry (see Section 2.3). Measuring the precise heading angles of dancers as they finish wagging is challenging, as it becomes difficult (and potentially subjective) to distinguish between a gradual decrease in wagging and the beginning of the dancer's turning motion. Therefore, we use the model to test this prediction and incorporate variability such that the dancer's heading angle at the end of a waggle phase is sampled from the von Mises mixture distribution shown in Fig. 3.7a.

Gardner¹⁰² defined a 'predictability index' to measure the consistency of alternating between left and right turns following consecutive waggle phases in natural dances. This index has a value of 0.5 when the current side that the dancer turns to has no predictive value concerning the next turn made and a value of 1 when the current turn provides complete certainty about the next turn to be performed (i.e. perfect alternations). The results of three independent colonies of *A. mellifera* reported in the study are overlaid in Fig. 3.7b (grey lines and markers). Interestingly, whilst the colonies do not perfectly alternate the consecutive turns in their dances, they do appear to alternate more than random. This pattern is mostly consistent across increasing feeder distances up to 500 m. As we might expect, the random sampling from the von Mises distribution for the simulated dancer's final heading results in a random pattern of alternating turns by the path integration model. Thus, applying the conservative assumption that dancers finish off-centre after wagging does not solely account for the levels of alternations observed in natural dances. Unlike the simulated environment, the natural dance floor is often a busy area of the hive which contains many nestmates, including those that are engaged with following the dance. The discrepancy could be reflecting the influence that real nestmates have on the structure of the dance path.

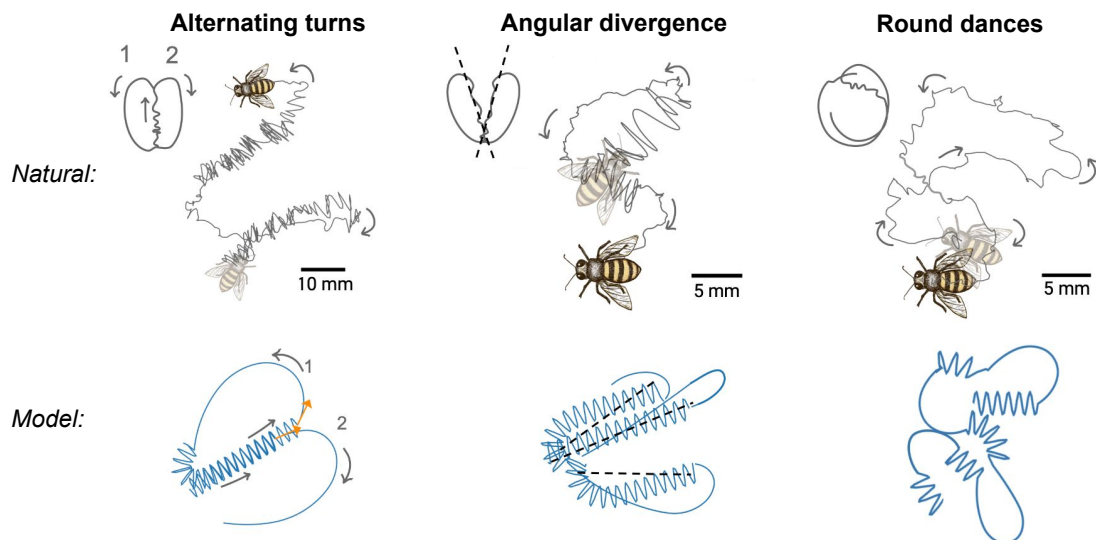


Figure 3.6. Natural (grey) and simulated (blue) paths of three features of dance communication. Natural paths from automated tracking of dance circuits by Landgraf et al.¹⁷⁴. Simulated paths from the path integration network shown in Fig. 3.4. The network makes the assumption that the dancer finishes off-centre after wagging and experiences a physical constraint if attempting to adjust her path direction when wagging.

To explore this further, we recorded the zonal position of each follower bee at the end of a dancer's waggle phase and the side the dancer turned to. The data was extracted from the same dance recordings used in Fig. 3.3 and followers were defined as a bee that was facing towards the dancer and within one bees length. Heatmaps showing the correlation coefficients of these features against the dancer turning left or right at the end of the phase (left) or in the previous phase (right) are shown in Fig. 3.7c. The most striking correlations are observed between a higher proportion of followers positioned behind and to the right of the dancer while she turns to the left; and a higher proportion behind and on the left while she turns to the right. While it might seem intuitive to assume that followers in front of the dancer could obstruct her movement and encourage her to turn to the opposite side, it is worth noting that in almost all of the recorded circuits, there were bees (followers and otherwise) occupying the space around the front such that dancers rarely had an unobstructed path in either direction and often turned to a side irrespective of whether another bee was there. It is not yet known whether the alternation of turns is of functional significance in communicating the dance vector. Landgraf et al.¹⁷⁴ suggest that a group of followers that continue to pursue the dancer on return phases help to clear the otherwise chaotic area for the rest of the dance. Alternating the turns of return phases might serve to increase the area that is cleared. We interpret our findings to be indicative of there being a certain flow associated with the interactions and movement between the dancers and followers during the dance, which is not solely determined by the dancer's path integration system.

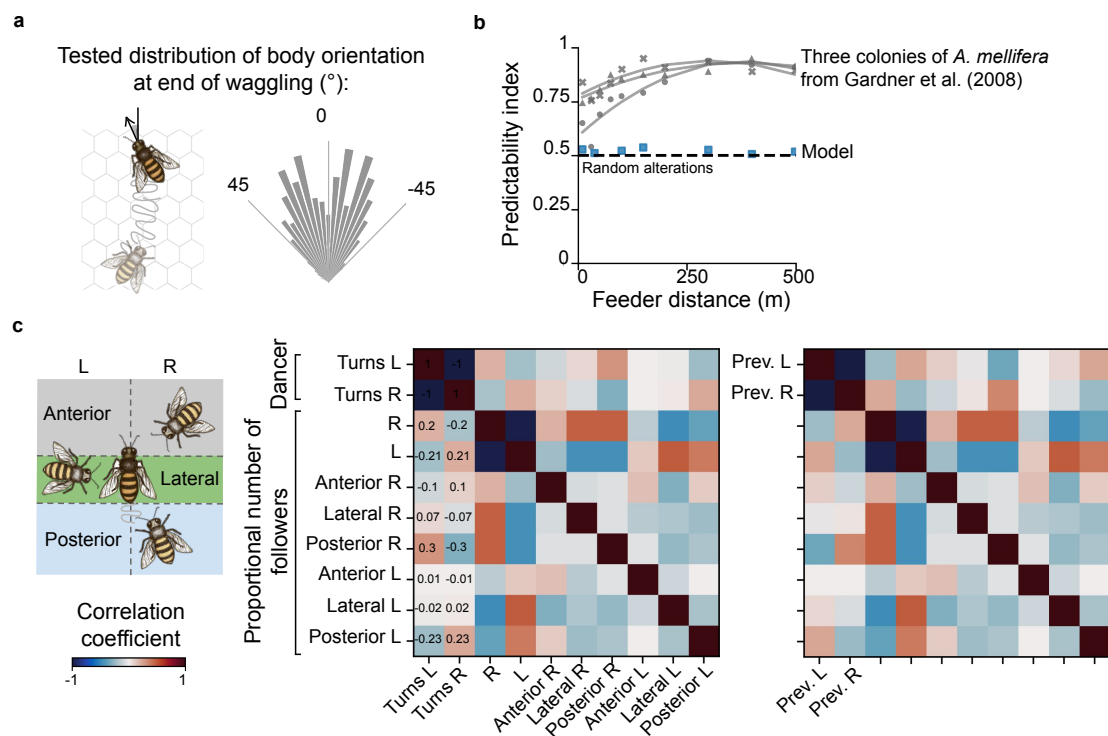


Figure 3.7. Alternating turns during natural and simulated dances. **a**, Circular histogram showing samples from the mixture of von Mises distribution ($\mu = \pm 20^{\circ}$, $\kappa = 15$) used to determine the heading angle of the dancer at the end of a waggle phase for the path integration dance model. **b**, The predictability indexes for three colonies of *A. mellifera* from Gardner et al.¹⁰⁴ (grey markers) and the model (blue markers). **c**, Heatmaps showing how the proportion of followers in positional zones around the dancer correlates with the side to which the dancer turns to at the end of the waggle phase. For brevity, values are only labelled for comparisons with the side that the dancer turns.

3.4.2 Angular divergence

We also investigated whether imposing limitations on how much a dancer can modify her path direction when wagging would yield comparable levels of angular divergence to those reported in natural dances. Such an outcome would lend support to the ‘physical constraint’ hypothesis proposed to elucidate the patterns of angular scatter seen in natural dances. We simulated foraging routes and subsequent dances for greater feeder distances and varied the maximum angular velocity at which the dancer could adjust her path direction during each waggle phase, exploring a range between $\pm 10^{\circ}/s$ and $\pm 80^{\circ}/s$. Feeder distances were mapped to waggle durations using the calibration curve reported by Kohl and Rutschmann¹⁶⁵ (Fig. 3.8a). To then quantify the resulting levels of angular divergence, we calculated the standard metric of the mean absolute angular difference between consecutive waggle phases.

Fig. 3.8b shows that a path integration model can effectively reproduce patterns of scatter observed in natural dances, where the mean angular divergence generally decreases with feeder distance. This trend is exemplified against a colony of *A. mellifera* reported by Towne and Gould³³⁰, using a version of the model with a maximum angular velocity restriction of

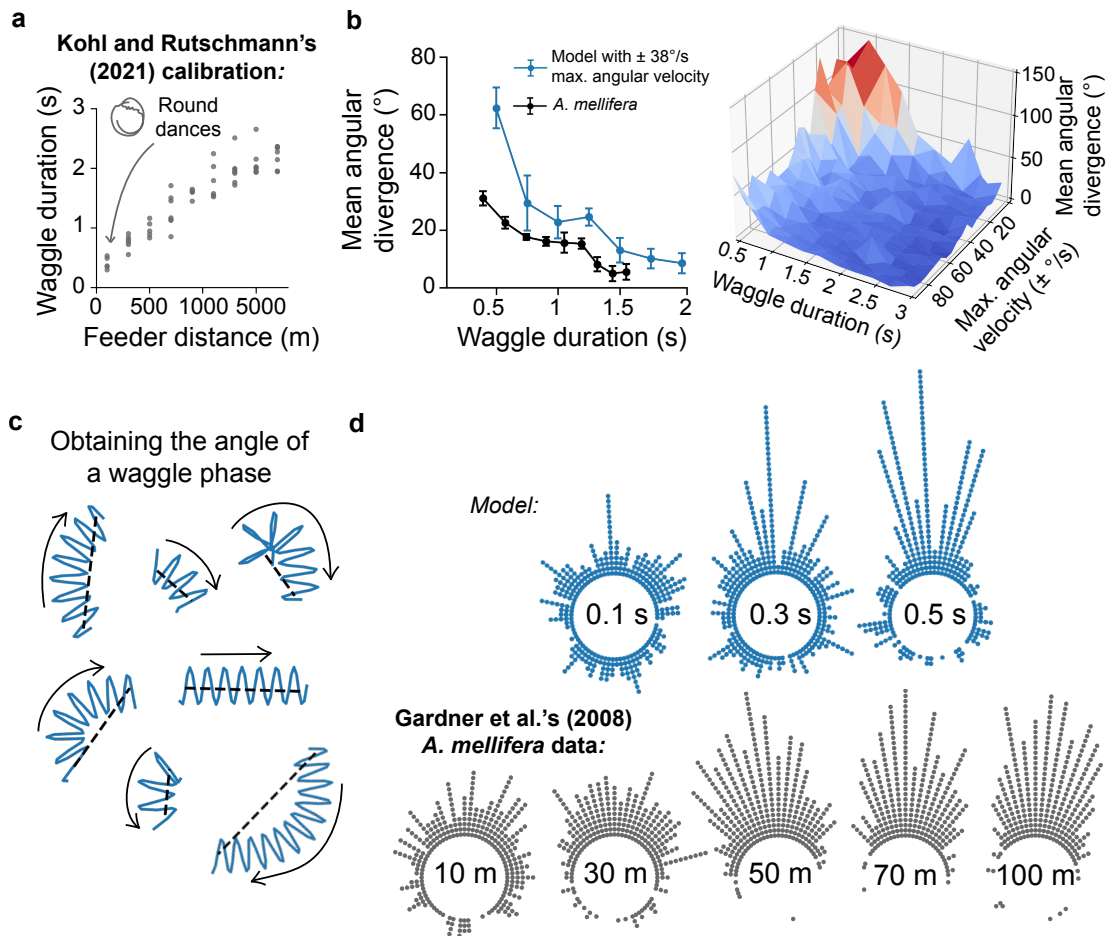


Figure 3.8. Angular scatter during natural (grey) and simulated (blue) dances for distant and nearby food sources. **a**, Feeder distance to waggle duration calibration data from Kohl and Rutschmann¹⁶⁵ is used to estimate the most appropriate waggle durations for comparing simulated and natural dance data. **b**, Mean \pm s.e.m. angular divergence between consecutive waggle phases for (left) natural dances of *A. mellifera* from Fig. 12 in Towne and Gould³³⁰ and the model for different waggle durations, and (right) the model configured with different maximum angular velocities. **c**, Examples of the angles of simulated waggle phases estimated using the line of best fit through the first and last segments of the phase (dashed lines). **d**, Circular plots showing the angular scatter of simulated dances with brief waggle phases against natural dances of *A. mellifera* from Gardner et al.¹⁰⁴ (Colony C) for nearby feeder distances, eliciting round dances. The model was configured to dance with a maximum angular velocity of $\pm 70^\circ/s$. The target angle of the feeder has been normalised to 0° North on the plots.

$\pm 38^\circ/s$ (Fig. 3.8b, left). Distinct profiles and rates of divergence also emerge from different configurations of the model (Fig. 3.8b, right), with tighter restrictions on the angular velocity generally resulting in a larger scatter between consecutive phases. While Beekman et al.¹⁹ concluded a general trend of decreasing divergence with increasing feeder distance across honeybee species, their data also suggests that the rate of this decrease could vary (see Fig. 2 of Beekman et al.¹⁹). For example, although most variations in dances between species remain subtle to human observers, the giant honeybee, *A. dorsata*, exhibits a visually conspicuous and distinctive waggle which involves dorsoventral abdominal movements¹⁶⁶, in addition to the lateral movements observed in other species. This raises the possibility that such a conspicuous physical characteristic may influence their rate of angular divergence and potentially reflect a specific configuration of the path integration system, compared to other species.

The angles of the simulated waggle phases were estimated using a line fit through the midpoints of the first and last segments of the phase (dashed lines in Fig. 3.8c). We chose this approach to mirror the conventional method used to measure waggle phase angles in natural dances: the straight line connecting the location of the thorax in the first and last frames of visible wagging. This method of estimating the angle, combined with idea that bees are physically constrained when updating their path direction during wagging (Section 3.2), offers an explanation for the apparent trends in angular divergence: longer waggle durations provide dancers with more time to align their waggle trajectory to the target foodward angle, resulting in a seemingly reduced divergence angle than would be possible for short waggle durations.

3.4.3 Round dances

We lastly compared the performance of simulated dances at one extreme end of the recruitment system: for resources less than 50 m from the hive. Throughout his work, von Frisch¹⁰⁰ repeatedly asserted that bees distinctly use round dances for signalling such nearby food sources and waggle dances for sources further away, and that round dances show no directional bias in their signalling or recruitment. He characterised them as the forager making “swift, tripping steps” to run in a circle before suddenly reversing the direction of travel and circling around again, before repeating (p. 29). Curiously, von Frisch did describe a gradual transition from round dances to waggle dances when a feeder’s distance is increased from 10 to 100 m (p. 61), but he never emphasised the similarity in their form or the continuation between them. There have been few attempts to quantify path statistics of round dances and they are often described as differing from waggle dances in that their waggle phases are extremely short and their path can appear quite random¹¹⁹. In 2008, Gardner et al.¹⁰⁴ showed that round dances actually exhibit a progressively strengthening directional bias in their brief waggle phases, corresponding to the feeder’s location (see also Jensen et al.¹⁴²; Kirchner et al.¹⁵⁸). Griffin et al.¹¹⁹ later confirmed that this bias could also recruits follower bees to the feeder, even when controlling for bee presence and the Nasonov pheromone. We tested whether the path integration circuit could support the hypothesis that the round dance is not a distinct dance type, but rather can emerge from the same underlying neural mechanism.

We calculated the angular scatter resulting from simulating dances with brief waggle phases

Table 3.1. Circular statistics for natural and simulated dances. MVB and MVL indicate mean vector bearing and mean vector length, respectively. All Rayleigh’s Z tests for uniformity were statistically significant ($P < 0.01$).

(a) *A. mellifera* from Gardner et al.¹⁰⁴ (colony C)

Distance (m)	10	30	50	70	100
n (waggles)	294	280	350	301	320
MVB ($^{\circ}$)	-14.15	-10.59	8.23	-7.35	-9.66
MVL	0.404	0.605	0.850	0.895	0.877
Rayleigh’s test (Z)	48.08	102.48	252.58	241.10	246.01

(b) Simulated dances from path integration model

Duration (s)	0.1	0.3	0.5
n (waggles)	309	367	355
n (dances)	13	28	32
MVB ($^{\circ}$)	-6.39	3.72	3.94
MVL	0.158	0.327	0.622
Rayleigh’s test (Z)	7.72	39.26	137.19

and compared them to a colony of *A. mellifera* collected by Gardner et al.¹⁰⁴. For each waggle phase duration, we computed the mean vector bearing (MVB, the mean direction of all waggle phases), the mean vector length (MVL, a measure of dispersion about the mean) and Rayleigh’s Z tests for uniformity, with the null hypothesis that the circular distribution of all angles comes from a uniform circular distribution. The circular scatter plots are shown in Fig. 3.8d and the statistics are given in Table 3.1. Both demonstrate that the model exhibits considerably greater angular scattering when expressing brief waggle phases, whilst also displaying a similar strengthening of the directional bias that is characteristic of natural dances. But, how can seemingly random waggle phase directions arise from a model that has an accurate encoding of the foodward vector? In the model, when nearing the end of the return phase, the vector memory reactivates depending on the amplitude of the CPU₄ activity that indicates whether *home* has been reached. The next waggle phase initiates when the dancer enters this boundary (set to an equivalent of 5 mm), regardless of her approach angle. Consequently, the especially brief waggle durations, along with the maximum angular velocity constraint, gives the dancer little time to correct her directionality, and thereby produces wide angular scatter.

Beyond their angular scatter, direct comparison between the dance paths of the model and natural round dances is difficult, as natural round dances can appear random and lack the detailed quantitative descriptions available for waggle dances. Fig. 3.9 therefore provides a visual comparison of a simulated round dance and two tracings of natural round dances: one that has been extracted for the purpose of this work and one adapted from Fig. 3 of Jensen et al.¹⁴².

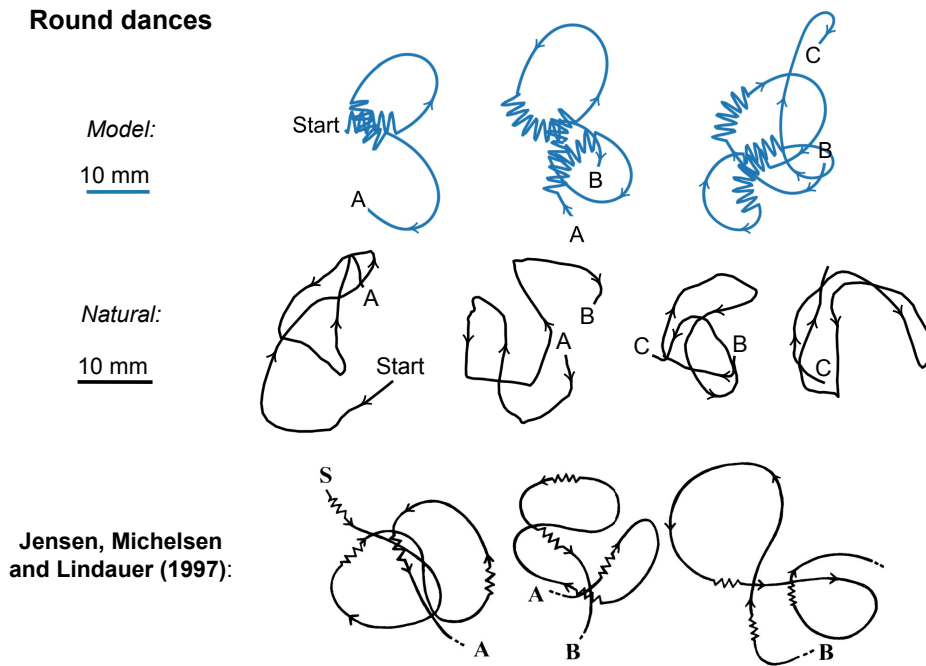


Figure 3.9. Traces of natural and simulated dance paths for nearby food sources. For clarity, the dance paths have been cut into sections. S, Start; A, end of the first section and the beginning of the second section; B, end of the second section, and so on. Zigzags indicate the presence and direction of any waggle phases. **Top**, The simulated dance path generated by the path integration model for a waggle duration of 0.25 s and maximum angular velocity of $\pm 80^\circ/s$. **Middle**, A tracing of a natural round dance signalling an unknown food source by *A. mellifera mellifera*. **Bottom**, Adaptation of Fig. 3 of Jensen et al.¹⁴²; a tracing of a natural round dance to a feeder 1 m from the hive by *A. mellifera carnica*.

3.5 Discussion

We have proposed how an anatomically grounded model of path integration could be adapted to navigate on a small-scale and operate in the context of the dance. This repurposing involves activating an existing vector memory to emulate travelling to the feeder via the waggle phase on the comb, whilst the parallel charging of a home vector retains an estimate of the starting point of the dance that can guide the return phase. We also analysed properties of natural dances to define appropriate restrictions for the simulated model. We identified that dancers could seemingly adjust the trajectory of their dance path during the waggle phase but these adjustments appeared to be limited, as if operating with physical constraints on these movements. Based on this, we assumed that different modes of movement (e.g. flight, walking and wagging) differ their ability to update the path direction of the circuit and imposed a parameter to limit the rate at which a dancing bee can adjust her path trajectory when wagging (i.e. the maximum angular velocity). Various features of natural dances arose from the model, particularly with respect to the angular scatter observed in waggle phases. The same model also displayed directional scatter and an overall dance path that is consistent with round dances when communicating nearby feeder locations, suggesting that a path integration control system can explain features that exist across the spectrum of the recruitment system.

The quantification of waggle phase angles serve as a fundamental metric in decoding direction in bee dances and are often simplified as the straight line connecting the start and end points of the bee's movement. Using this method, we showed how trends in angular divergence could potentially arise from the path integration circuit: longer waggle durations provide dancers with more time to align their waggle trajectory to the target foodward angle, resulting in a seemingly reduced divergence angle than would be possible in dances with short waggle durations. Our work highlights that waggle phase trajectories can deviate from linearity and that the methods we use to approximate certain dance features may influence our subsequent interpretations of it. Earlier studies, such as Towne and Gould³³⁰ in 1988, measured the waggle phase angle by aligning a large protractor against the computer monitor to record the dancer's body orientation five times per waggle phase. This typically yielded a low variance across the repeated measurements and was used to argue that the waggle phase angle had been measured accurately, e.g. that "the true mean direction of a waggle phase was likely to be within $\pm 2^\circ$ [of their estimated average]"³³⁰. The timing intervals between these repeated measurements were not explicitly stated but there was also a traditional characterisation of the waggle phase being a 'straight-run', described by von Frisch¹⁰⁰ himself (p. 57), that was emphasised at that time. We believe it is likely that researchers may have biased these repeated measurements towards the middle or straighter portions of the phase. Whilst these methods may be appropriate for estimating the general angle of the resources that the bees are foraging from, they underestimate the challenge faced by follower bees attempting to decode the dance, given that many would follow the dance during these misaligned or curved portions too.

There are two aspects of our model that drive the observed trends in the angular divergence. The first is the physical restrictions that controls the angular velocity in different modes of movement; in particular, different degrees of angular divergence can be seen depending on the strength of restriction used, i.e. how much can the control system adjust the waggle trajectory by. However, the path integration circuit will only adjust the trajectory if it is misaligned with the target angle in the first place. This can happen in subsequent waggle phases since during the return phase, the dancer will reactivate the vector memory as she enters the 'home distance' threshold, regardless of her approach angle or whether she has completed the full return loop. Curiously, whilst researchers have not yet quantified the potential curvature of waggle phase trajectories, others have reported a reduction in the duration of return phases in waggle dances for nearby feeders^{16;103}. Beekman et al.¹⁶ inferred that dances would have to be "performed more speedily" in order to be more accurate, i.e. a dancer does not have enough time to precisely reorient before starting the next phase, which is consistent with the behaviour of our model.

In an automated analysis of over a thousand natural dances, Landgraf et al.¹⁷⁴ reported a slight forward drift in the starting point of consecutive waggle phases. Seeley²⁸² also noted that dancers tend to separate across the comb due to a slight offset in their return path towards the foodward direction. Dormagen et al.⁶⁶ suggested that this drift could influence nestmates to favour following different dances that lead to similar food locations. In the current model, the path integrator is not reset after each waggle phase. This means that the starting point of the dance persists as the initial reference point to return back to, rather than the starting location

of the previous waggle phase. It is possible that small levels of drift could emerge if the home distance threshold is increased and the path integrator is reset after each dance circuit.

The current model does not incorporate the potential influence of nestmates, which could impact the dancer's path within the natural environment of the hive. For example, extending beyond the control of a path integration circuit, we hypothesise that further modelling of the dancer-follower interactions would be necessary to explain the observed degree of the alternating turning behaviour of dancers between consecutive waggle phases. While the path integration circuit would predict that the dancer would turn to the side she finishes her wagging, or the side which is not obstructed with other bees, there were rarely any instances in our behavioural data where the space ahead of the dancer was clear at the end of a waggle phase. Sampling the alternation of turns in dances throughout the foraging season, as comb occupancy fluctuates, would be necessary to confirm this prediction.

3.6 Methods

3.6.1 Honeybee dance datasets

External datasets. Dance datasets for *A. florea* from Makinson et al.¹⁹² and *A. mellifera* from Landgraf et al.¹⁷⁴ were obtained and analysed with permission, to study how angular divergence progresses throughout a dance. Angular divergence was calculated as the absolute angular difference between consecutive waggle phases (Fig. 3.2, the signed angular differences are shown in Fig. A.1). Whilst both datasets have a similar mean \pm s.d. absolute difference in angular divergence (*A. florea* = $28.44^\circ \pm 27.31^\circ$, *A. mellifera* = $29.65^\circ \pm 20.77^\circ$), the *A. florea* dataset appears to have more outliers (e.g. divergences larger than 90° , Fig. 3.2a). This could be due to the potential bias associated with this dataset since it is substantially larger by comparison (4900 versus 457 phases) and manually annotated by Timothy Schaerf's group. On the other hand, the *A. mellifera* dances were detected automatically by a method described in Landgraf and Rojas¹⁷³. Examples of these automatically segmented waggle trajectories are shown in Fig. 3.10. These trajectories were also used to exemplify the three features of dances being examined in the comparison between natural and simulated dances (Fig. 3.6).

Dances of *A. mellifera* collected by Gardner et al.¹⁰⁴ were also obtained and analysed with permission, to compare the predictability (defined in Section 3.6.3) of alternating turns in natural dances to those of the model (Fig. 3.7b, see Fig. 6 and Table 7 of Gardner et al.¹⁰⁴), as well as the scatter in the signalled waggle phases for nearby resources (Fig. 3.8d). We also traced the data from Fig. 12 in Towne and Gould³³⁰ to compare the angular divergence across longer waggle durations (Fig. 3.8b). For both datasets, since the original results were reported with respect to the feeder distance, as opposed to the waggle duration, we used Kohl and Rutschmann¹⁶⁵'s feeder distance-calibration curve (Fig. 3.8a) to estimate the most appropriate waggle durations when conducting a comparable experiment with the model.

Internal datasets. To investigate whether dancers adjust the course of their trajectory during a waggle phase (Fig. 3.3), we analysed video recordings of dances that we obtained from the

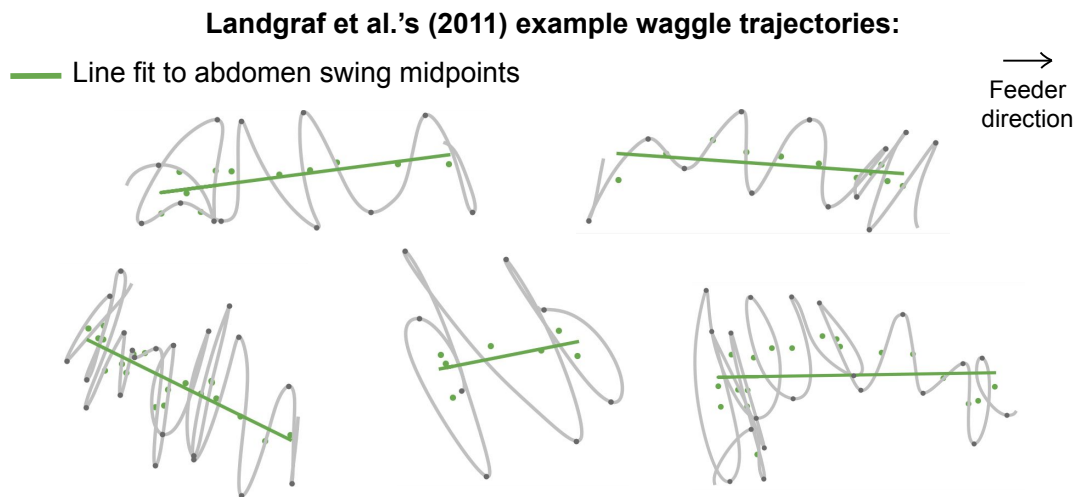


Figure 3.10. Example waggle phase trajectories from Landgraf et al.¹⁷⁴. Landgraf et al.¹⁷⁴ used an automated method¹⁷³ to track dances of foragers that had been trained to a feeder 230 m away. We calculated the angle of a waggle phase as the linear least squares fit (green line) through the consecutive midpoints (green dots) of each waggle in a waggle phase relative to the feeder (grey dots indicate waggle change points).

behavioural experiment conducted as part of Chapter 5. The dances were performed by a group of foragers that had been trained to a feeder that was positioned within a patterned tunnel. Full details of the training protocol is outlined in Section 5.4. From these video recordings, we also recorded the number of followers around the dancer at the end of each waggle phase, their positional zone, and the side to which the dancer then turned to for the return phase (Fig. 3.7c). The proportional number of followers in each zone was calculated for each waggle phase to investigate its relationship with which side the dancer turned to. The positional zone was determined by whether the follower's head was within a particular boundary with respect to the dancer. Followers that were anterior to the dancer were defined as those whose head was positioned in the space aligned with, or in front of, the head of the dancer. Followers that were posterior were defined as those whose head was located behind the dancer's abdomen, and followers that were lateral to the dancer were those in between these zones, with their head being alongside the dancer's body (see left of Fig. 3.7c).

Natural round dance traces. For a visual comparison of dances simulated by the path integration model for nearby resources and natural round dances, we obtained two tracings of natural round dances (Fig. 3.9). The first was extracted from a video we recorded in August 2022, of a round dance to an unknown natural resource by *A. mellifera mellifera* in Scotland. The dance was filmed at 200 fps under infrared illumination (690 nm), using a Basler acA1440-220UM ace camera and a 6 mm lens. The trace was obtained by manually tracking the thorax of the dancer in each frame and then smoothing the trajectory by applying a Savitzky-Golay filter using the Scipy³³⁶ Python library. The dance was identified based on being a series of rapid, short and circular movements performed in response to food (similar to descriptions by Frisch¹⁰⁰). These movements elicited interest from nearby fellow nestmates and trophallactic exchanges. As one of the only examples of a round dance trajectory in published literature,

the second dance trace in Fig. 3.9 was adapted from Fig. 3 of Jensen et al.¹⁴² in 1997. This provided a trace of a round dance to a feeder positioned 1 m from the hive by *A. mellifera carnica*. While Jensen et al.¹⁴² do not specify how the trace was generated (e.g. manually or automatically), their data was obtained from video recordings.

3.6.2 Path integration model

The following details accompany those already given in Section 3.3.

Model source and formulation. Our model source code is based on previous work^{217;305} that we extended. A comprehensive formulation of the underlying rate-based model can be found in the STAR methods of Stone et al.³⁰⁵, with the vector memory extension detailed in Moël et al.²¹⁷. We use the partially holonomic version of this model (as presented in Stone et al.³⁰⁵). This model captures holonomic movements within $\pm 90^\circ$ deviation of body axis and movement direction using TN2 neurons, which respond to forward movement. This subtly differs from the fully holonomic version used in Moël et al.²¹⁷, which utilises both TN2 and TN1 neurons to capture the full range of holonomic motion (i.e. $\pm 180^\circ$). Additionally using the TN1 neurons, which also respond to backwards movement, means that the CPU4 memory layer can be affected in an additive or subtractive manner, which results in its mean activity remaining centred on 0.5. This property is exemplified in Fig. 1c of Moël et al.²¹⁷.

Environment and agent. We simulate an agent moving in a two-dimensional environment using Python 3.9. There are two distinct environments: a foraging environment which contains both a hive and a feeder, and an environment representing the comb inside the hive. In the former, the hive and feeders are circular with a small defined radius (10 m) within which the agent is assumed to have landed successfully at the target. The agent is assumed to have sensory information about its heading direction in an absolute external reference frame, as supplied by the insect’s celestial compass (see Section 2.3). It is also assumed to have information about its instantaneous speed of movement in its heading direction (ground velocity), as could be supplied by optic flow or self-motion (i.e. proprioception or motor efference). These provide inputs to the central complex circuit for path integration. For each simulation, the agent’s starting position is set to a point of origin ($x^0 = 0, y^0 = 0$), which is at the hive when foraging, or the centre of the comb when in the nest. Its position is updated iteratively depending on its heading ($\theta_{heading}$, in degrees) and speed (s , in m/s when outside the hive and cm/s when within the hive):

$$\theta_{heading}^{t+1} = \theta_{heading}^t + \text{rot}^t \Omega dt \quad (3.2)$$

$$v^t = \begin{bmatrix} \cos(\theta_{heading}^t) \\ \sin(\theta_{heading}^t) \end{bmatrix} s^t dt \quad (3.3)$$

$$x^{t+1} = x^t + v_0^t \quad (3.4)$$

$$y^{t+1} = y^t + v_1^t \quad (3.5)$$

where,

$$s^t = \left\{ \begin{array}{l} s^0 = 0 \\ acc_{drag} = B(s^t)^2 \\ s^{t+1} = s^t + (acc_{fixed} - acc_{drag})dt \end{array} \right\} \begin{array}{l} \text{when flying outside hive (m/s)} \\ \text{when walking in hive (cm/s)} \\ \text{when wagging in hive (cm/s)} \end{array} \quad (3.6)$$

and rot is the angular velocity ($^\circ/s$) at the current simulation time step t , Ω is the parameter to control the maximum angular velocity of the agent (see Section 3.2), dt is the sampling time interval (set to 0.01, i.e. 10 ms intervals), and v is the displacement vector (in metres when outside the hive or cm when inside the hive). The acceleration, acc , is only used when outside the hive and is set to 29.76 m/s^2 to achieve a maximum speed of 6 m/s when flying. The acceleration due to drag when flying, acc_{drag} , is computed using $B = (0.5 C_D \rho \text{ area})/mass$ where C_D is the drag coefficient (set to 0.45, based on Nachtigall and Hanauer-Thieser²²³), ρ is the air density (set to 1.225 kg/m^3), $area$ is the reference area (set to 0.0003 m^2) and $mass$ is the mass of the bee (set to 0.0001 kg). When on the outbound journey of a foraging trip to discover a feeder, the heading is controlled by a random walk process, where a rot is sampled from a von Mises distribution, with parameters $\mu = 0$ and $\kappa = 2$, and $\Omega = 1$. When returning home, or at any point within the hive, rot is determined by the outputs of the central complex steering neurons (CPUs). During the waggle phase, the Ω parameter is set such that the desired maximum angular velocity is achieved ($10 \leq \Omega \leq 200$).

During the waggle phase of a dance, a lateral displacement is added to the agent's position to generate the characteristic waggle oscillations, which is implemented as a sine function. The $\theta_{heading}$ and v are modified as follows:

$$y^t = A \sin(\omega \sum dt + \phi) \quad (3.7)$$

$$\theta_{waggle}^t = \theta_{heading}^t + \frac{dy^t}{dt} dt \quad (3.8)$$

$$v_{waggle}^t = v^t + \begin{bmatrix} -\sin(\theta_{smooth}^t) \\ \cos(\theta_{smooth}^t) \end{bmatrix} \frac{dy^t}{dt} dt \quad (3.9)$$

where A is the amplitude, ω is the frequency (set to 15 Hz), ϕ is the phase and θ_{smooth} is a moving average of the previous $\theta_{heading}$ (window size set to 10). θ_{waggle} and v_{waggle} are updated using different sine functions, such that $A_{heading} = 30^\circ$ and $\phi_{heading} = 0$ when updating θ_{waggle} , and $A_v = 1 \text{ cm}$ and $\phi_v = \pi$ when updating v . The shifted phases mean that the displacement vector and heading are modified in opposing directions. For example, when the bees abdomen shifts to the right, its heading direction shifts to the left. The output of the sine functions (y) are interpreted as the positional or rotational displacements at a given time in the simulation. To obtain an update for θ_{waggle} and v_{waggle} in a single time step, we

numerically integrate the rate of change of the corresponding sine function ($\frac{dy^t}{dt}$). The input for the optic flow sensitive TN cells on the left and right side, I_{TN_L} and I_{TN_R} , is then given by,

$$I_{TN_L}^t = \begin{bmatrix} \cos(\theta_{heading}^t - \frac{\pi}{4}) \\ \sin(\theta_{heading}^t - \frac{\pi}{4}) \end{bmatrix}^T v^t \alpha \quad I_{TN_R}^t = \begin{bmatrix} \cos(\theta_{heading}^t + \frac{\pi}{4}) \\ \sin(\theta_{heading}^t + \frac{\pi}{4}) \end{bmatrix}^T v^t \alpha \quad (3.10)$$

where $\theta_{heading}^t = \theta_{waggle}^t$ and $v^t = v_{waggle}^t$ when in the waggle phase of a dance. The model then follows onward from Eq. 7 in Moël et al.²¹⁷. α is the sensitivity parameter that is tuned to achieve maximal TN cell activity at the desired speeds ($\alpha = 23.57$ when flying and $\alpha = 33.33$ when in the hive).

Dance simulations. The experimental simulations in Section 3.4 consist of two stages. Starting at the hive ($x = 0, y = 0$), a simulated bee first embarks on a random foraging trip where a feeder is discovered at a predetermined distance from the hive (ranging from 10 m to 5.5 km), and stores its final integrator state as a new vector memory. Then, after being reset to the nest (coordinates reset to $x = 0, y = 0$; CPU₄ integrator reset to baseline = 0.5), the vector memory is then recalled within the hive and allowed to drive dance behaviour (see Section 3.3). The distance of the feeder, represented by the amplitude of the vector memory (the inbound route) is mapped to a waggle duration using the calibration curve reported by Kohl and Rutschmann¹⁶⁵. Where possible, the metrics for each feature of the model (i.e. alternating turns and angular scatter) were calculated over a comparable number of dances or waggle phases as in the corresponding natural dance dataset used for comparison. When the corresponding dataset only provided the total number of waggle phases, a bout of dancing for an individual was simulated for long enough to produce between 18 and 25 waggle phases. A single experimental trial therefore represents a bout of dancing simulated for an individual forager trained on a random foraging route. No simulated forager was excluded from analysis.

3.6.3 Data analysis and statistics

Polar plots. The polar plots in Fig. 3.3a,d and Fig. 3.8d present the angular data relative to a target angle which has been normalised to 0° (North on the plots). A positive angle indicates a deviation to the left of the target angle (counterclockwise rotation) and a negative error indicates a deviation to the right (clockwise).

Predictability index. In order to determine how consistent simulated dances contained alternating turns when initiating the return phases of consecutive waggle phases, we computed the predictability index of dances for different foraging distances. Defined by Gardner et al.¹⁰⁴, the predictability index attempts to measure the consistency in alternating between left and right turns at the end of waggle phases using transition probabilities (TP),

$$predictability_index = 1 - (TP_{RR} \times TP_{RL} + TP_{LR} \times TP_{LL}) \quad (3.11)$$

where TP_{LR} is the probability of turning right at the end of a waggle phase after turning left in the previous phase, and so on. This index has a value of 0.5 when the current state has no predictive value concerning the next act to be performed and a value of 1.0 when the current states provides complete certainty about the next act (i.e. perfect alternations).

Estimating the angles of waggle phases. The angle of a simulated waggle phase was estimated using linear least squares to fit a line through the midpoints of the first and last waggle segments in the phase (Fig. 3.8c), relative to the feeder or gravity on the comb. The same approach was employed to calculate the angle of the raw waggle phase trajectories from Landgraf et al.¹⁷⁴, used in Figs. 3.2 and A.1 (green lines in Fig. 3.10). This approach was chosen to be consistent with the conventional method used to define the angle in natural dances: the straight line connecting the location of the thorax in the first and last frames of visible wagging (which was used when collecting the data in Fig. 3.3). In Fig. 3.8c, these angles have been visualised as circular histograms, with 0° straight up depicting the expected angle, i.e. the difference between the sun's azimuth and the feeder's direction.

Angular divergence. The angular divergence of a dance (or a simulated dance) was calculated as the mean angular difference between consecutive waggle phases (Fig. 3.2a-c and Fig. 3.8b). We computed divergence as an absolute (unsigned) value ranging between minimum 0° to maximum 180° (except for Fig. A.1, where the signs have been conserved).

Cumulative distributions. To analyse whether the first waggle phase is performed with greater precision than the rest of the dance in natural dances, the cumulative distributions of these differences were calculated for dances containing at least six circuits (Fig. 3.2d). Each step in a distribution is from a different dance: the value on the y-axis at the top of a step is the fraction of dances which have a difference between the first waggle phase and the mean divergence across the rest of the dance which is less than or equal to the value on the horizontal x-axis.

Analysis software. Data analysis and modelling was carried out using Python, relying on Numpy¹²⁷, Scipy³³⁶, and Pandas²⁰⁰ libraries. Seaborn³⁴² and Matplotlib¹⁴⁰ were used for plots.

Statistical tests. All plots show the mean \pm s.d. unless stated otherwise. Circular equivalents were used where appropriate. A Kruskal–Wallis H test was used to compare differences in the absolute mean difference in angular divergence per dance between dancers carrying pollen and those not carrying pollen (Fig. 3.2b) (as data non-normal, tested by Levene's test for equal variance and Shapiro-Wilk normality test). Pearson's r correlations were used to measure the strength of the relationship between proportional positioning of followers around the dancer and the side to which the dancer turned (Fig. 3.7c). Rayleigh's Z test⁹⁰ was used to test for directionality in the scatter of signalled foodward angles in natural and simulated dances (Table 3.1 and Fig. 3.8d), with the null hypothesis that the circular distribution of all angles comes from a uniform circular distribution.

4

Assimilating the flight vector information

The initial proposal that honeybees possess such an abstract system of communication was not easily accepted by the research community; although correlations between field site and dance properties existed, it could not immediately be concluded that nestmates decode and actually use the vector information available (i.e. distance and direction). In fact, Wenner³⁵³ and Johnson¹⁴³ initially proposed that recruitment of nestmates could be explained by a simple odour search in which naïve bees could rely on a resource's scent alone, provided by the dancer. Debate over whether the recruitment might actually be driven by scents, rather than dances, continued until 1975, when Gould¹¹⁴ published a study in which he manipulated the perceived position of the sun when bees were dancing to induce them signalling locations they had never visited, and found that recruits arrived at the deceptively advertised locations. After decades of further honeybee dance research, new findings still support the notion that dance vector information is indeed decoded by nestmates and can be used to locate the resource. This includes evidence from radar tracking of recruits' search flights following displacement upon leaving the hive²⁵⁷, as well as nestmates directing stop signals towards a dancer if they had previously encountered danger at the resource being signalled¹⁴¹ (suggesting that they decode the dance at the time of performance). It remains likely that honeybees use both (and many) kinds of information to locate the resource and the use of olfactory stimuli or dance vector information are not exclusive search strategies. In this chapter, we concentrate on the latter: how nestmates assimilate their own flight vector that they can follow to the resource.

Although the honeybee waggle dance has been widely studied as a communication system, we know surprisingly little about how nestmates assimilate the information needed to navigate towards the signalled resource. They are required to detect the orientation of the dancer relative to gravity and the duration of the waggle phase and translate this into a flight vector with a direction relative to the sun⁹⁸ and a distance to be travelled from the hive^{87;301}. While verbal models have been discussed within the field and describe the presumed necessary processing of

this information at a coarse level, a definitive neural mechanism for this process has yet to be identified. In this chapter, we study in detail the positioning of nestmates and their antennae as they follow the waggle phases of a dance. We find that nestmates follow dances from varied, dynamically changing, positions around the dancer and uncover a previously unremarked correlation between antennal position and the relative body axes of dancer and follower bees. Combined with new information about antennal inputs^{56;195} and spatial encoding in the insect central complex^{189;190}, we show how a neural circuit first proposed to underlie path integration can be adapted to decoding the dance. This provides the first plausible account of how the bee brain could support the interpretation of its dance language.

4.1 Perspectives on following behaviour

Von Frisch¹⁰⁰ originally termed nestmates around the dancer *followers* due to their apparent motivation to follow behind the general path of the dancer. That is, some nestmates position themselves towards the dancer and follow behind them during the waggle phase and sometimes the return phase too. Several studies since have used this *active* following movement as a strict criteria for identifying valid followers (e.g. Božič and Abramson²⁹; Božič and Valentinčič³⁰; George et al.¹⁰⁶; Gil and Marco¹⁰⁸; Tautz and Rohrseitz³²⁰). For example, Božič and Valentinčič³⁰ categorised bees that extended their antennae towards the dancer but only occasionally moved with them as ‘dance attendants’ and excluded them from being followers. Reinforcing this notion, an early assumption^{146;209;262} was that nestmates could determine the signalled direction by aligning their body to be parallel with the dancer’s, such that their own heading angle equals the waggle phase foodward angle (Fig. 4.1, left). This ‘follow-behind’ idea is consistent with the behaviour of experienced stingless bees leading the inexperienced to the resource¹⁴⁷, and horizontal open-nesting honeybee species *Apis florea* dancing directly towards the resource instead of relative to gravity¹⁸³.

The most naïve proposal for a mechanism underlying this classical behaviour is that following behind the dancer allows nestmates to directly assimilate a foodward flight vector with respect to their own frame of reference. This is rather intuitive with respect to the path integration network described in Chapter 3: by aligning their body to be parallel with the dancer’s, nestmates could hypothetically charge the amplitude (length) of their foodward vector in tandem with the length of the waggle phase, whilst accumulating this in the correct direction to the resource. With an appropriate feeder distance to waggle duration mapping, followers could charge their vector at an accelerated rate in the hive. This approach would be akin to accumulating a flight vector should the nestmate happen to fly a straight path when foraging and discover the feeder. However, this means that only one follower bee can comfortably obtain the dance vector from directly behind the dancer at a time.

Whilst several experiments support the importance of follower bees being positioned behind the dancer^{108;146;209;262}, others suggest that this is not always the case^{30;152;318}. Earlier observations by Božič and Valentinčič³⁰ argued that nestmates appear to maintain their body to be nearly perpendicular to the dancer during waggle and return phases. In support of

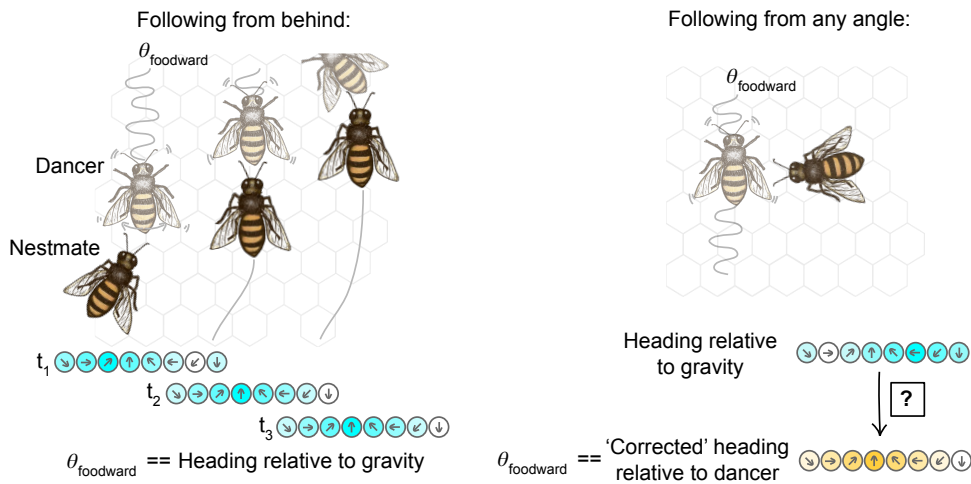


Figure 4.1. Assimilating the foodward angle (θ_{foodward}) when following from behind (left) versus from any angle (right) relative to the dancer. When following from behind, θ_{foodward} is equivalent to the nestmate's heading angle and we propose that the assimilation of vector could arise from the same neural circuitry that performs path integration when foraging. When following from any angle, a nestmate's heading angle must be corrected by its angle to the dancer in order to assimilate its foodward vector in the signalled direction. It is currently unknown how this is achieved.

this, Tanner and Visscher³¹⁸ reported that at least 35% of follower bees (9/26) that were successfully recruited to the resource by a dance had exclusively followed dancers from side-on. Such lateral positioning is common amongst subspecies of Asian honeybees too¹⁰⁶. This does not necessarily mean that information from the dance is collected better from the side of the dancer; in fact, Tanner and Visscher³¹⁸ found there was no significant difference in the accuracy between the bees following from behind versus side-on, as measured by their distribution in feeder traps positioned $\pm 45^\circ$ either side of the intended feeder. Most recently, Kietzman and Visscher¹⁵² observed that successfully recruited nestmates (i.e. recruits that arrived at the advertised feeder) could have occupied at least any one of the positions around the dancer (posterior, lateral or even anterior), even when only following for one dance circuit. Thus, nestmates appear capable of assimilating the vector information whether following *along* or following *behind*; although the collective mechanism underlying these abilities was unclear. When following from side-on or head-on, nestmates must proportionally adjust the angle in which they charge their foodward vector by their angle relative to the dancer (Fig. 4.1, right). Existing hypotheses have focused on how nestmates interpret signals to ultimately position themselves behind the dancer (e.g. near sound fields^{213;214}, and temporal patterns of antennal contact^{108;262}, see Section 2.2.3), instead of how this angle might be detected and corrected.

To examine which features of sensory input experienced by follower bees may enable them to detect this angle, we filmed Scottish black honeybees, *A. mellifera mellifera*, following dances in the hive advertising natural resources. This is a vertical cavity nesting species that is native to Scotland, whose common name is derived from their predominant brown-black colour and fewer yellow spots on the abdomen.

4.2 An observational study of follower bees

4.2.1 Dynamic variation of relative body axes

We first studied the positioning of 47 follower bees' relative body axes around dancers in the hive (Fig. 4.2a-c). The body axis was defined using the line connecting the centre of the thorax to the midpoint between the antennal bases. This meant that the axes of follower bees were not influenced by the possible bending of their abdomen when trying to maintain contact with the dancer²⁹⁶ and aligned more closely with their true head direction. Nestmates were defined as following a dance if facing towards the dancer and within one bees' length. We observed that follower bees were positioned all around the dancer. Most exhibited considerable changes in the angle of their body axis relative to the dancer throughout a waggle phase (Fig. 4.2b). Plotting this angle over time as a path, straightness values (straight-line distance divided by path length, i.e. consistency in maintaining the same angle to the dancer) were observed across almost the entire range of Batschelet's¹⁵ straightness index. Those that started to follow from particular angles (e.g. behind the dancer) did not appear to be any more consistent at maintaining it than those starting at other angles (Fig. 4.2b, right). In fact, few nestmates appeared truly consistent at maintaining an angle and these tended to be those that followed for a short time (Fig. 4.2c).

In contrast to previous studies¹⁰⁸, follower bees appeared to finish in various positions around the dancer instead of solely being clustered behind (Fig. 4.2c). This could reflect the different criteria used to identify follower bees; namely, such studies include only those that actively follow the dancer around the comb (which are also more likely to finish behind the dancer) and exclude those that face towards the dancer within a distance to receive contact but appear less motivated to actively move across the comb to pursue the dancer. No definition of valid follower bees can truly detract from the uncertainty surrounding (1) which nestmates are decoding the dance, (2) which will act on the information, and (3) which are following for some reason other than active foraging, such as waiting to unload nectar from the dancer²⁸³. There is no evidence to suggest that even the latter category of bees are not decoding the information, despite performing a different task. Therefore, we adopted an inclusive criteria, encompassing all nestmates facing the dancer within potential contact distance, regardless of active pursuit, as a proxy for interest in the dance.

It has been proposed that mechanosensory input via the antennae allows nestmates to assimilate the dance vector information when not aligned behind the dancer, a possibility known as the tactile hypothesis¹⁰⁸. Nestmates appear to position themselves at a distance where their antennae receive repeated contact with the dancer as it waggles by. Actual contact appears passive, that is nestmates do not actively touch the dancers with their antennae but instead are simply hit by the body moving past and exhibit no signs of collision avoidance^{30;108;262}. Recent work has also shown that genes are upregulated in the antennae of bees that use the dance (or *social*) information compared to those that rely on their own *private* information of route memories acquired during previous foraging trips¹⁴⁹. Using the antennae to obtain the information when positioned at any angle to the dancer should provide several advantages. It

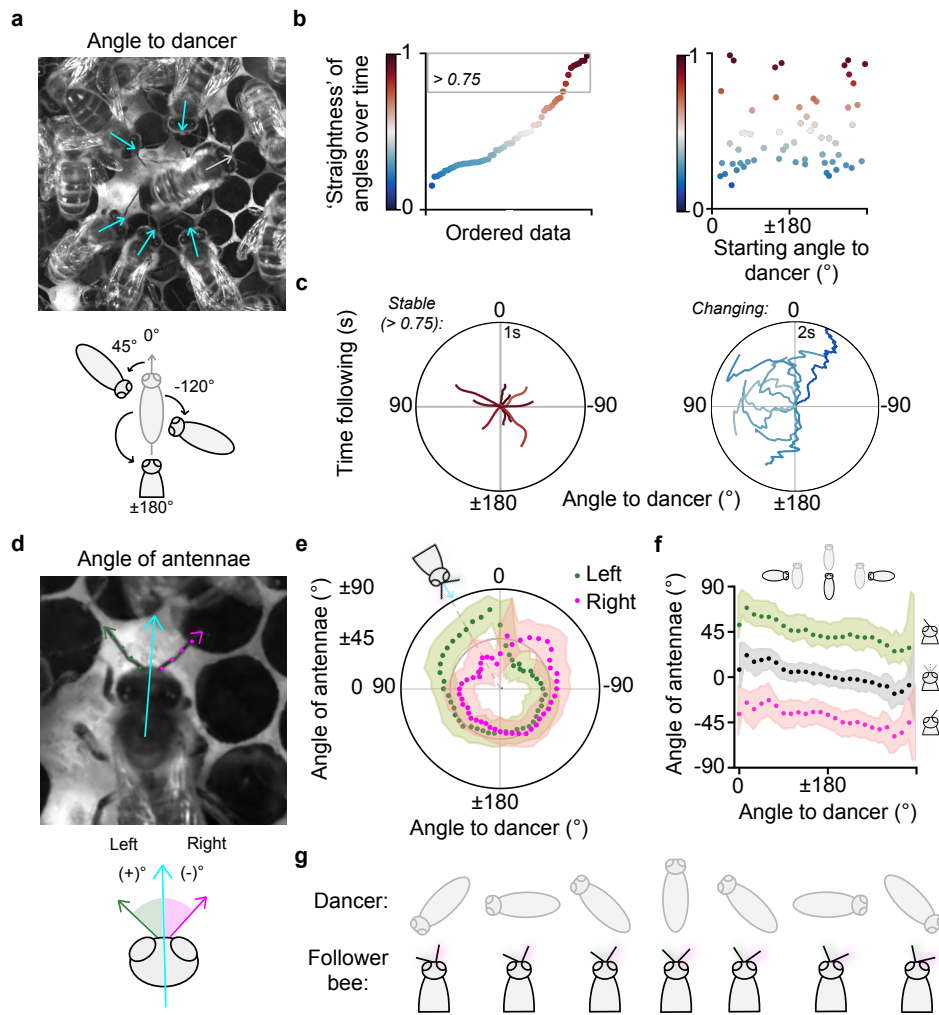


Figure 4.2. Positioning of follower bees and their antennae when following waggle phases.

Data from 47 bees across $n = 59$ total phases. **a**, Measuring the angle of follower bees' relative body axes (blue) with respect to the dancer (grey) when following the waggle phase. **b**, Batschelet's straightness index¹⁵ of bees' angles to the dancer treated as a path over time. A constant angle would have a value of 1. **c**, Stable (index > 0.75) and changing (index < 0.5) example paths coloured by their straightness index. **d**, Measuring the angle of a bee's left (green) and right (pink) antenna relative to its body axis (blue). Angles of the left antenna are denoted as positive angles and the right antenna denoted as negative. **e**, Angle of nestmates' antennae when positioned around the dancer. The distance from the origin indicates the antennal angles. The two circular boundaries indicate antennal angles of $\pm 45^\circ$ and $\pm 90^\circ$. Dots indicate the circular mean of left and right antennae angles computed across nestmates in 5° bins of angles to the dancer; shaded area represents mean \pm s.d. Dancers' directions have been normalised to 0° . **f**, The mean midpoint of nestmates' antennae (grey) along with the same data as in **e**. Data computed in 15° bins of angle to dancer; shaded area represents mean \pm s.d. Midpoint data circular correlation coefficient of -0.56 ($F = -56.76$, $P < 0.001$). **g**, Real nestmates' antennae when positioned at 45° (left) through to -45° (right) to the dancer. Adapted from Hadjitofi and Webb¹²² under CC BY 4.0.

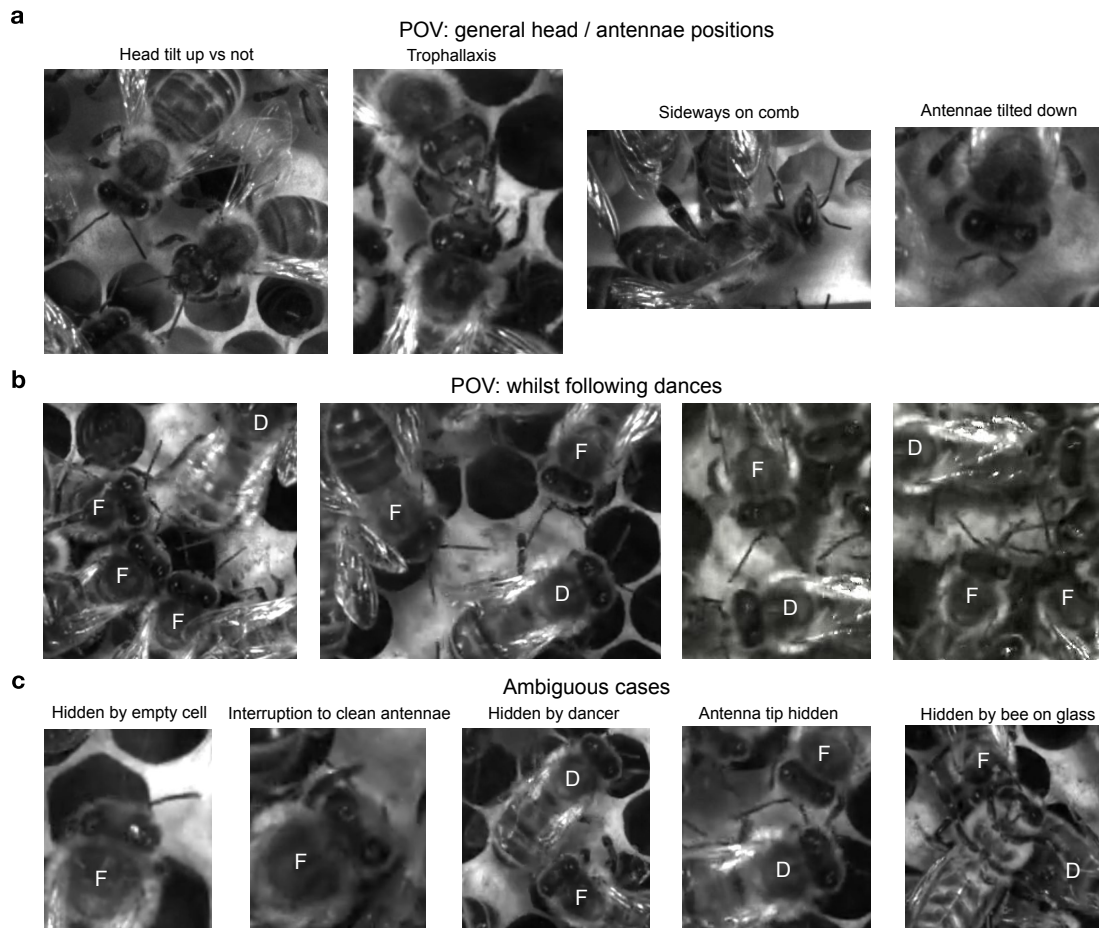


Figure 4.3. Point of view (POV) from camera positioned perpendicular to honeycomb. a, Examples of general head and antennae positions from around the hive. In such cases, the varying pitch and roll of head and antennae make it difficult to determine their true orientation. **b,** When following dances, nestmates' antennae are outstretched and they show a stable positioning of head, making it feasible to measure antennal angles from a top-down camera view. D and F indicate dancer and follower bee, respectively. **c,** Intermittent cases where determining the angle of antennae is not possible and excluded from the dataset. Adapted from Hadjitofi and Webb ¹²² under CC BY 4.0.

alleviates the constraint of limited space around and behind the dancer³²⁰. It does not rely on visual input, allowing communication in the darkness of a cavity nest, and removes any need for accurate positioning capabilities of a follower bee in relation to a dance. But how could antennae be used to detect the actual angle of the dancer relative to gravity from an arbitrary – and changing – relative angle between dancer and follower?

4.2.2 A relationship between antennal positioning and angle to dancer

We next tested whether antennal positioning could be used by nestmates to distinguish their angle relative to the dancer by tracking the antennae positions of followers in high-speed, high-resolution video (Fig. 4.2d-g). Compared to their movement elsewhere in the hive, when nestmates approach a dancer they exhibit a notably consistent posture, with antennae evenly

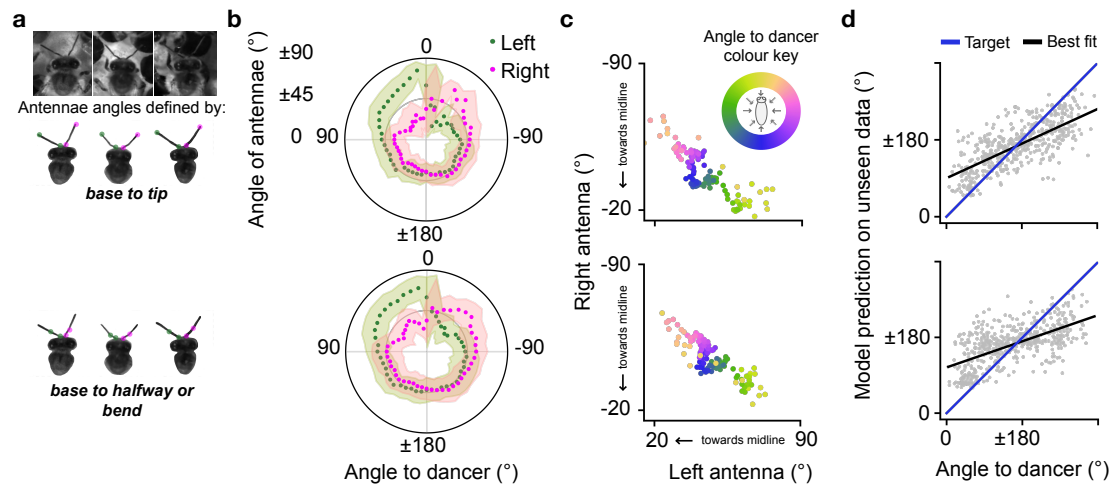


Figure 4.4. A similar relationship between antennal positioning and angle to the dancer is seen irrespective of whether the antennal angles are determined using the full length of the antenna (top row) or its base to halfway point (bottom row). **a**, Segmented bees with labels for defining the antennal angle using its full length ($n = 54$ total phases) or its halfway point or visible bend between the scape and pedicel ($n = 59$ total phases). **b**, Angle of nestmates' antennae when positioned around the dancer. Dots indicate circular mean computed in 5° bins of angle to dancer; shaded area represents mean \pm s.d. **c**, Mean positioning of the left versus right antennae computed for 3° bins of angle to dancer. Colour indicates angle to the dancer. **d**, Test predictions of a multivariate Gaussian process regressive model using antennal positioning to predict a nestmates angle to the dancer. Blue indicates target encoding and black is the best fit through the predictions using the angle defined by the full length of antennae (Pearson's $r = 0.68$, $P < 0.0001$), or the halfway point (Pearson's $r = 0.61$, $P < 0.0001$). Adapted from Hadjitofi and Webb¹²² under CC BY 4.0.

outstretched from their midline and their roll and pitch head orientation aligned with the plane of the comb (Fig. 4.3). The angle of an antenna could hence be estimated as the angle of the line connecting the base of the antenna to its tip.

We identified that the position of nestmates' antennae relative to their midline followed a unique relationship according to their positional angle to the dancer (Fig. 4.2d-g). When positioned on the left side of the dancer (e.g. between 0° and $+90^\circ$), the left antenna (green) is angled further away from the nestmates' midline whereas the right antenna (pink) is angled much closer. A similar but opposite effect is seen when on the right of the dancer (e.g. between 0° and -90°), with a smooth transition in between. We also found a statistically significant circular correlation coefficient of -0.56 for the relationship between the midpoint between nestmates' antennae and their angle to the dancer ($P < 0.001$, Fig. 4.2f). Earlier work¹⁰⁸ recorded the angle formed between the two antennae (rather than the angle of each antennae) at the end of each wagging movement but did not identify a consistent relationship of this angle to the follower's angle to the dancer. Recording at 200 frames per second (fps) captured around eight frames per waggle of the dancer's abdomen and indicates that this relationship is continual across wagging movements, i.e. it exists even when the dancer's abdomen had swung away from the follower.

Similar results were obtained when the angle of each antenna was defined as the angle of the line between the base of the antenna and the halfway point along it (Fig. 4.4). This reinforces the notion that the antennae are outstretched while dance-following. If there was a visible bend in the antenna (i.e. between the pedicel elbow-like joint and scape of the antenna), the position of this bend was used instead of the halfway point. This observation is consistent with early experiments where clipping the tips of both antennae did not lead to a reduction in the number of recruits arriving at the feeder⁷⁰. We also fitted a multivariate Gaussian process regression model to see how well the pairs of left and right antennae angles (using either tip or halfway point) could predict the angle of the nestmate relative to the dancer (Fig. 4.4d). The predictions on the test set confirm that the antennal angles are informative towards this angle, despite a degree of noise in the data.

4.3 A proposed circuit to recover the dance vector

The antennal relationship in Section 4.2.2 could allow the nestmate to detect its orientation relative to the dancer, but how could this be transformed into a flight vector towards food? In this section, we propose how a neural circuit modelled on the central complex (see Section 2.3) might use the antennal input that nestmates experience to acquire the signalled information as a flight vector that they can follow to the resource. This allows us to infer the food location after observing a single follower bee, which has never been possible before.

4.3.1 Vector assimilation by the central complex

Recent research^{189;190} has shown that the insect central complex contains circuitry that supports the transformation of angular variables from egocentric (body-centred) to allocentric (world-centred) coordinates. Optic flow-sensitive neurons (TN cells in the sweat bee³⁰⁵; LNO in the fruit fly^{189;190}) fire proportionally to the velocity component in directions of $\pm 45^\circ$ and $\pm 135^\circ$ around the insect. This motion appears to modulate the relative amplitudes of left and right (for front and back) sinusoidal bumps of activity in the brain that are otherwise yoked to the insect's head direction¹⁹⁰. Sinusoidal activity across a neural population can represent a flight vector, where the phase encodes the angle of the vector and the amplitude represents its length³²⁹. The projection pattern of these neurons to the fan-shaped body in the central complex supports a vector sum computation that results in an allocentric travel vector, enabling the insect to accurately track its ground velocity even when its motion is not directly aligned with its head direction (holonomic motion)¹⁹⁰. Moreover, it has been proposed that continuous integration of either the components³⁰⁵ or the downstream allocentric vector¹³⁹ could provide the neural basis for path integration. That is, a foraging bee that continually sums its travel vector (over a flight path varying in direction) will thereby maintain a 'home-vector' indicating the straight-line direction and distance it has travelled from its nest²¹⁶. Our key hypothesis is that a nestmate following a dance is similarly (and using the same neural circuitry) converting its egocentric orientation to the dancer to an allocentric estimate of the dancer's direction. This means that the follower uses its antennal positions to decode the angle

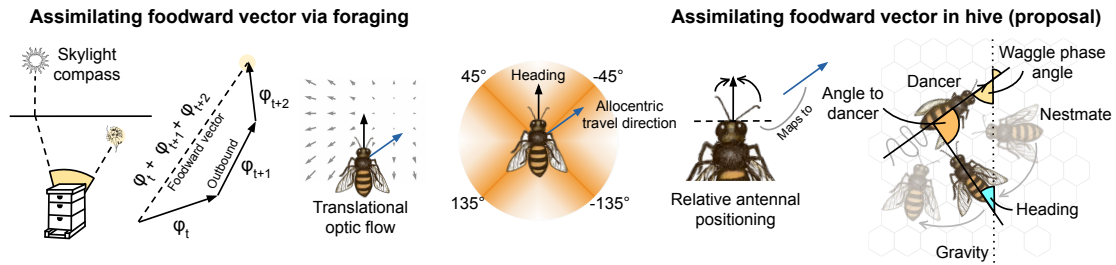


Figure 4.5. Proposed mechanism to assimilate the foodward vector (overview). **Left**, A foraging bee combines skylight compass information with optic flow to integrate ground velocity on the outbound path (segments indicated by φ_n) into a vector between home and food. **Middle**, The neurons sensing optic flow form an orthogonal basis to derive the allocentric ground velocity for holonomic motion (blue arrow). **Right**, By the same principle, a nestmate combines gravity sensing with antennal position to integrate the allocentric motion of the dancer during the waggle phase as a vector towards food. Adapted from Hadjitofti and Webb¹²² under CC BY 4.0.

between its body orientation and that of the dancer. Knowing its own orientation relative to gravity, this allows the follower to deduce the dancer's orientation relative to gravity, which is the direction of the food source relative to the sun⁹⁸. Crucially, this estimate of the dancer's orientation remains consistent (relative to gravity) over continuously varying angles of the follower to the dancer, so that by continuous integration of this estimate during a waggle phase the follower can obtain a corresponding foodward vector (Fig. 4.5).

Our model thus assumes that the relative positions of the antennae whilst following the waggle phase could modulate four sinusoidal gravity bumps to allow nestmates to charge their flight vector in the foodward direction, irrespective of their (changing) angle to the dancer (Fig. 4.6). This modulation is determined by first mapping the antennal angles to a 360° representation from their position within $\pm 90^\circ$ of the bee's midline, the maximum angle of either antennae observed (Fig. 4.6a). Within the central complex (Fig. 4.6b), the direction relative to gravity produces a sinusoidal bump in the ellipsoid body, and the antennal input differentially modulates four sets of neurons that convey the bump from the protocerebral bridge to the fan-shaped body with $\pm 45^\circ$ and $\pm 135^\circ$ anatomical offsets (Fig. 4.6c). Modulation is equal when the nestmate is directly behind the dancer, and varies proportionally as the antennal position becomes more extreme (Fig. 4.6d), such that the sum in the fan-shaped body always represents the allocentric orientation of the dancer (Fig. 4.6e). Simulating this circuit (Fig. 4.6f) shows that in principle this works perfectly to allow the dancer's vector direction to be recovered, for an arbitrarily changing nestmate position, and is robust to simulated noise in the antennal input.

This hypothesis requires two further assumptions:

1. The first is that bees can track their head direction relative to gravity within the hive. It is unknown how gravity is represented in the central complex, although it is well established that the head direction bump of activity in the central complex is influenced by a number of cues in the environment, including celestial¹³⁰, visual²⁸⁹ and proprio-

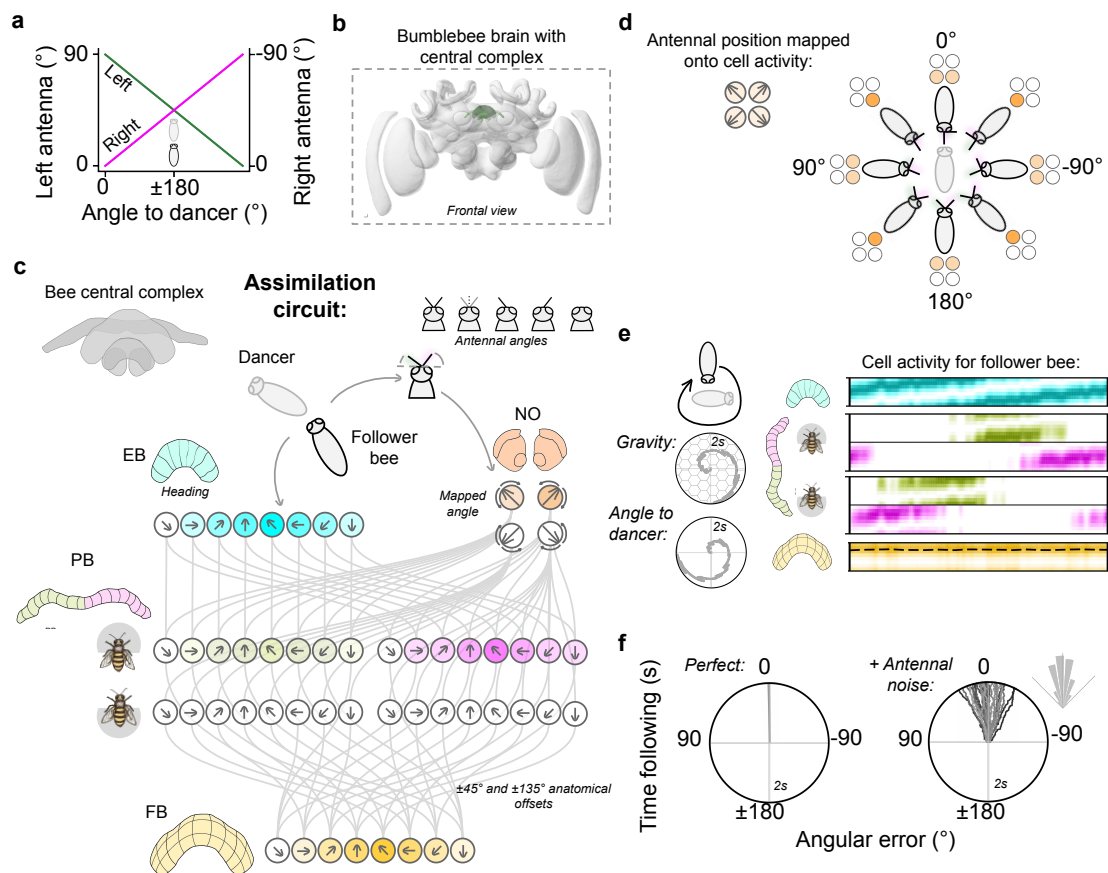


Figure 4.6. A central complex circuit to recover the allocentric dance angle. **a**, Relationship of the angle of a nestmate’s antennae to their angle to the dancer used in testing the circuit. **b**, Frontal view of a three-dimensional reconstruction of the bumblebee *Bombus terrestris* brain, with central complex neuropils illustrated in green (obtained from the insect brain database¹²⁸, www.insectbraindb.org; data from Rother et al.²⁶⁴). **c**, Example cell activations in the proposed assimilation circuit for a nestmate positioned at 147° relative to the dancer. Cells in the left and right sides of the protocerebral bridge (PB) (green and purple, for front and back) receive inputs from head direction cells in the ellipsoid body (EB) (blue) of the central complex which are multiplied by mapped antennal input from the noduli (NO) (orange), resulting in an amplitude modulation. Summing the four PB cell populations result in a vector that represents the signalled foodward direction relative to gravity in the fan-shaped body (FB) (yellow). Schematic illustration of the central complex neuropils shown in top left. Circuitry adapted and inspired by Lyu et al.¹⁹⁰. Connections between the EB and PB backward-sensitive cell populations are not shown for brevity. **d**, Example antennal positions mapped onto noduli cell activity, as a result of different orientations of the follower bee relative to the dancer. **e**, Example activity patterns of cell populations in **c** simulated for a nestmate (dark grey bee) changing orientation whilst following a dance (light grey bee). Dashed line indicates target allocentric orientation of dancer. **f**, Angular error of accumulated foodward vectors ($n = 25$) resulting from (top) perfect simulation of relationship and (bottom) simulation with noise added to antennae at each time step, drawn from von Mises distribution on the right ($\mu = 0^\circ$ and $\kappa = 10$). Adapted from Hadjitofi and Webb¹²² under CC BY 4.0.

ceptive³³³ cues. Bees are believed to mainly sense their orientation to gravity via sensory neurons of the neck hair plates^{35;187}. The removal of these hairs resulted in disoriented dancing on vertical combs in the dark but bees could still be able to orient with respect to the sun when on open horizontal combs¹⁸⁷. This loosely aligns with the idea that they detect their angle to the dancer using their antennae too; sensing their orientation to gravity with respect to their head direction may avoid having to further account for any bending of the abdomen while attempting to maintain contact with the dancer²⁹⁶.

2. The second assumption is that antennal position or motion can influence the processing of the directional bump. There is evidence from bees¹³⁴, locusts¹³⁵, cockroaches²⁶⁰ and flies^{56;238} that mechanical signals from antennae reach the central complex. Significantly, a recent study has found a basis vector representation (that is, neurons with peak sensitivity at $\pm 45^\circ$) encodes wind direction sensed via displacement of antennae in the fruit fly⁵⁶, similar to the optic flow input described above. In a following study¹⁹⁵, the authors' proposed that similar modulation of the head direction bump could allow an allocentric estimate of wind direction.

4.3.2 Real antennae data as input

We used the real set of antennae positions from each follower bee as input to the model to measure the directional accuracy of the assimilated foodward vectors (Fig. 4.7). We assume that the integration occurs during the frames in which the nestmate satisfies the 'follower' criteria (see Section 4.2.1) and the dancer is wagging. Note that this inherently produces a correlation between the length of the integrated vector and the waggle duration, implicitly encoding distance. In the bee, such gating of the integration could occur in the central complex¹⁹⁵. We suggest that the input could come from an auditory interneuron that has been observed³⁵ to have stopwatch-like behaviour encoding sounds^{208;213} emitted by the dancer during the waggle phase (see Section 2.2.3), the duration of which signals distance to the food source^{87;301}. Lacking information about this sound signal in our recordings, and also lacking 'ground truth' for the intended distance communication, our analysis focuses on the direction of the vector estimate rather than the length. However, our inclusive estimate of the waggle could also contribute to error in the direction that could be reduced by more precise gating of the integration period and thereby represents an upper bound on the error.

Antennal modulation improves accuracy of assimilated foodward vectors

We compared the performance of the assimilation circuit to the performance predicted by the simple 'follow-behind' hypothesis by calculating the vectors that would be assimilated if nestmates solely use their heading orientation relative to gravity to assimilate the vector (i.e. no antennal modulation). We found that simulated nestmates' estimated the average direction towards food significantly more accurately when using antennal information than when estimating based on their own orientation alone ($P < 0.005$, Fig. 4.7a). Angular error was largest for nestmates positioned anterior to the dancer and lowest for those positioned behind (Fig. 4.7b). Although some bees appear motivated to more actively pursue the dancer

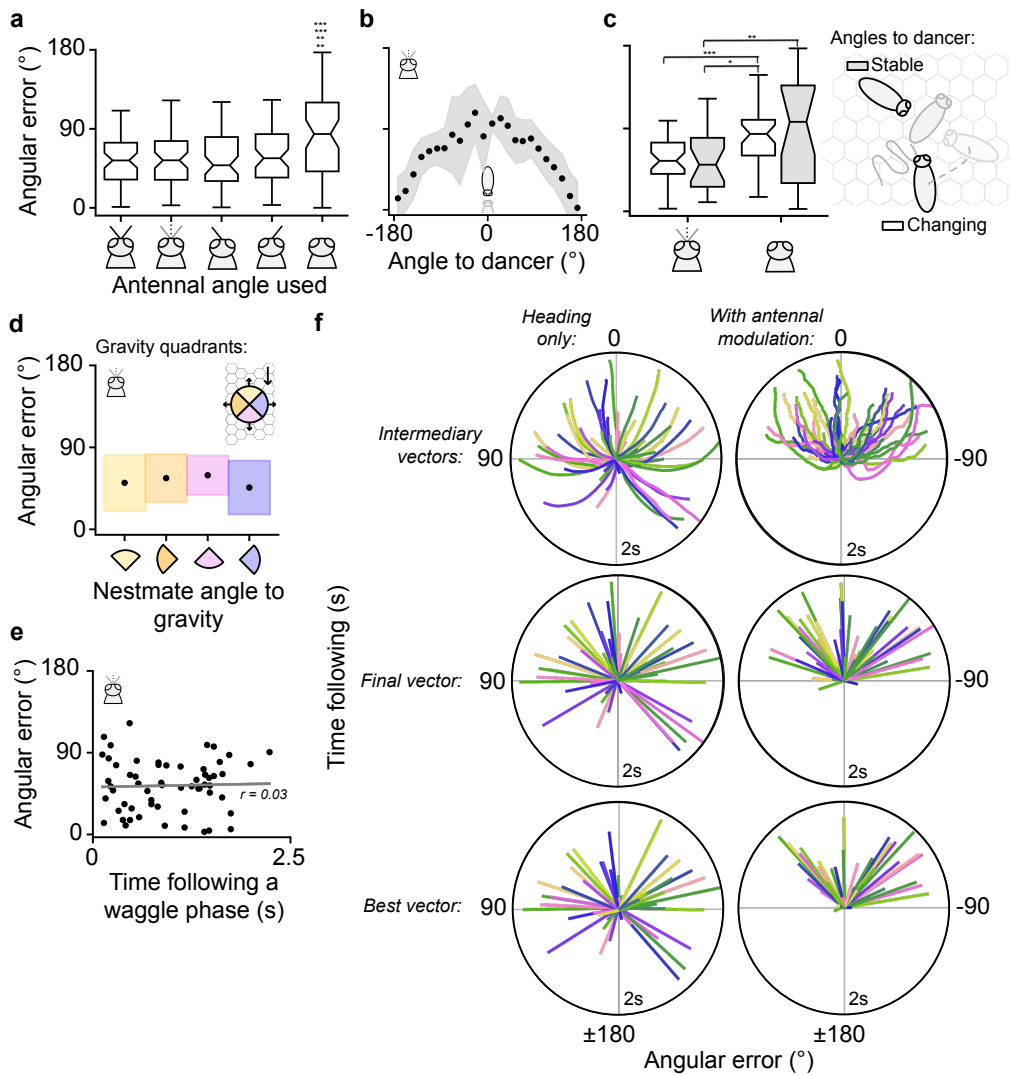


Figure 4.7. Deviation of decoded foodward vectors of nestmates relative to the dancer's mean waggle phase angle, as a result of feeding antennal positioning data to the assimilation circuit. Data from 47 bees across $n = 59$ total phases. **a**, Absolute angular error of assimilated vectors according to the feature of antennal position used: information from both antennae, midpoint of antennae, left antenna, right antenna or gravity heading only (without antennal modulation). Notches on boxplots indicate 95% confidence intervals for the median value. Asterisks indicate statistical significance between conditions (* if $P < 0.05$; ** if $P < 0.01$; *** if $P < 0.001$). **b**, Mean absolute angular error according to nestmates' angles to the dancer computed for 15° bins when using midpoint feature; shaded area represents mean \pm s.d. **c**, Absolute angular error according to nestmates that have more stable (straightness index > 0.5 , $n = 22$) or changing (index < 0.5 , $n = 37$) angles to the dancer. **d**, Mean absolute angular error according to nestmates' mean angle relative to gravity computed for four quadrants ($n = 16$, $n = 12$, $n = 15$, $n = 16$ phases, respectively). Dots indicate mean and height of coloured boundaries indicate s.d. **e**, Mean absolute angular error according to the time nestmates spent following a waggle phase (Pearson's $r = 0.032$, $P = 0.807$). **f**, Angular error at each time step (top row), at the end of following a waggle phase (middle row) or when most accurate (bottom row), using heading only (left) or antennal modulation (right). Colours for each nestmate are consistent across panels. **b-f** use antennal midpoint feature. See also Figs. A.2 and A.3. Adapted from Hadjitofi and Webb¹²² under CC BY 4.0.

around the comb whilst others do not, the accuracy of assimilation when using antennal information was independent of whether nestmates exhibited a changing or stable angle relative to the dancer during a waggle phase (determined using a straightness index threshold of 0.5) (Fig. 4.7c). Moreover, neither the nestmates' angles to gravity nor the time spent following a phase gave an apparent advantage to assimilating the foodward direction (Fig. 4.7d,e).

The performance of the 'heading only' condition will depend on the distribution of nestmates in a given dataset. For example, a dataset containing only follower bees behind the dancer will perform very well. Fig. A.2 shows that a hypothetical improvement is possible when nestmates are simulated in a uniform distribution around the dancer.

Recruits flight vectors are scattered but centred on the feeder

Fig. 4.7f shows the angular error of each nestmates' vector estimates at different points throughout following a waggle phase: the successive vector on each time step, the final vector accumulated at the end of following a waggle phase (i.e. to be stored in long term memory) and the most accurate vector. A positive angle indicates deviation to the left of the signalled food, and negative angle indicates a deviation to the right. Fig. A.3a shows the individual vectors for all four features of the antennal input. Utilising antennal positioning information considerably reduced the overall spread of recruits' flight vectors compared to when using the heading angle alone. Each vector type results in search flights that would be centred on the food source and fanned out in directions across the correct hemisphere containing the food. This spread is slightly larger than the range predicted when researchers have examined how much directional information is conveyed by dancers. Haldane and Spurway¹²⁵ estimated the directional indication in the dances from von Frisch's publications to have an information value of 2 bits (or Binary units), where a bit represents a single choice between two options. The more bits you have, the more complex information you can store. With 2 bits of directional data, a follower bee must theoretically choose between four 90° sectors for its outbound flight. More recently, Schürch and Ratnieks²⁷⁵, based on their own measurements, estimated it to be 2.9 bits, suggesting that followers have eight sectors of 45° each to choose from.

Vector averaging over multiple waggle phases improves angular accuracy

Previous work suggests that recruited nestmates fly in a direction that more closely resembles an average of many waggle phases, rather than any single phase³⁵. In line with this, whilst the length of time that nestmates followed an individual phase showed no effect on accuracy (Fig. 4.7e), we found that averaging the final vectors that nestmates assimilated at the end of consecutive waggle phases led to a significant reduction in the error ($P < 0.01$, Fig. 4.8a). Furthermore, the tendency for nestmates to switch sides of the dancer during consecutive waggle phases suggests that any errors that may be present on one side are likely to be counteracted over time (Fig. 4.8b). Fig. 4.8c shows an example of this apparent benefit, where an individual follower bee averages its vectors obtained over three consecutive waggle phases to yield a more accurate estimate of the foodward direction. Note that the estimate of vector length across these phases in this example are consistent too. Such vector averaging could also

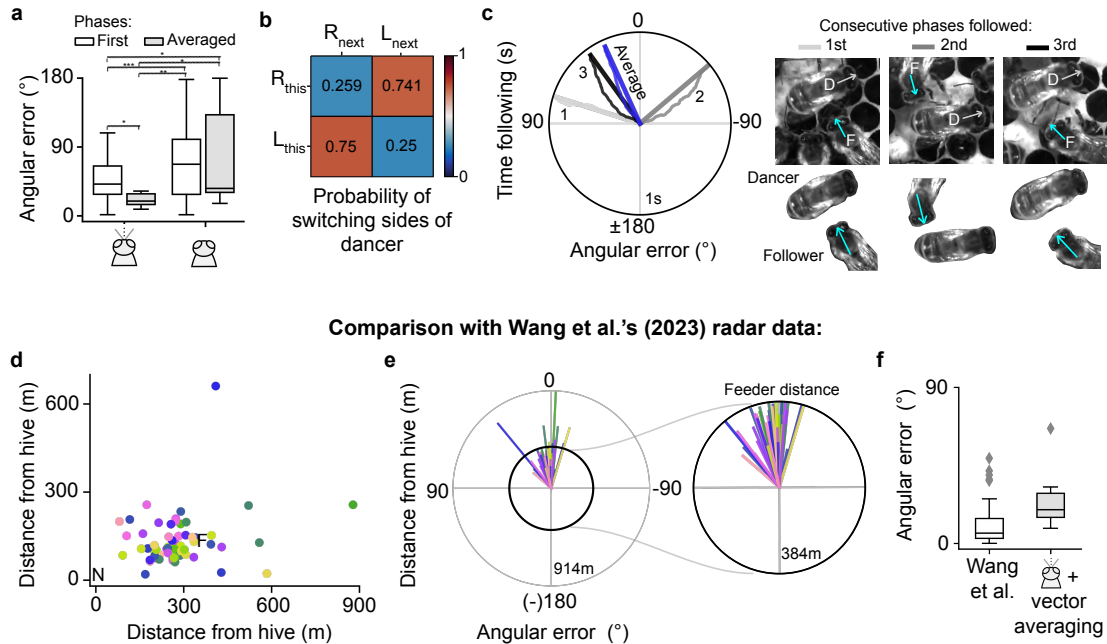


Figure 4.8. Averaging over consecutive waggle phases improves angular accuracy of the vector estimate. **a**, Absolute angular error of the final vector for nestmates that only followed one waggle phase (‘first’, $n = 38$) or when the final vector is averaged for nestmates that followed more than one consecutive phase (‘averaged’, $n = 12$). **b**, The probability of nestmates ($n = 27$) changing sides of the dancer when transitioning from ‘this’ to the ‘next’ waggle phase. L and R indicate left and right sides of the dancer, respectively. χ^2 test of independence: $P = 0.001$. **c**, Foodward vectors from a nestmate following three consecutive waggle phases. Thin lines indicate error at each time step; thick indicate the final vector for that phase; blue is the vector that arises if averaging across waggle phases. **d-f**, Comparison with recruits’ flight vectors from Wang et al.³⁴⁰ open source radar data. **d**, Final locations of the flight vector phases of follower bees ($n = 61$) recruited to a feeder via dancing. N and F represent the nest and feeder, respectively. **e**, Same data as **d** but the final positions are plotted as an angular error relative to the feeder. **f**, Absolute angular error for the harmonic radar dataset³⁴⁰ and our dataset when using the assimilation circuit with midpoint feature and vector averaging. Radar data URL: https://osf.io/a59rs/files/osfstorage?view_only=6da39e230c8d4072b27ab70ccecb06e2. Accessed: 2023-08-15. Adapted from Hadjitofi and Webb¹²² under CC BY 4.0.

minimise the impact of systematic curvatures in the waggle phase trajectories. For example, as noted in Chapter 3, it is possible that the dancer briefly indicates the incorrect direction as she begins to adjust her waggle angle to the intended foodward direction. If this occurs on both consecutive leftward and rightward deviated waggle phases, their effect on assimilation should be negligible when the vectors are averaged. Studies have shown nestmates following up to 15 consecutive waggle phases³⁵, although evidence also suggests that following four consecutive waggle phases is sufficient to estimate the variation of dancers across their entire dance⁵³. We observed nestmates following up to three waggle phases, a feasible number considering the resources required for annotating and tracking their antennae at 200 fps.

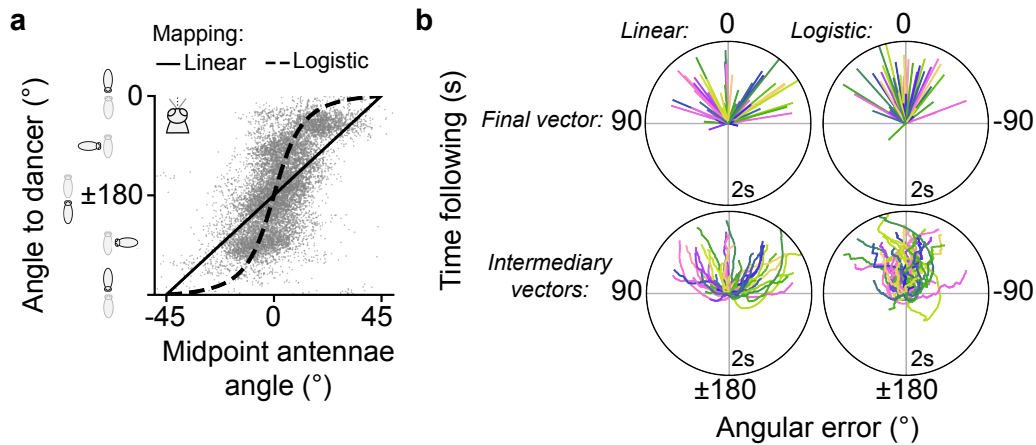


Figure 4.9. A non linear function improves the mapping of antennal angle to dancer angle. a, The original linear and the new logistic ($k = 11.2$) relationships tested when mapping the antennal midpoint to a corresponding angle to the dancer. **b,** Resulting angular error of the decoded vector relative to the dancer’s mean waggle phase angle, at the end of following a waggle phase (top row) and at each time step (bottom row).

Comparison with existing radar data

We have also plotted open source data from Wang et al. ³⁴⁰ showing recruits’ final vector search positions tracked via harmonic radar, after following dances within the hive signalling a new feeder (Fig. 4.8d-f). The performance of the assimilation circuit (augmented with vector averaging) appears to be comparable, even though the recruits in the Wang et al. ³⁴⁰ study likely followed multiple waggle phases and may have used additional cues for interpreting the waggle (discussed below in Section 4.4). We thus consider it to be fairly conservative to compare these data to our proposed assimilation circuit with vector averaging. We also note that the spread is larger for recruits that have been displaced from the hive before flying their dance-acquired vector (see Fig. 3 in Wang et al. ³⁴⁰) but the authors attribute this to other navigational influences so we have not included these data in the comparison.

A non linear antennal mapping function

We lastly experimented with using a non linear function to map the antennal midpoint to an angle to the dancer across the range of 360° (Fig. 4.9a). Fig. 4.9b shows the assimilated vectors, in their final and intermediate forms, produced from the assimilation circuit when using a logistic mapping function ($k = 11.2$) compared to the original linear mapping function. The mean \pm s.d. for the final vectors obtained from the different functions are $2.68^\circ \pm 34.71^\circ$ and $-2.03^\circ \pm 52.46^\circ$, respectively. Whilst the logistic mapping increases the sensitivity near the antennal midpoint values around 0° (i.e. the steepest section of the function), as evidenced by the variability of intermediary vectors, the overall spread of the final vectors is significantly smaller based on an Equal Kappa test for the homogeneity of the distributions’ concentration parameters ($\chi^2 = 7.18$, $P = 0.0074$). Thus, non linear functions may allow the model to better capture the relationship between the antennal position and the angle to the dancer.

4.4 Discussion

We have reported a novel feature of antennal positioning of bees following a dance: that it correlates to their angle to the dancer. Combining this with recent insights in the vector-processing circuitry of the central complex, we proposed a plausible mechanism by which the follower could assimilate a vector indicating the resource being advertised. Specifically, supported by recent characterisation of pathways between antennal input and the central complex^{56;195;238}, we suggested that antennal positioning during the dance maps to an orthogonal basis vector representation that is known to exist for other cues: wind⁵⁶ (also sensed via the antennae) and optic flow¹⁹⁰. Then, following the previously proposed principle for using such a basis to map head direction to allocentric ground velocity and integrate this into a home vector³⁰⁵, we demonstrated through modelling that, in principle, the same neural circuit could be used to integrate the dancer's direction relative to gravity, forming a food vector.

An antennal response for orientation and tracking tasks has been identified in several insects. In crickets, the antenna closest to an object moving horizontally in the visual field will track the object whilst the head remains fixed^{136;362}. In the fruit fly, the difference between left and right antennal displacements generates a linear code for wind direction³¹¹ and can be further tuned by active antennal movements³¹². In this work we have tacitly assumed that the nestmate's antennal position is a consequence of its angle to the dancer, e.g. the antennae are passively deflected further by the dancer's body when at more extreme angles to it. However we cannot rule out that some other sensory cue provides the information about this angle and leads the nestmate to actively adopt different antennae positions. Indeed it seems likely that the mechanosensory experience of the bee, either through other antennal cues such as the force exerted on them, or other tactile, wind, or electric-field¹¹⁸ sensing systems, is substantially richer than the one simple kinematic measurement we have made. The integration of such cues (although difficult to measure) could significantly improve the estimate of the angle, and consequently the accuracy of the vector. Towards this, developments in biomimetic robotic dancers^{171;172} present a potential future avenue to measure other aspects of the interaction. For example, the force or timing of antennal contact perceived by the follower could be measured by equipping the robot's abdomen or body with force sensors. There are many additional sensory cues emitted by the dancer in the hive that may also play a role in communication, including olfactory and chemical cues³²⁴, temperature³⁰², and comb vibrations^{232;267;320} (see Tables 2.1 and 2.2). These may assist nestmates in identifying, localising, and broadly orientating towards dancers within an area of the hive, but seem unlikely to provide accurate information about relative angles.

This work also assumes that follower bees have an internal representation of their head direction relative to gravity that arrives at the ellipsoid body in the central complex. Gravity is most likely detected through mechanosensors (e.g. antennae in *Drosophila*^{148;309}, and sensory neurons of the neck hair plates in bees¹⁸⁷) and we would hypothesise that the mechanosensory pathway via the ring neurons²³⁸ would subserve the formation of a 'gravity bump', whereas the pathway via the noduli to the fan-shaped body⁵⁶ would subserve the orthogonal basis

representation that transforms this to an allocentric direction estimate. We initially considered whether the vertical comb's regular hexagonal pattern of cells could also help bees sense their angle relative to gravity. However, there are clear contexts whereby the regular pattern of the comb is not available, such as in swarming and other species of honeybee where the dancing takes place on top of other bees¹⁸³.

It is difficult to ascertain what accuracy should be expected for the nestmates' assimilation of the foodward vector. The unpredictability of the dispersal and quality of foraging patches for bee colonies may reduce the evolutionary pressure to minimise communication error²³⁴. Determining the true nature of the information transfer requires a sophisticated setup: (1) the foraging of prospective dancers constrained to a known location, (2) the identity and behaviour of both the dancers and naïve followers recorded in detail in the hive, and (3) accurate tracking of every follower bee's immediate subsequent search flight, ideally after displacement so that only vector information can be used to direct their path. Historically there have been several attempts to characterise the accuracy of information transfer, e.g., from the distribution of recruited nestmates on an arc of feeders surrounding the one to which the dancer was trained^{99;315}. Alternatively, harmonic radar has also been used for tracking flight behaviour. We have plotted open source data from Wang et al.³⁴⁰ showing recruits' final vector search positions obtained from the dancer to a previously unknown feeder (Fig. 4.8d-f). We note that the recruits are scattered in varied directions (and distances) centred on the feeder, and believe it is plausible that such a distribution could arise from the base model described here with appropriate vector-averaging over consecutive waggle phases or augmented with additional mechanosensory cues (Fig. 4.8f). In Chapter 5, we conduct an experiment to explore the accuracy of the recruitment system and test the predictions of the assimilation circuit against the flight vectors expressed by real bees.

This work only provides a proof of principle: given the follower's antennal positions as input, a model of the neural circuitry of the central complex could recover the vector signalled by the dancer. It is currently beyond the state-of-the-art to directly measure the neural activity in actively dancing bees or their nestmates at the level of detail needed to test our hypothesis for assimilation of the vector. However, some new developments are bringing this possibility closer^{20;39} and our model predicts a particular convergence of sensory pathways in the central complex. Experiments in other insects, such as *Drosophila*, might meanwhile provide evidence for (or against) some of our key predictions: that a vertically oriented insect experiences a gravity orientation bump in the ellipsoid body and protocerebral bridge; and that antennal inputs can modulate the processing of an orientation bump in an equivalent coordinate transformation as seen for optic flow inputs to the fan-shaped body (i.e. an egocentric to allocentric frame of reference).

4.5 Methods

4.5.1 Honeybee data

Data collection and labelling. Honeybee data was collected during late summer (August 2022) and complied with the ‘Principles of Animal Care’, publication No. 86-23, revised 1985 by the National Institute of Health, and with the current laws of the country in which the bees were kept (Scotland). We filmed a colony of *A. mellifera mellifera* bees housed in a three-frame observation hive. Waggle dances of bees foraging at natural food sources were filmed at 200 fps under infrared illumination (690 nm), using a Basler acA1440-220UM ace camera and a 6 mm lens. The start and end of the waggle phase was determined by the first and last video frames where the dancer’s abdomen had swung to one side relative to its head direction. In each frame of the waggle phase, we extracted the angle of each follower bee relative to the dancer as well as the angle of their antennae relative to their body axis angle (also called ‘midline’). This was done by manually annotating key body parts using the DeepLabCut interface^{196;225} (Fig. 4.10a). A honeybee antenna is divided into three main sections: the scape, pedicel and flagellum. These are described in Section 2.2. When visible, we labelled the centre point of a bee’s thorax as well as the base, halfway point and tip of their left and right antennae. In cases where there was a bend in the antenna (i.e. between scape and pedicel), this point was labelled instead of the halfway point.

Extracting angles. From the labelled body parts, we determined the angle of each follower bee relative to the dancer, where the angle of a bee was defined using the straight line stemming from their thorax to the midpoint between the bases of the left and right antenna. The angle of an antenna relative to the midline was determined using the straight line stemming from the base to the tip of the antenna, or the base to the halfway point (or bend) in the case the tip was not visible. We depict these using negative angles for a clockwise rotation and positive angles for a counterclockwise rotation (in degrees). For example, 0° corresponds to the situation in which the follower faces the dancer head-on in the case of body axis orientation, or an antenna being directly aligned with the follower bee’s own body axis. 90° refers to the follower facing eastward towards the dancer or an antenna being positioned 90° to the left relative to their body axis. Fig. 4.10b shows an example of how we compute and present these angles on a polar plot. The bees’ heading relative to gravity is also determined from the angle of their body axis relative to the vertical axis (both the hive and filming rig were aligned beforehand using a spirit level and weighted string). Follower bees were also tracked over as many consecutive waggle phases that they followed, where their angles, identity and the side they followed from were recorded. The final dataset included the data of a total of 47 follower bees as they followed waggle phases of a dance. Each follower was measured from the start to end of their time following each waggle phase, with a minimum of 0.3 s and a maximum of 2 s (the full length of a waggle phase in the dataset). The dataset is deposited at Figshare¹²³.

External datasets. Wang et al.³⁴⁰’s open source harmonic radar data was used to compare the general range of accuracy predicted by the assimilation circuit with real vectors flown by recruits (see Fig. 4.8d-f). The published dataset was accessed and analysed based on the documentation

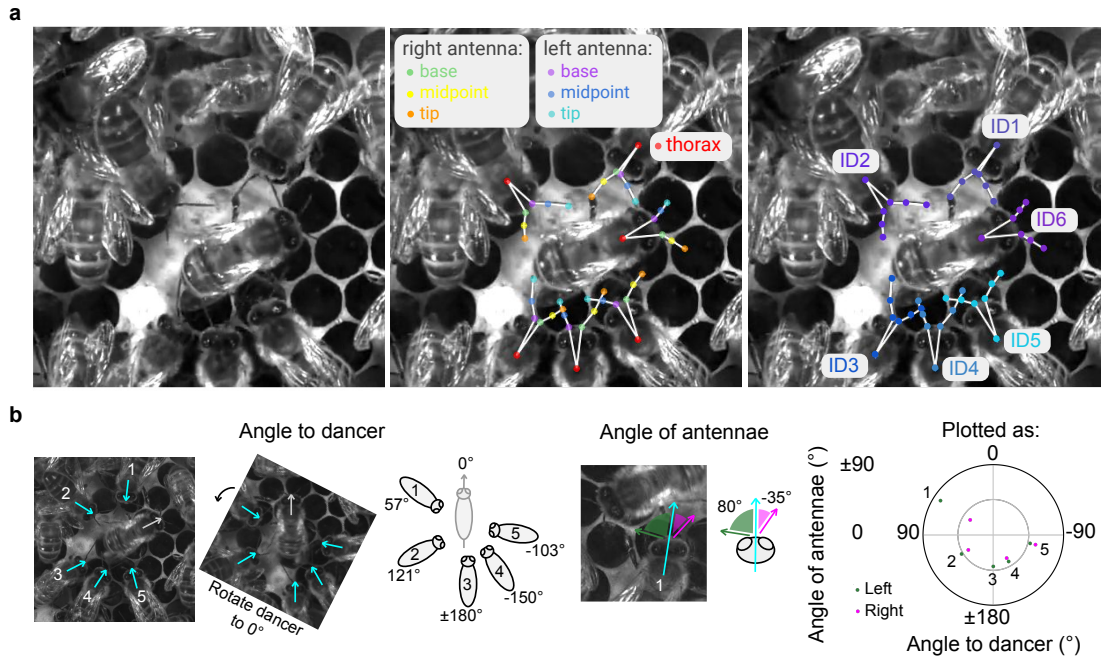


Figure 4.10. Labelling and visualisation pipeline of follower bees. **a**, Nestmates following a dancer in the midst of a waggle phase (left) with labels on the central points of each bees’ thorax and its connection to the base, halfway point and tip of each antenna (skeleton shown in white) (middle). Identities are tracked across frames to obtain trajectories (right). **b**, Example computation and plot of follower bees relative to the dancer and the angles of their antennae relative to their body axes. The distance along the radius of the polar plot indicates the antennae angle (positive for the left antenna and negative for the right) and the angle of the data points (relative to 0°) indicates the angle to the dancer. Adapted from Hadjitofi and Webb¹²² under CC BY 4.0.

provided by Gallistel and Beetz¹⁰¹. In their experiment, foragers were signalling a feeder that was 384 m from the hive and at a compass bearing of 60° relative to North. Recruits were captured upon leaving the hive after following a dance and fixed with a radar transponder to track their subsequent flight path. Fig. 4.8 presents the last recorded locations of the *vector* portion of the flights, which were separated from any final *search* portions by identifying sudden turns between two consecutive radar readouts that were larger than 60°.

4.5.2 Rate-based assimilation circuit

Antennal input. The angles of the left and right antennae (θ_L and θ_R) are first determined with respect to the nestmate’s heading (described in Extracting angles in Section 4.5.1) and clipped between a minimum and maximum position determined by the data. In our case, this is between 0° and ±90°,

$$0 \leq \theta_L \leq \frac{\pi}{2} \quad -\frac{\pi}{2} \leq \theta_R \leq 0 \quad (4.1)$$

We also investigated other maximum antennae angles, e.g. down to ±60°, to test the limits

of the relationship; these led to more variable vector estimates, in particular when using information from the left or right antenna only, or both (Fig. A.3b). The model uses the relative positions of the antennae whilst following the waggle phase to differentially modulate four sinusoidal gravity bumps to change their flight vector in the foodward direction (Fig. 4.6). To determine the modulation, features of antennal position are mapped onto the activity of four neurons (two in each hemisphere), corresponding to peak sensitivity at 45° , -45° , 135° and -135° , respectively. These are based on the optic flow sensing cells in the noduli – TN cells in the sweat bee³⁰⁵; LNO in the fruit fly^{189;190} – which fire proportionally to the velocity component in their preferred directions, modelled as a dot product. The antenna-induced output (AIO) of these cells is defined by,

$$f(x) = [\cos x, \sin x] \quad (4.2)$$

$$g(\theta_{pref}) = [f(\theta_{heading} - \theta_{pref})f(\phi_L)^T, f(\theta_{heading} + \theta_{pref})f(\phi_R)^T] \quad (4.3)$$

$$AIO_{front} = g\left(\frac{\pi}{4}\right) \quad AIO_{back} = g\left(\frac{3\pi}{4}\right) \quad (4.4)$$

where $\theta_{pref} = \frac{\pi}{4}$ and $\theta_{pref} = \frac{3\pi}{4}$ are the offset preference angles for each pair of front ($\pm 45^\circ$) and back ($\pm 135^\circ$) sensitive neurons respectively, and ϕ_L and ϕ_R are antennal features (described below) for the left and right sides. To test whether the accuracy of vector assimilation varied when different features were used (see Fig. 4.7), the activity of these neurons was determined using the midpoint of the antennae, where we set $\phi_L = \phi_R = s(\mu)$; information from the left antenna only, $\phi_L = \phi_R = s(\theta_L)$; right antenna only, $\phi_L = \phi_R = s(\theta_R)$; and information from both, $\phi_L = s(\theta_L)$, $\phi_R = s(\theta_R)$,

$$\mu = \text{atan2}\left(\sum_{i \in \{L,R\}} \sin \theta_i, \sum_{i \in \{L,R\}} \cos \theta_i\right) \quad (4.5)$$

$$s(x) = \theta_{heading} + \lambda x \quad (4.6)$$

where s is a linear mapping function to scale the range of possible antennae positions to a range of angles relative to the dancer. We set $\lambda = 4$ to map to a 360° range of possible angles (shown as $\pm 180^\circ$). We also investigated a modified logistic function to map the midpoint antennal feature to an angle to the dancer instead of a linear function (Fig. 4.9). For this case, Eq. (4.6) becomes,

$$s(x) = \theta_{heading} + \left(\frac{1}{1 + e^{-k(x-\frac{1}{2})}}\right) \quad (4.7)$$

where k is a parameter representing the steepness of the function, which was optimised against the data to be $k = 11.2$ using orthogonal distance regression²⁵. Using this logistic function to determine the mapped angle appears to lead to an improvement for the majority of the assimilated vectors (Fig. 4.9b).

Gravity bump. The head direction is calculated relative to gravity (described in Extracting angles in Section 4.5.1) and represented as a sinusoidal bump of activity, akin to the head direction bump seen in the ellipsoid body and known to be influenced by celestial¹³⁰, visual²⁸⁹ and proprioceptive³³³ cues. At each time step, the model creates a sinusoidal encoding of the heading ($Bump_{gravity} \in \mathbb{R}^8$) across a population of eight neurons representing eight cardinal directions relative to gravity,

$$Bump_{gravity} = \frac{1 + \cos(\theta_{cardinal} + \theta_{heading})}{2} \quad (4.8)$$

where $\theta_{cardinal} = [0, \frac{1\pi}{4}, \frac{2\pi}{4}, \frac{3\pi}{4}, \frac{4\pi}{4}, \frac{5\pi}{4}, \frac{6\pi}{4}, \frac{7\pi}{4}]$ and \cos is applied element-wise. The peak activity of the bump therefore tracks the angular movements of the bee relative to gravity whilst following a dance.

Sinusoid modulation. Four copies of the $Bump_{gravity}$ are replicated in the protocerebral bridge. The amplitude of each is modulated proportionally by the corresponding projection of the angle to the dancer, inferred from the antennal input, onto the four *AIO* projection axes. Hence there are modulated copies on the left and right sides of the bridge for both front ($Bump_{mod_{front}} \in \mathbb{R}^{16}$) and back ($Bump_{mod_{back}} \in \mathbb{R}^{16}$) *AIO* axes,

$$Bump_{mod_{front}} = (AIO_{front} W_{AIO \rightarrow Bump_{mod}}) \odot (Bump_{gravity} W_{Bump_{gravity} \rightarrow Bump_{mod}}) \quad (4.9)$$

$$Bump_{mod_{back}} = (AIO_{back} W_{AIO \rightarrow Bump_{mod}}) \odot (Bump_{gravity} W_{Bump_{gravity} \rightarrow Bump_{mod}}) \quad (4.10)$$

where \odot is element-wise multiplication, and $W_{Bump_{gravity} \rightarrow Bump_{mod}}$ is the matrix representing the connectivity pattern between the $Bump_{gravity}$ and $Bump_{mod}$. Fig. 4.11 visualises the connectivity matrices. These neurons are based on the populations of protocerebral bridge-fan-shaped body-noduli (PFN) neurons, PFN_d and PFN_v , in the fruit fly¹⁹⁰ (see Section 2.3).

Allocentric orientation of the dancer. Following observations by Lyu et al.¹⁹⁰, the projections of the $Bump_{mod}$ neuron populations from the bridge to neurons in the fan-shaped body result in anatomically shifted inputs that implement a vector sum, where the amplitudes and phases of the sinusoids correspond to the length and angles, respectively (see Fig. 4.11; see Lyu et al.¹⁹⁰ for a detailed description of the projection anatomy). This promotes sinusoidal activity across eight neurons that represent the allocentric bump relative to the dancer's orientation ($Bump_{dancer}$), which accumulates in short-term memory ($Memory_{Bump_{dancer}}$) with a gain (*gain*, set to 0.005),

$$Bump_{dancer} = Bump_{mod_{front}} W_{Bump_{mod_{front}} \rightarrow Bump_{dancer}} + Bump_{mod_{back}} W_{Bump_{mod_{back}} \rightarrow Bump_{dancer}} \quad (4.11)$$

$$Memory_{Bump_{dancer}}^{t+1} = Memory_{Bump_{dancer}}^t + gain Bump_{dancer} \quad (4.12)$$

This bump is then decoded at each timestep t (Fig. 4.7f) using the fast fourier transform²³³, and the error between the angle of the decoded vector and target vector is calculated. A positive error angle indicates that the assimilated vector is deviated to the left of the target angle (counterclockwise rotation) and a negative error indicates it deviates to the right (clockwise).

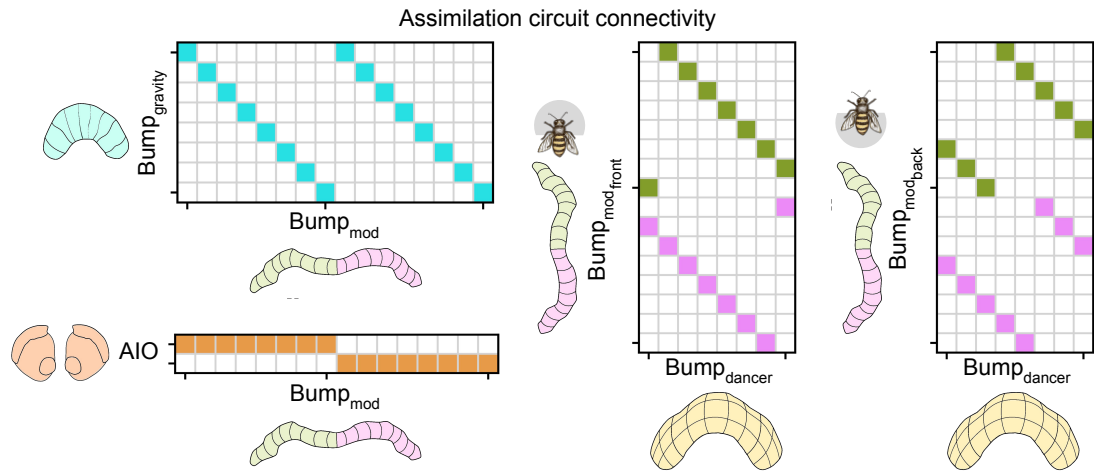


Figure 4.11. Connectivity of the assimilation circuit. See Section 4.5.2 for corresponding details on cell populations in the ellipsoid body (blue), noduli (orange, where AIO refers to antennal induced output), protocerebral bridge (green and pink) and the fan-shaped body (yellow). Cells were modelled as excitatory and colours indicate a value of 1. The projections that convey the four modulated bumps in the bridge ($Bump_{mod_front}$ and $Bump_{mod_back}$ for both the left (green) and right (pink) hemisphere) to the fan-shaped body ($Bump_{dancer}$) assume equal weighting. Read matrices as: e.g. the top matrix represents the connectivity between $Bump_{gravity}$ and $Bump_{mod}$, referred to as $W_{Bump_{gravity} \rightarrow Bump_{mod}}$ in the Methods. Adapted from Hadjitofi and Webb¹²² under CC BY 4.0.

4.5.3 Data analysis and statistics

Analysing changes in body orientation. To determine whether nestmates maintain a particular body orientation whilst following a dance, we constructed trajectories composed of their angles to the dancer along constant step-size points in time (i.e. viewing a trajectory as a stream of body axis angles for a bee). The Batchelet’s straightness index¹⁵ was then computed as D/L , where D is the straight-line distance between the first and last points in the trajectory, and L is the path length travelled (Fig. 4.2b). The index ranges between 0 and 1, where 1 indicates a constant angle. The raw body axis angles of nestmates show a small oscillation due to the dancers’ waggles and the angle of nestmates being recorded relative to the dancer in each frame. We smoothed these oscillations in this part of the analysis by applying a Savitzky-Golay filter using the `traja`²⁹² Python library prior to computing the straightness index. The values of each nestmates’ index were later used to categorise them into stable and changing orientations using a threshold of 0.5, when evaluating the circuit’s performance (Fig. 4.7c).

Multivariate Gaussian Process regression. We fitted a multivariate Gaussian Process regression model (see Schulz et al.²⁷³) to see how well pairs of left and right antennae angles could be used to predict the angle of the nestmate relative to the dancer (Fig. 4.4d). The cosine and sine transformations of the left and right antennae angles were used as features for the model. The data was divided into training and test sets using a 70 / 30 split, with individual nestmates featuring in only one set. Model fitting and optimisation of parameters was performed using the `mgpr` R library³³⁵, and predictions on the unseen test data were obtained. Pearson’s r coefficients were calculated to evaluate the predictions.

Model performance. The neural model was evaluated based on the angular error of the decoded vectors relative to the signalled food (normalised to 0° across dancers) when using antennal positioning information or heading orientation relative to gravity as input (Fig. 4.7). The latter assumes that follower bees assimilate the vector from their heading orientation only, as suggested by early hypotheses that nestmates vie for a position directly behind the dancer¹⁴⁶, where their angle to the gravity equals the waggle phase foodward angle. For each nestmate, the mean absolute vector error was computed with respect to the mean orientation of the dancer over the period that the nestmate had followed for (Fig. 4.7a-e, Fig. 4.8a). Fig. 4.7f shows the (signed) vector error for each time step. The mean error for a nestmate was determined by either using all intermediary vectors accumulated successively throughout following a waggle phase (Fig. 4.7a-f, Fig. 4.8c), the final vector accumulated by the end of following a waggle phase (the vector stored in long-term memory) (Fig. 4.7f, Fig. 4.8c) or the most accurate vector at any point during following a phase (Fig. 4.7e,f). The mean error of vectors averaged over consecutive waggle phases was computed as the circular mean of the final vectors assimilated from consecutive waggle phases (Fig. 4.8a). For brevity, model results after Fig. 4.7a are only reported for the antennal midpoint feature along with the condition without antennal modulation.

Transition counts. The tendency for nestmates to switch sides of the dancer for consecutive waggle phases that they followed was determined by calculating the first-order Markov transition probabilities (Fig. 4.8b). For example, the transition probability (TP) of following the dancer on her right side after just following on her left side (LR) was calculated as, $TP_{LR} = LR/(LL + LR)$, where LR indicates the corresponding frequency counts for that sequence across the data and so on. The observed counts were evaluated using a chi-square test of independence, $\chi^2 = 10.359$, $P = 0.001$.

Analysis software. Data analysis and modelling was carried out using Python or R code, relying mainly on Numpy¹²⁷, Scipy³³⁶, and Pandas²⁰⁰ libraries. Seaborn³⁴² and Matplotlib¹⁴⁰ were used for plots. This code is publicly available on GitHub (<https://github.com/annahadji/dance2vec>). The code contains the necessary elements reproduce results in this chapter (e.g. model simulation, processing of raw antennal data).

Statistical tests. All plots show the mean \pm s.d. unless stated otherwise. Circular equivalents were used where appropriate. Groups were compared using two-sided statistical tests, including Kruskal–Wallis H test (as data non-normal, tested by Levene’s test for equal variance and Shapiro–Wilk normality test) with post hoc Dunn’s testing for pairwise comparisons, and chi-square test of independence. The Wilcoxon signed-rank W test was used to compare groups of paired data (i.e. different antennal features or modulation conditions across the same bees), and for comparing more than two paired groups, the Friedman test was used with Bonferroni adjusted post hoc tests. Pearson’s r correlations were used to investigate data and model fit relationships. P value ranges are reported in the figure legends, and we provide the full list of statistics here.

The following P values are associated with Fig. 4.7a, comparing the angular errors obtained with no antennal information (termed ‘without modulation’) against different features of

antennal position (Friedman test $\chi^2 = 32.66$, $P = 0.0000014$): without modulation versus both antennae, $P = 0.00011$; without modulation versus midpoint, $P = 0.00011$; without modulation versus left antenna only, $P = 0.0021$; and without modulation versus right antenna only, $P = 0.0028$. The following P values are associated with Fig. 4.7c, comparing the angular errors obtained for nestmates that exhibited changing versus stable angles relative to the dancer for the midpoint antennal feature and without modulation: changing-midpoint versus changing-without modulation, $W = 66.0$, $P = 0.000017$; stable-midpoint versus changing-without modulation, $H = 5.60$, $P = 0.018$; and stable-midpoint versus stable-without modulation, $W = 45.0$, $P = 0.0066$. The following P values are associated with Fig. 4.8a, comparing the angular errors of bees that followed only one waggle phase versus the average final vectors from bees that followed consecutive waggle phases followed for the midpoint antennal feature and without modulation: first phase-midpoint versus average-without modulation, $H = 5.47$, $P = 0.019$; first phase-midpoint versus first phase-without modulation, $W = 88.0$, $P = 0.000042$; first phase-midpoint versus average-midpoint, $H = 5.28$, $P = 0.022$; average-midpoint versus first phase-without modulation, $H = 7.61$, $P = 0.0058$; and average-midpoint versus average-without modulation, $W = 2.0$, $P = 0.012$. All other comparisons were non-significant.

5

Testing dance recruitment

Whilst many have studied the error in the dancers' signalling, few have explored how variations in the experience of a nestmate following the dance influences their accuracy when searching for the signalled resource. In Chapter 4, we reported a previously unremarked correlation between antennal position and the relative body axes of dancer and follower bees. Based on this, we then proposed a plausible neural mechanism that enables followers to assimilate a flight vector that they can follow to the resource. This allowed us to infer the estimated food location after observing a single follower bee. Using real data from tracked dance followers in our model, we obtained appropriately centred but widely distributed estimates of the vector direction. To follow up on this result, in this chapter, we devise an experiment to compare the predictions of this model with the vectors expressed by real bees recruited to a feeder, as well as foragers returning to a feeder, inspired by the forced-detour paradigm in ants. By continuously updating their internal representation of their position via path integration, a foraging ant that has been forced away from its direct route can reorient towards its original goal as soon as its path is unconstrained⁴⁹. Following a similar idea, we tracked the correction angle made by bees attempting to navigate to a feeder after an imposed detour, as a measure of how accurately they had estimated the food location.

This chapter presents a final investigation into whether a path integration circuit, based on the central complex, is sufficient to explain the core aspects of how a flight vector is accumulated and expressed as part of dance communication. In Chapter 3, we focused on how the circuit could perform the dance, based on a hypothesis that the dance resembles a miniature replay of a return flight to food^{12;83}. This was built upon previous research that described how return flights could be produced if the bee can store and recall a 'vector memory' as a snapshot of the state of its path integrator when food is encountered²¹⁷. We now test the concept that the same mechanism is used with a food vector acquired from dance following (as in Chapter 4) to allow the nestmate to fly to the food for the first time.

5.1 A detour experiment in bees

The primary objective was to design an experiment which could provide an unbiased measure of how well foragers and new recruits had estimated the location of a feeder when returning to it or navigating to it for the first time. To directly compare these real-world vectors with the flight vectors predicted by the assimilation circuit in Chapter 4, it was crucial that the bees relied upon their vector information when navigating in the experiment. This required minimising the influence of external stimuli that might normally aid bees in finding the resource, such as landmarks and other bees (see Table 2.2). Several methodologies have been employed in the past to gauge the accuracy of foraging activity. In this section, we discuss these existing approaches and introduce our proposed experiment within this context.

5.1.1 Approaches to studying foraging accuracy

Harmonic radar

One of the most appealing options for our use case could have been a harmonic radar system. This technology operates by sending out a stimulus signal to a harmonic reflecting tag (or transponder) which once received, then generates a second harmonic that is transmitted back out to a receiving system. Measuring the time delays between the transmitted and the received signals allows one to determine the distance of the transponder and its direction on the horizontal plane. By tagging insects with tiny transponders, weighing only a few milligrams²⁵⁹, harmonic radars have been effective at tracking insects flying at low altitudes and over flat terrain^{36;175;191;239;258}. Recent experimental tracking systems that utilise cameras mounted on drones to track retroreflective tags³³⁸ suggests that it could be possible to track insects continuously in the near future and overcome the limited readouts associated with radar (e.g. one every three seconds³⁴⁰). Such expensive specialised systems were unfortunately beyond the scope of our experiment. Nonetheless, the harmonic radar has been used previously to demonstrate that after following a dance, recruits that are immediately displaced from the hive embark on flight paths that resemble the signalled dance vector^{207;257;340} (in fact, we plotted some of this data in Fig. 4.8d-f of Chapter 4). Unfortunately, these radar studies did not include accompanying data of the dancer-follower interactions in the hive, which might have otherwise offered an alternative data source from which we could obtain the antennal positioning of followers and their subsequent vectors expressed. Neither Riley et al.²⁵⁷ nor Wang et al.³⁴⁰ indicate the use of any video recordings in their methodologies and while Menzel et al.²⁰⁷ provided summary statistics on the average number of waggle phases followed by recruits, the underlying raw data or video recordings are not publicly available. Compared to other dance features or dancer-follower interactions, the antennal positioning is difficult to capture in enough detail to be able to consistently measure it. It is therefore unlikely that studies without the intention to analyse the antennae would have recorded dancer-follower interactions with the necessary level of detail.

Feeder traps

Traditional experiments have also attempted to characterise the final accuracy of recruits by geometrically arranging feeder traps around the intended feeder location^{99;114;143;315;318;353}. For example, the final distribution of recruits arriving at particular traps that have been arranged in an arc (equidistant from the hive) has been used to measure the directional error, whilst their arrangement along a straight line has been used as a measure of distance estimation. With an upper bound on the feasible number of traps, this approach collects data on the accuracy of recruits within discrete bins of angles or distances rather than continuous data. Unless a large enough array is used, it is difficult to measure the estimation of either the distance or direction whilst controlling the other. In directional feeder trap experiments, traps have been arranged at a maximum of 45° either side of the intended direction, which limits the measurable distribution of recruits to be within this range. One of the behavioural predictions of the assimilation circuit in Chapter 4 was that recruits would be directed across almost the whole correct hemisphere containing the food (i.e. potentially up to ±90° on either side). For this reason, our experiment required a more unrestricted readout of recruits' flight paths.

Vanishing bearings

One approach that provides a more continuous measure of the intended flight is through determining the angle of a bee as she departs from a location, such as the nest, feeding site or experimental release site, and soon *vanishes* into the distance when navigating to the next goal^{37;46;72;73;77;105;115;201;277}. Reportedly visible for up to 25 m away, the bee's position is tracked by the human eye and the bearing is typically recorded using a compass relative to North⁷². If guided by a vector memory of her goal and using her path integration circuitry, this bearing should represent the direction of the straight-line vector that she will fly the length of, before initiating a search for the estimated goal location. However, as the bees disappear quickly from view, we cannot observe the final vector length using this approach and thus cannot obtain an indication of the intended distance of travel.

Forced detour

Performing path integration while heading towards a goal makes it possible to recover from an imposed detour and such experiments have been used to demonstrate the use of path integration by ants whilst homing²⁷¹ and returning to a feeder⁴⁹. Ants will immediately redirect their trajectory at the end of a detour channel, where this corrective bearing indicates their predicted *location* of the original goal (i.e. not just its predicted *direction* as measured by a vanishing bearing) in terms of its path integration coordinates. Thus, we sought to design a similar experiment in bees which could measure their in-flight correction bearings when leaving an unexpected imposed detour when navigating to the feeder. To the best of our knowledge, we are unaware of any previous attempts to use detours to study the angles of departing bees when attempting to navigate to a known or signalled feeder.

5.1.2 Training phase

The first step was to establish a feeder location that foragers would be trained to and subsequently signal in their dances back in the hive. Provoking distinct waggle phases was preferable as this would provide a comparable context of dancing to that in Chapter 4 when measuring the antennal positioning of the recruited bees. Food sources normally need to be over several hundred metres away to invoke waggle dances with such phases and structured dance paths. Previous work has shown that bees can be trained to forage from a feeder positioned within a narrow tunnel with patterned walls^{87;299–301}. Flying past these patterns exploits the bees' visually-gauged odometer and causes them to perceive that they have flown a much farther distance (several hundred metres) than they have (six metres), which is accordingly signalled in the dance. A transparent roof or mesh ceiling enables the bees to still monitor their direction when flying through the tunnel using the celestial cues in the visible sky⁹⁸. The tunnels also ensure consistency of the foraging routes experienced across the bees and thus provide an appropriate context in which foraging behaviour can be controlled.

Fig. 5.1 provides two aerial views of our experimental site. We trained a group of bees to forage from a long training tunnel with randomly patterned (Julesz) walls, which was positioned 3 m from the hive. This layout mirrored the setup of previously published tunnel experiments^{87;298}. The tunnel was composed of several smaller segments that were connected and placed 1 m above the ground. Bees would exit the hive and fly the short route to the tunnel before flying along to the feeder positioned at the far end (Fig. 5.2). The tunnel was closed at the other side, which forced the foragers to return back to the hive via the same route. Foragers were tagged with numbered discs attached to their thorax and these identities were recorded when at the feeder throughout the experiment. The dances of the foragers were then filmed, along with the nestmates following the dance, whose identities were also recorded. Dance followers were identified using the same criteria as in Chapters 3 and 4: nestmates that were within one bees length of the dancer and oriented towards her with their antennae extended. The full experimental protocol is given in Section 5.4.

5.1.3 Testing phase

Once a nestmate had followed a dance and obtained her own foodward vector, the next stage was to determine how well she had estimated the signalled location. Both dancers and recruits that were motivated to leave the hive to fly their vector to the food were immediately captured upon exiting and released into a shorter version of the training tunnel that was oriented at a different angle and positioned in a different part of the field. This *detour* tunnel was open at the far end, such that bees were forced to fly along the detour but could then exit and make the corrective turn necessary to intersect their estimated location of the food. Note that because they have been displaced upon leaving the hive, the feeder is now *virtual*, that is, it will not actually be present at their estimated location. We recorded the silhouette of a bee against the sky as they left the detour tunnel and subsequently tracked their trajectory across a 1.56 m long and 0.84 m wide area on the horizontal plane at the tunnel's height. Recording the silhouette yields a more reliable and unbiased estimate of the flight trajectory than the manual

(52°27'34.0"N 13°17'59.7"E)



Figure 5.1. Top-down views of experimental area in Berlin. One arrangement of training and detour tunnels shown. Photos obtained via a drone piloted by Pranav Kedia, July 2023, and used with permission. Bees were trained to forage from a feeder positioned at the end of the training tunnel. Their dances and interactions with nestmates were then filmed upon returning to the hive. As a forager or a new recruit was leaving the nest to then fly their foodward vector, they were caught and displaced to the entrance of a different tunnel that forced the first segment of their journey to be a detour in a different direction. The angle of the bee's trajectory immediately post detour was tracked, allowing us to analyse the accuracy of their estimated food location under the theory that they would immediately reorient towards their original goal location once released from the detour. See also Fig. A.4.

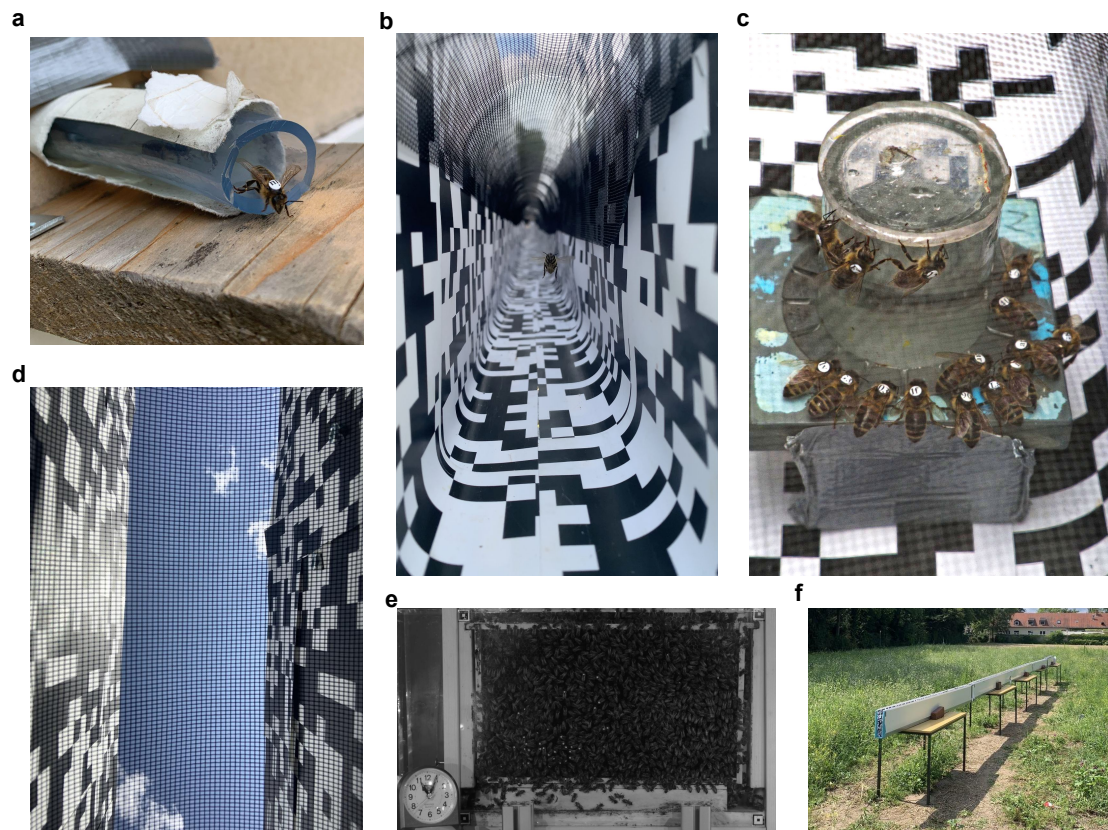


Figure 5.2. Equipment for the detour experiment. **a**, A tagged forager exiting the hive during the experiment. The specialised ‘bee tube’ entrance makes it easier to capture bees as they leave the hive. **b**, A forager flying through the patterned training tunnel with a mesh roof. **c**, Tagged foragers around the feeder positioned at the end of the training tunnel. **d**, Bottom-up view from within the tunnel and beneath the mesh. **e**, View of the colony in the observation hive from the filming rig used to monitor dancing and following behaviour. **f**, The training tunnel was positioned in the field at 3 m from hive. Photos by Anna Hadjitofi, July 2023.

approach used for traditional vanishing bearings. We interpret the angle of the bee’s flight to represent the correction that the bee has deemed necessary in order to fly directly towards its estimated location of the feeder. This angle can then be correlated with features experienced when following the dance, or features signalled in the dance, in the case of returning foragers. We focused solely on the initial trajectory where the bee first leaves the tunnel because as they fly further into the natural environment, they may realise their actual proximity to the hive (i.e. that they have not travelled as far as they perceived) and change behaviour, such as returning to the hive. The procedure was repeated for different relative orientations of the detour (Fig. 5.3) and can be used to study how accurately a forager or recruit has estimated the location of a known or new feeder, as well as how a recruit’s accuracy is related to what they experience in the hive. Although tunnels have been used to manipulate aspects of the dancer’s signalling and return to feeder behaviours, to our knowledge, this is the first attempt to involve recruits with the apparatus.

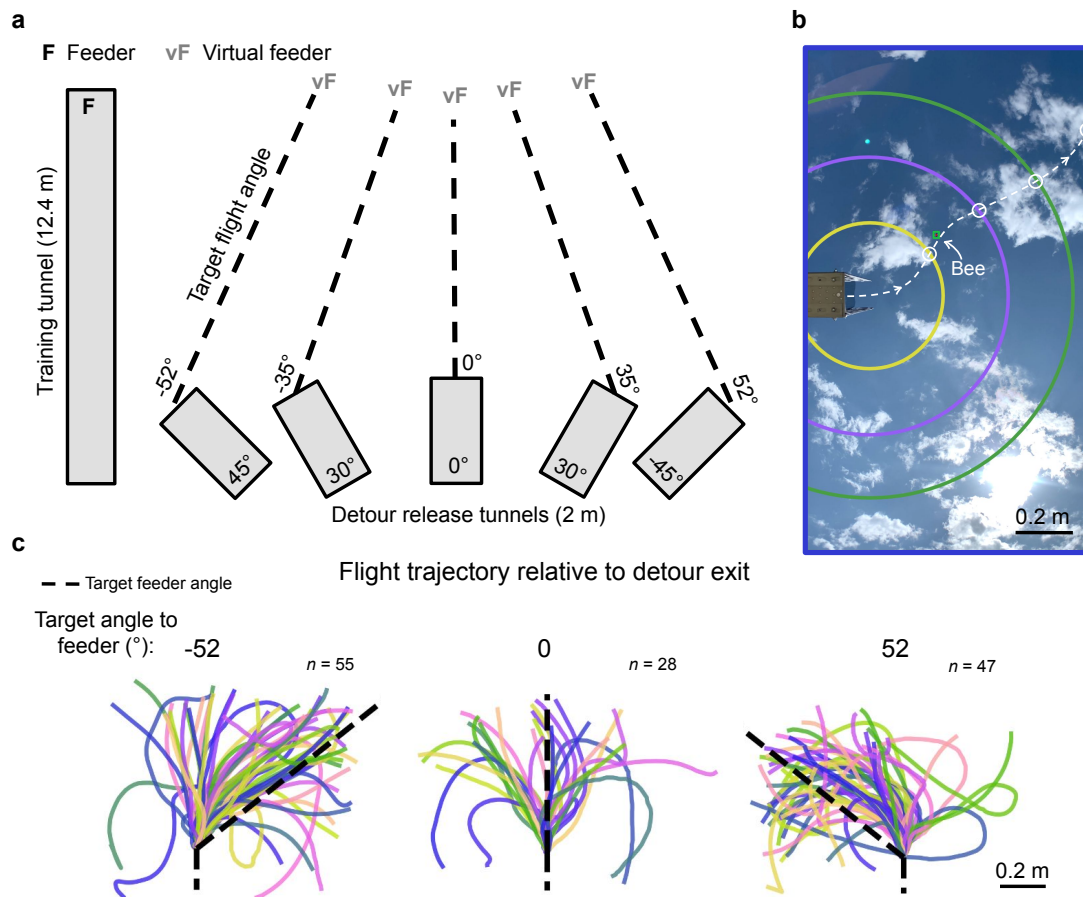


Figure 5.3. Configuration of tunnels during the experiment and the view of bees exiting the detour. **a**, Relative configuration of training and detour tunnels tested during the experiment. F and vF respectively indicate the location of the feeder during training and its target *virtual* location when forced along a detour. Sizes and angles of tunnels are not drawn to scale. **b**, Bottom-up view from the camera used to track the flight trajectory of a bee leaving the detour tunnel. The angle of the bee relative to the tunnel exit is later examined at four boundaries: the yellow, purple and green concentric circles, as well as its last visible position in the frame (blue). On the horizontal plane at the height of the tunnel, the concentric circles represent distances of 0.22 m, 0.44 m, and 0.56 m from the tunnel exit, respectively. **c**, Top-down view of the raw trajectories of foragers' flight paths post detour for relative detour tunnel angles of 45°, 0° or -45°.

5.2 Accuracy of location estimation and sharing

In this section, we present the results of the experiment focusing on the nature of flight trajectories following the detour, their relationship to the precision of dances by returning foragers and the vectors assimilated by recruits when simulating their antennal positioning using the assimilation circuit proposed in Chapter 4.

5.2.1 Flight trajectories post detour

Dancers

We initially focused on testing the experienced foragers who consistently returned to the feeder in the training tunnel to determine some of the unknown parameters of the experiment. For example, it became clear that detour angles that were too extreme relative to the feeder (e.g. $\pm 60^\circ$ and $\pm 90^\circ$) often resulted in foragers refusing to fly the detour altogether. Instead, they would simply fly back and forth near their release point at the start of the detour tunnel whilst oriented towards the feeder's general location. To promote a consistent motivation to fly the detour, we continued with a range of smaller detour angles ($\pm 45^\circ$ and $\pm 30^\circ$) and tested a detour of 0° to include a condition where no corrective turn would be necessary (Fig. 5.3b).

As prior detour experiments had recorded post detour adjustments in walking insects, we were also unsure where this turn or final directed bearing angle would be visible within the trajectories of flying bees. For this reason, we calculated the angle of a bee as she crossed three boundaries extending from the detour exit, as well as her final visible angle before leaving the frame. The three boundaries were at 0.22 m, 0.44 and 0.56 m from the bees' first visible position upon emerging from the tunnel on the horizontal plane at the tunnel's height (i.e. 1 m off the ground). Fig. 5.4a shows the recorded angles of the foragers when crossing these boundaries. Examples of the full trajectories of the foragers' flight paths are shown in Fig. 5.3c. These angles are visualised relative to the exit of the detour tunnel (i.e. at 0° North on the circular plots) and display dashed lines that indicate the target bearings to the location (black) and direction (grey) of the feeder. Whilst bees can fly up to 6 m/s when foraging in their natural environment³⁵², they fly slower in the tunnels (which is consistent with the intended manipulation of increased optic flow). The mean speed when flying midway along the detour was estimated to be 0.44 m/s ($n = 30$). The recorded trajectories were at most a couple of seconds long and corrective flight adjustments were made quickly and within the observed zone, likely facilitated by the bees' reduced speed inside the tunnel. In support of this, Fig. 5.4a demonstrates a progressive shift in the bearing distributions across the boundaries for bees that experienced angled detours. The circular mean (\pm s.d.) of each distribution is shown in Fig. 5.6a and further circular statistics in Table A.1a. The distribution of the final visible bearing angle (blue) shows the greatest shift away from the tunnel exit and is the most centred on the feeder location. The observation that the bearing angles remained centred on the feeder with the distance-only detour (i.e. a 0° relative detour angle) confirms that the other observed shifts are not simply due to an urge to circle away following a detour. We thus consider the final visible bearing angle to be a reliable indicator of the foodward location estimated by the bees and use it for the remainder of the results. However, it is also interesting that even as soon as the path is unconstrained (yellow), a slight bias towards the appropriate side containing the feeder can be seen. Hence, even though in flight, these observations align with the immediate initiation of a turn in walking insects released from a detour and is consistent with a path integration control system acting to immediately steer towards the direction that minimises the angle between the current and desired headings.

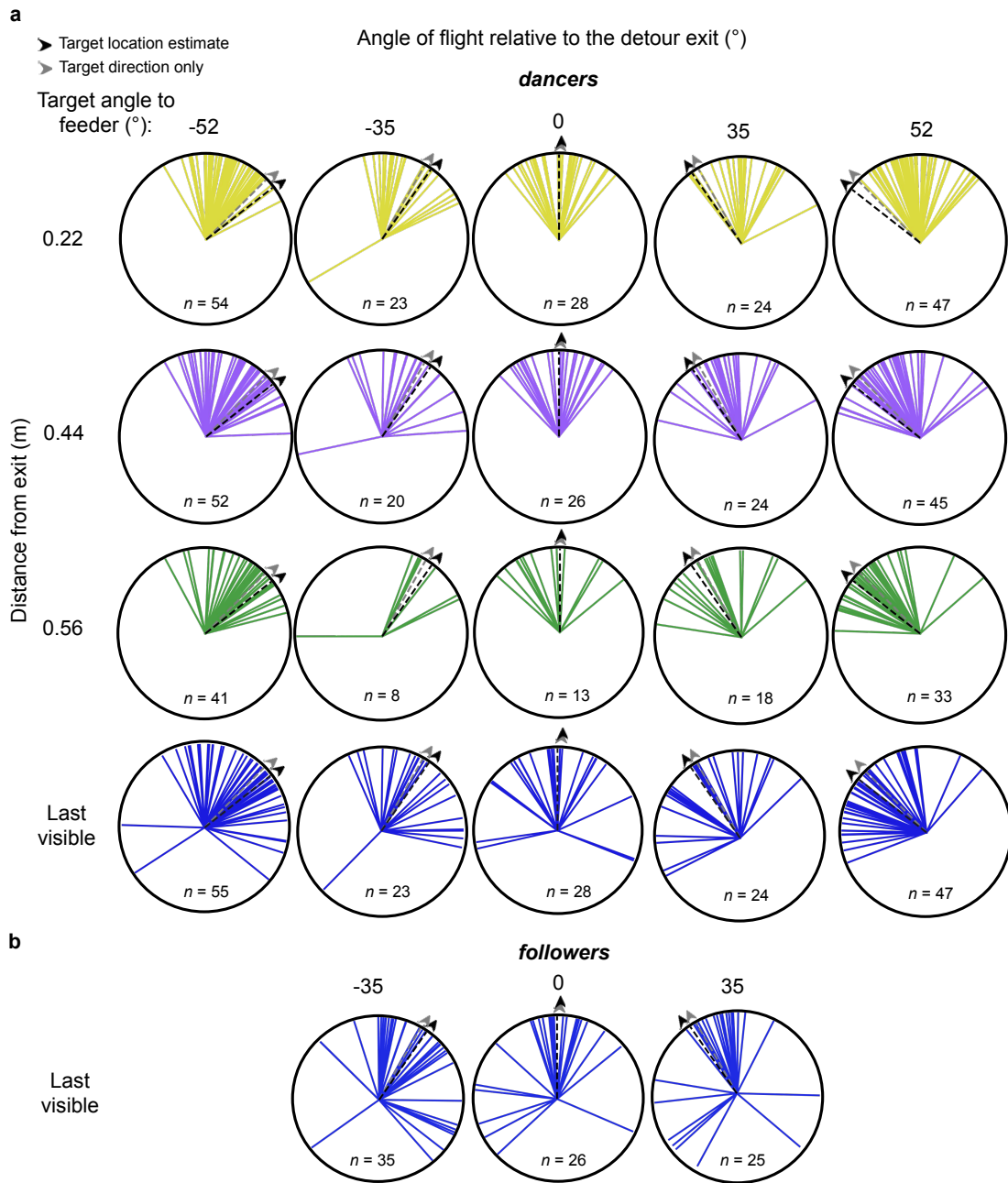


Figure 5.4. Distributions of the angles of flight post detour relative to the tunnel exit for a, dancers (returning foragers) and b, followers (recruits). Target directions are shown for two hypotheses: bees navigate based on the location of the feeder (black dashed lines and arrows) or follow the direction of the feeder only (grey dashed lines and arrow). Columns indicate different target angles required to reach the feeder and rows indicate the distribution of flight angles at different distance boundaries from the detour exit (see Fig. 5.3b). See also Table A.1.

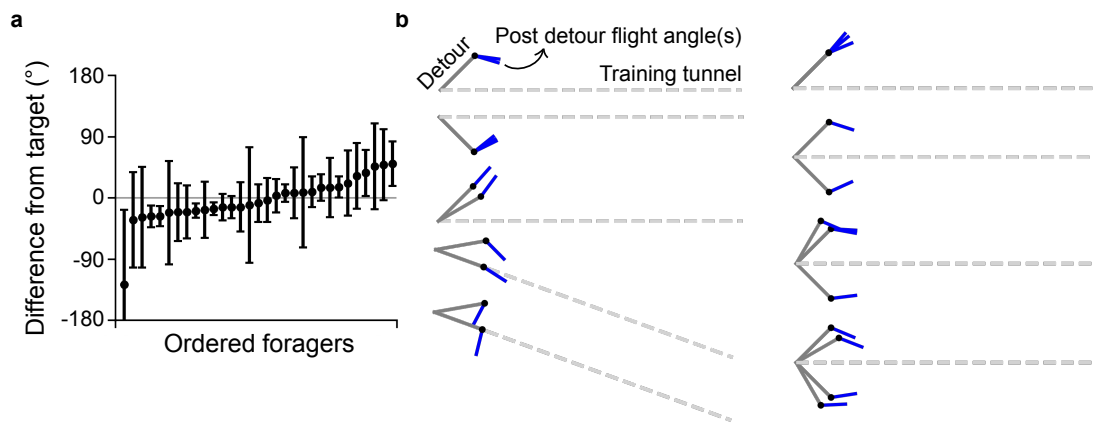


Figure 5.5. Returning foragers tested on multiple detour release sites. **a**, The mean \pm s.d. difference between the final bearing angles of foragers post detour ($n = 31$) relative to the target feeder angle, when tested on the same detour angle multiple times within the same day. **b**, Examples of the final bearing angles (blue) of individual foragers when tested at the same or different detour angles (solid grey lines) relative to the feeder (dashed grey lines).

There were also instances where the same forager was caught at different times throughout the day and tested in the detour multiple times. This revealed that the majority of these foragers exhibited a mostly consistent flight vector (Fig. 5.5a); a good indicator that they were attempting to navigate to a specific target location. There were also a few foragers who were tested in several different angles of detour routes. Despite this, the different flight paths for an individual appeared to converge to a similar location, even if not perfectly oriented towards the feeder (Fig. 5.5b). This further demonstrates that the bees were motivated to navigate to a particular target location and not just a direction.

Followers

The distributions and statistics of the final bearing angles of the recruited follower bees are given in Fig. 5.4b, Fig. 5.6b and Table A.1b. Both populations of returning foragers and these recruits show a remarkable centring around the expected target angle that would be required to intersect the feeder. Although nearly all bees flew out in a direction across the correct hemisphere containing the food, it is also notable that both populations exhibit a considerable spread on either side of the feeder. This supports the nature of flight vectors predicted by the assimilation circuit in Fig. 4.7 when we decoded the follower bees' foodward vectors. Whilst the overall concentration of the dancers' and recruits' distributions showed no statistically significant differences between each other, there appears to be a few more recruits that exhibited a much larger deviation from the expected angle (i.e. $> \pm 90^\circ$). Although determining a recruit's true intention is impossible, these outliers might represent bees returning to the nest after the unexpected disruption of the detour. At the time of its collection, the data was filtered based on the bee's performance in the tunnel. If any bee stopped flying within the tunnel or took longer than 30 s to exit, their data was excluded from later analysis. This means that the data presented contains only the bees that flew sensibly along the tunnel, but it might include bees that emerged from the tunnel with a reduced motivation for foraging.

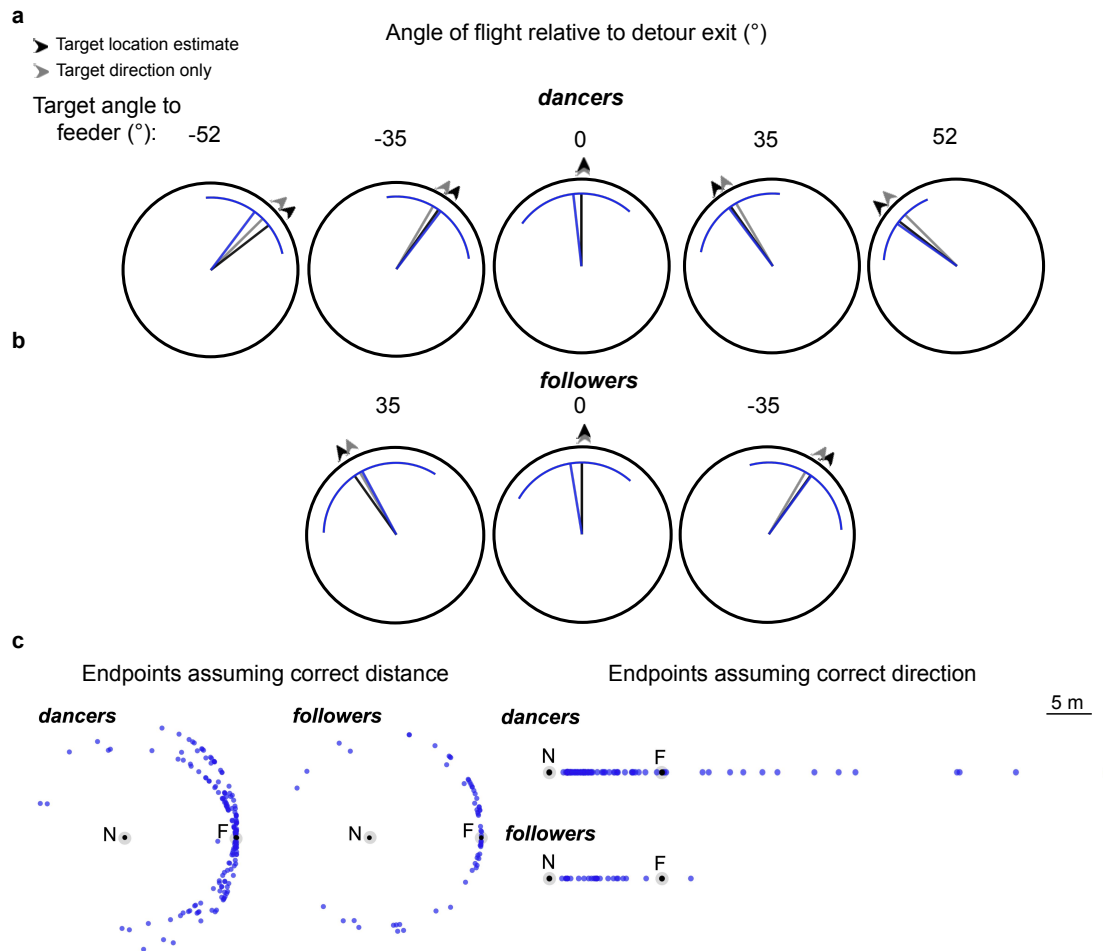


Figure 5.6. Mean distributions \pm s.d. of flight angles post detour relative to the tunnel exit for a, dancers (returning foragers) and b, followers (recruits). Same data and symbols as in Fig. 5.4, except only the bees' angle at the final distance is shown for the dancers. **c**, Predicted endpoints of the bees' flight vectors calculated under the assumption that they had correctly estimated the (left) distance or (right) direction to the food. The latter excludes bees whose flight path would not intersect the line connecting the hive and the feeder. N and F indicate the nest and feeder, respectively. See also Table A.1.

We also extrapolated the bees' flight vectors to predict their endpoints relative to the feeder (Fig. 5.6c). Previous feeder trap studies have reported the recruits' accuracy in terms of either the distance^{99;114;353} or direction^{99;114;143;315;318} alone; treating the other component as fixed during the experiment. By interpreting the final bearing angle after the initial detour as the bee's intended flight vector to the food, we can predict the bee's location at the end of following this vector for the cases that they have correctly estimated the distance (i.e. where do they end up if their vector is extended in their chosen direction for the correct distance?) or the direction (i.e. where does their flight path intersect the straight line connecting the hive and feeder?). When assuming the distance has been correctly estimated (left of Fig. 5.6c), the predicted end locations of dancers and recruits are scattered on either side of the feeder, with the majority arriving within $\pm 45^\circ$. When assuming the direction has been correctly estimated (right of Fig. 5.6c), both dancers and recruits have reasonably conservative estimates of the

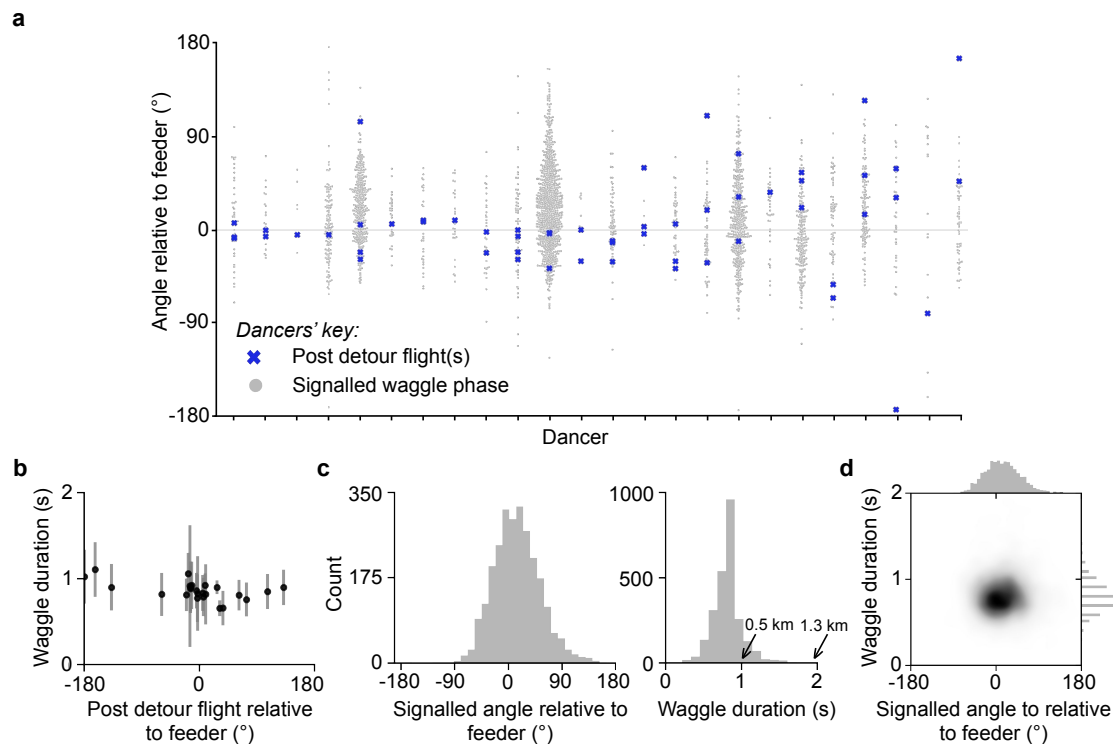


Figure 5.7. Features of the waggle phases of dancers ($n = 24$) ordered by their post detour accuracy. **a**, Foodward angles signalled (grey dots) in the waggle phases ordered by their post detour accuracy (blue crosses). **b**, Mean post detour flight angle according to the mean \pm s.d. duration of each dancer's waggle phases. **c**, Histogram of data in **a**, showing the waggle phase (left) angles and (right) durations across all dances. Arrows indicate equivalent feeder distances when in the natural environment¹⁶⁵. **d**, Kernel density estimation plot of the relationship between the duration and angle of waggle phases. Darker regions indicate higher density of observations. Marginal distributions shown on the top and right.

distance and most would arrive short of the feeder. There are also comparatively fewer recruits whose vectors would lead them far beyond the feeder, which may imply that overshooting could be more costly for them than experienced foragers returning to the site.

5.2.2 Precision of dances

The wide distribution of bearing angles of foragers returning to the feeder raises the question of whether this variation is also reflected in their dances. Do foragers with more accurate flight vectors signal more accurate foodward directions to nestmates? From the video data, we retrieved the dance sessions for a random sample of foragers before they were caught and tested in the detour tunnel ($n = 24$). The angle of each waggle phase was determined using the line connecting the thorax in the first and last frames of visible wagging (as in Chapter 3). A consistent pattern can be seen across dancers in Fig. 5-7: waggle phases (grey dots) signalled directions that were considerably scattered around the feeder, with nearly all signalling at least one or two phases that deviated by more than $\pm 60^\circ$. The dancers have been ordered according to the accuracy of their post detour flight (blue crosses). While the overall spread of

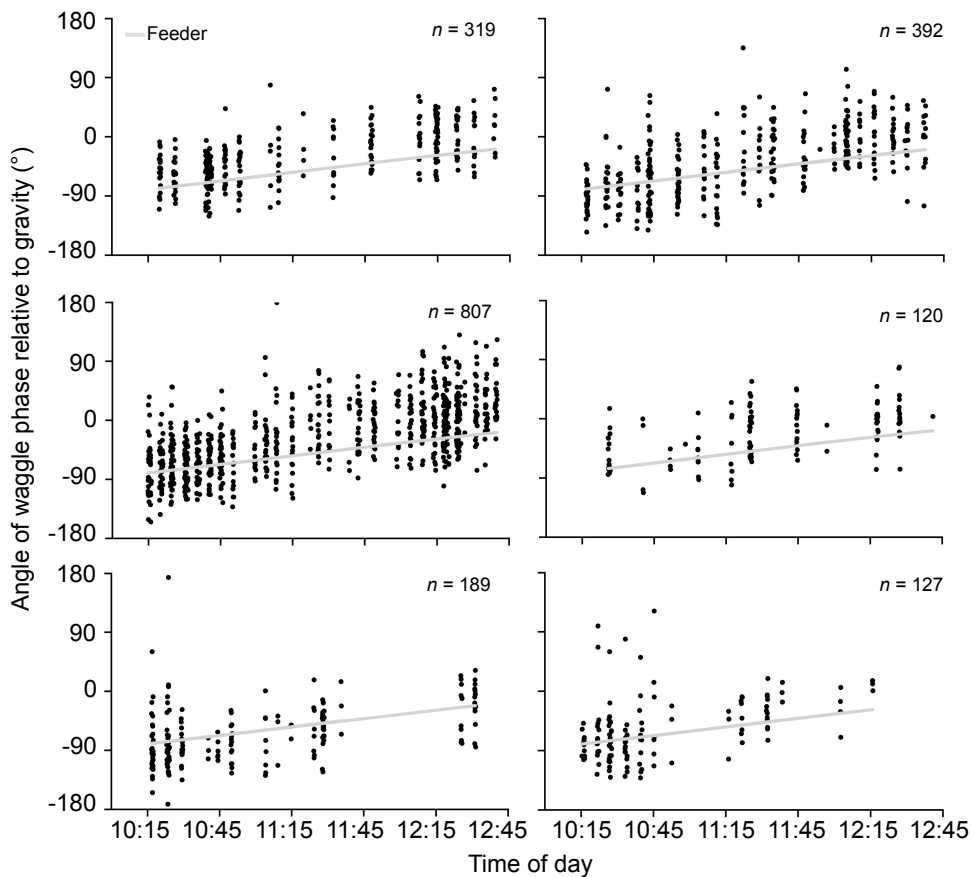


Figure 5.8. Angles of waggle phases by six dancers relative to gravity across all dances within a 2.5 hour foraging period to the trained feeder. Each black circle represents a waggle phase signalled by a dancer. The grey line indicates the expected angle of the waggle phase on the comb for that time of day. 0° is upwards on the vertical comb, 90° is leftwards, -90° is rightwards and $\pm 180^\circ$ is directly downwards. Time of day specified using a 24 hour clock. See also Fig. A.5.

the signalled directions align with the variation observed in the flight paths at the population level, the ordering does not reveal any obvious trend between the accuracy of a dancer's post detour flight and the precision of her waggle phases. Thus, the degree of signalled scatter appears to be consistent across dancers, regardless of the accuracy of their estimated location. A similar observation exists when comparing the signalled distances across dances (Fig. 5.7b).

Fig. 5.8 visualises the angles signalled (black dots) in each bout of dancing for a sample of these foragers across the same 2.5 hour period ($n = 6$, angles relative to the feeder are shown in Fig. A.5). A bout of dancing was defined as containing dance circuits that were performed continuously without pauses exceeding 15 s between circuits. Throughout the foraging period, the bees can be seen gradually shifting the orientation of their waggle dances in accordance with the sun's changing position. Although individual foragers exhibit variation in the number of bouts, dance circuits per bout, and the time between bouts (where they either revisit the feeder or remain in the hive), the pattern of scattering across waggle phase again remains remarkably consistent. The signalling of distance by foragers' overall appears to be more concentrated

(Fig. 5.7c), with a tight clustering of waggle durations around 0.8 s (measured to the nearest 0.05 s). This duration would typically indicate a feeder that was perceived to be around 60 m away¹⁶⁵, a distance where angular divergence could be noticeable^{19;330}. Within this range of duration, there is no apparent relationship between the duration of an individual waggle phase and its angular deviation from the feeder (Fig. 5.7d).

5.2.3 Predictions of the assimilation circuit

We finally examined whether the spread in the bearing angles of nestmates that were recruited to the feeder could be explained by what they experienced when following the dance. There were two sources of video data: one that was continuously running and provided a record of the dances and interactions of all bees in the hive on one side of the comb, and a second from a higher-resolution camera that provided shorter, close up recordings of the dance followers that had been initiated once the dance had been localised within its much smaller field of view. From the first source, we were able to obtain the angle of each waggle phase that the recruits had followed just before being caught and tested in the detour (Fig. 5.9). Recruits followed a variable number of waggle phases, with some following only one or two and others following more than twelve. Given the variability observed in the overall signalling of direction across the waggle phases (Figs. 5.7 and 5.8), it is perhaps unsurprising that the angles followed by recruits were also quite scattered. In Fig. 5.9a, the recruits have been sorted in ascending order according to the angular difference between their post detour flight and the mean angle of the phases they followed. Exceeding what would be expected from a random relationship, we observe a trend of the post detour flight angles generally falling within the range predicted by the angle of the phases they had followed. Fig. 5.9b shows the vectors for each recruit, vertically arranged in the order of their sequence in the dance and coloured by the deviation of their angle from the flight vector that the recruit expressed. These results suggest that the recruits do not necessarily fly in the direction that was signalled at a particular point in the dance, i.e. they do not bias their flight towards the information they received first or most recently.

While the second higher resolution video source offered the potential to track the antennal positions of the dance followers, there were still instances where the antennae of some followers were obscured or not visible during a phase. Consequently, we focused on a smaller subset of this data where complete interactions of the follower with the dancer were available for every waggle phase they followed (Fig. 5.10). For each of these recruits, we fed their antennal positioning data to the assimilation circuit in Chapter 4 and obtained the vectors that were assimilated at the end of each waggle phase using the midpoint feature of the antennae as input. These vectors were also averaged to obtain the mean direction of the final vector estimate (dashed line; the mean direction when weighted by the lengths of the individual vectors is shown in Fig. A.6). Following a similar observation that was seen for the angles of the phases followed, the post detour flights of these recruits appear to align reasonably well with the vectors predicted by the model. Fig. 5.10b shows a similar relationship for the recruits as in Fig. 5.9b, i.e. across the bees, there is no specific bias towards them expressing a vector that they obtained from any particular phase in the dance sequence.

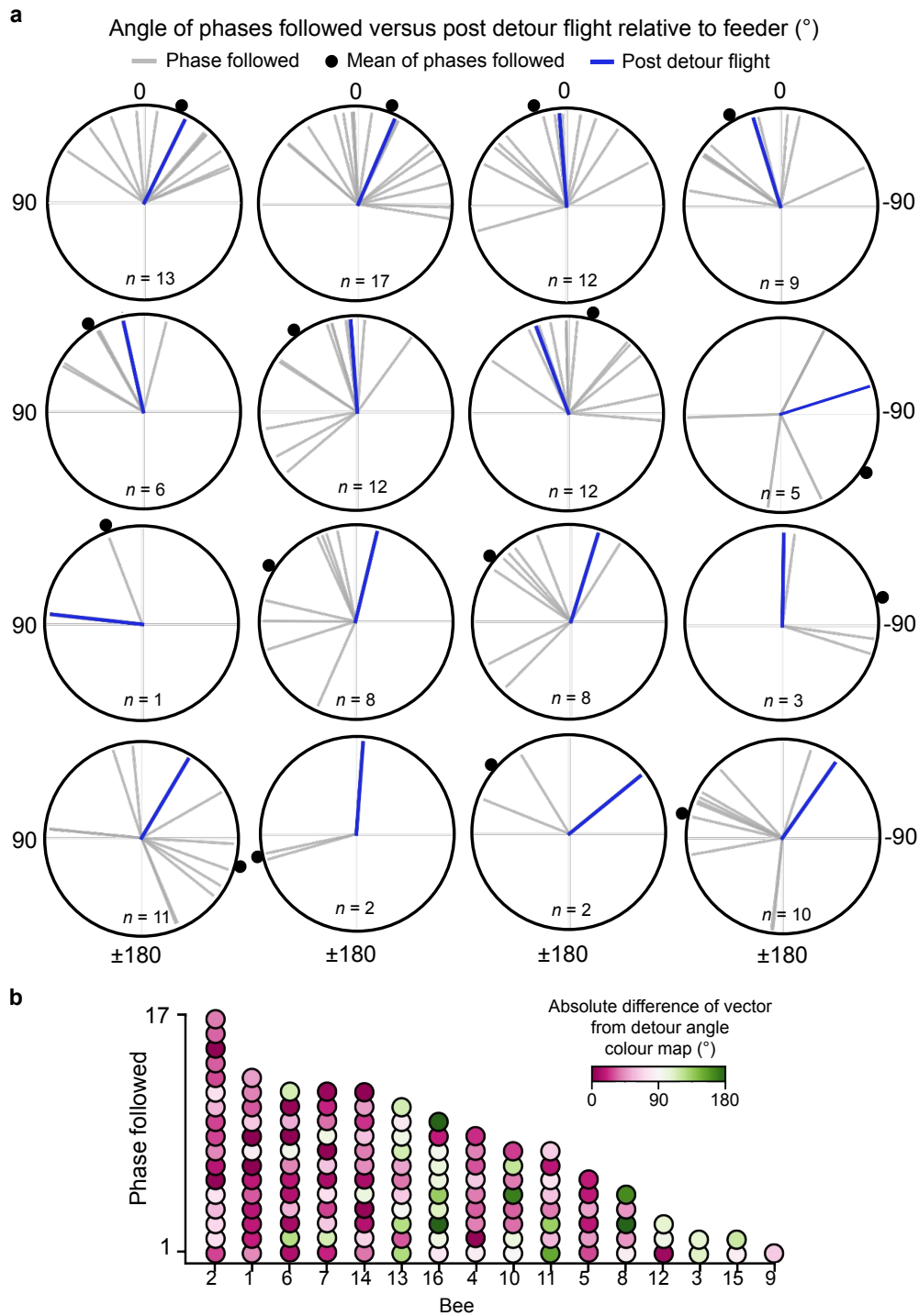


Figure 5.9. The angles of waggle phases followed (grey) by new recruits ($n = 16$) and their subsequent angle of flight post detour (blue). All angles indicated relative to feeder. **a**, Recruits have been ordered according to the angular difference between the post detour flight angle and the circular mean angle of the phases they had followed before captured (black dots). **b**, Same recruits as in **a**, but each phase they followed is coloured by the absolute difference between its angle and the final detour angle. The x-axis refers to the index of the bee in **a**, read as left-to-right and top-to-bottom.

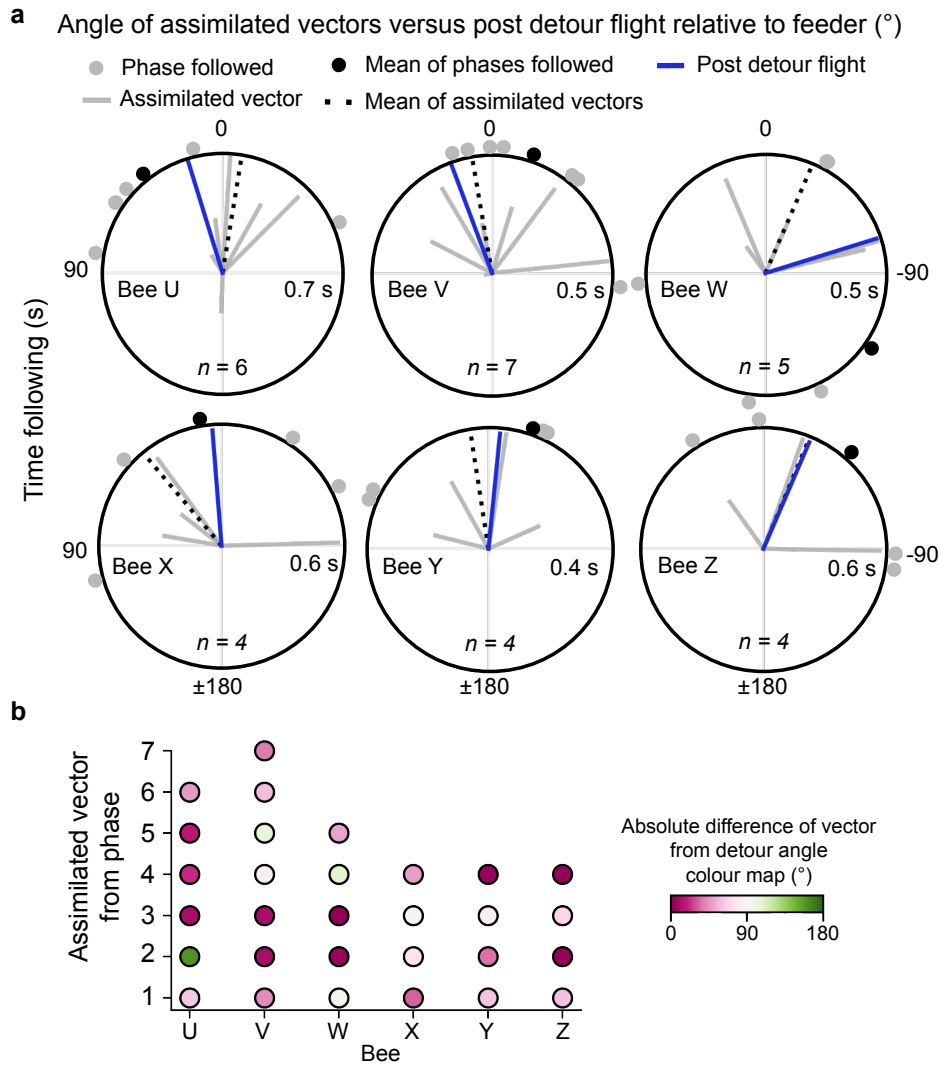


Figure 5.10. The assimilated vectors of six new recruits predicted by the assimilation circuit and their subsequent angle of flight post detour. **a**, The vectors assimilated at the end of each waggle phase (lines) and the angle of phases followed (circles) by six new recruits and their subsequent angle of flight post detour (blue). The midpoint of their antennae was used as the antennal input feature in the circuit. All angles indicated relative to feeder. **b**, Same recruits as in **a**, each phase they followed is coloured by the absolute difference between its angle and the final detour angle. See also Fig. A.6.

Collectively, these findings offer promising support for the model’s overall hypothesis and suggest that the spread in the bearing angles within the wider population of recruits could be partially attributed to variability in the assimilated vectors derived from their antennal positioning. Moreover, whilst only for an overall small sample size, some of the assimilated vectors demonstrate a higher degree of accuracy relative to the feeder compared to the corresponding angles signalled in the waggle phase (e.g. Bees ‘V’, ‘W’, ‘Y’ and ‘Z’ in Fig. 5.10a). Thus, although experimenters often predict recruits’ search flights based on the angles of the waggle phases they follow, recruits might be able to obtain a better vector estimate from their antennal positioning.

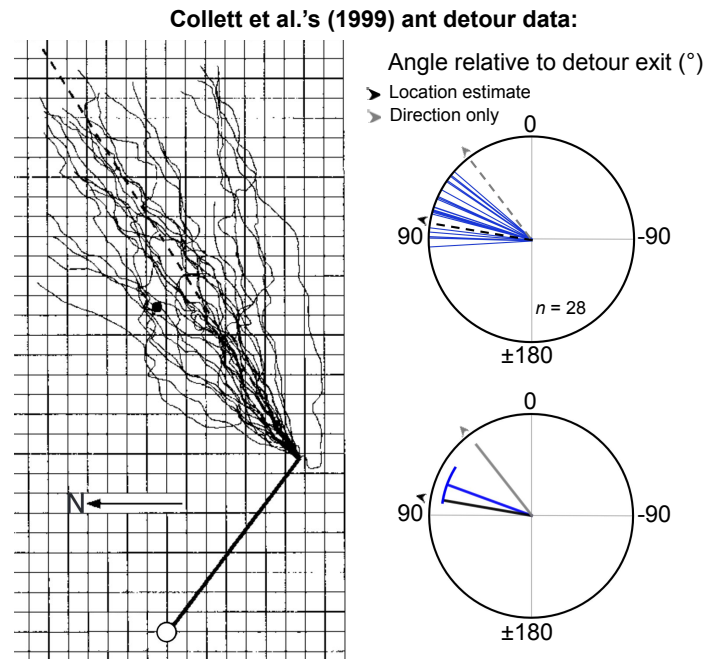


Figure 5.11. Ant detour data from Collett et al. ⁴⁹. **Left**, Original data as shown in Fig. 1d in Collett et al. ⁴⁹. Grid lines are spaced at 1 m. Filled circle marks the usual position of the food which is absent in the test. **Right**, Same data as in **Left**, but only angular error of the final vector endpoints for each individual is plotted relative to detour exit. Same style and symbols as in Figs. 5.4 and 5.6.

5.3 Discussion

We have conducted a novel detour experiment to study the distributions of honeybee foragers when returning to a feeder and of recruits when flying to an advertised feeder. The angle of the bee's trajectory immediately following an imposed detour was used as a measure of their estimated location of the food. Both foragers and recruits displayed a characteristic pattern: the flight vectors were scattered across the expected hemisphere and centred on the feeder. This observation aligns with the predictions of the assimilation circuit at the population level of recruits in Chapter 4, indicating that its seemingly broad distribution of predicted flight paths may indeed be biologically accurate. For a sample of six recruits, we were also able to record their antennal positioning data for every waggle phase of a dance they followed, before their first attempted flight to the feeder. Comparing the model's predicted flight vectors to the real flight vectors expressed by the recruits revealed a correspondence between them, exceeding what would be expected if the model's predictions were random or unrelated. This demonstrates that it is possible to obtain a reasonable readout of a recruit's recovery of the signalled dance vector by modelling their antennal positioning data with a network for path integration that is based on the insect central complex.

Although this is the first work to employ this paradigm in flying bees, similar imposed-detour experiments have been performed in ants returning to a known feeder ^{49;271}. We have plotted the data from an almost parallel experiment in *Cataglyphis fortis* conducted by Collett et al. ⁴⁹,

using the same style of visualisation to our own (Fig. 5.11). The angle of their trajectories show a similar trend of centring around the feeder, though with a potentially narrower spread overall. It is interesting the nature of the results are similar, considering that the ants underwent a proportionally longer detour (over half their training route) compared to the bees in our experiment. The ants had also been trained to the feeder for several days before testing, but their narrower spread could also reflect the inherent difference in the guidance precision between walking and flying, for example, relating to the manoeuvrability. Nonetheless, our data shows several instances of foragers or recruits who lie outside the clustering around the feeder. It is unclear whether the ant data has been filtered; but Collett and Collett⁴⁸ note that disturbed foraging ants often return to the nest rather than continue foraging when being displaced. Moreover, Wang et al.³⁴⁰ describe that some of the honeybee recruits initiated a straight homing flight after close exploration around a release site without performing a vector or search flight. These recruits were not included in their analyses. In contrast, our data includes all bees that successfully navigated the detour, regardless of the subsequent angle of their flight trajectory following the detour. Consequently, we believe it is likely that the outlying flight vectors in our dataset may represent bees returning to the hive.

At the population level of the colony it may be advantageous to scatter recruits when foraging, however, an interesting question that remains is whether the follower bees with more deviated vector estimates (e.g. more than $\pm 45^\circ$ from the feeder) could still find the advertised resource. After all, historically, various studies have reported that a surprising number of recruits can successfully arrive at the intended feeder, even if it is only a small saucer located within a large field¹⁰⁰. For a long time, it has been known that ants perform a stereotyped search strategy in which during a search for its nest after following a vector home, it performs a number of loops of ever-increasing size, starting and ending at the origin and pointing at different azimuthal directions³⁴⁷. Reynolds et al.²⁵⁶ observed similar search flights in honeybees too when tracked using radar whilst returning to a learned food source which had been removed. They show examples where search loops can deviate up to 30 to 50 m from the vector portion of their flight. Moreover, a radar study by Menzel and Greggers²⁰⁵ suggest that foragers that are following a vector to a known feeder may deviate from their intended vector upon detecting a familiar odour that was learned from the original food source. Foragers could be redirected by the odour within an angle that deviates from their vector by up to 60° . Thus, it is possible that a wide search centred on a vector that deviates from the food could still discover the food, especially if there are pheromone attractants left by conspecifics around the target.

5.4 Methods

5.4.1 Experimental protocol

Study site. The study site was located near Freie Universität Berlin in the district of Dahlem (Berlin, Germany). The data were collected between June 6 to July 27, 2023. The first month was spent setting up and testing different aspects of the experiment, including the patterning on the tunnel walls and floor, training protocol and the total length of the training tunnel

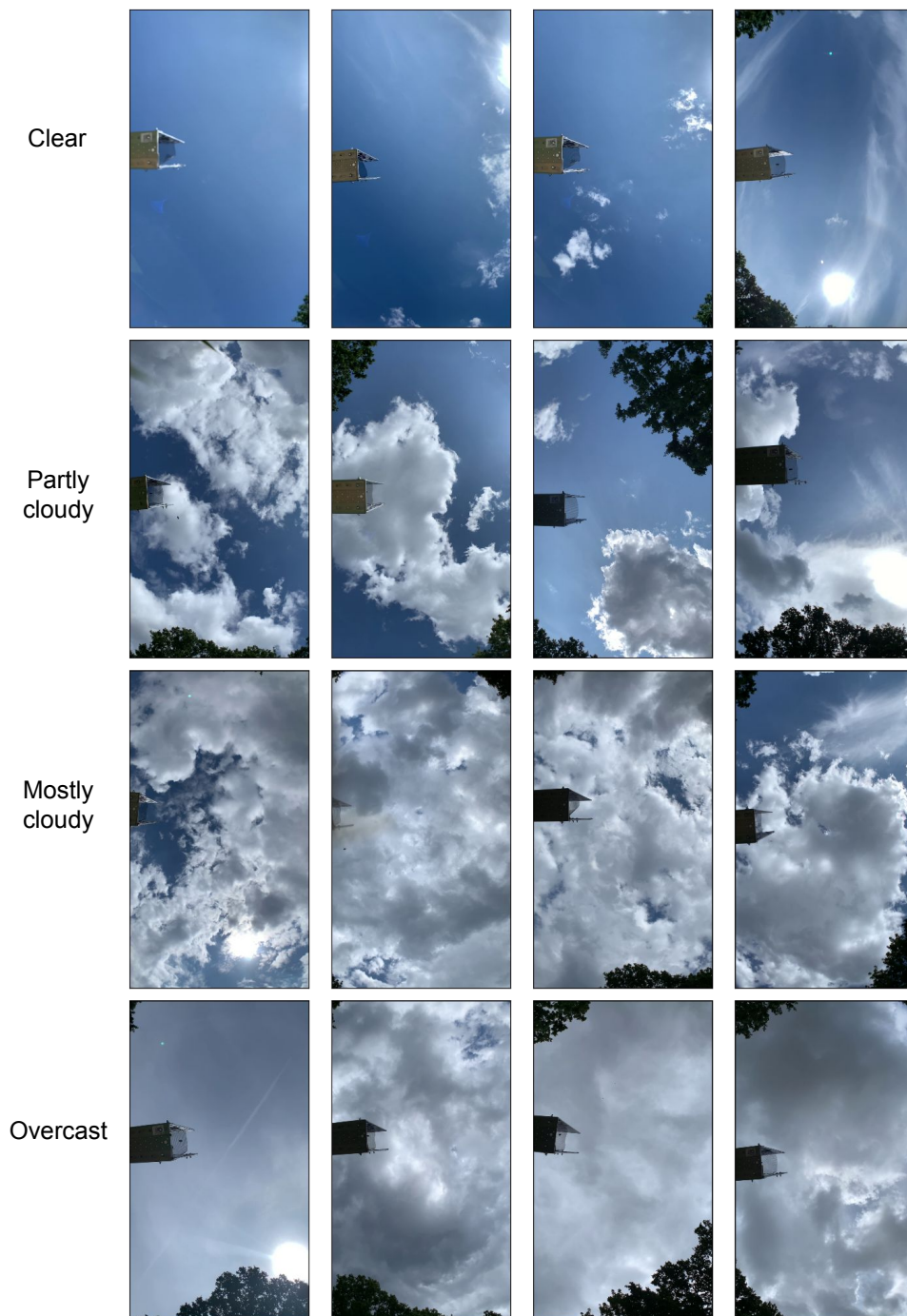


Figure 5.12. Sky conditions throughout the detour experiment. When testing each bee in the detour tunnel, the weather condition was categorised as clear ($n = 40$), partly cloudy ($n = 117$), mostly cloudy ($n = 66$) or overcast ($n = 40$).

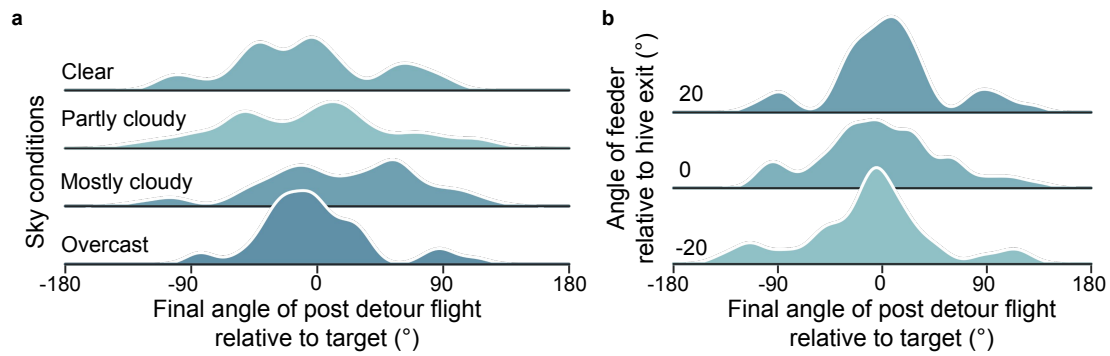


Figure 5.13. Post detour flight angles in relation to the a, sky conditions and b, angle of the feeder. The ridge plots visualise the kernel density estimates of the distributions across the given categories.

required to elicit distinct waggle phases. A small colony of *A. mellifera carnica* was housed in a two-frame observation hive within a trailer positioned at one end of a field (Fig. 5.1). A short transparent tube provided an entrance and exit to the hive for the bees and pointed outwards into the centre of the field (Fig. 5.2a). Weather conditions were mostly fine throughout the study but there were periods of cloud (Fig. 5.12). For each bee tested, the sky condition was later categorised from the video recordings of the bees' post detour flights. Fig. 5.13a shows that the accuracy of flights distributed across these categories is reasonably consistent. It is potentially surprising that the bees in overcast conditions also performed well, however, it is possible that the limited view of the video could have overlooked patches of clear sky that were available at the time. Data collected on windy days were excluded as bees visibly struggled to fly in the tunnels in these conditions.

Marking bees. Prior to conducting the experiment, any bee leaving the hive was captured in a queen marking tube and circular numbered tags were attached to their thorax using shellac glue (Fig. 5.2c). The hairs on the thorax of a bee were first removed with a wet toothpick to help the tag adhere to the bee. Marking sessions took place regularly over June to increase the chances of being able to identify a follower bee that was seen interacting with a dancer that had been trained to our feeder to then test their subsequent post detour flight trajectory.

Tunnels. Tunnels were assembled everyday from rectangular segments that were each 2.6 m long, 9 cm wide and 26 cm high. The tunnel used for the detour testing phase was assembled from two segments, each 1 m long. The side walls and floor of the tunnel were lined with waterproof paper that displayed a random white and black Julesz pattern with each block being 1 cm by 1 cm (Fig. 5.2b). The non-periodic nature of these patterns prevents the use of navigational cues based on counting a sequence of landmarks or features. A fine black mesh was used as a roof for the tunnels, which allowed light into the tunnel and a view of the sky so that the bees could still perceive directional cues (Fig. 5.2d). This layout mirrored the setup of previously published tunnel experiments^{87;298}. The mesh was affixed at mid-height within the tunnel, which prevented the bees from flying near the top and viewing nearby landmarks, such as tall trees at the edge of the field.

Training. A group of foragers were trained to a feeder placed inside the training tunnel whose entrance was 3 m from the hive exit. The feeder offered sugar water at a ratio of 1 : 1 and was initially placed at the entrance to the tunnel, before being gradually moved further inside until it was at the end (12.7 m) (Fig. 5.2c). Any foragers that landed on the mesh on top of the tunnel were placed at the tunnel entrance. The final distance of the feeder within the tunnel remained constant after training. The orientation of the tunnel relative to the hive exit was also constant within a given day but was changed across days to be either 0° or $\pm 20^\circ$. Fig. 5.13b shows that the accuracy of flights distributed across these different feeder angles was very consistent. Based on this observation, we pooled the data from the different feeder angles for the main analyses. The identities of foragers arriving at the feeder and the time of day were recorded in short intervals (every 5 minutes). A lower frame rate camera (20 fps) filmed the observation hive within the trailer under red light illumination (640 nm) throughout the entire day and recorded any dancing behaviour of the foragers as they returned from the feeder. Training would continue until a group of at least ten foragers were consistently visiting the feeder at its final position and signalling it in their dances. This would normally take around one to two hours.

Testing. Following the training phase, a shorter, 2 m long tunnel was setup to serve as the imposed detour. When not in use, both ends of this detour tunnel were kept closed so that bees could not enter. One experimenter would remain in the trailer and wait for a dance to begin by a bee that had been foraging from the feeder. The identity of the dancer and any nestmates following the dance would be recorded and an experimenter on the outside of the trailer would start capturing bees in queen marking tubes as they were leaving the hive. The dance-following interactions were filmed at a higher resolution and frame rate (80 fps) to see the antennae, using a Basler acA1440-220UM ace camera and a 50 mm lens. The captured bees were then filtered for those that were seen either dancing or following and released into the detour tunnel individually, whilst the time of day was recorded. Subsequently, this time of day, the date and location of the study site's hive was later used to calculate the target angle of the feeder relative to the sun. The time between the capture and release of a bee into the detour was between five to eight minutes. The flight trajectory of the bee leaving the tunnel was recorded within a 1.56 m by 0.84 m zone using an iPhone XR camera at 60 fps from beneath. The camera was positioned on a flat surface on the ground and recorded the silhouette of the bee against the sky. During testing, the training tunnel remained accessible for the other foragers. This procedure was repeated with different orientations of the testing tunnel relative to the training tunnel (see Fig. 5.3). The detour tunnel was positioned at different locations in the centre of the field, so that the bees leaving the detour could not see the long white exterior of the training tunnel (see Fig. 5.1 and Fig. 5.2f).

Bees flying in tunnels. Not all bees initially flew well in the tunnels. Some bees would repeatedly fly upwards, leading to them bouncing along the mesh roof. We initially speculated that this might be reflective of them attempting to regulate the amount of optic flow experienced beneath them (i.e. they were experiencing optic flow that indicated that they were too close to the ground), but we soon noticed that this behaviour more often appeared when they were returning from the feeder but not en route to the feeder. A couple of unique foragers

would also consistently land on top of the mesh at the distance of the feeder but fly perfectly through when released at the tunnel entrance. We also noticed that if the detour angle was too large ($> 60^\circ$), bees would fly up and down the first half of the tunnel but were resistant to fly through and exit. Only bees that flew sensibly and straight out of the detour were presented in the final results (Fig. 5.4). The criteria for determining whether a bee flew well in the detour tunnel (i.e. spent more than 30 s to fly out of the tunnel, needed manual intervention to leave or landed on the mesh or tunnel walls) was decided and recorded at the time of testing and usually before the bee had even left the tunnel.

Pilot study. A pilot study had also been conducted from August to September 2022, near the Roslin Institute (Edinburgh, United Kingdom). This tested some preliminary configurations of the tunnel (in terms of patterning and dimensions) and the feasibility of connecting a tunnel to the hive exit.

5.4.2 Video analysis

There were four sources of video data analysed during the experiment.

Automated tracking of post detour flights. Bees were automatically tracked as they exited the tunnel using a custom Python script that made use of the OpenCV library³¹ and a custom-built GUI. There were several steps required (Fig. 5.14). The first frame where the bee was visible upon exiting the tunnel was selected and a Gaussian blur with a kernel size of (35, 35) was applied to the video to remove noise. A Gaussian Mixture-based background subtraction algorithm^{365;366} was then applied to the remaining frames to isolate the bee from the background as it moved. Contours in the resulting binary images were filtered to an appropriate bee size and the nearest contour to the bee's position in the previous frame was selected. The centre 'x' and 'y' Cartesian coordinates of the contour's bounding box were used as the bee's position in that frame. The flight path was reliably tracked in most cases because the bees often left the tunnel and field of view within less than a couple of seconds, making them the only notable set of moving pixels within that time. In the few cases where there was strong wind that caused other objects to move within the video, the bee's position was tracked manually. The angle of the straight line connecting the coordinates of the bee in each frame with respect to its position when first exiting the tunnel was calculated relative to the angle of the tunnel exit (which had been normalised to East in the recorded videos). These angles were then presented at four boundaries: three concentric circles representing 0.22 m, 0.44 m and 0.56 m from the tunnel exit on the tunnel's horizontal plane, as well as the last visible position of the bee in the frame. Fig. 5.3c and Fig. 5.4 visualise these angles from a top-down view. The number of bees recorded at each consecutive circle generally decreased, as some bees may have left the frame before reaching the outermost circles (e.g. if they immediately turned home). Under normal circumstances, bees tend to fly upwards when travelling outwards from their hive. In our experiment, the mesh roof of the detour tunnel meant that the bees had generally become accustomed to flying at that altitude as they emerged from the tunnel and most were seen gradually ascending as they travelled further into the natural environment.

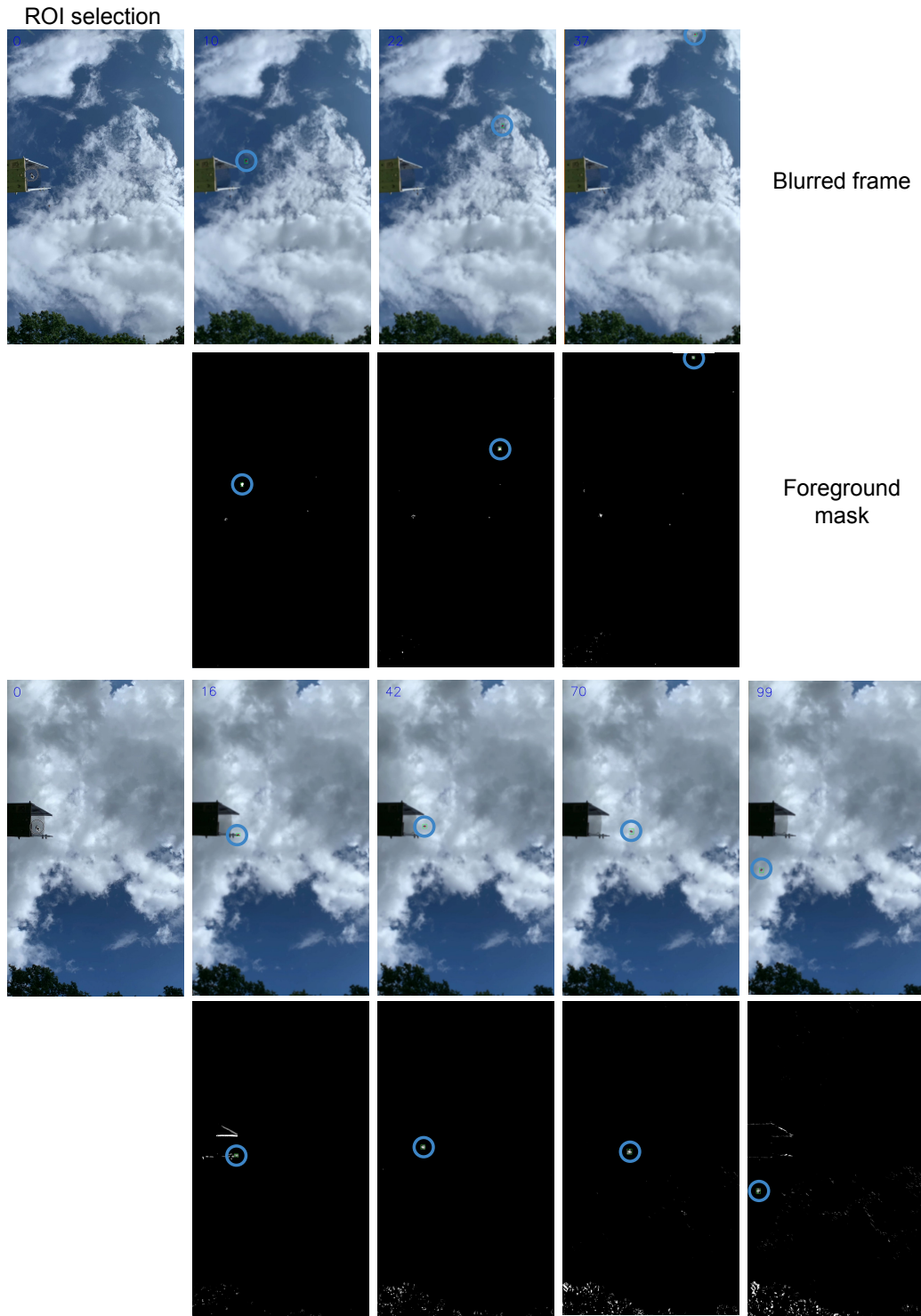


Figure 5.14. Two examples of automated tracking of bees' flight paths post detour. A region of interest (ROI) pertaining to the bee is first selected. An adaptive background subtraction algorithm is then applied to the blurred video frames to isolate the bee from the background. Candidate contours in the foreground mask (white) are filtered based on size and the contour nearest to the last known position is selected. The centre of the selected contour (bee) is shown in red and its bounding box in green. The blue circle has been added as a visual aid.

Measuring the precision of dances. There were two cases when the angles of dances were estimated. The first was when the angles of all waggle phases performed by a sample of dancers were measured based on the angle of the straight line connecting their thorax in the first to the last frame that wagging was seen (Figs. 5.7, 5.8 and A.5). The second was when the angle of the dances were measured between the first and last frame that a particular nestmate of interest was following (Figs. 5.9 and 5.10). In both cases, the angles were manually labelled with respect to gravity on the comb using a custom-built GUI. These angles were then transformed to be relative to the true angle of the feeder by calculating the expected angle of the feeder on the comb based on the position of the sun at the time and date that the dance had been performed (Figs. 5.7, 5.9, 5.10 and A.5). For the sample of foragers in Fig. 5.7, the duration of each waggle phase was also measured to the nearest 0.05 s, alongside the angle of the waggle phase.

Measuring antennal positioning. The same method from Section 4.5.1 was used to obtain and determine the angles of the dancer, follower bees and their antennae.

Mean flight speed in the detour tunnel. The mean flight speed of foragers within the detour tunnel was calculated from video recordings of a random sample of foragers flying through the tunnel at 60 fps using an iPhone XR camera. The time taken to travel 0.2 m along a portion of the midsection of the tunnel was measured to the nearest 0.016 s. The flight data was recorded from the midsection of the tunnel to avoid the initial acceleration phase of the bee.

5.4.3 Data analysis and statistics

Comparing angles. In keeping with Chapter 4, any comparisons between angles are presented such that a positive error angle indicates a deviation to the left of the target angle (counterclockwise rotation) and a negative error indicates a deviation to the right (clockwise), where the target angle can be the feeder relative to the sun, gravity, detour tunnel exit, or the training tunnel.

Assimilation circuit results. For each follower bee that was recorded interacting with a dancer that had been trained to the feeder in the training tunnel, the angles of their heading relative to gravity and their antennal positioning data were fed into the assimilation circuit, as described in Section 4.5.2. Fig. 5.10 shows the results when using the midpoint of a bee's antennae as the input feature for antennal modulation. The vector assimilated at the end of each waggle phase followed was visualised with respect to the true angle of the feeder. The mean vector direction was calculated across the phases (dashed line in Fig. 5.10). To account for the varying durations of the phases that were followed, Fig. A.6 shows the weighted mean where the weight of each vector was proportional to its length.

Analysis software. Data analysis and modelling was carried out using Python or R code, relying mainly on Numpy¹²⁷, Scipy³³⁶, and Pandas²⁰⁰ libraries. Seaborn³⁴² and Matplotlib¹⁴⁰ were used for plots. Astropy²⁶¹ was used to determine the angle of the feeder relative to the sun on a given date at the location of the study site and a given time of day. Computer vision methods for tracking bees flight trajectories post detour were implemented using OpenCV³¹

and tkinter²²⁰ was used to build the GUIs to orchestrate manual labelling of the dance angles, and the automated tracking of post detour flights. The annotation and tracking source code are publicly available on GitHub at <https://github.com/annahadji/videopyer> and <https://github.com/annahadji/bee-flight-tracer>, respectively.

Statistical tests. All plots show the mean \pm s.d. unless stated otherwise. Circular equivalents were used where appropriate. Rayleigh's Z test⁹⁰ was used to test for directionality in the scatter of the final flight angles of dancers and followers (Fig. 5.4 and Table A.1), with the null hypothesis that the circular distribution of angles for each configuration of the detour comes from a uniform circular distribution. All conditions tested significant at the level of $P < 0.001$. Equal Kappa tests for the homogeneity of concentration parameters were used to compare whether the spread of the distributions of final flight angles differed between dancers and followers for the same target angles. The following P values are associated with Figs. 5.4 and 5.6, comparing dancers and followers for the target angles: 0° , $\chi^2 = 0.083$, $P = 0.773$; 35° , $\chi^2 = 2.001$, $P = 0.157$; and -35° , $\chi^2 = 0.294$, $P = 0.588$.

Preliminary randomisation tests. We also performed randomisation tests to try to determine whether the mean angle of the waggle phases followed (Fig. 5.9a) or assimilated (Fig. 5.10a) by a recruit could predict their subsequent flight vector better than the equivalent data obtained from random samples generated from each respective dataset. For each bee, we calculated the absolute difference between their final bearing angle following the detour and their mean angle of the phases followed, or assimilated, respectively. Over 10,000 iterations, we then compared this *observed* statistic to the those generated from random samples of the entire dataset containing the same number of phases as the given bee. We calculated the proportional number of times that the randomised statistic was less than or equal to the observed statistic (the P value). The results are shown in Table 5.1. The majority of the bees showed relatively high P values, meaning that the statistics computed from the random samples often performed better their own data alone. We believe that these results might actually be reflecting a limitation of the randomisation test that is driven by the characteristics of our dataset. For example, the fact that each of the recruits were receiving information about the *same* target and that the distribution of detour angles flown was relatively narrow, means that any random samples drawn from across the data will also predominantly contain points that are clustered around this same target. We have therefore chosen to present these results as a preliminary exploration, acknowledging the need for a larger sample size and a wider range of feeder directions for a more robust conclusion in this context.

External dataset. We visualised the detour data from a comparable ant experiment by Collett et al.⁴⁹ in a similar style to our own detour data to enable an approximate comparison (see Fig. 1d in Collett et al.⁴⁹). The dataset was plotted based on the information provided by its original caption.

Table 5.1. Randomisation test results for the angles of the vectors **a, followed (see Fig. 5.9a) and **b**, assimilated (see Fig. 5.10a) by recruits.** The statistic computed was the absolute difference between the final bearing angle of the bee post detour and the mean phase **a**, followed or **b**, assimilated. The bee number in **a**, refers to the index of the bee in Fig. 5.9a, as read left-to-right and top-to-bottom.

(a) Vectors followed			(b) Vectors assimilated		
Bee	Observed statistic (°)	<i>P</i>	Bee	Observed statistic (°)	<i>P</i>
1	4.58	0.013	U	26.43	0.59
2	5.00	0.014	V	10.73	0.23
3	12.22	0.40	W	49.30	0.22
4	12.08	0.42	X	35.60	0.73
5	19.98	0.53	Y	14.50	0.34
6	33.00	0.83	Z	0.72	0.016
7	35.68	0.92			
8	51.455	0.12			
9	62.71	0.43			
10	72.44	0.96			
11	68.75	0.93			
12	74.37	0.89			
13	74.46	0.92			
14	108.29	0.924			
15	100.58	0.77			
16	111.51	0.99			

5.4.4 Acknowledgements

I would like to express my sincere gratitude to Prof. Tim Landgraf for hosting me in his lab group in Berlin to conduct the detour experiment, as well as Marie Messerich for helping me with the daily setup, training and testing of the bees throughout the entire experiment. In addition, my thanks go to David Dormagen for his expertise and technical support with the filming setup, Pranav Kedia for the providing stunning drone footage and Alexander Shtol for assistance with training the bees.

6

Conclusion

This thesis adopted a new approach to explore the neural mechanisms underlying the long-studied dance communication system of bees, by evaluating computational models of the insect brain against observed dance and foraging behaviour. Due to the newly established role of the central complex in the acquisition and utilisation of vectors for navigation, we focused on how this neural circuit could provide the necessary connectivity and computation for the encoding, decoding and expression of spatial information in dance communication. This chapter summarises the contributions of the thesis, as well as directions for future research.

6.1 Overview

In Chapter 3, we adapted an existing model of how vector memory recall in the central complex controls the return to a feeder to produce a corresponding miniature version of this trip as a dance. We concluded that angular scatter seen in natural dances was not the result of accumulating errors and was irrespective of the type of resource being signalled (nectar or pollen). Rather, our analysis of natural dances and simulations of the circuit suggested that the patterns of angular scatter could arise from the dynamics of activating a vector memory for consecutive waggle phases, alongside a physical constraint on the rate at which the dancer can update her path direction when wagging. Simulating these properties in dances reproduced the different scatter patterns observed in natural dances for nearby and distant feeders, indicating that the circuit can explain features that exist across the spectrum of the recruitment system. This is the first simulation of a biologically plausible circuit that is capable of producing a dance path based on a prior foraging trip.

In Chapter 4, we provided the first detailed explanation, at the sensory and neural level, of how follower bees could recover the vector information signalled by dancers. This work was based

on two key factors: (1) high-speed, high-resolution videography within which the antennal positions of follower bees were tracked in more detail than any previous study, and (2) recent insights into the vector-processing circuitry of the fruit fly central complex that revealed a neural substrate for converting egocentric motion signals in varying orientations into a consistent allocentric travel vector^{189;190}. Our modelling showed that the same anatomically grounded circuit could allow the antennal position signals of the follower over varying orientations to the dancer to be converted to a consistent allocentric estimate of the dancer's direction. By processing the positional data from real follower bees using this 'assimilation circuit', we were able to infer the location signalled by the dancer.

In Chapter 5, we conducted a novel experiment to study the accuracy of real vectors expressed by bees recruited to a feeder, as well as experienced foragers returning to a feeder. This experiment was the first application of the forced-detour paradigm, commonly used in ant studies, to bees, as well as the first to utilise the patterned tunnels apparatus to study the search flights of recruits. The correction angle made by the bees provided a continuous measure of their estimated location of the food source, incorporating both the distance and direction. This experiment indicated that a broad distribution of flight paths to the signalled feeder, as predicted by the assimilation circuit in Chapter 4, may indeed be biologically accurate. The circuit was able to provide a readout of the mean flight vectors predicted from the dancer-follower interactions of six recruits that differed from the actual vectors that were expressed by a minimum of 1° and a maximum of 49°.

By considering each of the key requirements of the system – performing the dance (Chapter 3), recovering the signalled dance vector (Chapter 4) and navigating to the resource (Chapter 5) – this thesis establishes the central complex as a plausible common neural substrate for dance communication. There have been speculations in the past that have alluded to this idea. In 2007, Brockmann and Robinson³⁵ concluded that there were no dance-specific sensory projections in the brains of honeybees, suggesting that the neural circuitry facilitating dance behaviour was likely to overlap with other behaviours. Esch⁸³ in 2011 commented on the similarity between the dance and a re-enactment of the foraging trip, but the possible neurobiological basis for vectors in the insect brain was unknown at that time. As new insights began to emerge, Barron and Plath¹² were the first to recognise their implications and hypothesised in 2017 that the central complex could be the neurobiological link between dance and orientation behaviours. This thesis has now extended and translated this hypothesis into concrete computational models that demonstrate how the central complex could explain the observed dance and following behaviours. By making this explicit connection between bee dance communication behaviour and the central complex, we have been able to ground the system within a rapidly developing account of the neural basis of navigation in insects.

6.2 Rethinking the dance

Honeybee dance communication has been a subject of scientific interest for many years, with its earliest known reference dating back to Aristotle's *History of Animals*²⁵¹ (400 B.C.E.). The

field arguably reached its peak with Karl von Frisch's Nobel Prize-winning work in 1973. Since then, researchers have documented nearly every aspect of the dancing bee according to some of his early conceptions of the dance. Should we be rethinking some of these conceptions in our current interpretation of the dance?

Von Frisch¹⁰⁰ described the waggle phase as the 'straight-run' portion of the dance where *'the bee runs straight ahead for a short distance [whilst wagging]'* and researchers since have measured the angle of this straight portion under numerous foraging conditions. He also briefly stated that the wagging can begin earlier, i.e. during the turn into the waggle phase, or even extend beyond it as the dancer turns into the return phase (p. 59). This property is often not accounted for but can introduce ambiguity when estimating the angle of the waggle phase. For example, in such cases, deriving the angle using the line from the start to end of wagging can differ from the angle obtained by fitting a line to the straightest portion of wagging, especially for phases of greater length. In Chapter 3, we demonstrated how misaligned portions of a waggle phase could in fact arise from an artefact of a path integration control system incorporating a vector memory and a parameter to constrain how much the dancer can update its waggle path direction. While many research questions are likely to be unaffected by this subtle detail, the problem potentially becomes more apparent when one considers what follower bees contend with to obtain their own flight vector to the resource. For example, some nestmates continuously follow the dancer through all phases of the dance, including the return phase, rather than just its straight-run portion. We can predict the effect that these misaligned portions would have on the accuracy of the information transfer using the assimilation circuit in Chapter 4. For a follower that can average her vector estimates across multiple waggle phases, the effect of such inconsistencies could actually be negligible if they occur symmetrically throughout the dance.

Early studies wishing to analyse dance followers within the hive decided to exclude nestmates that did not actively move along with the dancer, under the assumption that these 'dance attendants' were not decoding the information³⁰. Even though there is no evidence that this is the case, this criteria has been adopted by more recent works too, including Gil and Marco¹⁰⁸ in 2010, who excluded these nestmates when measuring the antennal positioning of dance followers. In Chapter 4, we included these nestmates as followers and found that the accuracy of vector estimates, as predicted by the antennal positioning data, was not significantly affected by whether their orientation relative to the dancer was stable or changing. These examples highlight the advantages of the approach taken in this thesis: computational models not only allow us to test hypotheses for the neural processing underlying naturalistic behaviour, but also make it possible to evaluate the system in different contexts and highlight the plausible assumptions required to match observations.

The initial controversy between Karl von Frisch^{99;116} and Adrian Wenner^{143;353;354} about the role of the dance versus odour cues in honeybee recruitment led to somewhat polarised perspectives on the dance. The behavioural models that arose from these discussions attributed either the dance or odour cues alone as being responsible for the *entire* path of recruits from the hive to the food source. By 1973, Wenner had largely stepped away from dance research and

a consensus had formed in favour of von Frisch’s interpretation²²². This led to a prevailing narrative – particularly emphasised in popular accounts of the dance³¹⁹ – that recruits could pinpoint the correct food location based on their vector obtained from the dance alone. We believe that the assimilation circuit contributes a *lower bound* on the accuracy of location information that a follower could extract from the dance. With no other cues available, the effects of following the dancer on the follower’s antennal positions (as we measured) combined with their orientation to gravity (as we modelled) is sufficient to create an estimate of the direction and distance to the food location signalled by the dancer. This will allow the follower to get closer to the feeder than they would otherwise. While real bees might use additional factors to improve their estimates, they should be no worse than our model. Indeed we found this to be the case in Chapter 5: the circuit predicted a broad spread of estimates which is consistent with the broad spread of initial flight paths we observed from the detour experiment. However, the extent of the spread we observed arguably exceeds what might be expected from von Frisch’s experiments^{99;100} as well as others³¹⁸. For example, von Frisch⁹⁹ had observed that the majority of recruits caught in feeder traps deviated no more than $\pm 15^\circ$ from the direction of the feeder. So, how is it that, despite variability in the message of dancers and a broad scatter of initial flight paths, recruits have historically still been able find the goal, even when it is a small saucer of sugar water in a field? We believe that the *approximate* vector that nestmates obtain from the dance can be used for the initial stages of orientation to the distant goal and that a structured search based on this vector²⁵⁶ along with other orientation aids, such as scents and the presence of other bees, can be used in the final stages of locating the food source. It is also possible that bees project this vector into a remembered map of the landscape and can then use landmarks to improve their accuracy at finding the source³⁴⁰. These perspectives shift the view of the dance towards the idea that the recovered dance vector need not pinpoint the exact correct location but nonetheless, can guide them closer to the food than would otherwise be possible. A recent book by Tautz³¹⁹ in 2022 strongly advocates for further research on the behaviour and communication of bees outside the hive that could accompany this interpretation.

It is easy to overlook the challenges faced by the earliest bee researchers, who decoded dances in real-time using stopwatches and protractors positioned over the glass of the observation hive – a testament to their dedication in a time before recording technologies became commonplace. Most of the work presented in von Frisch’s book¹⁰⁰ used such methods. However, it is worth considering whether the reliance on real-time observation could have introduced bias to the measured data. Given the emphasis on alternating turn directions in consecutive waggle phases, could the experimenter’s anticipation of a *leftward* or *rightward* phase subtly influence their measurement of its angle? The ability to record and store high-speed, high-resolution videos enables reproducibility and repeated re-analysis of the data to test different hypotheses; something we did frequently throughout Chapters 3 to 5. This technological preservation of the data is also invaluable in terms of data sharing. Throughout this thesis, we were able to make use of several datasets collected by other research groups, enriching the scope of comparisons for our models. There are also new automated methods for tracking bees^{24;28}, decoding dances^{237;341}, and even generalised methods for pose estimation of animals

in laboratory environments^{225;244}. Although these are powerful tools for data analysis, their predictions often still require human validation, as even the most sophisticated algorithms can struggle to accurately capture fine-grained features, such as antennae movements, in a natural setting. Nonetheless, the increasing quality and scale of data within the bee community enables a more robust analysis of dance communication.

6.3 Future directions

In order to facilitate the development of the computational models in this thesis, we introduced plausible assumptions that also implicate areas for further research. For example, in Chapter 3, the path integration circuit controlled the general path direction of the dancer through its PFL motor commands (known as CPUs in bee nomenclature) that specify leftward or rightward turns. Whilst Tautz et al.³²¹ recorded the positioning of the dancer's feet on the comb when wagging, the specific muscles and motor patterns involved in generating the dance remain unknown. For this reason, we added a lateral displacement to the position when wagging to generate the abdomen oscillations. However, it may be possible to record electrograms from muscles in a dancing bee in order to obtain a detailed understanding of their activation and coordination, especially when combined with improved tracking methods¹¹.

We also assumed the existence of a 'gravity bump' in the ellipsoid body and protocerebral bridge of the central complex, similar in nature to the activity observed for other pertinent cues in the environment, including celestial¹³⁰, visual²⁸⁹ and proprioceptive³³³ cues. In bees, the neck and abdomen hairs are believed to be candidate sensory organs for detecting the orientation relative to gravity¹⁸⁷. Whilst it appears that the sensory information from the neck hair plates projects to the antennal mechanosensory and motor centre (AMMC) of the brain¹⁵⁴, how the gravity information could then be relayed to the central complex is an active area of research in bees and in other insects too. It is interesting that the open-nesting species of honeybee, *A. florea*, that dance on the horizontal portion of their comb can only use the celestial cues for orienting their waggle dances (and not gravity, like in other species of honeybee)¹⁸³. Confirming how gravity is represented in the brain could therefore offer an insight into the evolution of the dance and its divergence from other forms of signalling behaviour.

In Chapter 4, our hypothesis that the follower's antennal positioning could reach the central complex was supported by research showing that antennal displacements in the fruit fly, evoked by wind, could yield a basis vector representation in the fan-shaped body of the central complex⁵⁶. We assumed that the follower bee exhibits a similar representation from passive antennal deflections that arise from contact with the dancer's body when positioned at extreme angles to it. Since the equivalent genetic tools are not yet available to test this assumption in honeybees at the neural level, comparing their antennal displacements in response to wind direction to those recorded in fruit flies²³⁸ could meanwhile reveal any differences in the response characteristics of bee and fruit fly antennae. It is possible that modelling the complete honeybee antennal pathway could account for any observed differences. There could

also be other sensory cues that provide followers with the information about the dancer's angle or lead them to actively adopt the observed antennal positions. An interesting avenue of future research could use the inverse methodology of trying to understand what the follower is experiencing by measuring the force or timing of antennal contact perceived on the abdomen of a robotic dancer^{171;172}. Moreover, whilst our observations offer an explanation for the antennal positioning of nestmates that immediately surround the dancer, other cues, such as the electrostatic field¹¹⁸, may be able to influence nestmates positioned beyond this range. In our recordings, we did not observe any *outer* nestmates showing interest in the dance or orienting towards the dancer so did not examine this idea.

One could also further validate the proposed circuit in Chapter 4 by manipulating the positions of nestmates' antennae whilst following a dance. For example, if their antennae were held in a constant position whilst following, according to the assimilation circuit, their recovered vector should accumulate in the direction specified by the now predetermined allocentric angle of the dancer. If the follower changes their position relative to gravity they will experience the dancer as changing its direction correspondingly and thus, it is likely that they would end up integrating a variety of directions. With their tracked data, we could obtain a prediction of this vector and compare it to their actual flight vector flown. Manipulating the antennae of bees for experimental purposes is challenging, as bees rely on their antennae for a wide range of functions both within and outside the hive. Thus, whilst it might be feasible to fix the bases of the antennae with glue, or potentially use piezoelectric actuators to control their position (e.g. see Okubo et al. ²³⁸), it would be preferable to devise a method that transiently manipulates their position only when following, for example, by using magnetic paint on the antennae and precisely positioned magnets. Researchers have identified genetic lines in *Drosophila* that allow for experimental control over antennal movement³¹², with their activation causing a forward and upward antennal movement, similar to those induced by the start of flight. This suggests that similar tools might eventually be possible in bees.

Although our work did not explicitly examine the role of age in dance following behaviour, it could also be interesting avenue for future exploration. Dong et al. ⁶⁵ identified that young bees spend a few days observing experienced bees before attempting to dance themselves. However, whether there are differences in the following behaviour of young versus experienced bees remain unexplored. Investigating this could potentially explain the styles of following behaviour that have been noted over the years, such as the aforementioned dance follower versus dance attendant debate. For example, do young followers exhibit the more *active* style of behaviour where they pursue the dancer around the comb? Kumaraswamy et al. ¹⁶⁹ identified changes in the dendritic density and firing rate of the vibration-sensitive interneuron (DL-Int-1) between newly emerged adult bees and mature foragers. This suggests that age-dependent adaptations might be required for processing the dance's duration information (i.e. the distance to the signalled resource). In the assimilation circuit, we proposed that DL-Int-1 could gate the accumulation of the follower's vector during the train of pulses within the waggle phase. In Section 4.1, we discuss how the circuit could also accumulate the distance information according to the length of the waggle phase on the comb if following directly behind the dancer, i.e. the way that distance information would normally be accumulated via path integration when

walking. Alongside tracking the age of members within the colony, comparing the vector estimates when integrating across these different gating periods – e.g. the more precise sound pulse stimuli versus the distance travelled on the comb – could reveal whether age-related differences influence the temporal cue used for the integration and accuracy of the recovered dance vector.

The dance's dynamic and social nature necessitates free movement and interaction of the bees, which precludes the use of existing electrophysiological approaches that require an isolated or restrained insect to study its neural activity. The availability of advanced neurogenetic tools in some insects has allowed researchers to perform sophisticated experiments to explore the neural circuits underlying behaviour by manipulating gene expression and neuron function. However, developing techniques that allow for the neurogenetic manipulation of eusocial insects, such as honeybees, has been challenging due to the difficulties associated with breeding and more complex genetics¹⁶⁸. Thus, it is currently beyond the state-of-the-art to directly measure the neural activity in dancing bees, or their followers, with the detail needed to verify some of the predictions of the computational models in this thesis. Whilst parallel studies using model organisms like *Drosophila* could meanwhile be valuable, recent advances offer a promising path forward for bee neuroethology in the future. In 2023, Carcaud et al.³⁹ generated a pan-neuronal genetic driver in the honeybee, allowing them to widely express a calcium indicator in neurons across the brain and study the activity in multiple regions upon olfactory stimulation. Although these recordings were in restrained bees, the technique holds promise as the first neurogenetic tool for recording neural activity in an eusocial insect and could potentially be combined with a virtual reality setup or used to investigate neural responses to controlled interactions.

In conclusion, this thesis has explored how computational models of the central complex circuit could accommodate the dance and foraging behaviours observed in honeybee communication. We have offered a neurobiological explanation for how follower bees decode and extract the vector information available in a dance, addressing a key question that arose from von Frisch's seminal work. It is our hope that the models presented here will provide a framework for guiding future investigations, particularly as neurogenetic tools become increasingly available in honeybees. As a compelling example of how social interactions can be implemented within a compact and efficient neural architecture, honeybees and the wider insect world will undoubtedly continue to invite many years of research.

Bibliography

- [1] Ai, H. and Hagio, H. 2013, 'Morphological analysis of the primary center receiving spatial information transferred by the waggle dance of honeybees', *Journal of Comparative Neurology* **521**(11), 2570–2584.
- [2] Ai, H. and Itoh, T. 2011, *The Auditory System of the Honey Bee*, Springer Netherlands, pp. 269–283.
- [3] Ai, H., Kai, K., Kumaraswamy, A., Ikeno, H. and Wachtler, T. 2017, 'Interneurons in the honeybee primary auditory center responding to waggle dance-like vibration pulses', *Journal of Neuroscience* **37**(44), 10624–10635.
- [4] Ai, H., Nishino, H. and Itoh, T. 2007, 'Topographic organization of sensory afferents of Johnston's organ in the honeybee brain', *Journal of Comparative Neurology* **502**(6), 1030–1046.
- [5] Ai, H., Rybak, J., Menzel, R. and Itoh, T. 2009, 'Response characteristics of vibration-sensitive interneurons related to Johnston's organ in the honeybee, *Apis mellifera*', *Journal of Comparative Neurology* **515**(2), 145–160.
- [6] Arias, M. C. and Sheppard, W. S. 2005, 'Phylogenetic relationships of honey bees (Hymenoptera: Apinae: Apini) inferred from nuclear and mitochondrial DNA sequence data', *Molecular Phylogenetics and Evolution* **37**(1), 25–35.
- [7] Baddeley, B., Graham, P., Husbands, P. and Philippides, A. 2012, 'A model of ant route navigation driven by scene familiarity', *PLoS Computational Biology* **8**(1), e1002336.
- [8] Baird, E., Boeddeker, N. and Srinivasan, M. V. 2021, 'The effect of optic flow cues on honeybee flight control in wind', *Proceedings of the Royal Society B: Biological Sciences* **288**.
- [9] Baird, E., Srinivasan, M. V., Zhang, S., Lamont, R. and Cowling, A. 2006, *Visual Control of Flight Speed and Height in the Honeybee*, Springer Berlin Heidelberg, pp. 40–51.
- [10] Balbuena, M. S., González, A. and Farina, W. M. 2019, 'Characterizing honeybee cuticular hydrocarbons during foraging', *Sociobiology* **66**(1), 97.
- [11] Banerjee, A., Wu, S., Cheng, L. and Aw, S. S. 2020, 'Fully automated leg tracking in freely moving insects using feature learning leg segmentation and tracking (FLLIT)', *Journal of Visualized Experiments* (158).
- [12] Barron, A. B. and Plath, J. A. 2017, 'The evolution of honey bee dance communication: a mechanistic perspective', *Journal of Experimental Biology* **220**(23), 4339–4346.
- [13] Barron, A. B., Zhu, H., Robinson, G. E. and Srinivasan, M. V. 2005, 'Influence of flight time and flight environment on distance communication by dancing honey bees', *Insectes Sociaux* **52**(4), 402–407.

- [14] Barron, A. and Srinivasan, M. V. 2006, ‘Visual regulation of ground speed and headwind compensation in freely flying honey bees (*Apis mellifera* L.)’, *Journal of Experimental Biology* **209**(5), 978–984.
- [15] Batschelet, E. 1981, *Circular Statistics in Biology*, Mathematics in biology, Academic Press.
URL: <https://books.google.co.uk/books?id=ip5kQgAACAAJ>
- [16] Beekman, M., Doyen, L. and Oldroyd, B. P. 2005, ‘Increase in dance imprecision with decreasing foraging distance in the honey bee *Apis mellifera* L. is partly explained by physical constraints’, *Journal of Comparative Physiology A* **191**(12), 1107–1113.
- [17] Beekman, M., Gloag, R. S., Even, N., Wattanachaiyingchareon, W. and Oldroyd, B. P. 2008, ‘Dance precision of *Apis florea*—clues to the evolution of the honeybee dance language?’, *Behavioral Ecology and Sociobiology* **62**(8), 1259–1265.
- [18] Beekman, M. and Lew, J. B. 2007, ‘Foraging in honeybees—when does it pay to dance?’, *Behavioral Ecology* **19**(2), 255–261.
- [19] Beekman, M., Makinson, J. C., Couvillon, M. J., Preece, K. and Schaerf, T. M. 2015, ‘Honeybee linguistics - a comparative analysis of the waggle dance among species of *Apis*’, *Frontiers in Ecology and Evolution* **3**.
- [20] Beetz, M. J., Kraus, C. and el Jundi, B. 2023, ‘Neural representation of goal direction in the monarch butterfly brain’, *Nature Communications* **14**(1).
- [21] Behbahani, A. H., Palmer, E. H., Corfas, R. A. and Dickinson, M. H. 2021, ‘*Drosophila* re-zero their path integrator at the center of a fictive food patch’, *Current Biology* **31**(20), 4534–4546.e5.
- [22] Biesmeijer, J. C. and de Vries, H. 2001, ‘Exploration and exploitation of food sources by social insect colonies: a revision of the scout-recruit concept’, *Behavioral Ecology and Sociobiology* **49**(2–3), 89–99.
- [23] Biesmeijer, J. C. and Seeley, T. D. 2005, ‘The use of waggle dance information by honey bees throughout their foraging careers’, *Behavioral Ecology and Sociobiology* **59**(1), 133–142.
- [24] Boenisch, F., Rosemann, B., Wild, B., Dormagen, D., Wario, F. and Landgraf, T. 2018, ‘Tracking all members of a honey bee colony over their lifetime using learned models of correspondence’, *Frontiers in Robotics and AI* **5**.
- [25] Boggs, P. T. and Donaldson, J. R. 1989, *Orthogonal distance regression*.
- [26] Borst, A. and Heisenberg, M. 1982, ‘Osmotropotaxis in *Drosophila melanogaster*’, *Journal of Comparative Physiology* **147**(4), 479–484.
- [27] Bowker, G. E. and Crenshaw, H. C. 2007, ‘Electrostatic forces in wind-pollination – part 1: Measurement of the electrostatic charge on pollen’, *Atmospheric Environment* **41**(8), 1587–1595.

- [28] Bozek, K., Hebert, L., Portugal, Y., Mikheyev, A. S. and Stephens, G. J. 2021, 'Markerless tracking of an entire honey bee colony', *Nature Communications* **12**(1).
- [29] Božič, J. and Abramson, C. I. 2003, 'Following and attending: two distinct behavior patterns of honeybees in a position to collect the dance information'.
- [30] Božič, J. and Valentinčič, T. 1991, 'Attendants and followers of honey bee waggle dances', *Journal of Apicultural Research* **30**(3-4), 125–131.
- [31] Bradski, G. 2000, 'The OpenCV Library', *Dr. Dobb's Journal of Software Tools* .
- [32] Brandt, R., Rohlfing, T., Rybak, J., Kroficzek, S., Maye, A., Westerhoff, M., Hege, H.-C. and Menzel, R. 2005, 'Three-dimensional average-shape atlas of the honeybee brain and its applications', *Journal of Comparative Neurology* **492**(1), 1–19.
- [33] Brines, M. L. 1978, Skyline polarization patterns as cues for honey bee orientation; physical measurements and behavioral experiments, PhD thesis, The Rockefeller University.
- [34] Brockmann, A., Basu, P., Shakeel, M., Murata, S., Murashima, N., Boyapati, R. K., Prabhu, N. G., Herman, J. J. and Tanimura, T. 2018, 'Sugar intake elicits intelligent searching behavior in flies and honey bees', *Frontiers in Behavioral Neuroscience* **12**.
- [35] Brockmann, A. and Robinson, G. E. 2007, 'Central projections of sensory systems involved in honey bee dance language communication', *Brain, Behavior and Evolution* **70**(2), 125–136.
- [36] Cant, E. T., Smith, A. D., Reynolds, D. R. and Osborne, J. L. 2005, 'Tracking butterfly flight paths across the landscape with harmonic radar', *Proceedings of the Royal Society B: Biological Sciences* **272**(1565), 785–790.
- [37] Capaldi, E. A. and Dyer, F. C. 1999, 'The role of orientation flights on homing performance in honeybees', *Journal of Experimental Biology* **202**(12), 1655–1666.
- [38] Capaldi, E. A., Smith, A. D., Osborne, J. L., Fahrback, S. E., Farris, S. M., Reynolds, D. R., Edwards, A. S., Martin, A., Robinson, G. E., Poppy, G. M. and Riley, J. R. 2000, 'Ontogeny of orientation flight in the honeybee revealed by harmonic radar', *Nature* **403**(6769), 537–540.
- [39] Carcaud, J., Otte, M., Grünwald, B., Haase, A., Sandoz, J.-C. and Beye, M. 2023, 'Multisite imaging of neural activity using a genetically encoded calcium sensor in the honey bee', *PLOS Biology* **21**(1), e3001984.
- [40] Cardinal, S. and Danforth, B. N. 2011, 'The antiquity and evolutionary history of social behavior in bees', *PLoS ONE* **6**(6), e21086.
- [41] Cheeseman, J. F., Millar, C. D., Greggers, U., Lehmann, K., Pawley, M. D. M., Gallistel, C. R., Warman, G. R. and Menzel, R. 2014a, 'Reply to cheung et al.: The cognitive map hypothesis remains the best interpretation of the data in honeybee navigation', *Proceedings of the National Academy of Sciences* **111**(42).

- [42] Cheeseman, J. F., Millar, C. D., Greggers, U., Lehmann, K., Pawley, M. D. M., Gallistel, C. R., Warman, G. R. and Menzel, R. 2014b, 'Way-finding in displaced clock-shifted bees proves bees use a cognitive map', *Proceedings of the National Academy of Sciences* **111**(24), 8949–8954.
- [43] Cheung, A., Collett, M., Collett, T. S., Dewar, A., Dyer, F., Graham, P., Mangan, M., Narendra, A., Philippides, A., Stürzl, W., Webb, B., Wystrach, A. and Zeil, J. 2014, 'Still no convincing evidence for cognitive map use by honeybees', *Proceedings of the National Academy of Sciences* **111**(42).
- [44] Chiel, H. and Beer, R. 2009, *Computational Neuroethology*, Elsevier, pp. 23–28.
- [45] Chittka, L. and Geiger, K. 1995, 'Can honey bees count landmarks?', *Animal Behaviour* **49**(1), 159–164.
- [46] Chittka, L., Kunze, J., Shipman, C. and Buchmann, S. L. 1995, 'The significance of landmarks for path integration in homing honeybee foragers', *Naturwissenschaften* **82**(7), 341–343.
- [47] Clarke, D., Whitney, H., Sutton, G. and Robert, D. 2013, 'Detection and learning of floral electric fields by bumblebees', *Science* **340**(6128), 66–69.
- [48] Collett, M. and Collett, T. S. 2000, 'How do insects use path integration for their navigation?', *Biological Cybernetics* **83**(3), 245–259.
- [49] Collett, M., Collett, T. S. and Wehner, R. 1999, 'Calibration of vector navigation in desert ants', *Current Biology* **9**(18), 1031–31.
- [50] Collett, T., Fry, S. and Wehner, R. 1993, 'Sequence learning by honeybees', *Journal of Comparative Physiology A* **172**(6).
- [51] Collett, T. S. 1996, 'Insect navigation en route to the goal: Multiple strategies for the use of landmarks', *Journal of Experimental Biology* **199**(1), 227–235.
- [52] Collett, T. S. and Baron, J. 1994, 'Biological compasses and the coordinate frame of landmark memories in honeybees', *Nature* **368**(6467), 137–140.
- [53] Couvillon, M. J., Pearce, F. C. R., Harris-Jones, E. L., Kuepfer, A. M., Mackenzie-Smith, S. J., Rozario, L. A., Schürch, R. and Ratnieks, F. L. W. 2012, 'Intra-dance variation among waggle runs and the design of efficient protocols for honey bee dance decoding', *Biology Open* **1**(5), 467–472.
- [54] Couvillon, M. J., Phillipps, H. L. F., Schürch, R. and Ratnieks, F. L. W. 2012, 'Working against gravity: horizontal honeybee waggle runs have greater angular scatter than vertical waggle runs', *Biology Letters* **8**(4), 540–543.
- [55] Cruse, H. and Wehner, R. 2011, 'No need for a cognitive map: Decentralized memory for insect navigation', *PLoS Computational Biology* **7**(3), e1002009.

- [56] Currier, T. A., Matheson, A. M. and Nagel, K. I. 2020, 'Encoding and control of orientation to airflow by a set of drosophila fan-shaped body neurons', *eLife* **9**.
- [57] Dacke, M., Baird, E., Byrne, M., Scholtz, C. and Warrant, E. 2013, 'Dung beetles use the milky way for orientation', *Current Biology* **23**(4), 298–300.
- [58] Dacke, M. and Srinivasan, M. V. 2007, 'Honeybee navigation: distance estimation in the third dimension', *Journal of Experimental Biology* **210**(5), 845–853.
- [59] Dacke, M. and Srinivasan, M. V. 2008, 'Two odometers in honeybees?', *Journal of Experimental Biology* **211**(20), 3281–3286.
- [60] De Marco, R. J., Gil, M. and Farina, W. M. 2005, 'Does an increase in reward affect the precision of the encoding of directional information in the honeybee waggle dance?', *Journal of Comparative Physiology A* **191**(5), 413–419.
- [61] Degen, J., Kirbach, A., Reiter, L., Lehmann, K., Norton, P., Storms, M., Koblöfsky, M., Winter, S., Georgieva, P. B., Nguyen, H., Chamkhi, H., Greggers, U. and Menzel, R. 2015, 'Exploratory behaviour of honeybees during orientation flights', *Animal Behaviour* **102**, 45–57.
- [62] Degen, J., Kirbach, A., Reiter, L., Lehmann, K., Norton, P., Storms, M., Koblöfsky, M., Winter, S., Georgieva, P., Nguyen, H., Chamkhi, H., Meyer, H., Singh, P., Manz, G., Greggers, U. and Menzel, R. 2016, 'Honeybees learn landscape features during exploratory orientation flights', *Current Biology* **26**(20), 2800–2804.
- [63] Deisseroth, K. 2011, 'Optogenetics', *Nature methods* **8**(1), 26–29.
- [64] Dethier, V. G. 1957, 'Communication by insects: Physiology of dancing', *Science* **125**(3243), 331–336.
- [65] Dong, S., Lin, T., Nieh, J. C. and Tan, K. 2023, 'Social signal learning of the waggle dance in honey bees', *Science* **379**(6636), 1015–1018.
- [66] Dormagen, D. M., Wild, B., Wario, F. and Landgraf, T. 2023, 'Machine learning reveals the waggle drift's role in the honey bee dance communication system', *PNAS Nexus* **2**(9).
- [67] Dornhaus, A. 2002, The role of communication in the foraging process of social bees, PhD thesis, Universität Würzburg, Fakultät für Biologie.
- [68] Dornhaus, A. and Chittka, L. 1999, 'Evolutionary origins of bee dances', *Nature* **401**(6748), 38–38.
- [69] Dreller, C. and Kirchner, W. 1993a, 'Hearing in honeybees: localization of the auditory sense organ', *Journal of Comparative Physiology A* **173**(3), 275–279.
- [70] Dreller, C. and Kirchner, W. H. 1993b, 'How honeybees perceive the information of the dance language', *Naturwissenschaften* **80**(7), 319–321.

- [71] Dyer, F. C. 1987, 'Memory and sun compensation by honey bees', *Journal of Comparative Physiology A* **160**(5), 621–633.
- [72] Dyer, F. C. 1991, 'Bees acquire route-based memories but not cognitive maps in a familiar landscape', *Animal Behaviour* **41**(2), 239–246.
- [73] Dyer, F. C. 1993, 'How honey bees find familiar feeding sites after changing nesting sites with a swarm', *Animal Behaviour* **46**(4), 813–816.
- [74] Dyer, F. C. 2002, 'The biology of the dance language', *Annual Review of Entomology* **47**(1), 917–949.
- [75] Dyer, F. C. and Dickinson, J. A. 1994, 'Development of sun compensation by honeybees: how partially experienced bees estimate the sun's course.', *Proceedings of the National Academy of Sciences* **91**(10), 4471–4474.
- [76] Dyer, F. C. and Gould, J. 1983, 'Honey bee navigation: The honey bee's ability to find its way depends on a hierarchy of sophisticated orientation mechanisms', *American Scientist* **71**(6), 587–597.
URL: <https://www.jstor.org/stable/27852344>
- [77] Dyer, F., Gill, M. and Sharbowski, J. 2002, 'Motivation and vector navigation in honey bees', *Naturwissenschaften* **89**(6), 262–264.
- [78] Edrich, W. 2015, 'Honey bees can perform accurately directed waggle dances based solely on information from a homeward trip', *Journal of Comparative Physiology A* **201**(10), 1003–1010.
- [79] el Jundi, B., Smolka, J., Baird, E., Byrne, M. J. and Dacke, M. 2014, 'Diurnal dung beetles use the intensity gradient and the polarization pattern of the sky for orientation', *Journal of Experimental Biology*.
- [80] el Jundi, B., Warrant, E. J., Byrne, M. J., Khaldy, L., Baird, E., Smolka, J. and Dacke, M. 2015, 'Neural coding underlying the cue preference for celestial orientation', *Proceedings of the National Academy of Sciences* **112**(36), 11395–11400.
- [81] Engel, M. S. and Schultz, T. R. 1997, 'Phylogeny and behavior in honey bees (hymenoptera: Apidae)', *Annals of the Entomological Society of America* **90**(1), 43–53.
- [82] Esch, H. 1967, 'Die bedeutung der lauterzeugung für die verständigung der stachellosen bienen', *Zeitschrift für vergleichende Physiologie* **56**(2), 199–220.
- [83] Esch, H. 2011, *Foraging Honey Bees: How Foragers Determine and Transmit Information About Feeding Site Locations*, Springer Netherlands, pp. 53–64.
- [84] Esch, H. and Bastian, J. A. 1970, 'How do newly recruited honey bees approach a food site?', *Zeitschrift für Vergleichende Physiologie* **68**(2), 175–181.
- [85] Esch, H. E. and Burns, J. E. 1995, 'Honeybees use optic flow to measure the distance of a food source', *Naturwissenschaften* **82**(1), 38–40.

- [86] Esch, H. E. and Burns, J. E. 1996, 'Distance estimation by foraging honeybees', *Journal of Experimental Biology* **199**(1), 155–162.
- [87] Esch, H. E., Zhang, S., Srinivasan, M. V. and Tautz, J. 2001, 'Honeybee dances communicate distances measured by optic flow', *Nature* **411**(6837), 581–583.
- [88] Fernández, P. C. and Farina, W. M. 2001, 'Changes in food source profitability affect nasonov gland exposure in honeybee foragers *Apis mellifera* L.', *Insectes Sociaux* **48**(4), 366–371.
- [89] Ferrari, T. E. 2014, 'Magnets, magnetic field fluctuations and geomagnetic disturbances impair the homing ability of honey bees (*Apis mellifera*)', *Journal of Apicultural Research* **53**(4), 452–465.
- [90] Fisher, N. I. 1993, *Statistical Analysis of Circular Data*, Cambridge University Press.
- [91] Fisher, Y. E. 2022, 'Flexible navigational computations in the *Drosophila* central complex', *Current Opinion in Neurobiology* **73**, 102514.
- [92] Françon, J. 1939, *Die klugheit der bienen*, Neff.
- [93] Franconville, R., Beron, C. and Jayaraman, V. 2018, 'Building a functional connectome of the *Drosophila* central complex', *Elife* **7**, e37017.
- [94] Freas, C. A. and Cheng, K. 2018, 'Limits of vector calibration in the australian desert ant, *Melophorus bagoti*', *Insectes Sociaux* **65**(1), 141–152.
- [95] Free, J. B. and Williams, I. H. 1983, 'Scent-marking of flowers by honeybees', *Journal of Apicultural Research* **22**(2), 86–90.
- [96] Friesen, L. J. 1973, 'The search dynamics of recruited honeybees, *A. mellifera linguistica spinola*', *The Biological Bulletin* **144**(1), 107–131.
- [97] Frisch, K. and Jander, R. 1957, 'Über den schwänzeltanz der bienen', *Zeitschrift für Vergleichende Physiologie* **40**(3), 239–263.
- [98] Frisch, K. V. 1949, 'Die polarisation des himmelslichtes als orientierender faktor bei den tänzen der bienen', *Experientia* **5**(4), 142–148.
- [99] Frisch, K. V. 1967, 'Honeybees: Do they use direction and distance information provided by their dancers?', *Science* **158**(3804), 1072–1076.
- [100] Frisch, K. V. 1993, *The Dance Language and Orientation of Bees*, Harvard University Press.
- [101] Gallistel, C. and Beetz, J. 2012, 'Bee navigation with randolf menzel'.
URL: https://osf.io/a59rs/files/?view_only=6da39e230c8d4072b27ab70ccecb06e2
- [102] Gardner, K. E. 2007, 'A scientific note on the directional accuracy of the waggle dance over the course of a day', *Apidologie* **38**(3), 312–313.

- [103] Gardner, K. E., Seeley, T. D. and Calderone, N. W. 2007, 'Hypotheses on the adaptive-ness or non-adaptiveness of the directional imprecision in the honey bee's waggle dance (hymenoptera: Apidae: Apis mellifera)', *Entomologia Generalis* **29**(2-4), 285-298.
- [104] Gardner, K. E., Seeley, T. D. and Calderone, N. W. 2008, 'Do honeybees have two discrete dances to advertise food sources?', *Animal Behaviour* **75**(4), 1291-1300.
- [105] Geiger, K., Kratzsch, D. and Menzel, R. 1995, 'Target-directed orientation in displaced honeybees', *Ethology* **101**(4), 335-345.
- [106] George, E. A., Pimplikar, S., Thulasi, N. and Brockmann, A. 2020, 'Similarities in dance follower behaviour across honey bee species suggest a conserved mechanism of dance communication', *Animal Behaviour* **169**, 139-155.
- [107] Gil, M. and Farina, W. 2002, 'Foraging reactivation in the honeybee *Apis mellifera* L.: factors affecting the return to known nectar sources', *Naturwissenschaften* **89**(7), 322-325.
- [108] Gil, M. and Marco, R. J. D. 2010, 'Decoding information in the honeybee dance: revisiting the tactile hypothesis', *Animal Behaviour* **80**(5), 887-894.
- [109] Gilley, D. C., Kuzora, J. M. and Thom, C. 2011, 'Hydrocarbons emitted by waggle-dancing honey bees stimulate colony foraging activity by causing experienced foragers to exploit known food sources', *Apidologie* **43**(1), 85-94.
- [110] Giraldo, Y. M., Leitch, K. J., Ros, I. G., Warren, T. L., Weir, P. T. and Dickinson, M. H. 2018, 'Sun navigation requires compass neurons in drosophila', *Current Biology* **28**(17), 2845-2852.e4.
- [111] Giurfa, M. and Núñez, J. A. 1992, 'Honeybees mark with scent and reject recently visited flowers', *Oecologia* **89**(1), 113-117.
- [112] Goldschmidt, D., Manoonpong, P. and Dasgupta, S. 2017, 'A neurocomputational model of goal-directed navigation in insect-inspired artificial agents', *Frontiers in Neuro-robotics* **11**.
- [113] Goulard, R., Buehlmann, C., Niven, J. E., Graham, P. and Webb, B. 2021, 'A unified mechanism for innate and learned visual landmark guidance in the insect central complex', *PLOS Computational Biology* **17**(9), e1009383.
- [114] Gould, J. L. 1975, 'Honey bee recruitment: The dance-language controversy: Unambiguous experiments show that honey bees use an abstract language for communication.', *Science* **189**(4204), 685-693.
- [115] Gould, J. L. 1986, 'The locale map of honey bees: Do insects have cognitive maps?', *Science* **232**(4752), 861-863.
- [116] Gould, J. L., Henerey, M. and MacLeod, M. C. 1970, 'Communication of direction by

the honey bee: Review of previous work leads to experiments limiting olfactory cues to test the dance language hypothesis.’, *Science* **169**(3945), 544–554.

- [117] Green, J., Adachi, A., Shah, K. K., Hirokawa, J. D., Magani, P. S. and Maimon, G. 2017, ‘A neural circuit architecture for angular integration in drosophila’, *Nature* **546**(7656), 101–106.
- [118] Greggers, U., Koch, G., Schmidt, V., Dürr, A., Floriou-Servou, A., Piepenbrock, D., Göpfert, M. C. and Menzel, R. 2013, ‘Reception and learning of electric fields in bees’, *Proceedings of the Royal Society B: Biological Sciences* **280**(1759), 20130528.
- [119] Griffin, S. R., Smith, M. L. and Seeley, T. D. 2012, ‘Do honeybees use the directional information in round dances to find nearby food sources?’, *Animal Behaviour* **83**(6), 1319–1324.
- [120] Grimaldi, D. and Engel, M. 2005, *Evolution of the insects*, Cambridge University Press.
- [121] Grüter, C., Balbuena, M. S. and Farina, W. M. 2008, ‘Informational conflicts created by the waggle dance’, *Proceedings of the Royal Society B: Biological Sciences* **275**(1640), 1321–1327.
- [122] Hadjitofi, A. and Webb, B. 2024a, ‘Dynamic antennal positioning allows honeybee followers to decode the dance’, *Current Biology* **34**(8), 1772–1779.e4.
- [123] Hadjitofi, A. and Webb, B. 2024b, ‘Honeybee antennal positioning data when following dances’, *figshare* .
- [124] Haferlach, T., Wessnitzer, J., Mangan, M. and Webb, B. 2007, ‘Evolving a neural model of insect path integration’, *Adaptive Behavior* **15**(3), 273–287.
- [125] Haldane, J. B. S. and Spurway, H. 1954, ‘A statistical analysis of communication in “*Apis mellifera*” and a comparison with communication in other animals’, *Insectes Sociaux* **1**(3), 247–283.
- [126] Hardcastle, B. J., Omoto, J. J., Kandimalla, P., Nguyen, B.-C. M., Keleş, M. F., Boyd, N. K., Hartenstein, V. and Frye, M. A. 2021, ‘A visual pathway for skylight polarization processing in *Drosophila*’, *eLife* **10**.
- [127] Harris, C. R., Millman, K. J., van der Walt, S. J., Gommers, R., Virtanen, P., Cournapeau, D., Wieser, E., Taylor, J., Berg, S., Smith, N. J., Kern, R., Picus, M., Hoyer, S., van Kerkwijk, M. H., Brett, M., Haldane, A., del Río, J. F., Wiebe, M., Peterson, P., Gérard-Marchant, P., Sheppard, K., Reddy, T., Weckesser, W., Abbasi, H., Gohlke, C. and Oliphant, T. E. 2020, ‘Array programming with NumPy’, *Nature* **585**(7825), 357–362.
- [128] Heinze, S., el Jundi, B., Berg, B. G., Homberg, U., Menzel, R., Pfeiffer, K., Hensgen, R., Zittrell, F., Dacke, M., Warrant, E., Pfuhl, G., Rybak, J. and Tedore, K. 2021, ‘A unified platform to manage, share, and archive morphological and functional data in insect neuroscience’, *eLife* **10**.

- [129] Heinze, S., Florman, J., Asokaraj, S., el Jundi, B. and Reppert, S. M. 2012, 'Anatomical basis of sun compass navigation II: The neuronal composition of the central complex of the monarch butterfly', *Journal of Comparative Neurology* **521**(2), 267–298.
- [130] Heinze, S. and Homberg, U. 2007, 'Maplike representation of celestial e-vector orientations in the brain of an insect', *Science* **315**(5814), 995–997.
- [131] Heinze, S. and Homberg, U. 2008, 'Neuroarchitecture of the central complex of the desert locust: Intrinsic and columnar neurons', *Journal of Comparative Neurology* **511**(4), 454–478.
- [132] Heinze, S., Narendra, A. and Cheung, A. 2018, 'Principles of insect path integration', *Current Biology* **28**(17), R1043–R1058.
- [133] Heran, H. and Wanke, L. 1952, 'Beobachtungen über die entfernungsmeldung der sammelbienen', *Zeitschrift für Vergleichende Physiologie* **34**(4), 383–393.
- [134] Homberg, U. 1985, 'Interneurones of the central complex in the bee brain (*Apis mellifera*, L.)', *Journal of Insect Physiology* **31**(3), 251–264.
- [135] Homberg, U. 1994, 'Flight-correlated activity changes in neurons of the lateral accessory lobes in the brain of the locust *Schistocerca gregaria*', *Journal of Comparative Physiology A* **175**(5).
- [136] Honegger, H. W. 1981, 'A preliminary note on a new optomotor response in crickets: Antennal tracking of moving targets', *Journal of Comparative Physiology* <https://doi.org/10.1016/j.jinsphys.2013.11.006> **142**(3), 419–421.
- [137] Honkanen, A., Adden, A., da Silva Freitas, J. and Heinze, S. 2019, 'The insect central complex and the neural basis of navigational strategies', *Journal of Experimental Biology* **222**(Suppl 1).
- [138] Hubbell, S. P. and Johnson, L. K. 1978, 'Comparative foraging behavior of six stingless bee species exploiting a standardized resource', *Ecology* **59**(6), 1123–1136.
- [139] Hulse, B. K., Haberkern, H., Franconville, R., Turner-Evans, D., ya Takemura, S., Wolff, T., Noorman, M., Dreher, M., Dan, C., Parekh, R., Hermundstad, A. M., Rubin, G. M. and Jayaraman, V. 2021, 'A connectome of the *Drosophila* central complex reveals network motifs suitable for flexible navigation and context-dependent action selection', *eLife* **10**.
- [140] Hunter, J. D. 2007, 'Matplotlib: A 2d graphics environment', *Computing in Science & Engineering* **9**(3), 90–95.
- [141] Jack-McCollough, R. T. and Nieh, J. C. 2015, 'Honeybees tune excitatory and inhibitory recruitment signalling to resource value and predation risk', *Animal Behaviour* **110**, 9–17.
- [142] Jensen, I. L., Michelsen, A. and Lindauer, M. 1997, 'On the directional indications in the round dances of honeybees', *Naturwissenschaften* **84**(10), 452–454.

- [143] Johnson, D. L. 1967, 'Honey bees: Do they use the direction information contained in their dance maneuver?', *Science* **155**(3764), 844–847.
- [144] Johnston, C. 1855, 'Auditory apparatus of the *Culex Mosquito*', *Journal of Cell Science* **51-3**(10), 97–102.
- [145] Judd, S. P. D. and Collett, T. S. 1998, 'Multiple stored views and landmark guidance in ants', *Nature* **392**(6677), 710–714.
- [146] Judd, T. M. 1994, 'The waggle dance of the honey bee: Which bees following a dancer successfully acquire the information?', *Journal of Insect Behavior* **8**(3), 343–354.
- [147] Kajobe, R. and Echazarreta, C. M. 2005, 'Temporal resource partitioning and climatological influences on colony flight and foraging of stingless bees (*Apidae; Meliponini*) in Ugandan tropical forests', *African Journal of Ecology* **43**(3), 267–275.
- [148] Kamikouchi, A., Inagaki, H. K., Effertz, T., Hendrich, O., Fiala, A., Göpfert, M. C. and Ito, K. 2009, 'The neural basis of *Drosophila* gravity-sensing and hearing', *Nature* **458**(7235), 165–171.
- [149] Kennedy, A., Peng, T., Glaser, S. M., Linn, M., Foitzik, S. and Grüter, C. 2021, 'Use of waggle dance information in honey bees is linked to gene expression in the antennae, but not in the brain', *Molecular Ecology* **30**(11), 2676–2688.
- [150] Kerr, W. 1973, 'Sun compass orientation in the stingless bees *Trigona* (*Trigona*) *spinipes* (Fabricius, 1793)(*Apidae*)', *Anais da Academia Brasileira de Ciencias* **45**(2), 301–308.
- [151] Kerr, W. E. 1960, 'Evolution of communication in bees and its role in speciation', *Evolution* **14**(3), 386–387.
- [152] Kietzman, P. M. and Visscher, P. K. 2019, 'Follower position does not affect waggle dance information transfer', *Psyche: A Journal of Entomology* **2019**, 1–5.
- [153] Kim, I. S. and Dickinson, M. H. 2017, 'Idiothetic path integration in the fruit fly *Drosophila melanogaster*', *Current Biology* **27**(15), 2227–2238.e3.
- [154] Kim, S. S., Rouault, H., Druckmann, S. and Jayaraman, V. 2017, 'Ring attractor dynamics in the *Drosophila* central brain', *Science* **356**(6340), 849–853.
- [155] Kirchner, W. 1994, 'Hearing in honeybees: the mechanical response of the bee's antenna to near field sound', *Journal of Comparative Physiology A* **175**(3).
- [156] Kirchner, W. H. and Braun, U. 1994, 'Dancing honey bees indicate the location of food sources using path integration rather than cognitive maps', *Animal Behaviour* **48**(6), 1437–1441.
- [157] Kirchner, W. H., Dreller, C. and Towne, W. F. 1991, 'Hearing in honeybees: operant conditioning and spontaneous reactions to airborne sound', *Journal of Comparative Physiology A* **168**(1), 85–89.

- [158] Kirchner, W. H., Lindauer, M. and Michelsen, A. 1988, 'Honeybee dance communication: Acoustical indication of direction in round dances', *Naturwissenschaften* **75**(12), 629–630.
- [159] Kirschvink, J. L., Padmanabha, S., Boyce, C. K. and Oglesby, J. 1997, 'Measurement of the threshold sensitivity of honeybees to weak, extremely low-frequency magnetic fields', *Journal of Experimental Biology* **200**(9), 1363–1368.
- [160] Kiya, T. and Kubo, T. 2011, 'Dance type and flight parameters are associated with different mushroom body neural activities in worker honeybee brains', *PLoS ONE* **6**(4), e19301.
- [161] Klein, B. A., Vogt, M., Unrein, K. and Reineke, D. M. 2018, 'Followers of honey bee waggle dancers change their behaviour when dancers are sleep-restricted or perform imprecise dances', *Animal Behaviour* **146**, 71–77.
- [162] Kloppenburg, P. 1995, 'Anatomy of the antennal motoneurons in the brain of the honeybee (*Apis mellifera*)', *Journal of Comparative Neurology* **363**(2), 333–343.
- [163] Knaden, M. and Wehner, R. 2006, 'Ant navigation: resetting the path integrator', *Journal of Experimental Biology* **209**(1), 26–31.
- [164] Knierim, J. J. and Zhang, K. 2012, 'Attractor dynamics of spatially correlated neural activity in the limbic system', *Annual Review of Neuroscience* **35**(1), 267–285.
- [165] Kohl, P. L. and Rutschmann, B. 2021, 'Honey bees communicate distance via non-linear waggle duration functions', *PeerJ* **9**, e11187.
- [166] Kohl, P. L., Rutschmann, B. and Brockmann, A. 2023, *Dance Communication of Giant Honeybees*, CRC Press, pp. 104–122.
- [167] Kohl, P. L., Thulasi, N., Rutschmann, B., George, E. A., Steffan-Dewenter, I. and Brockmann, A. 2020, 'Adaptive evolution of honeybee dance dialects', *Proceedings of the Royal Society B: Biological Sciences* **287**(1922), 20200190.
- [168] Kohno, H. and Kubo, T. 2019, 'Genetics in the honey bee: Achievements and prospects toward the functional analysis of molecular and neural mechanisms underlying social behaviors', *Insects* **10**(10), 348.
- [169] Kumaraswamy, A., Ai, H., Kai, K., Ikeno, H. and Wachtler, T. 2019, 'Adaptations during maturation in an identified honeybee interneuron responsive to waggle dance vibration signals', *eneuro* **6**(5), ENEURO.0454–18.2019.
- [170] Lambinet, V., Hayden, M. E., Bieri, M. and Gries, G. 2014, 'Does the earth's magnetic field serve as a reference for alignment of the honeybee waggle dance?', *PLoS ONE* **9**(12), e115665.
- [171] Landgraf, T., Bierbach, D., Kirbach, A., Cusing, R., Oertel, M., Lehmann, K., Greggers,

- U., Menzel, R. and Rojas, R. 2018, 'Dancing honey bee robot elicits dance-following and recruits foragers'.
- [172] Landgraf, T., Oertel, M., Kirbach, A., Menzel, R. and Rojas, R. 2012, Imitation of the honeybee dance communication system by means of a biomimetic robot, *in* 'Biomimetic and Biohybrid Systems', Springer Berlin Heidelberg, pp. 132–143.
- [173] Landgraf, T. and Rojas, R. 2007, Tracking honey bee dances from sparse optical flow fields, Technical report, Institut für Informatik, Freie Universität Berlin.
- [174] Landgraf, T., Rojas, R., Nguyen, H., Kriegel, F. and Stettin, K. 2011, 'Analysis of the waggle dance motion of honeybees for the design of a biomimetic honeybee robot', *PLoS ONE* **6**(8), e21354.
- [175] Lee, D.-H., Park, C.-G., Seo, B. Y., Boiteau, G., Vincent, C. and Leskey, T. C. 2014, 'Detectability of *Halyomorpha halys* (Hemiptera: Pentatomidae) by portable harmonic radar in agricultural landscapes', *Florida Entomologist* **97**(3), 1131–1138.
- [176] Leucht, T. 1984, 'Responses to light under varying magnetic conditions in the honeybee, *Apis mellifica*', *Journal of Comparative Physiology A* **154**(6), 865–870.
- [177] Leucht, T. and Martin, H. 1990, 'Interactions between e-vector orientation and weak, steady magnetic fields in the honeybee, *Apis mellifica*', *Naturwissenschaften* **77**(3), 130–133.
- [178] Liang, C.-H., Chuang, C.-L., Jiang, J.-A. and Yang, E.-C. 2016, 'Magnetic sensing through the abdomen of the honey bee', *Scientific Reports* **6**(1).
- [179] Lin, C.-Y., Chuang, C.-C., Hua, T.-E., Chen, C.-C., Dickson, B., Greenspan, R. and Chiang, A.-S. 2013, 'A comprehensive wiring diagram of the protocerebral bridge for visual information processing in the *Drosophila* brain', *Cell Reports* **3**(5), 1739–1753.
- [180] Lindauer, M. 1952, 'Ein beitrag zur frage der arbeitsteilung im bienenstaat', *Zeitschrift für Vergleichende Physiologie* **34**(4), 299–345.
- [181] Lindauer, M. 1954, 'Dauertänze im bienenstock und ihre beziehung zur sonnenbahn', *Die Naturwissenschaften* **41**(21), 506–507.
- [182] Lindauer, M. 1955, 'Schwarmbienen auf wohnungssuche', *Zeitschrift für Vergleichende Physiologie* **37**(4), 263–324.
- [183] Lindauer, M. 1956, 'Über die verständigung bei indischen bienen', *Zeitschrift für Vergleichende Physiologie* **38**(6), 521–557.
- [184] Lindauer, M. 1960, 'Time-compensated sun orientation in bees', *Cold Spring Harbor Symposia on Quantitative Biology* **25**(0), 371–377.
- [185] Lindauer, M. and Kerr, W. E. 1958, 'Die gegenseitige verständigung bei den stachellosen bienen', *Zeitschrift für Vergleichende Physiologie* **41**(4), 405–434.

- [186] Lindauer, M. and Martin, H. 1972, 'Magnetic effect on dancing bees', *NASA Special Publication* **262**, 559.
- [187] Lindauer, M. and Nedel, J. O. 1959, 'Ein schweresinnesorgan der honigbiene', *Zeitschrift für Vergleichende Physiologie* **42**(4), 334–364.
- [188] Lo, N., Gloag, R. S., Anderson, D. L. and Oldroyd, B. P. 2010, 'A molecular phylogeny of the genus *Apis* suggests that the giant honey bee of the philippines, *A. breviligula* Maa, and the plains honey bee of southern india, *A. indica Fabricius*, are valid species', *Systematic Entomology* **35**(2), 226–233.
- [189] Lu, J., Behbahani, A. H., Hamburg, L., Westeinde, E. A., Dawson, P. M., Lyu, C., Maimon, G., Dickinson, M. H., Druckmann, S. and Wilson, R. I. 2022, 'Transforming representations of movement from body- to world-centric space', *Nature* **601**(7891), 98–104.
- [190] Lyu, C., Abbott, L. F. and Maimon, G. 2022, 'Building an allocentric travelling direction signal via vector computation', *Nature* **601**(7891), 92–97.
- [191] Maggiora, R., Saccani, M., Milanesio, D. and Porporato, M. 2019, 'An innovative harmonic radar to track flying insects: the case of *Vespa velutina*', *Scientific Reports* **9**(1).
- [192] Makinson, J. C., Schaerf, T. M., Wagner, N., Oldroyd, B. P. and Beekman, M. 2017, 'Collective decision making in the red dwarf honeybee *apis florea*: do the bees simply follow the flowers?', *Insectes Sociaux* **64**(4), 557–566.
- [193] Marco, R. D. and Menzel, R. 2005, 'Encoding spatial information in the waggle dance', *Journal of Experimental Biology* **208**(20), 3885–3894.
- [194] Martin, H. 1965, 'Osmotropotaxis in the honey-bee', *Nature* **208**(5005), 59–63.
- [195] Matheson, A. M. M., Lanz, A. J., Medina, A. M., Licata, A. M., Currier, T. A., Syed, M. H. and Nagel, K. I. 2022, 'A neural circuit for wind-guided olfactory navigation', *Nature Communications* **13**(1).
- [196] Mathis, A., Mamidanna, P., Cury, K. M., Abe, T., Murthy, V. N., Mathis, M. W. and Bethge, M. 2018, 'DeepLabCut: markerless pose estimation of user-defined body parts with deep learning', *Nature Neuroscience* **21**(9), 1281–1289.
- [197] Matsuo, E. and Kamikouchi, A. 2013, 'Neuronal encoding of sound, gravity, and wind in the fruit fly', *Journal of Comparative Physiology A* **199**(4), 253–262.
- [198] Maxwell, J. C. 1865, *A dynamical theory of the electromagnetic field*, The Royal Society.
- [199] McIndoo, N. E. 1914, 'The scent-producing organ of the honey bee', *Proceedings of the Academy of Natural Sciences of Philadelphia* pp. 542–555.
- [200] McKinney, W. 2010, Data structures for statistical computing in python, in 'Proceedings of the Python in Science Conference', SciPy.

- [201] Menzel, R., Brandt, R., Gumbert, A., Komischke, B. and Kunze, J. 2000, 'Two spatial memories for honeybee navigation', *Proceedings of the Royal Society of London. Series B: Biological Sciences* **267**(1447), 961–968.
- [202] Menzel, R., De Marco, R. J. and Greggers, U. 2006, 'Spatial memory, navigation and dance behaviour in *Apis mellifera*', *Journal of Comparative Physiology A* **192**(9), 889–903.
- [203] Menzel, R., Geiger, K., Jeorges, J., Müller, U. and Chittka, L. 1998, 'Bees travel novel homeward routes by integrating separately acquired vector memories', *Animal Behaviour* **55**(1), 139–152.
- [204] Menzel, R. and Giurfa, M. 2001, 'Cognitive architecture of a mini-brain: the honeybee', *Trends in Cognitive Sciences* **5**(2), 62–71.
- [205] Menzel, R. and Greggers, U. 2013, 'Guidance by odors in honeybee navigation', *Journal of Comparative Physiology A* **199**(10), 867–873.
- [206] Menzel, R., Greggers, U., Smith, A., Berger, S., Brandt, R., Brunke, S., Bundrock, G., Hülse, S., Plümpe, T., Schaupp, F., Schüttler, E., Stach, S., Stindt, J., Stollhoff, N. and Watzl, S. 2005, 'Honey bees navigate according to a map-like spatial memory', *Proceedings of the National Academy of Sciences* **102**(8), 3040–3045.
- [207] Menzel, R., Kirbach, A., Haass, W.-D., Fischer, B., Fuchs, J., Koblöfsky, M., Lehmann, K., Reiter, L., Meyer, H., Nguyen, H., Jones, S., Norton, P. and Greggers, U. 2011, 'A common frame of reference for learned and communicated vectors in honeybee navigation', *Current Biology* **21**(8), 645–650.
- [208] Michelsen, A. 2003, 'Signals and flexibility in the dance communication of honeybees', *Journal of Comparative Physiology A* **189**(3), 165–174.
- [209] Michelsen, A. 2012, How do honey bees obtain information about direction by following dances?, in 'Honeybee Neurobiology and Behavior', Springer, pp. 65–76.
- [210] Michelsen, A. 2014, *Mechanical Signals in Honeybee Communication*, Springer Berlin Heidelberg, pp. 333–347.
- [211] Michelsen, A., Andersen, B. B., Kirchner, W. H. and Lindauer, M. 1989, 'Honeybees can be recruited by a mechanical model of a dancing bee', *Naturwissenschaften* **76**(6), 277–280.
- [212] Michelsen, A., Andersen, B. B., Storm, J., Kirchner, W. H. and Lindauer, M. 1992, 'How honeybees perceive communication dances, studied by means of a mechanical model', *Behavioral Ecology and Sociobiology* **30**(3-4), 143–150.
- [213] Michelsen, A., Kirchner, W. H. and Lindauer, M. 1986, 'Sound and vibrational signals in the dance language of the honeybee, *Apis mellifera*', *Behavioral Ecology and Sociobiology* **18**(3), 207–212.

- [214] Michelsen, A., Towne, W. F., Kirchner, W. H. and Kryger, P. 1987, 'The acoustic near field of a dancing honeybee', *Journal of Comparative Physiology A* **161**(5), 633–643.
- [215] Mittelstaedt, H. 1962, 'Control systems of orientation in insects', *Annual Review of Entomology* **7**(1), 177–198.
- [216] Mittelstaedt, H. and Mittelstaedt, M. L. 1982, Homing by path integration, in 'Proceedings in Life Sciences', Springer Berlin Heidelberg, pp. 290–297.
- [217] Moël, F. L., Stone, T., Lihoreau, M., Wystrach, A. and Webb, B. 2019, 'The central complex as a potential substrate for vector based navigation', *Frontiers in Psychology* **6**(5), ENEURO.0454–18.2019.
- [218] Molina-Montenegro, M. A., Acuña-Rodríguez, I. S., Ballesteros, G. I., Baldelomar, M., Torres-Díaz, C., Broitman, B. R. and Vázquez, D. P. 2023, 'Electromagnetic fields disrupt the pollination service by honeybees', *Science Advances* **9**(19).
- [219] Montgomery, C., Vuts, J., Woodcock, C. M., Withall, D. M., Birkett, M. A., Pickett, J. A. and Robert, D. 2021, 'Bumblebee electric charge stimulates floral volatile emissions in *Petunia integrifolia* but not in *Antirrhinum majus*', *The Science of Nature* **108**(5).
- [220] Moore, A. D. 2018, *Python GUI Programming with Tkinter: Develop responsive and powerful GUI applications with Tkinter*, Packt Publishing Ltd.
- [221] Müller, M. and Wehner, R. 1988, 'Path integration in desert ants, *Cataglyphis fortis*', *Proceedings of the National Academy of Sciences* **85**(14), 5287–5290.
- [222] Munz, T. 2005, 'The bee battles: Karl von frisch, adrian wenner and the honey bee dance language controversy', *Journal of the History of Biology* **38**(3), 535–570.
- [223] Nachtigall, W. and Hanauer-Thieser, U. 1992, 'Flight of the honeybee: V. drag and lift coefficients of the bee's body; implications for flight dynamics', *Journal of Comparative Physiology B* **162**(3), 267–277.
- [224] Namiki, S., Iwabuchi, S., Pansopha Kono, P. and Kanzaki, R. 2014, 'Information flow through neural circuits for pheromone orientation', *Nature Communications* **5**(1).
- [225] Nath, T., Mathis, A., Chen, A. C., Patel, A., Bethge, M. and Mathis, M. W. 2019, 'Using DeepLabCut for 3d markerless pose estimation across species and behaviors', *Nature Protocols* **14**(7), 2152–2176.
- [226] Nieh, J. C. 1998, 'The food recruitment dance of the stingless bee, *Melipona panamica*', *Behavioral Ecology and Sociobiology* **43**(2), 133–145.
- [227] Nieh, J. C. 1999, 'Stingless-bee communication: Searching for a proto-dance language reveals possible stages in the evolution of methods by which experienced foragers lead others to food', *American Scientist* **87**(5), 428–435.
- [228] Nieh, J. C. 2004, 'Recruitment communication in stingless bees (Hymenoptera, Apidae, Meliponini)', *Apidologie* **35**(2), 159–182.

- [229] Nieh, J. C., Contrera, F. A. L. and Nogueira-Neto, P. 2003, 'Pulsed mass recruitment by a stingless bee, *Trigona hyalinata*', *Proceedings of the Royal Society of London. Series B: Biological Sciences* **270**(1529), 2191–2196.
- [230] Nieh, J. C. and Roubik, D. W. 1995, 'A stingless bee (*Melipona panamica*) indicates food location without using a scent trail', *Behavioral Ecology and Sociobiology* **37**(1), 63–70.
- [231] Nieh, J. C. and Roubik, D. W. 1998, 'Potential mechanisms for the communication of height and distance by a stingless bee, *Melipona panamica*', *Behavioral Ecology and Sociobiology* **43**(6), 387–399.
- [232] Nieh, J. and Tautz, J. 2000, 'Behaviour-locked signal analysis reveals weak 200–300 hz comb vibrations during the honeybee waggle dance', *Journal of Experimental Biology* **203**(10), 1573–1579.
- [233] Nussbaumer, H. J. 1982, The fast fourier transform, in 'Fast Fourier Transform and Convolution Algorithms', Springer Berlin Heidelberg, pp. 80–111.
- [234] Okada, R., Ikeno, H., Kimura, T., Ohashi, M., Aonuma, H. and Ito, E. 2014, 'Error in the honeybee waggle dance improves foraging flexibility', *Scientific Reports* **4**(1).
- [235] Okada, R., Ikeno, H., Sasayama, N., Aonuma, H., Kurabayashi, D. and Ito, E. 2008, 'The dance of the honeybee: How do honeybees dance to transfer food information effectively?', *Acta Biologica Hungarica* **59**(Supplement 2), 157–162.
- [236] O'Keefe, J. and Nadel, L. 1978, *The hippocampus as a cognitive map*, Oxford University Press.
- [237] Okubo, S., Nikkeshi, A., S. Tanaka, C., Kimura, K., Yoshiyama, M. and Morimoto, N. 2019, 'Forage area estimation in european honeybees (*Apis mellifera*) by automatic waggle decoding of videos using a generic camcorder in field apiaries', *Apidologie* **50**(2), 243–252.
- [238] Okubo, T. S., Patella, P., D'Alessandro, I. and Wilson, R. I. 2020, 'A neural network for wind-guided compass navigation', *Neuron* **107**(5), 924–940.e18.
- [239] O'Neal, M. E., Landis, D. A., Rothwell, E., Kempel, L. and Reinhard, D. 2004, 'Tracking insects with harmonic radar: a case study', *American Entomologist* **50**(4), 212–218.
- [240] OpenStreetMap contributors 2017, 'Planet dump retrieved from <https://planet.osm.org>', <https://www.openstreetmap.org>.
- [241] Otto, F. 1959, 'Die bedeutung des rückfluges für die richtungs- und entfernungsangabe der bienen', *Zeitschrift für Vergleichende Physiologie* **42**(4), 303–333.
- [242] Page, R. E. and Robinson, G. E. 1991, *The Genetics of Division of Labour in Honey Bee Colonies*, Elsevier, pp. 117–169.
- [243] Patel, R. N., Kempnaers, J. and Heinze, S. 2022, 'Vector navigation in walking bumblebees', *Current Biology* **32**(13), 2871–2883.e4.

- [244] Pereira, T. D., Tabris, N., Matsliah, A., Turner, D. M., Li, J., Ravindranath, S., Papadoyannis, E. S., Normand, E., Deutsch, D. S., Wang, Z. Y., McKenzie-Smith, G. C., Mitelut, C. C., Castro, M. D., D’Uva, J., Kislin, M., Sanes, D. H., Kocher, S. D., Wang, S. S.-H., Falkner, A. L., Shaevitz, J. W. and Murthy, M. 2022, ‘SLEAP: A deep learning system for multi-animal pose tracking’, *Nature Methods* **19**(4), 486–495.
- [245] Pfeiffer, K. and Homberg, U. 2014, ‘Organization and functional roles of the central complex in the insect brain’, *Annual Review of Entomology* **59**(1), 165–184.
- [246] Piéron, H. 1904, ‘Du rôle du sens musculaire dans l’orientation de quelques espèces de fourmis’, *Bulletin de l’Institut général de psychologie* **4**, 168–186.
- [247] Pisokas, I., Heinze, S. and Webb, B. 2020, ‘The head direction circuit of two insect species’, *eLife* **9**.
- [248] Portelli, G., Ruffier, F. and Franceschini, N. 2010, ‘Honeybees change their height to restore their optic flow’, *Journal of Comparative Physiology A* **196**(4), 307–313.
- [249] Portelli, G., Ruffier, F., Roubieu, F. L. and Franceschini, N. 2011, ‘Honeybees’ speed depends on visual control of flight speed and height in the honeybee dorsal as well as lateral, ventral and frontal optic flows’, *PLoS ONE* **6**(5), e19486.
- [250] Price, R. I. and Grüter, C. 2015, ‘Why, when and where did honey bee dance communication evolve?’, *Frontiers in Ecology and Evolution* **3**.
- [251] Rapp, C., ed. 2019, *Aristoteles: Historia Animalium – Books VIII and IX*, De Gruyter. Translated and explained by Stefan Schnieders.
- [252] Rayshubskiy, A., Holtz, S. L., D’Alessandro, I., Li, A. A., Vanderbeck, Q. X., Haber, I. S., Gibb, P. W. and Wilson, R. I. 2020, ‘Neural circuit mechanisms for steering control in walking *Drosophila*’.
- [253] Reinhard, J. and Srinivasan, M. V. 2009, *The role of scents in honey bee foraging and recruitment*, CRC Press, pp. 177–194.
- [254] Reinhard, J., Srinivasan, M. V., Guez, D. and Zhang, S. W. 2004, ‘Floral scents induce recall of navigational and visual memories in honeybees’, *Journal of Experimental Biology* **207**(25), 4371–4381.
- [255] Renner, M. 1960, ‘The contribution of the honey bee to the study of time-sense and astronomical orientation’, *Cold Spring Harbor Symposia on Quantitative Biology* **25**(0), 361–367.
- [256] Reynolds, A. M., Smith, A. D., Reynolds, D. R., Carreck, N. L. and Osborne, J. L. 2007, ‘Honeybees perform optimal scale-free searching flights when attempting to locate a food source’, *Journal of Experimental Biology* **210**(21), 3763–3770.
- [257] Riley, J. R., Greggers, U., Smith, A. D., Reynolds, D. R. and Menzel, R. 2005, ‘The flight paths of honeybees recruited by the waggle dance’, *Nature* **435**(7039), 205–207.

- [258] Riley, J. R., Greggers, U., Smith, A. D., Stach, S., Reynolds, D. R., Stollhoff, N., Brandt, R., Schaupp, F. and Menzel, R. 2003, 'The automatic pilot of honeybees', *Proceedings of the Royal Society of London. Series B: Biological Sciences* **270**(1532), 2421–2424.
- [259] Riley, J. R., Smith, A. D., Reynolds, D. R., Edwards, A. S., Osborne, J. L., Williams, I. H., Carreck, N. L. and Poppy, G. M. 1996, 'Tracking bees with harmonic radar', *Nature* **379**(6560), 29–30.
- [260] Ritzmann, R. E., Ridgel, A. L. and Pollack, A. J. 2008, 'Multi-unit recording of antennal mechano-sensitive units in the central complex of the cockroach, *Blaberus discoidalis*', *Journal of Comparative Physiology A* **194**(4), 341–360.
- [261] Robitaille, T. P., Tollerud, E. J., Greenfield, P., Droettboom, M., Bray, E., Aldcroft, T., Davis, M., Ginsburg, A., Price-Whelan, A. M., Kerzendorf, W. E., Conley, A., Crighton, N., Barbary, K., Muna, D., Ferguson, H., Grollier, F., Parikh, M. M., Nair, P. H., Günther, H. M., Deil, C., Woillez, J., Conseil, S., Kramer, R., Turner, J. E. H., Singer, L., Fox, R., Weaver, B. A., Zabalza, V., Edwards, Z. I., Azalee Bostroem, K., Burke, D. J., Casey, A. R., Crawford, S. M., Dencheva, N., Ely, J., Jenness, T., Labrie, K., Lim, P. L., Pierfederici, F., Pontzen, A., Ptak, A., Refsdal, B., Servillat, M. and Streicher, O. 2013, 'Astropy: A community python package for astronomy', *Astronomy & Astrophysics* **558**, A33.
- [262] Rohrseitz, K. and Tautz, J. 1999, 'Honey bee dance communication: waggle run direction coded in antennal contacts?', *Journal of Comparative Physiology A: Sensory, Neural, and Behavioral Physiology* **184**(4), 463–470.
- [263] Rossel, S. and Wehner, R. 1982, 'The bee's map of the e-vector pattern in the sky', *Proceedings of the National Academy of Sciences* **79**(14), 4451–4455.
- [264] Rother, L., Kraft, N., Smith, D. B., el Jundi, B., Gill, R. J. and Pfeiffer, K. 2021, 'A micro-ct-based standard brain atlas of the bumblebee', *Cell and Tissue Research* **386**(1), 29–45.
- [265] Roy Khurana, T. and Sane, S. P. 2016, 'Airflow and optic flow mediate antennal positioning in flying honeybees', *eLife* **5**.
- [266] Sadler, N. and Nieh, J. C. 2011, 'Honey bee forager thoracic temperature inside the nest is tuned to broad-scale differences in recruitment motivation', *Journal of Experimental Biology* **214**(3), 469–475.
- [267] Sandeman, D., Tautz, J. and Lindauer, M. 1996, 'Transmission of vibration across honeycombs and its detection by bee leg receptors', *Journal of Experimental Biology* **199**(12), 2585–2594.
- [268] Sayre, M. E., Templin, R., Chavez, J., Kempnaers, J. and Heinze, S. 2021, 'A projectome of the bumblebee central complex', *eLife* **10**.
- [269] Scheffer, L. K., Xu, C. S., Januszewski, M., Lu, Z., Takemura, S.-y., Hayworth, K. J., Huang, G. B., Shinomiya, K., Maitlin-Shepard, J., Berg, S., Clements, J., Hubbard, P. M.,

Katz, W. T., Umayam, L., Zhao, T., Ackerman, D., Blakely, T., Bogovic, J., Dolafi, T., Kainmueller, D., Kawase, T., Khairy, K. A., Leavitt, L., Li, P. H., Lindsey, L., Neubarth, N., Olbris, D. J., Otsuna, H., Trautman, E. T., Ito, M., Bates, A. S., Goldammer, J., Wolff, T., Svirskas, R., Schlegel, P., Neace, E., Knecht, C. J., Alvarado, C. X., Bailey, D. A., Ballinger, S., Borycz, J. A., Canino, B. S., Cheatham, N., Cook, M., Dreher, M., Duclos, O., Eubanks, B., Fairbanks, K., Finley, S., Forknall, N., Francis, A., Hopkins, G. P., Joyce, E. M., Kim, S., Kirk, N. A., Kovalyak, J., Lauchie, S. A., Lohff, A., Maldonado, C., Manley, E. A., McLin, S., Mooney, C., Ndama, M., Ogundeyi, O., Okeoma, N., Ordish, C., Padilla, N., Patrick, C. M., Paterson, T., Phillips, E. E., Phillips, E. M., Rampally, N., Ribeiro, C., Robertson, M. K., Rymer, J. T., Ryan, S. M., Sammons, M., Scott, A. K., Scott, A. L., Shinomiya, A., Smith, C., Smith, K., Smith, N. L., Sobeski, M. A., Suleiman, A., Swift, J., Takemura, S., Talebi, I., Tarnogorska, D., Tenshaw, E., Tokhi, T., Walsh, J. J., Yang, T., Horne, J. A., Li, F., Parekh, R., Rivlin, P. K., Jayaraman, V., Costa, M., Jefferis, G. S., Ito, K., Saalfeld, S., George, R., Meinertzhagen, I. A., Rubin, G. M., Hess, H. F., Jain, V. and Plaza, S. M. 2020, 'A connectome and analysis of the adult *Drosophila* central brain', *eLife* **9**.

- [270] Schlegel, P., Yin, Y., Bates, A. S., Dorkenwald, S., Eichler, K., Brooks, P., Han, D. S., Gkantia, M., dos Santos, M., Munnely, E. J., Badalamente, G., Serratos Capdevila, L., Sane, V. A., Fragniere, A. M., Kiassat, L., Pleijzier, M. W., Stürner, T., Tamimi, I. F., Dunne, C. R., Salgarella, I., Javier, A., Fang, S., Perlman, E., Kazimiers, T., Jagannathan, S. R., Matsliah, A., Sterling, A. R., Yu, S.-c., McKellar, C. E., Consortium, F., Costa, M., Seung, H. S., Murthy, M., Hartenstein, V., Bock, D. D. and Jefferis, G. S. 2024, 'Whole-brain annotation and multi-connectome cell typing of *Drosophila*', *Nature* **634**, 139–152.
- [271] Schmidt, I., Collett, T., Dillier, F. and Wehner, R. 1992, 'How desert ants cope with enforced detours on their way home', *Journal of Comparative Physiology A* **171**(3).
- [272] Schmitt, D. E. and Esch, H. E. 1993, 'Magnetic orientation of honeybees in the laboratory', *Naturwissenschaften* **80**(1), 41–43.
- [273] Schulz, E., Speekenbrink, M. and Krause, A. 2016, 'A tutorial on gaussian process regression: Modelling, exploring, and exploiting functions', *Journal of Mathematical Psychology*.
- [274] Schürch, R. and Couvillon, M. J. 2013, 'Too much noise on the dance floor: Intra- and inter-dance angular error in honey bee waggle dances', *Communicative & Integrative Biology* **6**(1), e22298.
- [275] Schürch, R. and Ratnieks, F. L. W. 2015, 'The spatial information content of the honey bee waggle dance', *Frontiers in Human Neuroscience* **3**.
- [276] Schürch, R., Zwirner, K., Yambrick, B. J., Pirault, T., Wilson, J. M. and Couvillon, M. J. 2019, 'Dismantling babel: creation of a universal calibration for honey bee waggle dance decoding', *Animal Behaviour* **150**, 139–145.

- [277] Schöne, H., Westermayr, P., Kühme, D., Kühme, L., Schöne, M. and Schöne, R. 1998, 'Searching behaviour and direction finding of differently motivated displaced honeybees—an 'etho-psychological' study of release behaviour', *Ethology* **104**(12), 1039–1055.
- [278] Schürch, R., Couvillon, M. J., Burns, D. D. R., Tasman, K., Waxman, D. and Ratnieks, F. L. W. 2013, 'Incorporating variability in honey bee waggle dance decoding improves the mapping of communicated resource locations', *Journal of Comparative Physiology A* **199**(12), 1143–1152.
- [279] Schürch, R., Ratnieks, F. L. W., Samuelson, E. E. W. and Couvillon, M. J. 2016, 'Dancing to her own beat: honey bee foragers communicate via individually calibrated waggle dances', *Journal of Experimental Biology* .
- [280] Seeley, T. D. 1983, 'Division of labor between scouts and recruits in honeybee foraging', *Behavioral Ecology and Sociobiology* **12**(3), 253–259.
- [281] Seeley, T. D. 1985, *Honeybee Ecology: A Study of Adaptation in Social Life*, Princeton University Press.
- [282] Seeley, T. D. 1994, 'Honey bee foragers as sensory units of their colonies', *Behavioral Ecology and Sociobiology* **34**(1), 51–62.
- [283] Seeley, T. D. 1996, *The Wisdom of the Hive*, Harvard University Press.
- [284] Seeley, T. D., Mikheyev, A. S. and Pagano, G. J. 2000, 'Dancing bees tune both duration and rate of waggle-run production in relation to nectar-source profitability', *Journal of Comparative Physiology A: Sensory, Neural, and Behavioral Physiology* **186**(9), 813–819.
- [285] Seeley, T. D. and Towne, W. F. 1992, 'Tactics of dance choice in honey bees: do foragers compare dances?', *Behavioral Ecology and Sociobiology* **30**(1).
- [286] Seeley, T. D. and Visscher, P. K. 2008, 'Sensory coding of nest-site value in honeybee swarms', *Journal of Experimental Biology* **211**(23), 3691–3697.
- [287] Seelig, J. D., Chiappe, M. E., Lott, G. K., Dutta, A., Osborne, J. E., Reiser, M. B. and Jayaraman, V. 2010, 'Two-photon calcium imaging from head-fixed drosophila during optomotor walking behavior', *Nature Methods* **7**(7), 535–540.
- [288] Seelig, J. D. and Jayaraman, V. 2013, 'Feature detection and orientation tuning in the drosophila central complex', *Nature* **503**(7475), 262–266.
- [289] Seelig, J. D. and Jayaraman, V. 2015, 'Neural dynamics for landmark orientation and angular path integration', *Nature* **521**(7551), 186–191.
- [290] Shafir, S. and Barron, A. B. 2009, 'Optic flow informs distance but not profitability for honeybees', *Proceedings of the Royal Society B: Biological Sciences* **277**(1685), 1241–1245.
- [291] Shakeel, M. and Brockmann, A. 2023, 'Temporal effects of sugar intake on fly local

- search and honey bee dance behaviour’, *Journal of Comparative Physiology A* **210**(3), 415–429.
- [292] Shenk, J., Byttner, W., Nambusubramaniyan, S. and Zoeller, A. 2021, ‘Traja: A python toolbox for animal trajectory analysis’, *Journal of Open Source Software* **6**(63), 3202.
- [293] Si, A., Srinivasan, M. V. and Zhang, S. 2003, ‘Honeybee navigation: properties of the visually driven ‘odometer’’, *Journal of Experimental Biology* **206**(8), 1265–1273.
- [294] Skiles, D. D. 1985, *The Geomagnetic Field Its Nature, History, and Biological Relevance*, Springer US, pp. 43–102.
- [295] Snodgrass, R. E. 1956, *The anatomy of the honey bee*, Cornell University Press.
- [296] Spaethe, J., Schaefer, S. and Tautz, J. 1997, ‘Active and passive thorax/abdominal flexion in dead, walking and dance following bees’, *Adv Ethol* **29**, 107.
- [297] Spangler, H. G. 1991, ‘Do honey bees encode distance information into the wing vibrations of the waggle dance?’, *Journal of Insect Behavior* **4**(1), 15–20.
- [298] Srinivasan, M. V., Zhang, S., Altwein, M. and Tautz, J. 2000, ‘Honeybee navigation: Nature and calibration of the “odometer”’, *Science* **287**(5454), 851–853.
- [299] Srinivasan, M. V., Zhang, S. W. and Bidwell, N. J. 1997, ‘Visually mediated odometry in honeybees’, *Journal of Experimental Biology* **200**(19), 2513–2522.
- [300] Srinivasan, M., Zhang, S. and Lehrer, M. 1998, ‘Honeybee navigation: odometry with monocular input’, *Animal Behaviour* **56**(5), 1245–1259.
- [301] Srinivasan, M., Zhang, S., Lehrer, M. and Collett, T. 1996, ‘Honeybee navigation en route to the goal: visual flight control and odometry’, *Journal of Experimental Biology* **199**(1), 237–244.
- [302] Stabentheiner, A. and Hagmüller, K. 1991, ‘Sweet food means ‘hot dancing’ in honeybees’, *Naturwissenschaften* **78**(10), 471–473.
- [303] Stabentheiner, A., Kovac, H. and Hagmüller, K. 1995, ‘Thermal behavior of round and wagtail dancing honeybees’, *Journal of Comparative Physiology B* **165**(6).
- [304] Steck, K., Hansson, B. S. and Knaden, M. 2009, ‘Smells like home: Desert ants, *Cataglyphis fortis*, use olfactory landmarks to pinpoint the nest’, *Frontiers in Zoology* **6**(1).
- [305] Stone, T., Webb, B., Adden, A., Weddig, N. B., Honkanen, A., Templin, R., Wcislo, W., Scimeca, L., Warrant, E. and Heinze, S. 2017, ‘An anatomically constrained model for path integration in the bee brain’, *Current Biology* **27**(20), 3069–3085.e11.
- [306] Stork, N. E. 2018, ‘How many species of insects and other terrestrial arthropods are there on earth?’, *Annual Review of Entomology* **63**(1), 31–45.

- [307] Su, S., Cai, F., Si, A., Zhang, S., Tautz, J. and Chen, S. 2008, 'East learns from west: Asiatic honeybees can understand dance language of european honeybees', *PLoS ONE* **3**(6), e2365.
- [308] Sumner-Rooney, L. 2023, "distributed' vision and the architecture of animal visual systems', *Journal of Experimental Biology* **226**(23).
- [309] Sun, Y., Liu, L., Ben-Shahar, Y., Jacobs, J. S., Eberl, D. F. and Welsh, M. J. 2009, 'TRPA channels distinguish gravity sensing from hearing in Johnston's organ', *Proceedings of the National Academy of Sciences* **106**(32), 13606–13611.
- [310] Sutton, G. P., Clarke, D., Morley, E. L. and Robert, D. 2016, 'Mechanosensory hairs in bumblebees (*Bombus terrestris*) detect weak electric fields', *Proceedings of the National Academy of Sciences* **113**(26), 7261–7265.
- [311] Suver, M. P., Matheson, A. M., Sarkar, S., Damiata, M., Schoppik, D. and Nagel, K. I. 2019, 'Encoding of wind direction by central neurons in *Drosophila*', *Neuron* **102**(4), 828–842.e7.
- [312] Suver, M. P., Medina, A. M. and Nagel, K. I. 2023, 'Active antennal movements in *Drosophila* can tune wind encoding', *Current Biology* .
- [313] Taisz, I., Doná, E., Münch, D., Bailey, S. N., Morris, B. J., Meechan, K. I., Stevens, K. M., Varela-Martínez, I., Gkantia, M., Schlegel, P., Ribeiro, C., Jefferis, G. S. and Galili, D. S. 2023, 'Generating parallel representations of position and identity in the olfactory system', *Cell* **186**(12), 2556–2573.e22.
- [314] Tanner, D. A. and Visscher, K. 2005, 'Do honey bees tune error in their dances in nectar-foraging and house-hunting?', *Behavioral Ecology and Sociobiology* **59**(4), 571–576.
- [315] Tanner, D. A. and Visscher, P. K. 2008a, 'Do honey bees average directions in the waggle dance to determine a flight direction?', *Behavioral Ecology and Sociobiology* **62**(12), 1891–1898.
- [316] Tanner, D. A. and Visscher, P. K. 2010a, 'Adaptation or constraint? reference-dependent scatter in honey bee dances', *Behavioral Ecology and Sociobiology* **64**(7), 1081–1086.
- [317] Tanner, D. A. and Visscher, P. K. 2010b, 'Does imprecision in the waggle dance fit patterns predicted by the tuned-error hypothesis?', *Journal of Insect Behavior* **23**(3), 180–188.
- [318] Tanner, D. and Visscher, K. 2008b, 'Does the body orientation of waggle dance followers affect the accuracy of recruitment?', *Apidologie* **40**(1), 55–62.
- [319] Tautz, J. 2022, *Communication Between Honeybees*, Springer International Publishing.
- [320] Tautz, J. and Rohrseitz, K. 1998, 'What attracts honeybees to a waggle dancer?', *Journal of Comparative Physiology A: Sensory, Neural, and Behavioral Physiology* **183**(5), 661–667.

- [321] Tautz, J., Rohrseitz, K. and Sandeman, D. C. 1996, 'One-strided waggle dance in bees', *Nature* **382**(6586), 32–32.
- [322] Tautz, J. and Sandeman, D. C. 2003, 'Recruitment of honeybees to non-scented food sources', *Journal of Comparative Physiology A* **189**(4), 293–300.
- [323] Tautz, J., Zhang, S., Spaethe, J., Brockmann, A., Si, A. and Srinivasan, M. 2004, 'Honeybee odometry: Performance in varying natural terrain', *PLoS Biology* **2**(7), e211.
- [324] Thom, C., Gilley, D. C., Hooper, J. and Esch, H. E. 2007, 'The scent of the waggle dance', *PLoS Biology* **5**(9), e228.
- [325] Titova, A. V., Kau, B. E., Tibor, S., Mach, J., Vo-Doan, T. T., Wittlinger, M. and Straw, A. D. 2022, 'Displacement experiments provide evidence for path integration in *Drosophila*'.
- [326] Tolman, E. C. 1948, 'Cognitive maps in rats and men.', *Psychological Review* **55**(4), 189–208.
- [327] Tomlinson, J., McGinty, S. and Kish, J. 1981, 'Magnets curtail honey bee dancing', *Animal Behaviour* **29**(1), 307–308.
- [328] Toufalia, H. A., Couvillon, M. J., Ratnieks, F. L. W. and Grüter, C. 2013, 'Honey bee waggle dance communication: signal meaning and signal noise affect dance follower behaviour', *Behavioral Ecology and Sociobiology* **67**(4), 549–556.
- [329] Touretzky, D. S., Redish, A. D. and Wan, H. S. 1993, 'Neural representation of space using sinusoidal arrays', *Neural Computation* **5**(6), 869–884.
- [330] Towne, W. F. and Gould, J. L. 1988, 'The spatial precision of the honey bees' dance communication', *Journal of Insect Behavior* **1**(2), 129–155.
- [331] Tsujiuchi, S., Sivan-Loukianova, E., Eberl, D. F., Kitagawa, Y. and Kadowaki, T. 2007, 'Dynamic range compression in the honey bee auditory system toward waggle dance sounds', *PLoS ONE* **2**(2), e234.
- [332] Turner-Evans, D. B., Jensen, K. T., Ali, S., Paterson, T., Sheridan, A., Ray, R. P., Wolff, T., Lauritzen, J. S., Rubin, G. M., Bock, D. D. and Jayaraman, V. 2020, 'The neuroanatomical ultrastructure and function of a biological ring attractor', *Neuron* **108**(1), 145–163.e10.
- [333] Turner-Evans, D., Wegener, S., Rouault, H., Franconville, R., Wolff, T., Seelig, J. D., Druckmann, S. and Jayaraman, V. 2017, 'Angular velocity integration in a fly heading circuit', *eLife* **6**.
- [334] Ueno, T., Tomita, J., Tanimoto, H., Endo, K., Ito, K., Kume, S. and Kume, K. 2012, 'Identification of a dopamine pathway that regulates sleep and arousal in *Drosophila*', *Nature Neuroscience* **15**(11), 1516–1523.

- [335] Varvia, P., Rätty, J. and Packalen, P. 2023, ‘mgpr: An r package for multivariate gaussian process regression’, *SoftwareX* **24**, 101563.
- [336] Virtanen, P., Gommers, R., Oliphant, T. E., Haberland, M., Reddy, T., Cournapeau, D., Burovski, E., Peterson, P., Weckesser, W., Bright, J., van der Walt, S. J., Brett, M., Wilson, J., Millman, K. J., Mayorov, N., Nelson, A. R. J., Jones, E., Kern, R., Larson, E., Carey, C. J., Polat, İ., Feng, Y., Moore, E. W., VanderPlas, J., Laxalde, D., Perktold, J., Cimrman, R., Henriksen, I., Quintero, E. A., Harris, C. R., Archibald, A. M., Ribeiro, A. H., Pedregosa, F., van Mulbregt, P., Vijaykumar, A., Bardelli, A. P., Rothberg, A., Hilboll, A., Kloeckner, A., Scopatz, A., Lee, A., Rokem, A., Woods, C. N., Fulton, C., Masson, C., Häggström, C., Fitzgerald, C., Nicholson, D. A., Hagen, D. R., Pasechnik, D. V., Olivetti, E., Martin, E., Wieser, E., Silva, F., Lenders, F., Wilhelm, F., Young, G., Price, G. A., Ingold, G.-L., Allen, G. E., Lee, G. R., Audren, H., Probst, I., Dietrich, J. P., Silterra, J., Webber, J. T., Slavič, J., Nothman, J., Buchner, J., Kulick, J., Schönberger, J. L., de Miranda Cardoso, J. V., Reimer, J., Harrington, J., Rodríguez, J. L. C., Nunez-Iglesias, J., Kuczynski, J., Tritz, K., Thoma, M., Newville, M., Kümmerer, M., Bolingbroke, M., Tartre, M., Pak, M., Smith, N. J., Nowaczyk, N., Shebanov, N., Pavlyk, O., Brodtkorb, P. A., Lee, P., McGibbon, R. T., Feldbauer, R., Lewis, S., Tygier, S., Sievert, S., Vigna, S., Peterson, S., More, S., Pudlik, T., Oshima, T., Pingel, T. J., Robitaille, T. P., Spura, T., Jones, T. R., Cera, T., Leslie, T., Zito, T., Krauss, T., Upadhyay, U., Halchenko, Y. O. and and, Y. V.-B. 2020, ‘SciPy 1.0: fundamental algorithms for scientific computing in python’, *Nature Methods* **17**(3), 261–272.
- [337] Visscher, P. K. and Seeley, T. D. 1982, ‘Foraging strategy of honeybee colonies in a temperate deciduous forest’, *Ecology* **63**(6), 1790.
- [338] Vo-Doan, T. T., Titov, V. V., Harrap, M. J., Lochner, S. and Straw, A. D. 2023, ‘High resolution outdoor videography of insects using fast lock-on tracking’.
- [339] von Hadeln, J., Hensgen, R., Bockhorst, T., Rosner, R., Heidasch, R., Pegel, U., Quintero Pérez, M. and Homberg, U. 2019, ‘Neuroarchitecture of the central complex of the desert locust: Tangential neurons’, *Journal of Comparative Neurology* **528**(6), 906–934.
- [340] Wang, Z., Chen, X., Becker, F., Greggers, U., Walter, S., Werner, M., Gallistel, C. R. and Menzel, R. 2023, ‘Honey bees infer source location from the dances of returning foragers’, *Proceedings of the National Academy of Sciences* **120**(12).
- [341] Wario, F., Wild, B., Rojas, R. and Landgraf, T. 2017, ‘Automatic detection and decoding of honey bee waggle dances’, *PLOS ONE* **12**(12), e0188626.
- [342] Waskom, M. 2021, ‘seaborn: statistical data visualization’, *Journal of Open Source Software* **6**(60), 3021.
- [343] Wedzony, M. and Filek, M. 1998, ‘Changes of electric potential in pistils of *Petunia hybrida* Hort. and *Brassica napus* L. during pollination’, *Acta Physiologiae Plantarum* **20**(3), 291–297.

- [344] Wehner, R. 1984, 'Astronavigation in insects', *Annual Review of Entomology* **29**(1), 277–298.
- [345] Wehner, R., Boyer, M., Loertscher, F., Sommer, S. and Menzi, U. 2006, 'Ant navigation: One-way routes rather than maps', *Current Biology* **16**(1), 75–79.
- [346] Wehner, R., Hoinville, T. and Cruse, H. 2023, 'On the 'cognitive map debate' in insect navigation', *Studies in History and Philosophy of Science* **102**, 87–89.
- [347] Wehner, R. and Srinivasan, M. V. 1981, 'Searching behaviour of desert ants, genus *Cataglyphis* (Formicidae, Hymenoptera)', *Journal of Comparative Physiology A* **142**(3), 315–338.
- [348] Wehner, R. and Srinivasan, M. V. 2003, *Path integration in insects*, Oxford University Press, pp. 9–30.
- [349] Weidenmuller, A. and Seeley, T. D. 1999, 'Imprecision in waggle dances of the honeybee (*Apis mellifera*) for nearby food sources: error or adaptation?', *Behavioral Ecology and Sociobiology* **46**(3), 190–199.
- [350] Wells, P. H. and Wenner, A. M. 1971, 'The influence of food scent on behavior of foraging honey bees', *Physiological Zoology* **44**(4), 191–209.
- [351] Wenner, A. M. 1962, 'Sound production during the waggle dance of the honey bee', *Animal Behaviour* **10**(1–2), 79–95.
- [352] Wenner, A. M. 1963, 'The flight speed of honeybees: a quantitative approach', *Journal of Apicultural Research* **2**(1), 25–32.
- [353] Wenner, A. M. 1967, 'Honey bees: Do they use the distance information contained in their dance maneuver?', *Science* **155**(3764), 847–849.
- [354] Wenner, A. M. 2002, 'The elusive honey bee dance "language" hypothesis', *Journal of Insect Behavior* **15**(6), 859–878.
- [355] Wenner, A. M., Wells, P. H. and Johnson, D. L. 1969, 'Honey bee recruitment to food sources: Olfaction or language?', *Science* **164**(3875), 84–86.
- [356] Westeinde, E. A., Kellogg, E., Dawson, P. M., Lu, J., Hamburg, L., Midler, B., Druckmann, S. and Wilson, R. I. 2024, 'Transforming a head direction signal into a goal-oriented steering command', *Nature* **626**(8000), 819–826.
- [357] Wiltschko, W. and Wiltschko, R. 2005, 'Magnetic orientation and magnetoreception in birds and other animals', *Journal of Comparative Physiology A* **191**(8), 675–693.
- [358] Wittlinger, M., Wehner, R. and Wolf, H. 2006, 'The ant odometer: stepping on stilts and stumps', *e-Neuroforum* **12**(3), 240–241.
- [359] Wolf, E. 1927, 'Über das heimkehrvermögen der bienen (zweite mitteilung.)', *Zeitschrift für Vergleichende Physiologie* **6**(2), 221–254.

- [360] Wolff, T. and Rubin, G. M. 2018, 'Neuroarchitecture of the *Drosophila* central complex: A catalog of nodulus and asymmetrical body neurons and a revision of the protocerebral bridge catalog', *Journal of Comparative Neurology* **526**(16), 2585–2611.
- [361] Wray, M. K., Klein, B. A. and Seeley, T. D. 2011, 'Honey bees use social information in waggle dances more fully when foraging errors are more costly', *Behavioral Ecology* **23**(1), 125–131.
- [362] Yamawaki, Y. and Ishibashi, W. 2014, 'Antennal pointing at a looming object in the cricket *Acheta domestica*', *Journal of Insect Physiology* **60**, 80–91.
- [363] Yorozu, S., Wong, A., Fischer, B. J., Dankert, H., Kernan, M. J., Kamikouchi, A., Ito, K. and Anderson, D. J. 2009, 'Distinct sensory representations of wind and near-field sound in the drosophila brain', *Nature* **458**(7235), 201–205.
- [364] Zhang, S., Lehrer, M. and Srinivasan, M. 1999, 'Honeybee memory: Navigation by associative grouping and recall of visual stimuli', *Neurobiology of Learning and Memory* **72**(3), 180–201.
- [365] Zivkovic, Z. 2004, Improved adaptive gaussian mixture model for background subtraction, in 'Proceedings of the 17th International Conference on Pattern Recognition, 2004.', IEEE.
- [366] Zivkovic, Z. and van der Heijden, F. 2006, 'Efficient adaptive density estimation per image pixel for the task of background subtraction', *Pattern Recognition Letters* **27**(7), 773–780.
- [367] Łopuch, S. and Tofilski, A. 2017a, 'Direct visual observation of wing movements during the honey bee waggle dance', *Journal of Insect Behavior* **30**(2), 199–210.
- [368] Łopuch, S. and Tofilski, A. 2017b, 'Importance of wing movements for information transfer during honey bee waggle dance', *Ethology* **123**(12), 974–980.
- [369] Łopuch, S. and Tofilski, A. 2020, 'Impact of the quality of food sources on the wing beating of honey bee dancers', *Apidologie* **51**(4), 631–641.

A

Supplementary Material

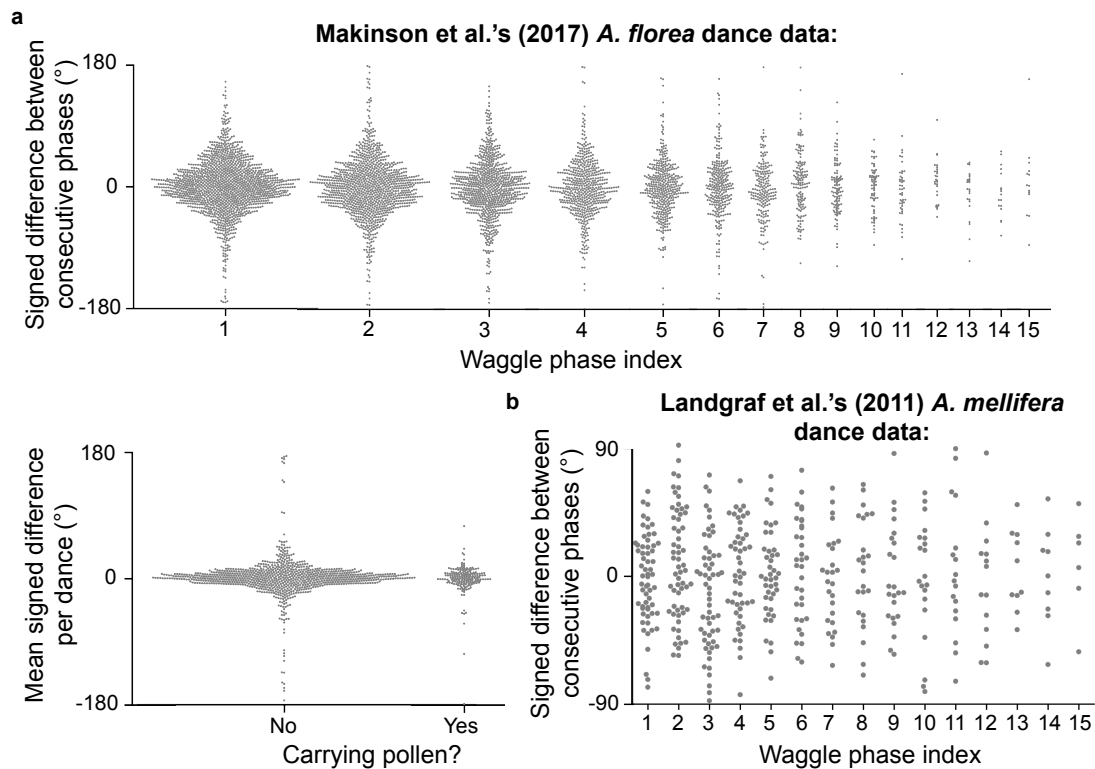


Figure A.1. Angular divergence across consecutive waggle phases (additional view). Related to Fig. 3.2. Same data as in Fig. 3.2 but plotted with signed (instead of absolute) angular differences between consecutive waggle phases. There appears to be no substantial change in the angular divergence over the course of a dance with regards to the absolute phase angles for either species. Both original data sources from **a**, Makinson et al.¹⁹² and **b**, Landgraf et al.¹⁷⁴ were analysed and used with permission.

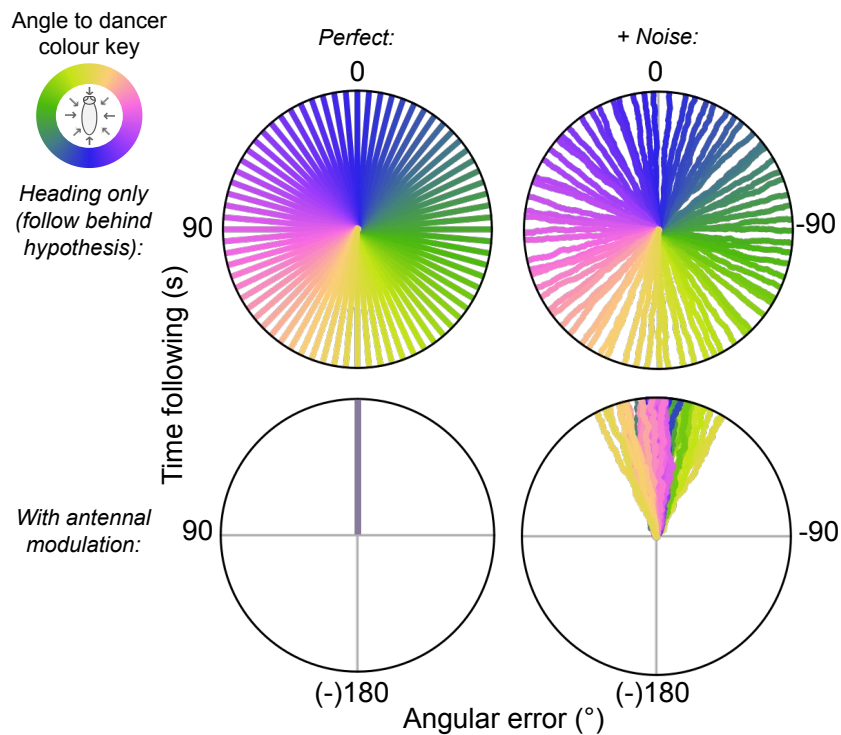


Figure A.2. The hypothetical gain in performance when comparing the ‘follow behind’ and antennal modulation conditions for a uniform distribution of nestmates around the dancer. Related to Fig. 4.7. Angular error of decoded vectors when using heading angle only (top row) or using antennal modulation with midpoint feature (bottom row) simulated under ‘perfect’ (left column) and noisy (right column) conditions. In the latter, noise was added to the heading angle (top right) or antennae (bottom right) at each time step, drawn from von Mises distribution ($\mu = 0$ and $\kappa = 10$). Nestmates’ vectors are coloured by their according angle to the dancer when following the waggle phase.

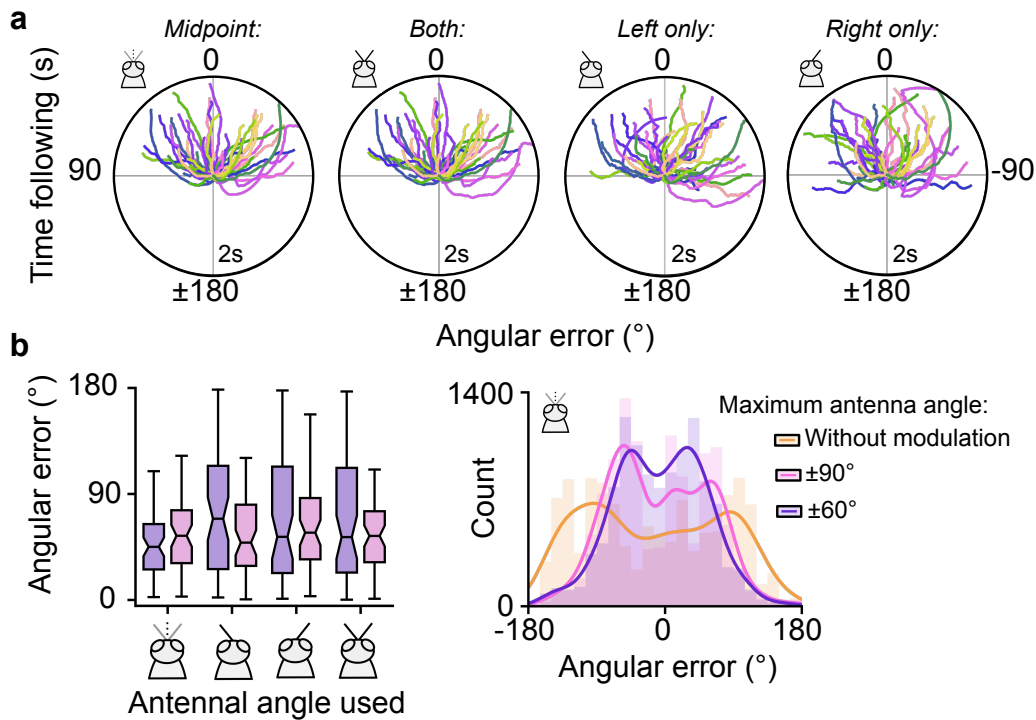


Figure A.3. Additional results of the assimilation circuit. Related to Fig. 4.7. **a**, Angular error of decoded vectors of simulated nestmates at each time step of following when using modulation with the four different features of antennal input. **b**, (Left) Absolute angular error of intermediary vectors accumulated when using $\pm 60^\circ$ (purple) or $\pm 90^\circ$ (pink) as the maximum antennae position that angles are mapped from according to the antennal feature used. Notches on boxplots indicate 95% confidence intervals for the median value. (Right) Angular error histogram for vectors assimilated with and without antennal modulation (orange). Solid lines indicate smoothed kernel density estimate curves.

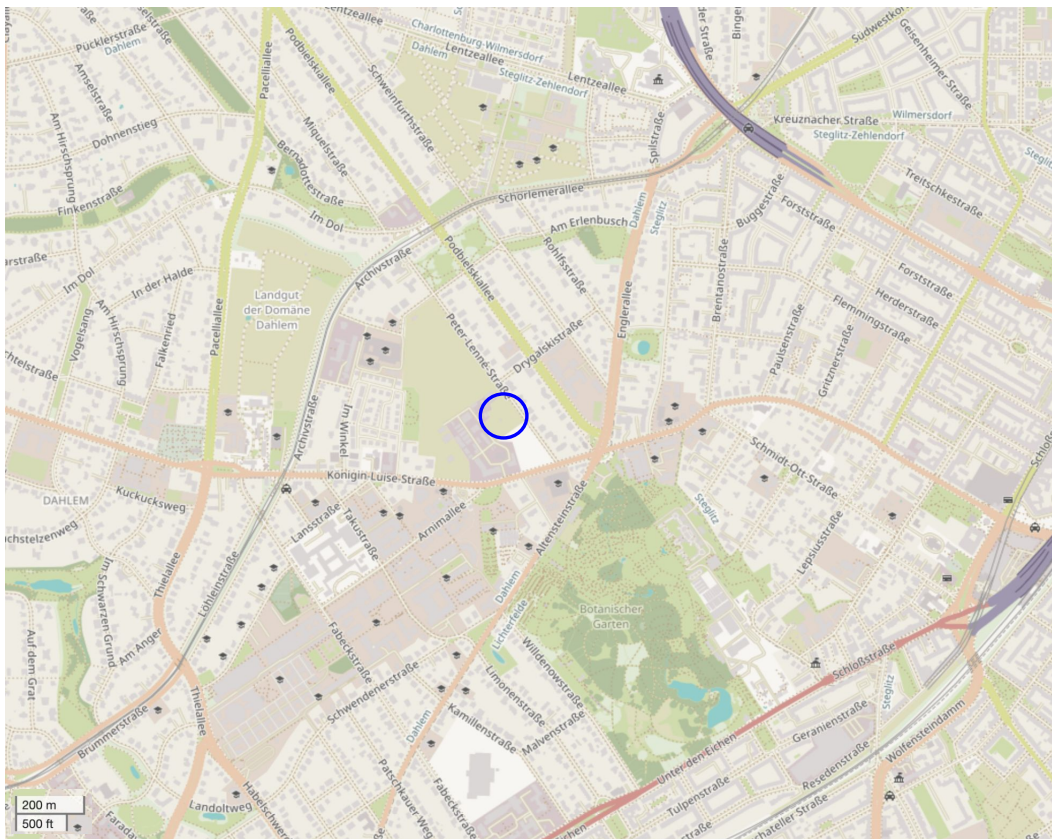


Figure A.4. Surrounding area of experimental site in Berlin ($52^{\circ}27'34.0''\text{N}$ $13^{\circ}17'59.7''\text{E}$) from OpenStreetMap²⁴⁰. Related to Fig. 5.1.

Table A.1. Circular statistics for post detour flight angles of a, dancers and b, followers relative to the detour tunnel exit. Related to Figs. 5.4 and 5.6. Row groups indicate the recorded data at different distance boundaries from the tunnel exit. MVB indicates the mean vector bearing. All Rayleigh's Z tests for uniformity were statistically significant ($P < 0.001$).

(a) Dancers

		Target angle (°)	52	35	0	-35	-52
0.22 m	<i>n</i>		47	24	28	23	54
	MVB (°)		7.81	1.22	-0.61	-18.54	-19.48
	s.d. (°)		22.6	23.33	20.83	33.15	19.27
	Rayleigh's test (Z)		40.22	20.33	24.53	16.46	48.23
0.44 m	<i>n</i>		45	24	26	30	52
	MVB (°)		26.44	13.28	-1.91	-20.83	-27.48
	s.d. (°)		26.83	27.98	25.04	36.91	25.61
	Rayleigh's test (Z)		36.14	18.91	21.48	13.2	42.58
0.56 m	<i>n</i>		33	18	13	8	41
	MVB (°)		44.03	24.17	-10.22	-29.88	-35.59
	s.d. (°)		26.03	32.29	29.47	41.61	23.03
	Rayleigh's test (Z)		26.65	13.10	9.98	4.72	34.88
Last visible	<i>n</i>		47	24	28	23	55
	MVB (°)		54.43	36.71	-6.39	-37.11	-36.6
	s.d. (°)		31.09	42.44	47.89	40.68	40.68
	Rayleigh's test (Z)		35.01	13.86	13.92	12.23	33.22

(b) Followers

		Target angle (°)	35	0	-35
Last visible	<i>n</i>		25	26	35
	MVB (°)		27.94	-9.20	-35.64
	s.d. (°)		60.74	51.31	51.17
	Rayleigh's test (Z)		8.15	11.66	15.76

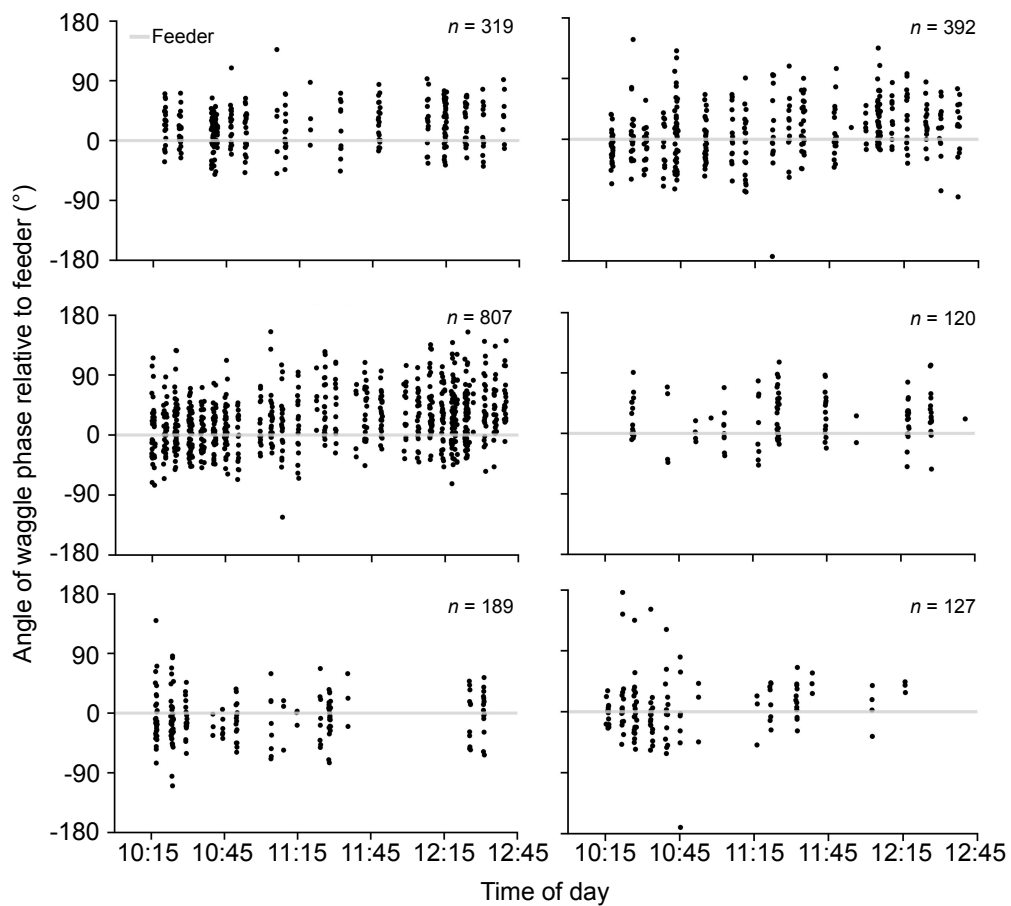


Figure A.5. Angles of waggle phases of six dancers relative to the feeder across all dances performed within a 2.5 hour foraging period to the trained feeder. Related to Fig. 5.8. Each black circle represents a waggle phase signalled by a dancer. 90° and -90° respectively indicate a signalled angle that is deviated to the left or right of the feeder, respectively. Time of day specified using a 24 hour clock. Same data as in Fig. 5.8 but signalled waggle phases have been visualised with respect to the feeder.

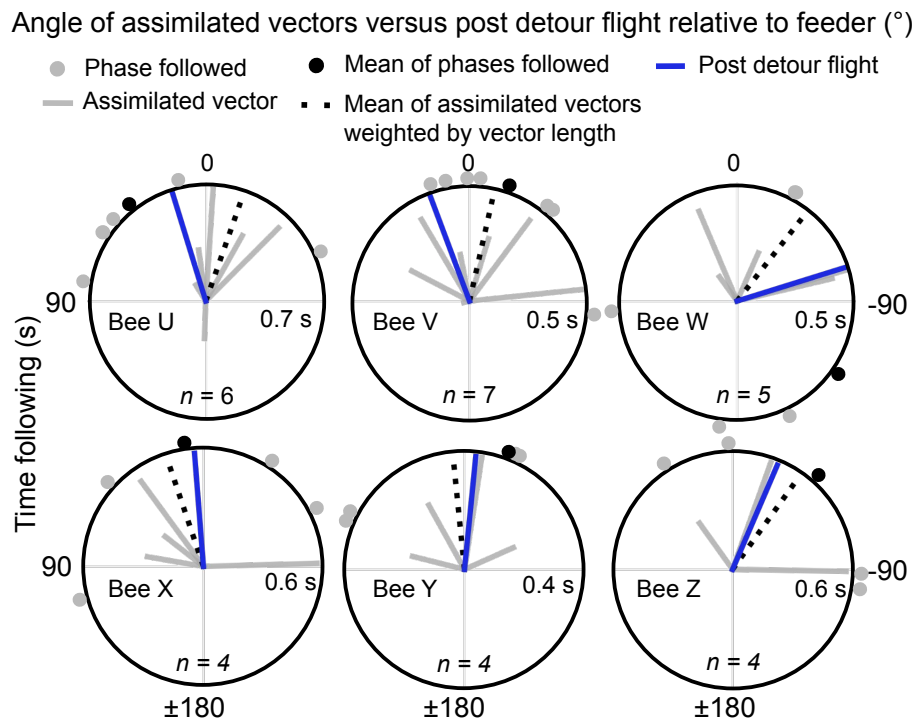


Figure A.6. The assimilated vectors of six new recruits with their mean vectors weighted by their length. Related to Fig. 5.10. The vectors assimilated at the end of each waggle phase (lines) and the angle of phases followed (circles) by six new recruits and their subsequent angle of flight post detour (blue). Same data as in Fig. 5.10 but the mean assimilated vector (dashed line) for each recruit has been weighted by the lengths of the individual vectors.